Delayed response of the Cys326 variant of the DNA repair protein OGG1 to cellular oxidative stress

By

Rachael Maria Kershaw

A thesis submitted to

The University of Birmingham

for the degree of

DOCTOR OF PHILOSOPHY

School of Biosciences

The University of Birmingham

August 2011

Abstract

Reactive oxygen species (ROS) are generated via endogenous and exogenous sources. ROS are involved in essential cellular processes but when present in excess, can overwhelm antioxidant defences and induce a range of damaging DNA lesions. The most commonly oxidised DNA base is guanine. This generates products including 7,8-dihydro-8-oxodeoxyguanine (8-oxo dG) which can result in G:C→T:A transversion mutations, frequently found in human cancers. Oxidative damage is also implicated in normal cellular ageing and degenerative diseases. 8-oxo dG repair is initiated by the base excision repair enzyme 8-oxoguanine DNA glycosylase 1 (OGG1). Modulation of OGG1 activity in oxidising conditions has implications for mutation prevention. This thesis investigates regulation of OGG1 under oxidising conditions using BSO, which increases intracellular ROS. Chapter 3 shows that following BSO treatment, mouse OGG1 activity in mouse embryonic fibroblast (MEF) cells increases with no change in mRNA levels, whereas identical treatment has no effect on rat OGG1 activity in MH1C1 cells but modulates protein levels. A human OGG1 (hOGG1) variant with serine exchanged for cysteine at codon 326 (Cys326-hOGG1) is associated with reduced repair ability under oxidising conditions. Chapter 4 describes the development of mOGG1$^{-/-}$ MEF cells stably expressing Ser326- or Cys326-hOGG1 and in chapter 5 these cells are used to investigate Ser326- and Cys326-hOGG1 activity, gene expression, protein localisation, homo-dimer formation and retention within an insoluble nuclear fraction following BSO treatment. Data presented shows that the activity of both Ser326- and Cys326-hOGG1 increase following BSO treatment but Ser326-hOGG1 peak activity occurs 12 hours prior to that of Cys326-hOGG1. This increased activity is not associated with increased gene expression or protein, or any protein localisation change; however, Cys326-hOGG1 is retained to a lesser extent in an insoluble nuclear fraction following BSO treatment. The findings presented in this thesis show that OGG1 activity is modulated post-transcriptionally in response to increased ROS and provide a possible mechanism behind impaired Cys326-hOGG1 repair in oxidising conditions, further supporting the role of Cys326-hOGG1 in the process of carcinogenesis.

Acknowledgements

I would like to thank Nik Hodges for his support, guidance and patience throughout the project and without whom I could not have completed my Ph.D. I would like to acknowledge the BBSRC for providing funding, both for the research project and for extra training, which has allowed me to attend valuable courses and conferences. I am grateful for the advice given by Chris Bunce during the project, both relating to the thesis and my future career. I am also grateful to Anne Pheasant for convincing me to study toxicology and encouraging me throughout my time here at Birmingham.

My thesis would not have been possible without the help of many people on the 4th floor and I am extremely grateful to all members of the Chipman/Hodges research group: Kevin Chipman, Shrikant Jondhale, Fiona McRonald, Lucy Wilkinson and Tim Williams. In particular, I would like to thank Richard Green for his considerable help at the beginning of my project. I am also grateful to Farhat Khanim, Nicola Cumley, Rachel Hayden and Bob Harris for invaluable advice.

I could not have survived without the daily Primula-centred tea breaks and the people who shared these with me made my Ph.D. hugely more enjoyable: Rhiannon David, Alex Gavin, Huw Jones, Zahra Khan, Leda Mirbahai, Sabrina Moro, Louise Stone, Nadine Taylor, Lorna Thorne, Mohammed Shuwaikan and Chibuzor Uchea.

Finally, I would like to thank my awesome parents, who will no doubt continue to be disappointed that I don't have a 'proper' job, and my siblings; Deb, Dave, Paul and Pip for their support and contributions. Last, but not least, I am extremely grateful to my wonderful boyfriend Chris for providing emotional support and a large gin and tonic after a bad day in the lab.

TABLE OF CONTENTS

LIST OF FIGURES

Chapter 1

Chapter 2

Chapter 3

Chapter 4

Chapter 5

LIST OF TABLES

LIST OF ABBREVIATIONS

$^1O_2$	Singlet molecular oxygen
4-HNE	4-hydroxynonenal
8-oxo dG	7,8-dihydro-8-oxodeoxyGuanine
ABC	ATP-binding cassette
Ah	Aromatic hydrocarbon
ANOVA	Analysis of variance
AP	Apurinic/apyridiminic
APE1	Apurinic/apyrimidinic endonuclease 1
APS	Ammonium persulphate
ARE	Antioxidant-response element
AU	Absorbance units
BER	Base excision repair
BiFC	Bimolecular fluorescence complementation
BPB	Bromophenol blue
BSA	Bovine serum albumin
BSO	L-buthionine-S-sulphoximine
C4	Cys326-hOGG1 MEF
CMV	Cytomegalovirus
CSK	Cytoskeleton
C_t	Cycle threshold
CYPs	Cytochrome P450 family of monooxygenases
DAB	4-dimethylaminephenylazobenzoic acid
DCF	Dichlorofluorescein
DMEM	Dulbecco's modified Eagle's medium
DMSO	Dimethylsulphoxide
DNA	Deoxyribonucleic acid
dNTP	Deoxyribonucleic triphosphate
dRP	5'-deoxyribose phosphate
DSB	Double strand break
DTT	Dithiothreitol

ECL	Enhanced chemiluminescence
EDTA	Ethylenediaminetetraacetic acid
EGFP	Enhanced green fluorescent protein
EGFR	Epidermal growth factor receptor
EMSA	Electrophoretic mobility shift assay
EtBr	Ethidium bromide
fapyG	2,6-diamino-4-hydroxy-5-formamidopyrimidine
FBS	Foetal bovine serum
Fen1	Flap endonuclease 1
FITC	Fluorescein isothiocyanate
FPG	Formamidopyrimidine DNA glycosylase
FRET	Fluorescence resonance energy transfer
GC/IDMS	Gas chromatography/isotope-dilution mass spectrometry
GCL	Glutamate-cysteine ligase
GG-NER	Global genome nucleotide excision repair
GMP	Guanosine monophosphate
GO	Guanine oxide
GS	Glutathione synthetase
GSH	Reduced glutathione
GSSG	Oxidised glutathione
GST	Glutathione-*S*-transferase
GTP	Guanosine triphosphate
Gu	Guanidinohydantoin
H_2DCF	2,7-Dichlorodihydrofluorescein
H_2DCF-DA	2,7-Dichlorodihydrofluorescein-diacetate
H_2O_2	Hydrogen peroxide
HEK293	Human embryonic kidney
HEPES	*N*-2-Hydroxyethylpiperazine-*N*'-2-ethanesulphonic acid
$HO^{\bullet}$	Hydroxyl radical
$HO_2^{\bullet}$	Hydroperoxyl
HOCl	Hypochlorite
hOGG1	Human 8-oxo-2'-deoxyguanosine DNA glycosylase 1

hph	Hygromycin B phosphotransferase
HPLC-ECD	High pressure liquid chromatography with electrochemical detection
HR	Homologous recombination
HRP	Horseradish peroxidase
hSMUG1	Single-strand selective monofunctional uracil DNA glycosylase
KO	mOGG1$^{-/-}$ null MEF, Knock-out
L$^{\cdot}$	Lipid radical
LB	Luria-bertani
LH	Polyunsaturated fatty acid
LOO$^{\cdot}$	Lipid peroxyl radical
LOOH	Lipid hydroperoxide
MBD4	Methyl-CpG-binding domain protein 4
MDA	Malondialdehyde
MEF	Mouse embryonic fibroblast
MH1C1	Rat Hepatoma cells
MMR	Mismatch repair
mOGG1	Mouse 8-oxo-2'-deoxyguanosine DNA glycosylase 1
MRN	Mre11/Rad50/Nbs1
MRP	Multidrug resistance-associated protein
MTT	3-[4,5-Dimethylthiazol-2-yl]-2,5-diphenyl tetrazolium bromide
MutM	Mutator gene M
MutT	Mutator gene T
MutY	Mutator gene Y
NADH	Nicotinamide adenine dinucleotide
NADPH	Reduced nicotinamide adenine dinucleotide
NEIL	Nei-like
neo	Neomycin
NER	Nucleotide excision repair
NHEJ	Non-homologous end joining
NLS	Nuclear localisation signal
NO^{-}	Nitroxyl anion
NO^{+}	Nitrosonium cation

$NO^{\cdot}$	Nitric oxide
Nrf2	Nuclear factor E2-related factor 2
$O_2^{\bullet-}$	Superoxide radical
OATP	Organic anion transporting polypeptide
OGG1	8-oxodeoxyguanine DNA glycosylase 1
$ONOO^-$	Peroxynitrite radical
OPA	*o*-Phthalaldehyde
PAGE	Polyacrylamide gel electrophoresis
PAH	Polyaromatic hydrocarbon
PBS	Phosphate buffered saline
PCNA	Proliferating cell nuclear antigen
PCR	Polymerase chain reaction
PKC	Protein kinase C
Pol β	DNA polymerase beta
qPCR	Quantitative polymerase chain reaction
Rif^R	Rifampicin resistant
RNA	Ribonucleic acid
RNAPIIo	RNA polymerase II complex
RNS	Reactive nitrogen species
$RO^{\cdot}$	Alkoxy radical
rOGG1	Rat 8-oxo-2'-deoxyguanosine DNA glycosylase 1
$ROO^{\cdot}$	Peroxy radical
ROOH	Organic hydroperoxide
ROS	Reactive oxygen species
RPA	Replication protein A
S2	Drosophila Schneider 2
S326C	Ser326Cys polymorphism
S5	Ser326-hOGG1 MEF
SDS	Sodium dodecyl sulphate
SEM	Standard error of the mean
SNP	Single nucleotide polymorphism
SOC	Superoptimal broth

SOD	Superoxide dismutase
SOH	Sulphenic acid
Sp	Spiroiminodihydantoin
SSB	Single strand break
T4 PNK	T4 Polynucleotide kinase
TBS	Tris buffered saline
TCA	Trichloroacetic acid
TC-NER	Transcription coupled nucleotide excision repair
TEMED	N,N,N,N,-tetramethylethylenediamine
TFIIH	Transcription factor II H
Tris	(Hydroxymethyl) methylamine
UNG	Uracil DNA glycosylase
UV	Ultraviolet
WT	Wild-type
XPA	Xeroderma pigmentosum complementation group A
XPC	Xeroderma pigmentosum complementation group C
XRCC1	X-ray cross complementing protein 1
YFP	Yellow fluorescent protein

Chapter 1 - Introduction

1.1 Reactive species and oxidative stress

1.1.1 Overview

Reactive oxygen species (ROS) are oxygen species which exist in a more reactive state than molecular oxygen. The production of low levels of ROS and reactive nitrogen species (RNS) is necessary for essential cellular processes including gene regulation, cell mediated immunity, cell differentiation, post translational processing of proteins and cellular signalling (Adler V. *et al.* 1999; Dröge W. 2002). The requirement for radical species has necessitated adaptive responses for their detoxification and a delicate cellular balance exists termed redox homeostasis. However, an interference of the balance between oxidative and reductive species by either increased ROS/RNS generation or decreased ROS/RNS removal can result in cellular oxidative/nitrosative stress and cellular components can become damaged (Kohen R. and Nyska A. 2002).

1.1.2 Types of reactive species

There are a variety of commonly occurring ROS and RNS (summarised in Table 1.1). The superoxide radical (O2•-), a primary ROS, is formed via the one-electron reduction of molecular oxygen and can exist at low pH as hydroperoxyl (HO2•) which penetrates biological membranes more easily than O2•- (Kohen R. and Nyska A. 2002). Although relatively unreactive, O2•- is capable of dis-mutating to form hydrogen peroxide (H2O2) [Equation 1] (Fridovich I. 1978). Hydrogen peroxide is stable and uncharged which allows it to easily diffuse across membranes (Paulsen C.E. and Carroll K.S. 2009). Although not a radical species, H2O2 can directly damage cellular components and can react via the Fenton [Equation 2] or the Haber-Weiss reaction [Equation 3] to create

hydroxyl radicals (HO•) and singlet molecular oxygen (1O2) (Kohen R. and Nyska A. 2002).

$O_2^{\bullet-} + O_2^{\bullet-} + 2H^+ \longrightarrow O_2 + H_2O_2$ [Equation 1]

$H_2O_2 + Fe^{2+}/Cu^+ \longrightarrow OH^- + {}^{\bullet}OH + Fe^{3+}/Cu^{2+}$ [Equation 2]

$H_2O_2 + O_2^{\bullet-} \longrightarrow {}^1O_2 + OH^- + {}^{\bullet}OH$ [Equation 3]

The half-life of hydroxyl radicals is short, typically ~10^{-9} seconds, which renders them highly reactive, unable to be eliminated by enzymic reactions and able to perpetuate a cascade of ROS production (Genestra M. 2007). Hydroxyl radicals have a high affinity for and react readily with many cellular molecules. Nitric oxide, produced by vascular endothelial cells and activated macrophages, reacts with $O_2^{\bullet-}$ to produce the peroxynitrite radical ($ONOO^-$) which is similar in reactivity to the hydroxyl radical and hence can damage many cellular constituents (Beckman J.S. *et al.* 1990).

Table 1.1: Summary of ROS and RNS.

Reactive Species			Examples of Formation	Properties
Superoxide	$O_2^{\cdot -}$	One electron reduction state of O_2	In autoxidation reactions and by the electron transport chain	Unreactive but can release Fe^{2+} from iron-sulphur proteins and ferritin
Nitric oxide	$NO^{\cdot}$	Gaseous free radical	Via nitric oxide synthase which catalyses biosynthesis of NO from L-arginine	Reacts with transition metals, alters protein activity by S-nitrosylation, reacts with $O_2^{\cdot -}$ to form peroxynitrite
Hydroxyl radical	$HO^{\cdot}$	Three-electron reduction state of O_2	By Fenton reaction, ionising radiation and decomposition of peroxynitrite	Short *in vivo* half-life, highly reactive, will attack most cellular components and damage all macromolecules
Hydrogen peroxide	H_2O_2	Two-electron reduction state of O_2	By dismutation of $O_2^{\cdot -}$ or direct reduction of O_2	One of the most powerful oxidisers known
Organic hydroperoxide	ROOH	Oxidant	By radical reactions with cellular components such as lipids and nucleobases	Interacts with cellular membrane components, oxidises plasma membrane sulfhydryl groups and disturbs transporters
Hypochlorite	HOCl	Oxidant	From H_2O_2 by myeloperoxidase	Lipid soluble and highly reactive, readily oxidises protein constituents
Alkoxy radical Peroxy radical	$RO^{\cdot}$ $ROO^{\cdot}$	Oxygen centred organic radicals	In the presence of oxygen by radical addition to double bonds or hydrogen abstraction	Lipid forms participate in lipid peroxidation reactions
Peroxynitrite	$ONOO^-$	An oxidant and nitrating agent	By a rapid reaction between $O_2^{\cdot -}$ and $NO^{\cdot}$	Lipid soluble and highly reactive, can damage a wide array of molecules in cells
Singlet oxygen	$^1O_2$	The lowest excited state of O_2	During photosynthesis and via decomposition of hydrogen peroxide	Reacts with many organic compounds, can induce lipid peroxidation

1.1.3 Sources of ROS and RNS

1.1.3.1 Endogenous sources

The consumption of oxygen in metabolic reactions takes place in several cellular locations by various enzymes and redox-reactive components and results in the release of ROS. Under certain physiological conditions mitochondria can be a major source of ROS, particularly in tissues such as the heart and brain. Aerobic respiration involves the transfer of electrons from NADH to oxygen and complexes I and III can release $O_2^{\bullet-}$ as a toxic by-product (Ježek P. and Hlavatá L. 2005; Murphy M.P. 2009).

As well as producing ROS, in certain tissues including liver (Giulivi C. *et al.* 1998) and brain (Lacza Z. *et al.* 2001), mitochondria have a nitric oxide synthase and can generate nitric oxide (Haynes V. *et al.* 2004). Nitric oxide synthase catalyses the oxidation of one of the terminal guanidonitrogen atoms of L-arginine and the nitric oxide generated can be converted to other RNS including peroxynitrite, the nitrosonium cation (NO^+) or the nitroxyl anion (NO^-) (Palmer R.M.J. *et al.* 1988; Stamler J.S. *et al.* 1992).

Many oxidase enzymes including the xanthine oxidase, peroxisomal oxidases and endoplasmic reticular oxidases release ROS. The xanthine oxidoreductase catalyses the hydroxylation of hypoxanthine to xanthine, and xanthine to urate. The reduction of molecular oxygen by this enzyme yields both superoxide and hydrogen peroxide (Harrison R. 2002; McNally J.S. *et al.* 2005). Hydrogen peroxide is also produced by peroxisomal oxidases as they transfer hydrogen to oxygen during metabolic processes such as the beta oxidation of fatty acids (Schrader M. and Fahimi H.D. 2006).

The oxidation of many endogenous and xenobiotic substances is catalysed by the cytochrome P450 family of monooxygenases (CYPs) which are part of a membrane bound multi-enzyme system present mainly in the endoplasmic reticulum. There are two mechanisms by which CYPs form the reactive intermediates H_2O_2 and $O_2^{\bullet-}$ and these are dependent on both the CYP enzyme and its substrate. The first mechanism is via O_2 reduction during the CYP catalytic cycle and the second is via the escape of an electron from flavins in the NADPH:P450 reductase enzyme (Ježek P. and Hlavatá L. 2005). Under certain conditions CYP metabolism can account for a high level of cellular ROS production. For example, CYP2E1, responsible for ethanol detoxification, is a potent radical producer as it is poorly coupled with the NADPH-cytochrome P450 reductase (Caro A.A. and Cederbaum A.I. 2004). Hence, in the liver, ethanol mediated induction of CYP2E1 can enable this to be a source of ROS either comparable to, or exceeding that of the mitochondria (Ježek P. and Hlavatá L. 2005).

Although often considered a toxic by-product, some cellular systems have evolved to produce ROS. The first identified example of a component with the primary role of ROS generation was the phagocyte NADPH oxidase system which produces reactive species responsible for mediating an immune response and killing pathogens. Found in many cell types, NADPH oxidases are a family of transmembrane proteins that transport electrons across biological membranes, catalysing the production of superoxide by taking reducing equivalents from the hexose monophosphate shunt and transferring them to molecular oxygen. Physiological functions of NADPH oxidase family members include cell signalling, cell differentiation, regulation of gene expression as well as host defence

(Bedard K. and Krause K.H. 2007). A detailed discussion of the physiological functions of ROS is beyond the scope of this thesis but is well reviewed by Valko *et al.* (2007).

1.1.3.2 Exogenous sources

There are a variety of exogenous sources linked with ROS production which include UV light, ionising radiation, metals, and polycyclic aromatic hydrocarbons (PAHs). Exposure to such compounds may be via cigarette smoke, environmental pollution, toxic food ingredients or sunlight (Limón-Pacheco J. and Gonsebatt M.E. 2009). During metabolic processes PAHs, such as benzo(*a*)pyrene, form quinone derivatives. These can be enzymatically reduced to semiquinones which donate their extra electron to oxygen resulting in superoxide formation as well as regeneration of the original quinone. This process, termed redox cycling, leads to PAH-induced ROS generation within cells (Kim K.B. and Lee B.M. 1997). Exposure to UVA or UVB light induces the formation of reactive species including superoxide, singlet oxygen and lipid peroxide radicals (Black H.S. 1987; Peak M.J. and Peak J.G. 1989). Ionising radiation cleaves water and predominantly generates the hydroxyl radical (Wallace S.S. 1998). The ability of metals to gain and lose electrons means they can directly or indirectly generate ROS and at high doses, a variety of metals including cadmium (Ikediobi C.O. *et al.* 2004), copper (Pourahmad J. and O'Brien P. J. 2000), chromium (Bagchi D. *et al.* 1995) and lead (Bokara K.K. *et al.* 2008) have been shown to induce oxidative stress conditions. An overload of iron can also result in increased radical generation and oxidative stress (Papanikolaou G. and Pantopoulos K. 2005).

1.1.4 Cellular targets of ROS

As a detailed discussion of RNS is beyond the scope of this thesis, the focus from this point forward will be on ROS. Reactive species can react with many cellular components including lipids, carbohydrates, proteins, mitochondrial and nuclear DNA. When ROS react with membrane lipids, a hydrogen atom can be abstracted from carbon atoms in the polyunsaturated fatty acid tail. The resulting reaction is termed lipid peroxidation (Figure 1.1) which leads to loss of membrane integrity and compromised cellular function, as well as the production of reactive end products; malondialdehyde (MDA) or 4-hydroxynonenal (4-HNE) (Brown G.C. and Borutaite V. 2004; Marnett L.J. 1999).

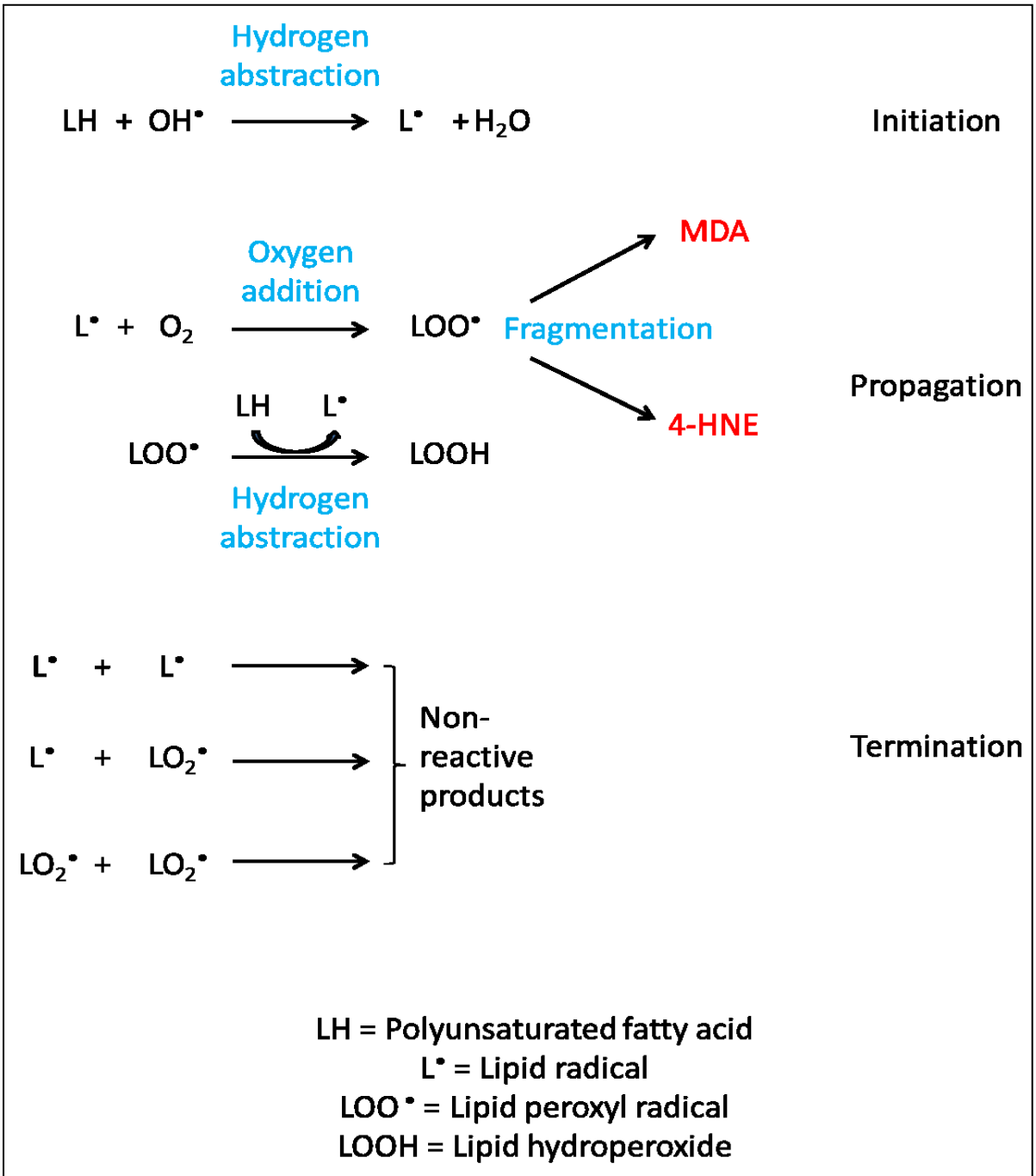

Figure 1.1: Lipid Peroxidation.
Initiation of lipid peroxidation occurs when the •OH radical abstracts a hydrogen atom from a polyunsaturated fatty acid, resulting in the generation of a lipid radical. Lipid radicals can react further with oxygen or a second fatty acid to generate lipid hydroperoxides and lipid peroxide radicals which can react further, or fragment to produce the reactive end products MDA and 4-HNE. Termination of lipid peroxidation occurs when radical species combine to generate non-reactive products (adapted from Niesink R.J.M. et al. 1996).

The reaction of ROS with proteins can result in the irreversible oxidation of amino acid side chains and the cleavage of polypeptide chains (Stadtman E.R. 1992). The reversible interaction between ROS and thiol groups present in proteins is necessary for signal transduction, resulting in either activation or inactivation of proteins including tyrosine kinases and transcription factors (Kamata H. and Hirata H. 1999). The thiol side chains of cysteine residues are susceptible to oxidation by H_2O_2. Their reactivity depends both on their accessibility to oxidants and the pK_a of the thiol group which determines whether it exists as the thiolate ion or in the thiol form. The pK_a of a thiol group is typically around 8.5 but can be reduced in the presence of polar or positively charged amino acids to as low as 3.5, allowing thiolate ion formation at physiological pH (Salsbury Jr. F.R. *et al.* 2008). The reaction with H_2O_2 yields a sulphenic acid (SOH) which can undergo several possible further reactions (Figure 1.2); disulphide formation with glutathione, disulphide formation with another cysteine, sulphenamide formation by attack of the amide nitrogen of a neighbouring residue or sulphinic and irreversible sulphonic acid formation by further reaction with H_2O_2. The thiols can be regenerated by reduction by the glutathione reductase or thioredoxin reductase systems (Paulsen C.E. and Carroll K.S. 2009).

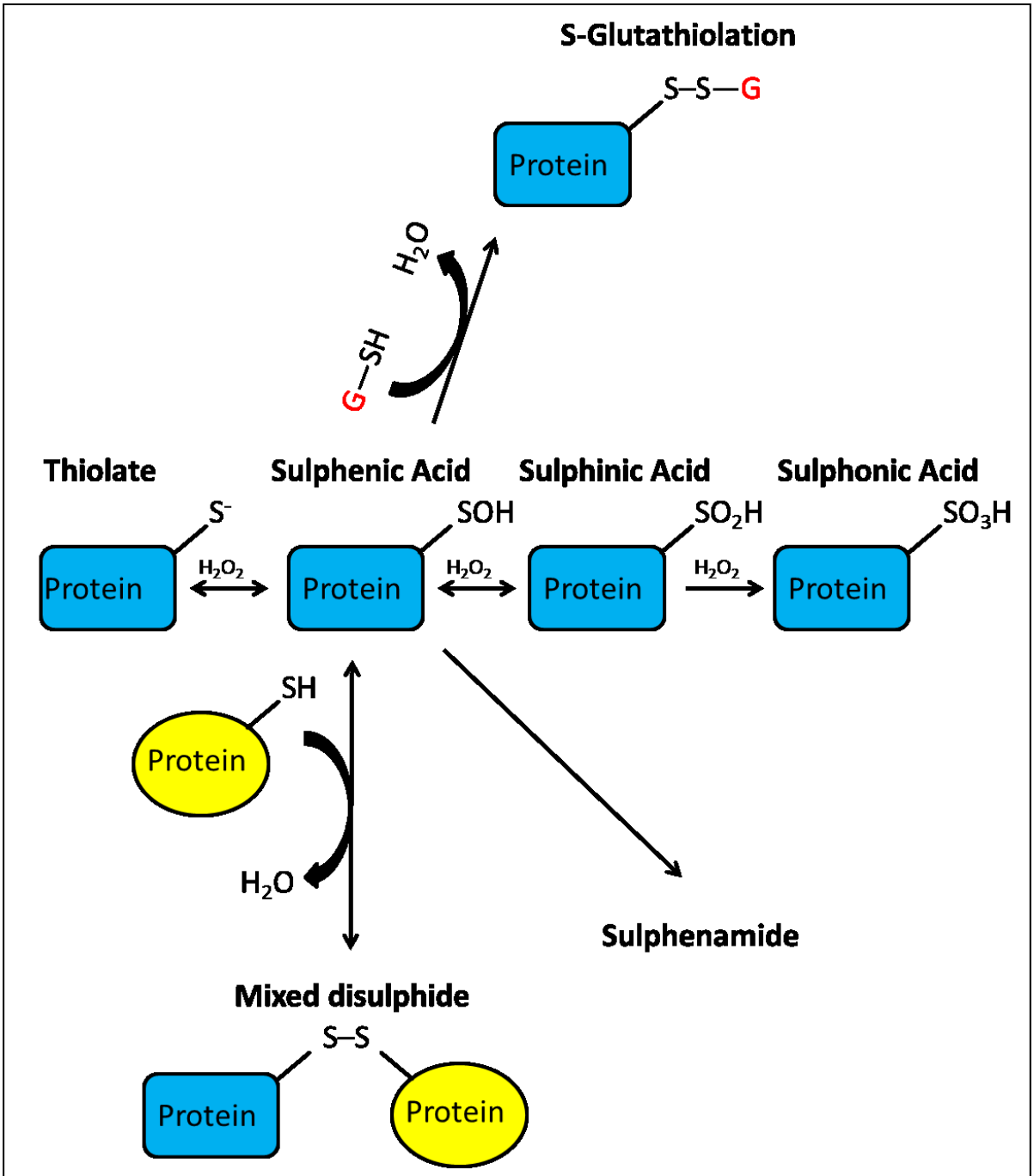

Figure 1.2: Reactions of sulphenic acid.
Reaction of protein thiolates with H_2O_2 results in formation of sulphenic acid which can either react with a second cysteine to yield a disulphide, form a disulphide with reduced glutathione or react with the amide nitrogen of the neighbouring protein to form a sulphenamide. In the presence of H_2O_2 the sulphenic acid can generate sulphinic and sulphonic acid (adapted from Paulsen C.E. and Carroll K.S. 2009).

The interactions between ROS and nuclear DNA are discussed in detail in section 1.3. Nuclear DNA is protected by both histones and DNA repair enzymes. In contrast, mitochondrial DNA lacks protective histones and furthermore is in close proximity to the electron transport chain rendering it vulnerable to oxidative stress (Ames B. *et al.* 2003). Mitochondrial DNA damage mediated by ROS has been linked with various cancers (Horton T.M. *et al.* 1996; Tamura G. *et al.* 1999) and ageing (Sastre J. *et al.* 2000). The mitochondrial theory of ageing (Harman D. 1956) proposes that as mitochondrial DNA is damaged by ROS and accumulates mutations, the oxidative phosphorylation activity is reduced resulting in enhanced ROS production and increased damage. This cycle of oxidative stress and mitochondrial DNA damage causes the accumulation of mutations resulting in mitochondrial dysfunction and cell death (Alexeyev M.F. *et al.* 2004).

1.1.5 Antioxidant defences

As reactive species can damage cellular macromolecules, a variety of antioxidant defences exist. Antioxidant enzymes include superoxide dismutase (SOD), which catalyses the conversion of superoxide ions to hydrogen peroxide, catalase and glutathione peroxidase which catalyse the conversion of hydrogen peroxide to oxygen and water, and peroxiredoxins which reduce peroxides directly, as well as in the presence of thioredoxins (Ma Q. 2009). Induction of these enzymes is regulated at the transcriptional level by the antioxidant-response element (ARE) (Rushmore T.H. and Pickett C.B. 1990), which responds to a variety of reactive compounds in order to maintain cellular redox homeostasis. Many transcription factors including Nrf, Jun, Fos Ah (aromatic hydrocarbon) receptor and the oestrogen receptor bind to the ARE (Dhakshinamoorthy S. *et al.* 2000) but it is Nrf2 (nuclear factor E2-related factor 2)

which is the primary mediator of gene transcription, controlling both the inducible and constitutive gene expression mediated by the ARE (Nguyen T. *et al.* 2009).

Non enzymatic antioxidants include amino acids, dietary components including beta carotene, ascorbate, alpha-tocopherol and glutathione. Glutathione (Figure 1.3A) is a tripeptide with a variety of important cellular functions (Figure 1.3B), in particular to help regulate and maintain redox homeostasis. In its reduced form (GSH), glutathione conjugates and detoxifies reactive metabolites and xenobiotics and is able to deactivate ROS. Conjugation reactions can be spontaneous or catalysed by glutathione S-transferase enzymes, with the conjugates converted by a series of further reactions to mercapturic acids (Meister A. and Anderson M.E. 1983). Redox-sensitive thiol groups are modulated by GSH either by direct interaction or via glutaredoxins, whose reduction by GSH allows them to reduce thiol groups. The oxidation of thiol groups is also prevented during oxidative stress by the formation of glutathione-protein mixed disulphides (Kalinina E.V. *et al.* 2008).

As the most abundant intracellular thiol, GSH is maintained in its reduced state by the NADPH-dependent glutathione disulphide reductase (GSSG reductase). High (0.2 – 10 mM) intracellular concentrations of GSH are maintained by constitutive *de novo* synthesis via a two-step pathway catalysed by the rate limiting enzyme glutamate-cysteine ligase (GCL) and glutathione synthetase (GS) (Figure 1.4) (Griffith O.W. and Meister A. 1979).

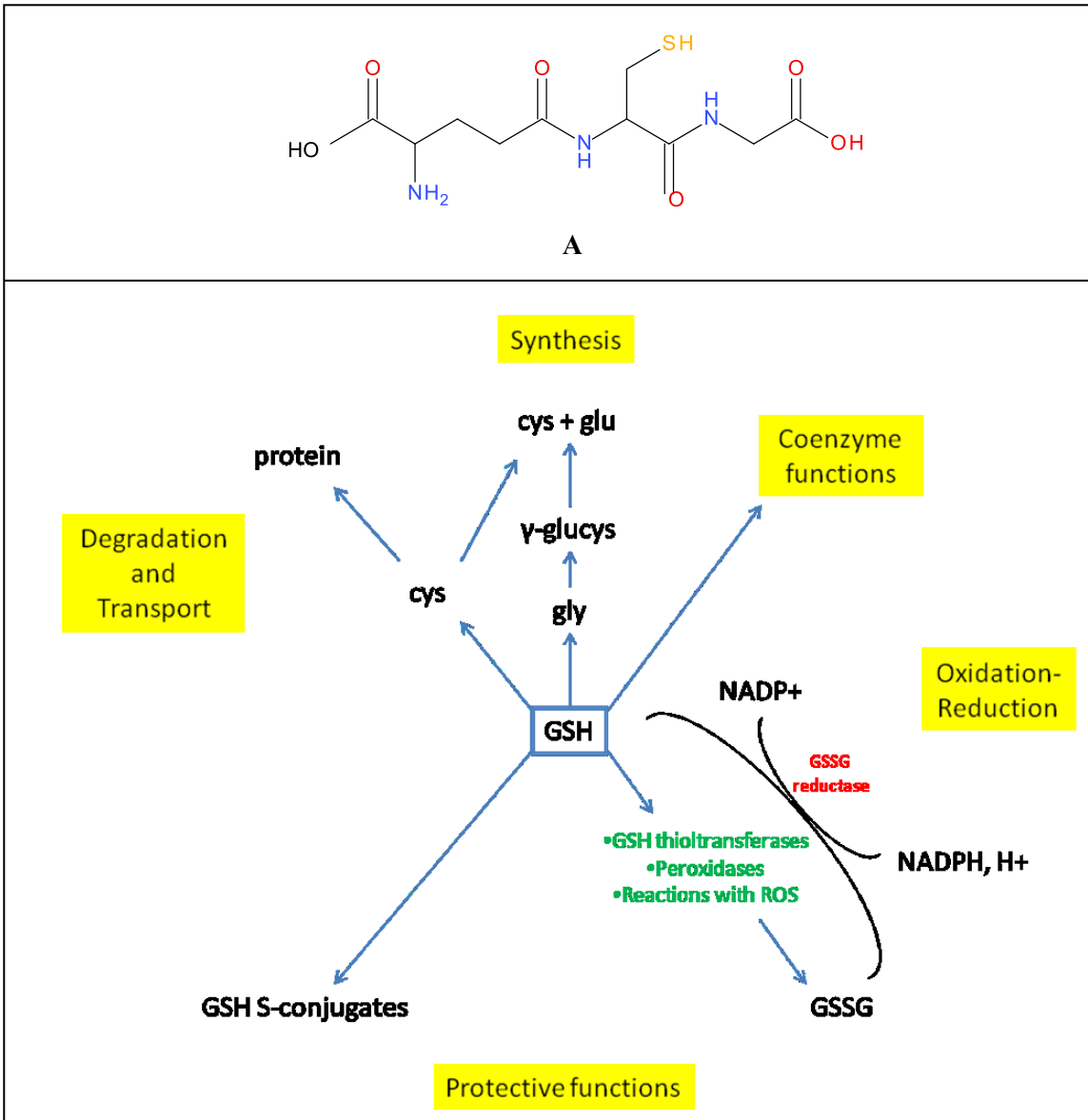

Figure 1.3: (A) The structure of GSH. (B) The metabolism and important cellular functions of GSH.

Glutathione is involved in several important intracellular functions including conjugation of reactive species, participation as a coenzyme, and amino acid transport. It is also involved in metabolism and the maintenance of thiol moieties of proteins and low molecular weight compounds (adapted from figure 2: Anderson M.E. 1998).

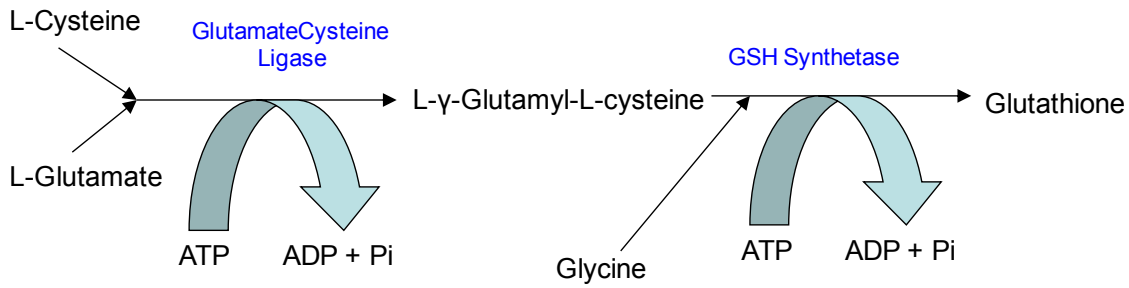

Figure 1.4: De novo GSH synthesis.

GSH is synthesised intracellularly from L-cysteine, L-glutamate and glycine. Synthesis proceeds via a two-step pathway catalysed by GCL and GSH synthetase. Inhibition of GCL by BSO (see section 1.2) results in depletion of intracellular GSH levels (adapted from Balendiran G.K. *et al.* 2004).

1.2 Buthionine Sulphoximine (BSO)

L-buthionine-S-sulphoximine (BSO) is a synthetic amino acid which depletes cellular GSH. It does this by inhibiting GCL, the enzyme which catalyses the reaction of L-glutamate with MgATP to form the enzyme bound intermediate γ-glutamylphosphate, which subsequently reacts with L-cysteine (see Figure 1.4). The phosphorylation of BSO is catalysed by GCL as BSO has a structure similar to that of the GCL cysteine adduct (Griffith O.W. *et al.* 1979). Phosphorylated BSO product binds the GCL active site tightly but non-covalently and inhibits the reaction with L-cysteine until the product dissociates. The inhibition of GCL by BSO occurs at low concentrations and is rapid, specific and potent (Griffith O.W. 1982).

Synthesis and catabolism of GSH occurs via the γ-glutamyl cycle which involves a series of enzymatic and membrane transport steps (Meister A. and Anderson M.E. 1983). The synthesis of GSH occurs intracellularly however the breakdown of GSH, involving the transfer of the γ-glutamyl moiety to acceptors including amino acids and water, is catalysed by γ-glutamyl transpeptidase which is on the external surface of the cell membrane. GSH is therefore transported across cell membranes by members of the multidrug resistance-associated protein (MRP/CFTR or ABCC) family of ATP-binding cassette (ABC) proteins and members of the organic anion transporting polypeptide (OATP) family of transporters (Ballatori N. *et al.* 2005). Most GSH is exported from cells, therefore administration of BSO and the consequent inhibition of GSH synthesis results in GSH depletion (Anderson M.E. 1998). In wild type and m*Ogg1*$^{-/-}$ null mouse embryonic fibroblast (MEF) cells BSO has been shown to deplete GSH from the cytoplasm in a concentration dependent manner, and deplete GSH from the nucleus and

mitochondria at concentrations ≥100 μM (Green R.M. *et al.* 2006). Green *et al.* (2006) additionally showed that significant depletion of cytoplasmic GSH, achieved at BSO concentrations ≥100 μM, also resulted in a significant increase in ROS formation, levels of lipid peroxidation and formation of oxidative DNA modifications. The use of BSO thus serves as an important experimental tool for depletion of GSH and subsequent induction of oxidative stress conditions within cells.

1.3 DNA damage

Antioxidants have limited capacity and can become overwhelmed giving rise to cellular oxidative stress. The accumulation of oxidative damage has been shown to contribute to the process of normal cellular ageing (Gruber J. *et al.* 2008) and various degenerative diseases including cancer (Matés J.M. *et al.* 2008), Alzheimer's disease (Lovell M.A. and Markesbery W.R. 2007), Parkinson's disease (Chinta S.J. and Anderson J.K. 2008) and cardiovascular disease (Ames B.N. *et al.* 1993).

Reactive oxygen species are genotoxic and able to induce a range of DNA lesions including abasic sites, DNA strand breaks, and base oxidations which, if replicated, can lead to apoptosis or mutation (Demple B. and Harrison L. 1994). The major reactions of the hydroxyl radical with DNA are additions to the π bonds of DNA bases or hydrogen abstractions from the deoxyribose sugar units (Breen A.P. and Murphy J.A. 1995). Hydrogen abstraction is possible from all carbon atoms of the sugar although the most common is C4 as its C-H bond is weakest and most sterically exposed in B-DNA (Pardo L. *et al.* 1991). Following hydrogen abstraction, in the absence of repair, the sugar-phosphate backbone is cleaved generating a single strand break (SSB) which can be mutagenic but often easily repaired due to the alternate intact DNA strand. However,

hydroxyl radical induced breaks generated near to each other on both strands generate a double strand break (DSB) which, if unrepaired, is much more likely to cause cell death due to the permanent damage to genetic information (Breen A.P. and Murphy J.A. 1995).

The reaction of hydroxyl radicals with DNA bases is favoured over deoxyribose sugar units and primarily occurs at C5 and C6 of the pyrimidines (von Sonntag C. 1987) and at C4 and C8 of the purines (Steenken S. 1989). Due to its low oxidation potential guanine is the most easily and most commonly oxidised base (Steenken S. and Jovanovic S.V. 1997) and the two most abundant products formed are 2,6-diamino-4-hydroxy-5-formamidopyrimidine (fapyG) and 7,8-dihydro-8-oxodeoxyguanine (8-oxo dG). Subsequent oxidation results in the formation of spiroiminodihydantoin and guanidinohydantoin (Figure 1.5) (Cadet J. *et al.* 2008):

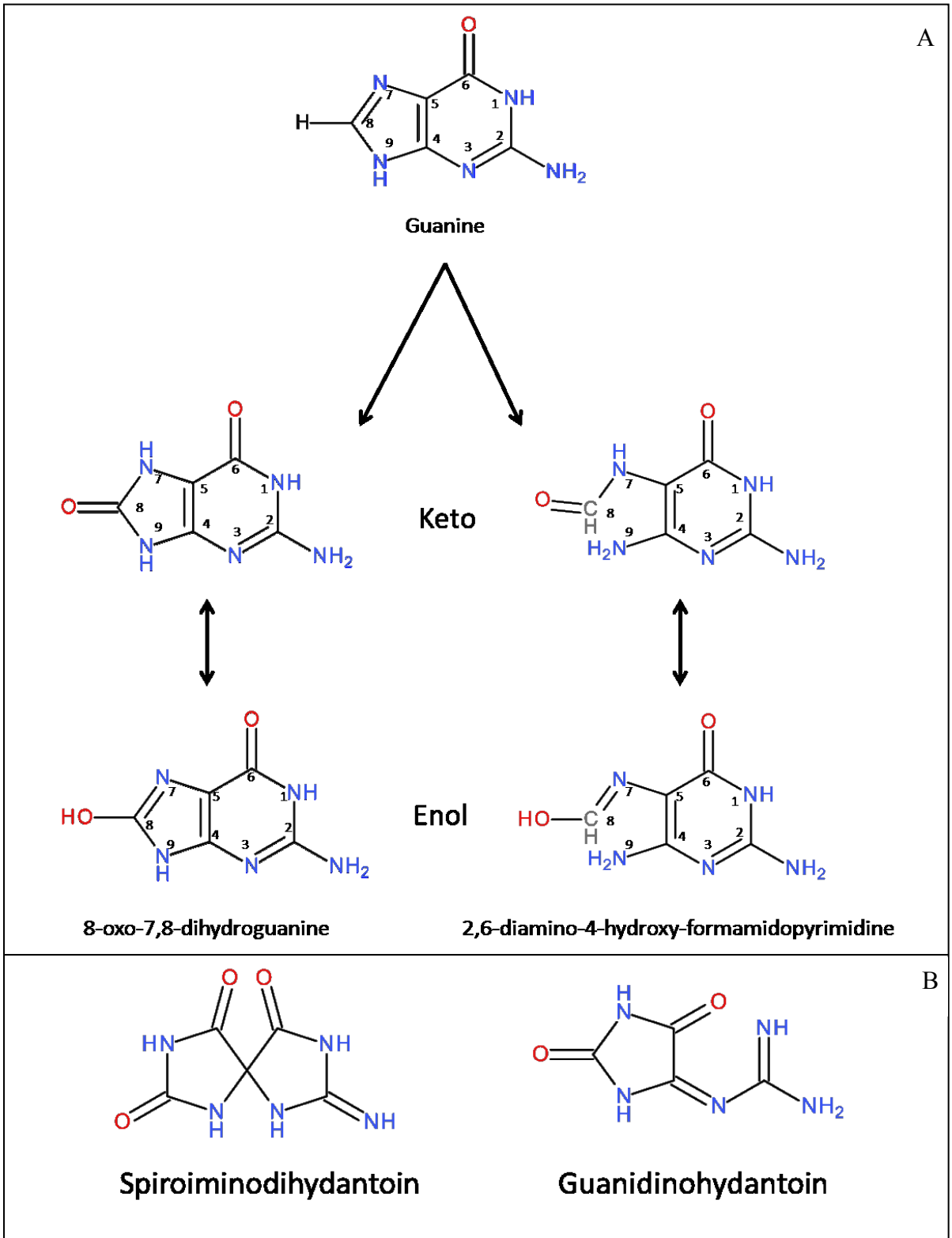

Figure 1.5: Oxidised forms of guanine.
The two most abundant products formed following oxidation of guanine are fapyG and 8-oxo dG (Figure 1.5A) with subsequent oxidation resulting in the formation of spiroiminodiydantoin and guanidinohydantoin (Figure 1.5B) (adapted from Malayappan B. *et al.* 2007).

1.3.1 8-oxo dG

First discovered in 1984 (Kasai H. and Nishimura S. 1984), 8-oxo dG is a pre-mutagenic lesion initially thought capable of mispairing with any base (Kuchino Y. *et al.* 1987). However, experiments with *Escherichia Coli (E. coli)* (Wood M.L. *et al.* 1990), *in vitro* and *in vivo* studies (Cheng K.C. *et al.* 1992; Moriya M. *et al.* 1991; Shibutani S. *et al.* 1991) and studies in mammalian systems (Klein J.C. *et al.* 1992) subsequently found that 8-oxo dG causes predominantly G:C→T:A transversions; among the most predominant somatic mutations in lung, breast, ovarian, gastric and colorectal cancers (Greenman C. *et al.* 2007) and frequent in the mutational spectrum of the tumour suppressor gene *p53* (Hollstein M. *et al.* 1996).

This can be explained by the conformation adopted by 8-oxo dG around the *N*-glycosidic bond. At physiological pH, 8-oxo dG exists in the keto form and in the normal *anti* conformation around the *N*-glycosidic bond 8-oxo dG forms a conventional Watson-Crick pair with cytosine (Figure 1.6A) (Wang D. *et al.* 1998). However, in the *syn* conformation it forms a Hoogsteen mispair with adenine (Figure 1.6B) (Bjørås M. *et al.* 2002). The capability for 8-oxo dG to cause G:C→T:A transversions is therefore attributed to its ability to form this base pair. It has also been found that 8-oxo dG can mispair with guanine (Figure 1.6C) (Thiviyanathan V. *et al.* 2003), introducing the possibility that 8-oxo dG also has the ability to induce G→C transversions.

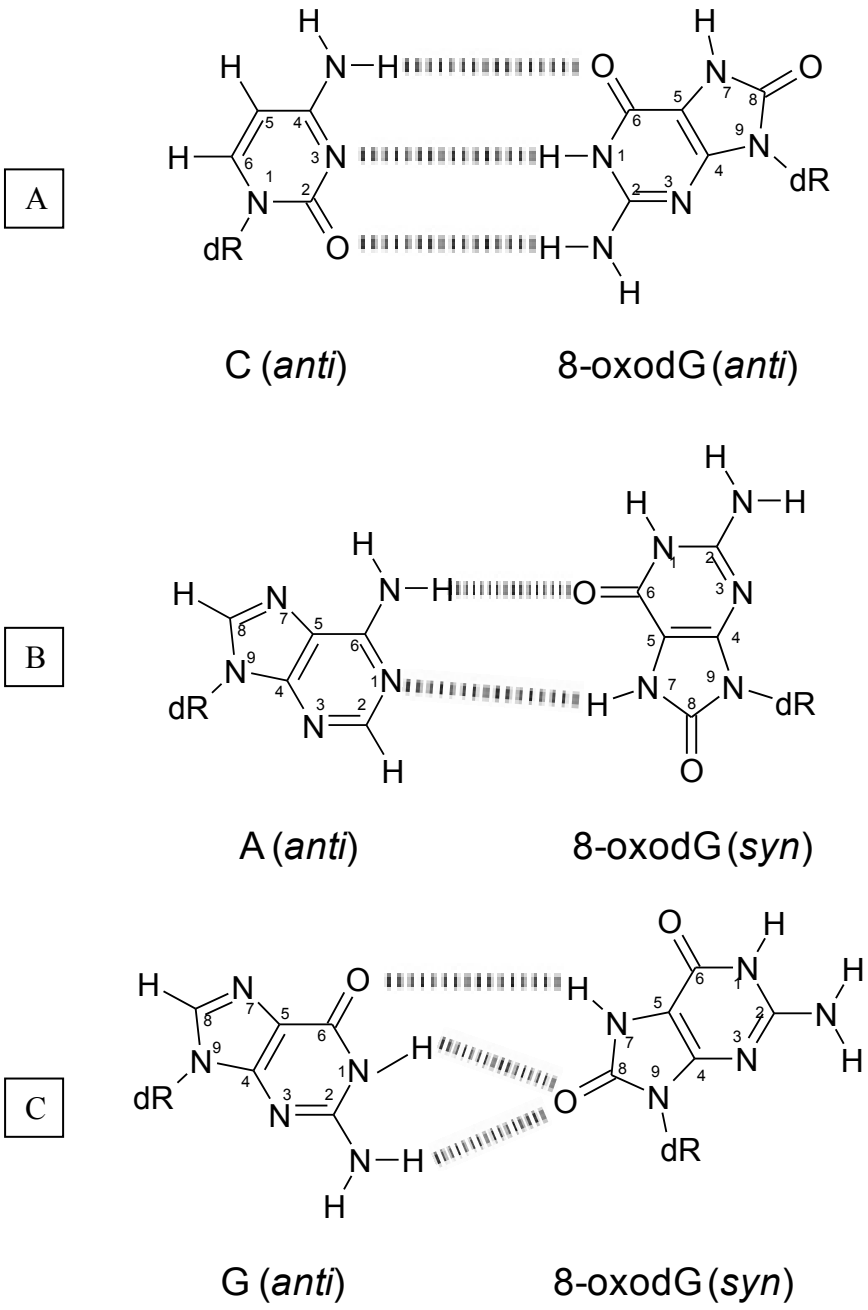

Figure 1.6: The conformation adopted by 8-oxo dG around the N-glycosidic bond. 8-oxo dG in the anti conformation around the N-glycosidic bond forming a stable Watson-Crick pair with cytosine (A). 8-oxo dG in the syn conformation around the N-glycosidic bond forming a stable Hoogsteen mispair with adenine (B). 8-oxo dG in the syn conformation around the N-glycosidic bond forming a mispair with guanine (C). (Figure 2: Klungland A. and Bjelland S. 2007).

1.3.2 8-oxo dG and disease

In normal tissues it is estimated that the steady-state rate of formation of 8-oxo dG lesions is approximately 10^3 per cell per day (van Loon B. *et al.* 2010). Although described as weakly mutagenic, with mutation frequencies of 2.5 – 4.8% in mammalian cells (Moriya M. 1993), the ability of 8-oxo dG to cause mutation combined with its abundance means it is considered to play an important role in carcinogenesis *in vivo* (Cooke M.S. *et al.* 2006; Floyd R.A. 1990). The process of carcinogenesis is complex and involves multiple stages at which oxidative stress can play a role (Guyton K.Z. and Kensler T.W. 1993). One of the crucial events is the mutation of DNA resulting in the activation of proto-oncogenes such as H-ras and/or inactivation of tumour suppressor genes such as p53. Numerous studies, reviewed by Evans *et al.* (2004), show increased levels of 8-oxo dG in tumour tissue (Gackowski D. *et al.* 2002; Inoue M. *et al.* 1998; Matsui A. *et al.* 2000; Romano G. *et al.* 2000; Sentürker S. *et al.* 1997) and urine from cancer patients (Erhola M. *et al.* 1997; Tagesson C. *et al.* 1995; Yamamoto T. *et al.* 1996). However, it is important to note that it is currently unclear whether this increase is causative of, or an effect of tumours.

As well as causing DNA mutations 8-oxo dG lesions can result in epigenetic alterations which modulate gene expression and may also contribute to carcinogenesis. Methylation patterns of adjacent cytosine residues can be altered by 8-oxo dG which may inhibit the initial binding of methylation binding proteins (Valinluck V. *et al.* 2004). This interferes with subsequent steps in the chromatin condensation cascade resulting in potentially heritable epigenetic alterations. Binding of transcription factors can also be modulated

by the presence of 8-oxo dG in promoter elements resulting in alterations in gene expression (Ghosh R. and Mitchell D.L. 1999; Ramon O. *et al.* 1999).

The involvement of 8-oxo dG has also been implicated in non-cancerous pathological conditions including Parkinson's disease (Alam Z.I. *et al.* 1997; Zhang K. *et al.* 1999), Alzheimer's disease (Lovell M.A. *et al.* 1999; Mecocci P. *et al.* 1998), Huntington's disease (Browne S.E. *et al.* 1997), multiple sclerosis (Vladimirova O. *et al.* 1998) and atherosclerosis (Martinet W. *et al.* 2001).

1.4 DNA damage repair

Throughout the lifetime of a cell nuclear DNA is subject to many different types of damage with the potential to cause cell death or mutagenesis. In order to reduce the occurrence of such events several mechanisms exist for repair including simple direct repair of the damaged base, for example dealkylation, and more complicated recombination repair or excision repair systems. Base excision repair (BER), nucleotide excision repair (NER), and mismatch repair (MMR) are all involved in the repair of damage to a single DNA strand and are able to use the undamaged strand as a repair template. In contrast, the repair of DSB, where both DNA strands are damaged, is complicated by the inavailability of a complementary strand and as a result has the potential to be error prone. Although less well characterised, mitochondrial DNA repair pathways also exist. Mitochondrial DNA is particularly susceptible to oxidative lesions hence mitochondria possess proficient BER (de Souza-Pinto N.C. *et al.* 2008). Mitochondria also possess MMR activity which is distinctive from nuclear MMR, as well as recombination repair for DSB (reviewed by Liu P. and Demple B. 2010).

This thesis focuses on oxidative DNA damage therefore the major DNA repair pathways will be briefly reviewed prior to a more in depth discussion of oxidative damage repair, with emphasis on nuclear DNA repair.

1.4.1 DNA double strand break repair

Endogenous factors including metabolites and ROS as well as exogenous factors such as ionising radiation and xenobiotics have the potential to induce DSB (Weterings E. and Chen D.J. 2008). They can also arise during DNA replication, as a replication fork passing through a template containing a SSB leads to conversion of this into a DSB on a sister chromatid. Additionally, DSB are generated during DNA replication and as intermediates during other essential cellular processes including meiosis and the assembly of mature immunoglobulin and T-cell receptor genes (van Gent D.C. *et al.* 2001). Cleavage of both DNA strands in close proximity causes the DNA molecule to break apart leading to chromosome breaks. The chromosome fragments produced can then be unequally distributed to daughter cells or translocated to other parts of the genome. The deleterious effects of such translocation events include cell death, or the inactivation of tumour suppressor genes or activation of oncogenes for example Philadelphia-chromosome translocation and chronic myeloid leukaemia (Borgaonkar D.S. 1973) hence DSB are potentially carcinogenic (Weterings E. and Chen D.J. 2008).

There are two major pathways involved in mammalian repair of DSB: homologous recombination (HR) (Figure 1.7) and non-homologous end joining (NHEJ) (Figure 1.8). Error-free HR begins with the processing of DNA ends mediated by the Mre11/Rad50/Nbs1 (MRN) complex creating single-strand overhangs. Rad51, Rad52 and replication protein A (RPA) associate with these overhands, search for the

homologous duplex DNA and generate a joint molecule between the damaged and undamaged strands. The template guides DNA synthesis and resolution of the two strands to complete DSB repair (Weterings E. and Chen D.J. 2008). The mechanism of NHEJ involves the processing and joining of broken non-compatible DNA ends, without the use of a template. Consequently more error-prone, NHEJ begins with the recognition of the DSB by the Ku70/80, DNA-PKcs complex which brings the ends of the broken DNA molecule together. Non-compatible ends are then processed prior to end-to-end ligation by the DNA ligase IV-XRCC4 complex (Phillips E.R. and McKinnon P.J. 2007; Weterings E. and Chen D.J. 2008).

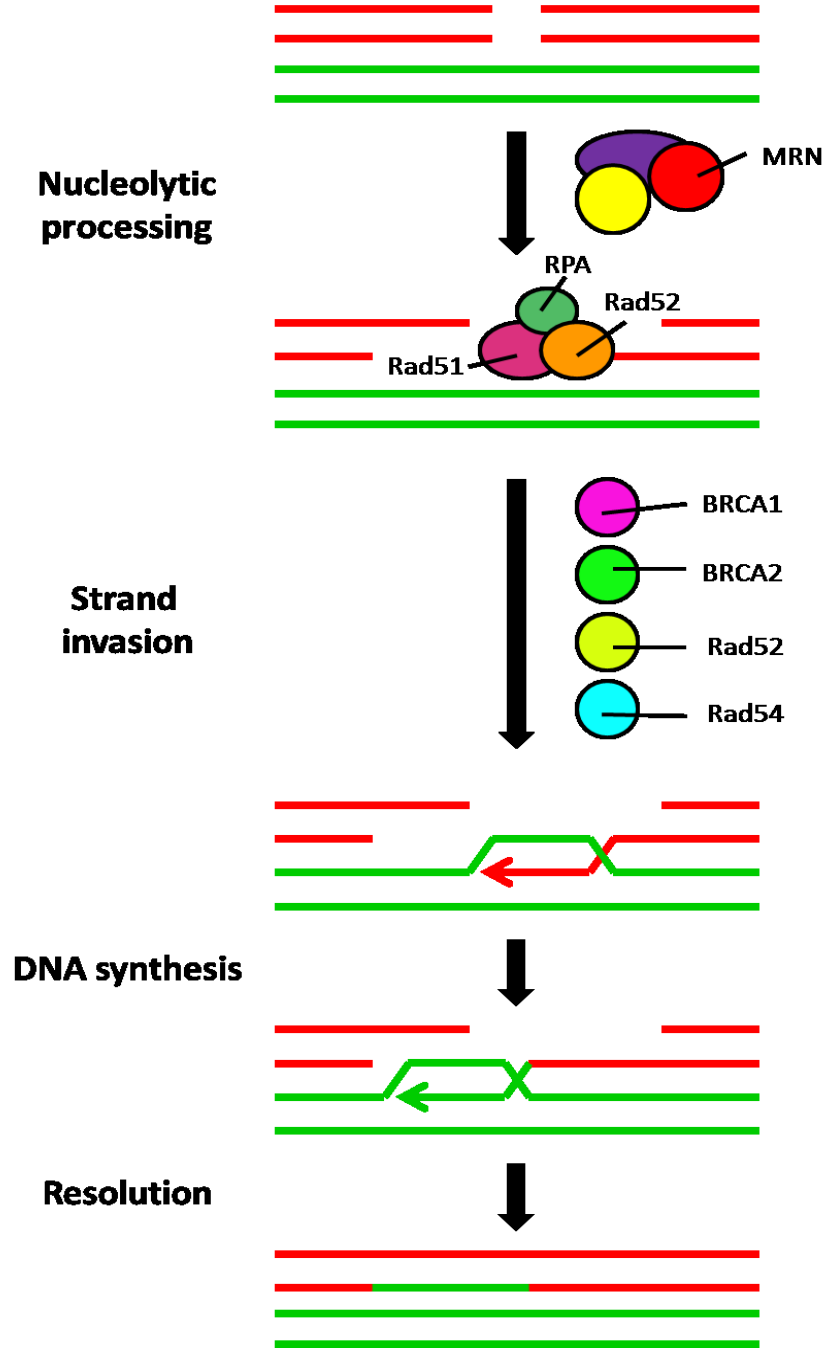

Figure 1.7: Homologous recombination.

HR begins with the nucleolytic processing of DNA ends mediated by the Mre11/Rad50/Nbs1 (MRN) complex creating single-strand overhands. Rad51, Rad52 and replication protein A (RPA) associate with these overhangs, search for the homologous duplex DNA and generate a joint molecule between the damaged and undamaged strands. The template guides DNA synthesis and resolution of the two strands which completes DSB repair (Weterings E. and Chen D.J. 2008).

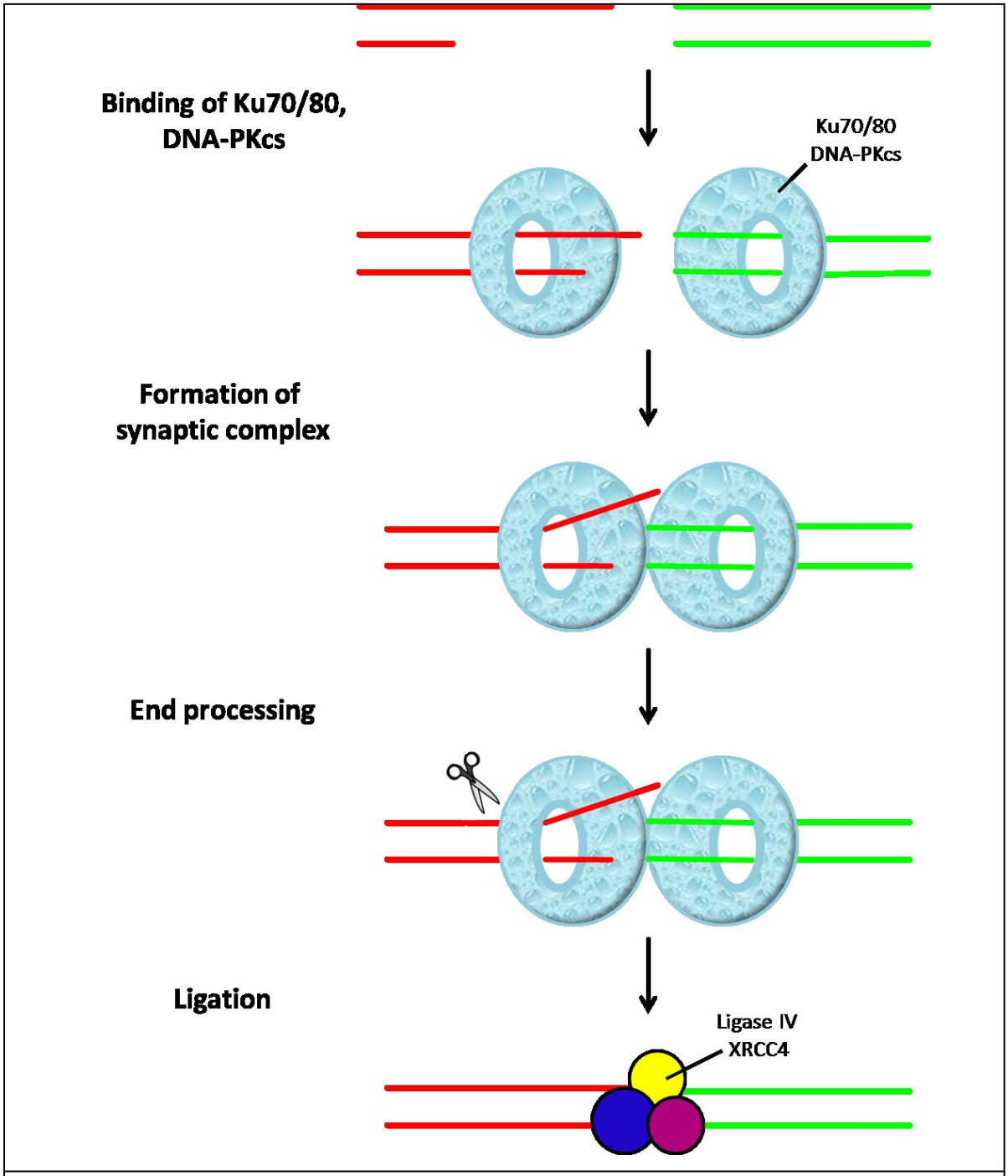

Figure 1.8: Non-homologous end joining.
NHEJ begins with the recognition of the DSB by the Ku70/80, DNA-PKcs complex which brings the ends of the broken DNA molecule together. Non-compatible ends are then processed prior to end-to-end ligation by the DNA ligase IV-XRCC4 complex (Weterings E. and Chen D.J. 2008).

1.4.2 Mismatch repair

The mismatch repair (MMR) system is responsible for the repair of DNA mismatches arising through spontaneous and induced base deamination, oxidation and methylation, as well as through replication errors (Modrich P. and Lahue R. 1996; Umar A. and Kunkel T.A. 1996). The DNA lesion that initiates the MMR machinery is recognised by either the MutSα complex (MSH2 and MSH6) or the MutSβ complex (MSH2 and MSH3), depending on its form. Following complex binding, MMR discriminates between the parental and newly synthesised DNA strand by an unclear mechanism that is thought to involve either the 'molecular switch model' or the 'hydrolysis-driven translocation model' reviewed by Christmann M. *et al.* (2003). Following strand discrimination a complex between MutSα and MutLα is formed which results in excision of the DNA strand containing the mispaired base by exonuclease I and resynthesis by Polδ (Figure 1.9).

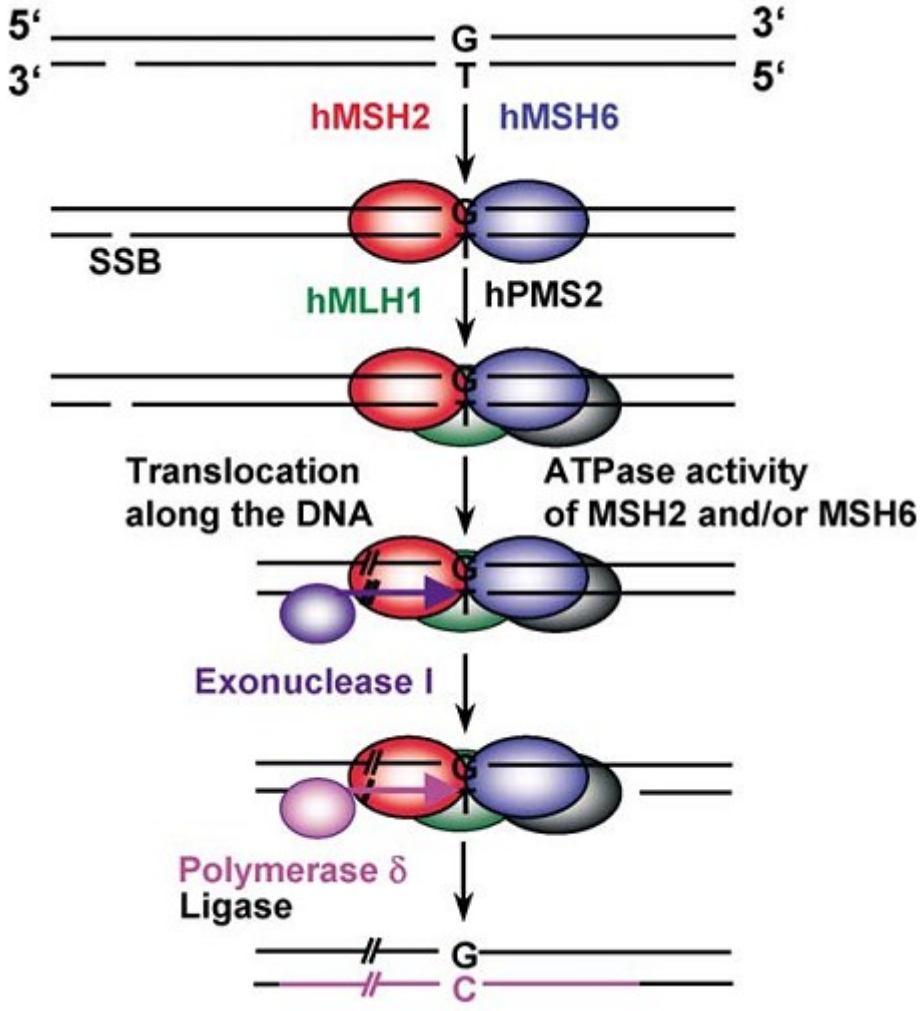

Figure 1.9: Mismatch repair.
Recognition of the DNA lesion by the MutSα complex (MSH2 and MSH6) leads to strand discrimination, resulting in the formation of a complex composed of MutSα and MutLα. Excision is then performed by ExoI and repair synthesis completed by polymerase δ and DNA ligase I (Figure 2, Christmann M. *et al.* 2003).

1.4.3 Excision repair

The process of excision repair was discovered in 1964 when two independent groups observed that following UV light exposure, bacteria such as *E.coli* excise small pieces of DNA from their genome (Boyce R.P. and Howard-Flanders P. 1964; Setlow R.B. and Carrier W.L. 1964). The distinction between NER and BER was made following the discovery by Lindahl (1974) that uracil is excised from DNA as a free base, in contrast to pyrimidine dimers which are excised as small oligonucleotide fragments.

1.4.4 Nucleotide excision repair

The NER pathway is often considered the most versatile and flexible known DNA repair pathway due to its ability to deal with a wide range of structurally unrelated DNA lesions and bulky DNA adducts such as PAHs (Costa R.M.A. *et al.* 2003). Lesions that distort the DNA helix, including UV light-induced cyclobutane pyrimidine dimers and 6-4 photoproducts, if unrepaired, interfere with base pairing and block DNA duplication and transcription. These lesions are repaired either by a mechanism which acts only on DNA lesions in transcribed strands and is coupled to active transcription; transcription coupled-NER (TC-NER), or by a mechanism that is able to repair DNA lesions throughout the genome; global genome-NER (GG-NER) (Fousteri M. and Mullenders L.H.F. 2008).

The damage recognition mechanisms of TC-NER and GG-NER are distinct but subsequent steps require identical core factors as the two pathways converge. Initiation of TC-NER begins following the generation of DNA lesions which block the elongating RNA polymerase II complex (RNAPIIo), which triggers the recruitment of TC-NER specific factors and NER proteins (Fousteri M. and Mullenders L.H.F. 2008). In

contrast, GG-NER begins with recognition of the DNA lesion by the UV-DDB and XPC-RAD23B protein complexes which recognise the distortion and have a binding affinity to damaged DNA (Shuck S.C. *et al.* 2008). Following recognition, TFIIH, XPA and RPA open the helix and verify the lesion prior to dual incision of the damaged strand by ERCC1-XPF and XPG endonucleases. A single strand gap is created which is filled by DNA polymerase δ, PCNA and RFC and then sealed by DNA ligase III-XRCC1 in non-dividing cells, or by DNA ligase III-XRCC1 plus DNA polymerase ε and DNA ligase I in dividing cells (Figure 1.10) (Fousteri M and Mullenders L.H.F. 2008). A detailed discussion of NER is beyond the scope of this thesis but is reviewed by Hoeijmakers J.H. (2001).

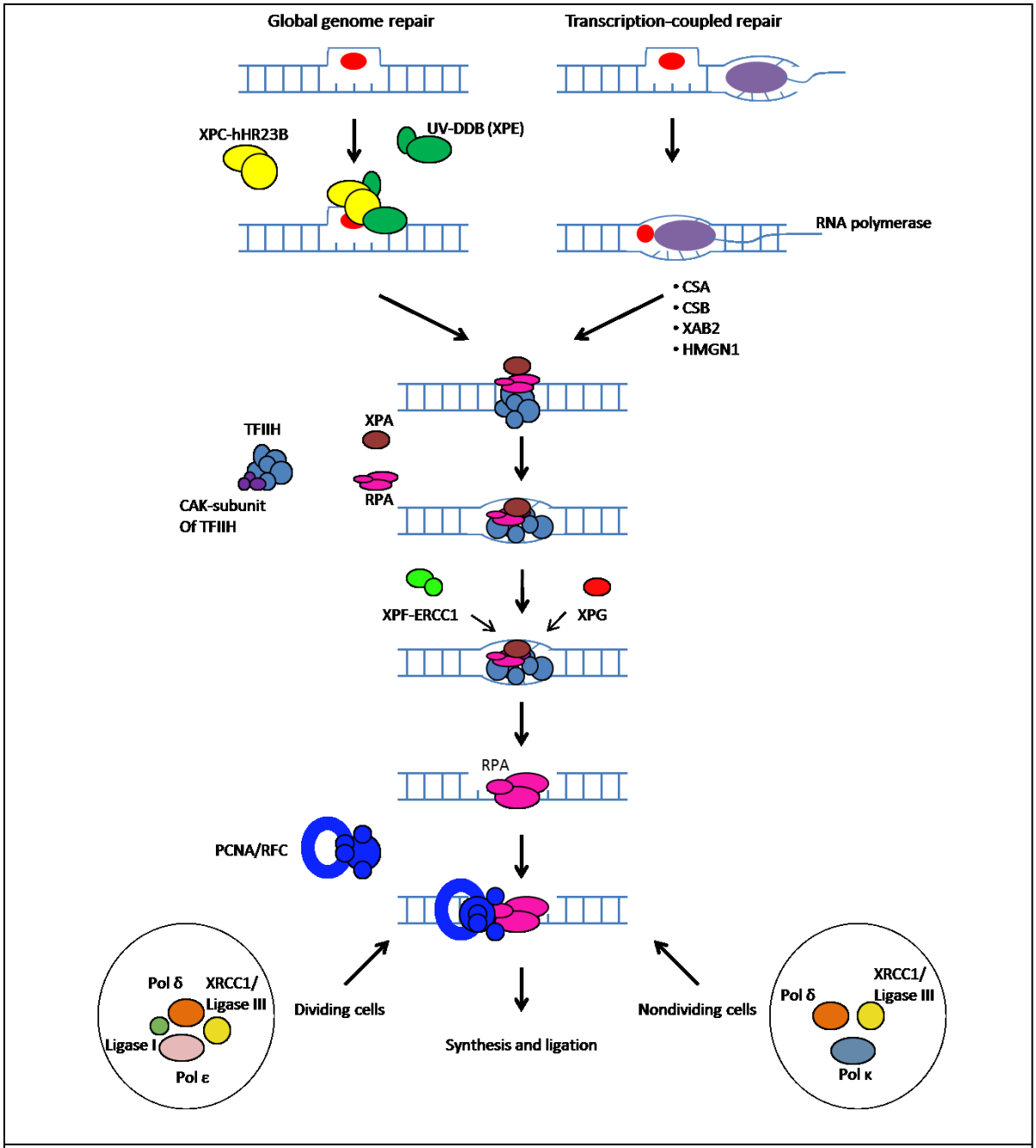

Figure 1.10: Nucleotide excision repair.
TC-NER begins with the binding of XPC-hHR23B and UV-DDB. GG-NER begins with the blockage of RNAPIIo. The two pathways then converge and TFIIH, XPA and RPA open the helix, prior to dual incision of the damaged strand by ERCC1-XPF and XPG endonucleases. DNA polymerase δ, PCNA and RFC fill the single strand gap prior to gap sealing by XRCC1/DNA ligase III or XRCC1/DNA ligase III plus DNA polymerase ε and DNA ligase I (adapted from figure 1, Fousteri M. and Mullenders L.H.F. 2008).

1.4.5 Base excision repair

Oxidative base lesions including 8-oxo dG and FapyG are repaired by the BER pathway. This highly conserved, versatile pathway is also responsible for the repair of products arising from spontaneous hydrolytic deamination e.g. uracil from deamination of cytosine (Krokan H.E. *et al.* 2002), alkylation e.g. 3-methyladenine (Sedgwick B. *et al.* 2007) and hydrolysis of the *N*-glycosidic bond producing an abasic site. Such modifications would lead to mispairs which could result in impaired genetic stability, hence their successful repair is necessary to maintain genomic integrity.

A lesion specific glycosylase (Table 1.2) initiates BER by excising the altered base, BER is then completed by either short-patch BER or long-patch BER; replacement of one, or two to thirteen bases respectively (Almeida K.H. and Sobol R.W. 2007). Following glycosylase excision of the damaged base an apurinic/apyridimic (AP) site is created within the DNA backbone. This is recognised and cleaved either by an AP-endonuclease, generating a 3′OH and a 5′-deoxyribose phosphate (dRP), or by the intrinsic AP-lyase activity of bi-functional DNA glycosylases. The latter generates 3′ blocking phosphoribose or phosphate termini together with 5′ phosphates which are subsequently cleaved by the 3′ phosphodiesterase activity of APE1. The resulting dRP is released by the intrinsic 5′-dRPase activity of β-polymerase (short-patch BER) or the 5′-flap endonuclease Fen1 (long-patch BER). The nucleotide gap is filled by β-polymerase and finally sealed by either DNA ligase I or a complex of DNA ligase III and XRCC1 (Figure 1.11) (Boiteux S. and Guillet M. 2004; Hazra T.K. *et al.* 2007).

Table 1.2: DNA glycosylases in human cell nuclei.

(Adapted from Table 1: Lindahl T. and Wood R.D. 1999 and Table 1: Hegde M.L. *et al.* 2008).

Enzyme	Altered base removal from DNA
UNG	U and 5-hydroxyuracil
TDG	U or T opposite G, ethenocytosine
hSMUG1	U (preferentially from single-stranded DNA)
MBD4	U or T opposite G at CpG sequences
hOGG1	8-oxoG opposite C, formamido-pyrimidine
MYH	A opposite 8-oxoG
hNTH1	Thymine glycol, cytosine glycol, dihydrouracil, formamido-pyrimidine
MPG	3-MeA, ethenoadenine, hypoxanthine
NEIL1	Fapy-A, 5-hydroxyuracil, thymine glycol
NEIL2	Hydantoin, 5-hydroxyuracil
NEIL3	FapyA, FapyG, 5-hydroxyuracil

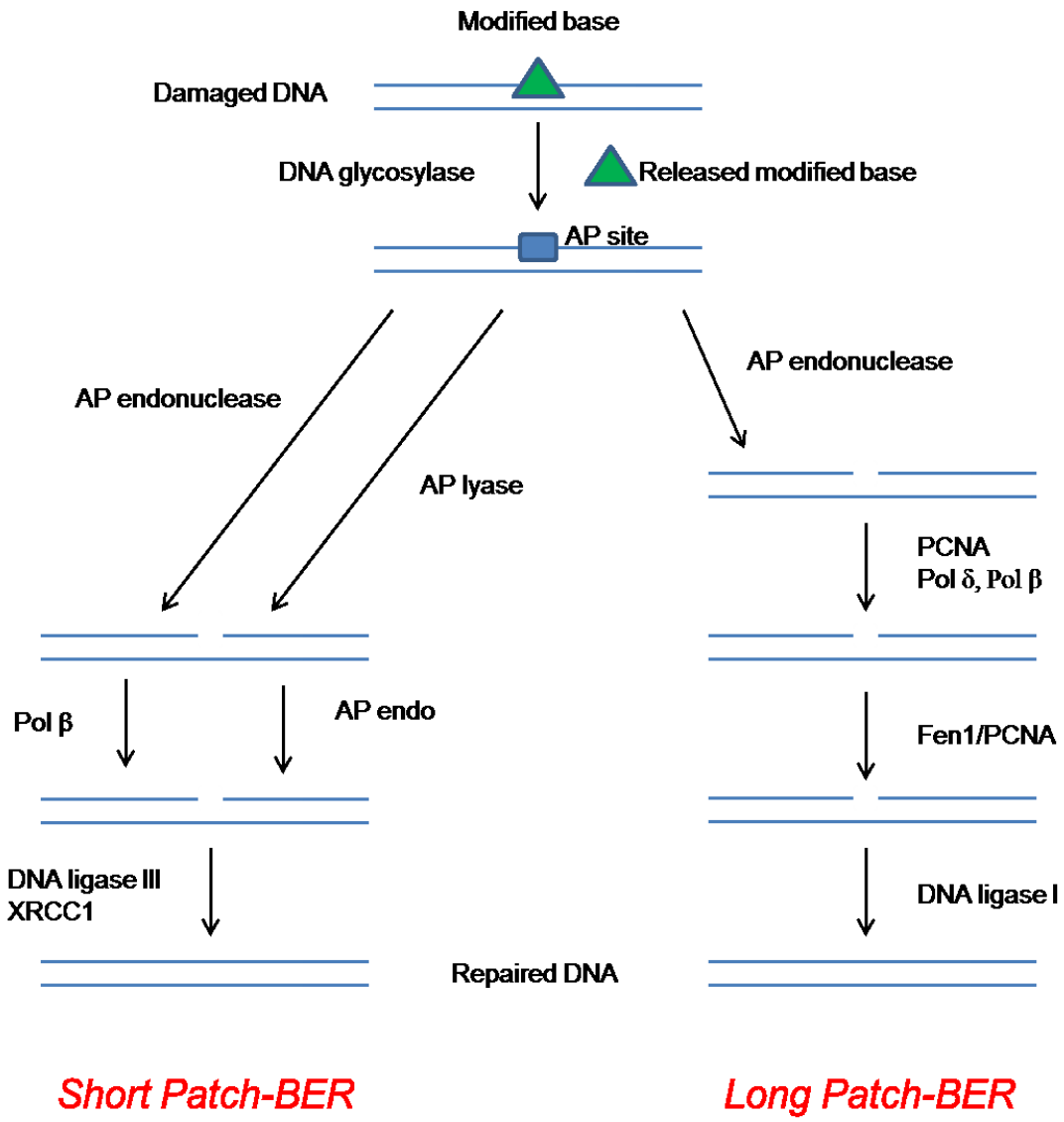

Figure 1.11: Monofunctional Base Excision Repair.
Initiation of BER involves recognition and glycosylase-mediated excision of the altered base, which generates an AP site in the DNA backbone. This is cleaved either by the intrinsic lyase activity of the glycosylase or by APE1 and then processed by either polymerase β, prior to religation by the XRCC1/DNA ligase III complex (short patch pathway), or PCNA, polymerase δ, polymerase β and Fen1 prior to religation by DNA ligase I (long patch pathway) (Scheme 1: Evans M.D. *et al.* 2004).

Glycosylase enzymes are highly conserved, do not require cofactors, and have broad substrate specificities, although most have a preference for either purine or pyrimidine derivatives. Their initial recognition of the deformed DNA helix results in their binding to the minor groove and subsequently flipping the lesion base out of the DNA major groove (Hegde M.L. *et al.* 2008). A number of base-specific DNA glycosylases have been identified in mammals including 8-oxodeoxyguanine DNA glycosylase 1 (OGG1), the endonuclease III homolog NTH1, and the *E.coli* Nth-like NEILs (NEIL1, NEIL2 and NEIL3). Base lesions are excised by OGG1 and NTH1 only from double-stranded DNA whereas the NEILs prefer single-stranded DNA and are thought to be involved in repair of oxidised bases during transcription and DNA replication (Dou H. *et al.* 2003). Specific to pyrimidines, NTH1 recognises a wide range of oxidised pyrimidine derivatives including thymine glycol, 5-hydroxycytosine, dihydrouracil, urea and the ring-opened structure of 1, N^6-ethenoadenine (Speina E. *et al.* 2001). Similarly, the NEILs prefer oxidised pyrimidines, NEIL1 has high affinity for ring-opened purines and thymine glycol whereas NEIL2 prefers cytosine-derived lesions including 5-hydroxyuracil and 5-hydroxycytosine. No glycosylase activity has been detected for NEIL3 (Hazra T.K. *et al.* 2007). The NEILs are also able to recognise and remove spiroiminodihydantoin and guanidinohydantoin (Hailer M.K. *et al.* 2005).

1.5 Base excision repair and the role of OGG1

In *E.coli.* defence against the mutagenic effects of 8-oxo dG is via an enzymatic pathway called the "guanine oxide (GO) system" (Figure 1.12). This includes an 8-oxodeoxyG-DNA glycosylase; formamidopyrimidine DNA glycosylase (Fpg/MutM), a mismatch-specific adenine-DNA glycosylase; MutY, and an 8-oxodGTPase; MutT (Zharkov D.O.

and Rosenquist T.A. 2002). An analogous BER system exists in mammalian cells, involving MTH1 (human MutT orthologue), MutYH (human MutY homologue) and the human Fpg functional analogue OGG1 with both N-glycosylase and β-lyase activities. *In vitro,* the OGG1 enzyme recognises oxoG:C pairs and catalyses both the removal of 8-oxo dG and cleavage of the DNA backbone (Bruner S.D. et al 2000). Although capable of bifunctional activity, recent evidence suggests that the AP lyase activity of human OGG1 is not essential and that the enzyme may operate as a monofunctional glycosylase *in vivo* (Dalhus B. *et al.* 2011).

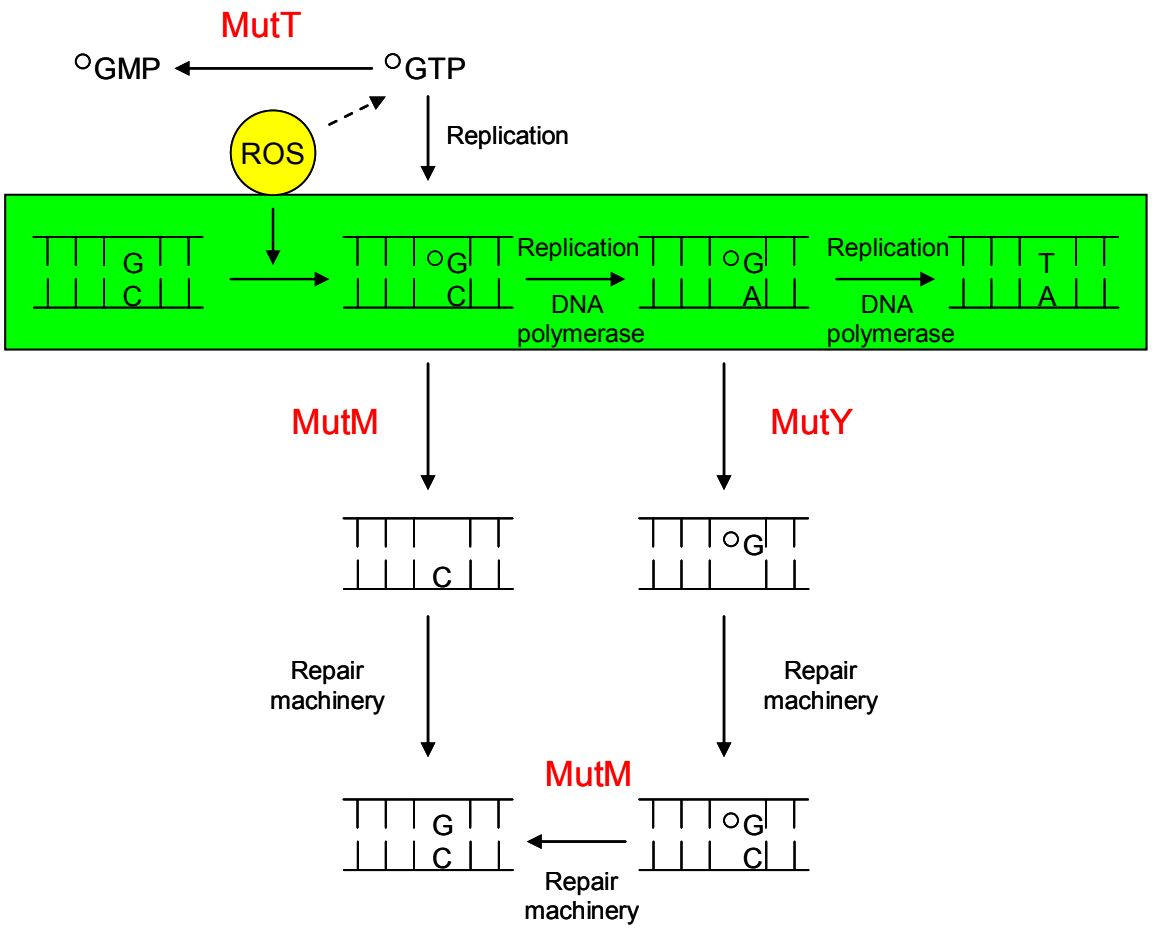

Figure 1.12: The *E.coli* "GO system".

°GTP/GMP = 8-oxo-dGTP/GMP. An 8-oxo dGTPase, MutT, is responsible for removing oxidatively damaged GTP from the nucleotide pool, thereby preventing its incorporation into nascent DNA. A DNA glycosylase, MutM, excises oxidised guanine from 8-oxoG:C pairs and a second DNA glycosylase, MutY, excises any adenine residues that have been misincorporated opposite 8-oxo dG (Adapted from Figure 1: Sampson J.R. *et al.* 2005).

The human *OGG1* (h*OGG1*) gene, isolated by several groups in 1997 (Arai K. *et al.* 1997; Aburatani H. *et al.* 1997; Lu R. *et al.* 1997; Rosenquist T.A. *et al.* 1997) has been mapped to chromosome 3p26.2 (Arai K. *et al.* 1997) and found to undergo alternative splicing (Aburatani H. *et al.* 1997). Two main forms of messenger RNAs are expressed with open reading frames which code for proteins of 345 and 424 amino acids; the 39kDa α-hOGG1 and 47kDa β-hOGG1 respectively. The first 316 amino acids are identical and contain a mitochondrial targeting sequence however the carboxy-terminal ends differ extensively, with that of α-hOGG1 containing a nuclear localisation sequence absent in β-hOGG1 (Boiteux S. and Radicella J.P. 2000). This PAKRRK sequence at position 333 in the C-terminus of α-hOGG1 targets it to the nucleus (Takao M. *et al.* 1998) and suppresses the mitochondrial targeting sequence which targets β-hOGG1 to the mitochondria (Nishioka K. *et al.* 1999). It was hypothesised that β-hOGG1 was responsible for mitochondrial BER however it has more recently been shown to lack glycoslyase activity (Hashiguchi K. *et al.* 2004), so it is thought instead that α-hOGG1 is responsible for mitochondrial DNA repair. Although interesting, β-hOGG1 is not the subject of investigation in this project which instead concentrates solely on α-hOGG1, which from this point forward will be referred to simply as hOGG1.

The structural features of hOGG1 include a helix-hairpin-helix followed by a Gly/Pro rich loop and a conserved aspartic acid (HhH-GDP motif) which is common to repair proteins with DNA glycosylase/AP-lyase activities. When DNA bound, hOGG1 is strongly bound to the DNA backbone of the 8-oxo dG containing strand but is not in contact with the backbone of the complementary strand. The 8-oxo dG residue extrudes from the helix and is inserted deeply into an extrahelical active-site cleft on the enzyme

(Bruner S.D. *et al.* 2000). The catalytic mechanism of the DNA glycosylase activity of hOGG1 involves an attack on C-1′ of the 8-oxo dG-containing nucleotide by the ε-NH_2 group of Lys249, with Asp268 playing a catalytic role, eliminating the 8-oxo dG base. The hOGG1 protein then forms a covalent enzyme-DNA intermediate which undergoes rearrangements and forms a ring-opened Schiff base resulting in scission of the sugar-phosphate backbone on the 3′-side of the AP site (Figure 1.13A).

In order to effectively initiate DNA repair hOGG1 must specifically excise 8-oxo dG but not guanine, and must only remove 8-oxo dG when bound to cytosine, not adenine. The structure of DNA bound hOGG1 compared with the structure of free hOGG1 revealed that conformational changes take place to allow recognition of 8-oxo dG:C to be coupled with catalysis. Asp268 and Asn149 are hydrogen bonded to the protonated N^{ε} of the catalytic Lys249 in the free enzyme. These hydrogen bonds serve as independent 'trigger-locks' with one linked to recognition of cytosine and the other to recognition of 8-oxo dG. The removal of both of these bonds is necessary in order to 'prime' the catalytic lysine for nucleophilic attack of the *N*-glycosidic bond (Bjørås M. *et al.* 2002).

As previously stated, recent evidence suggests that OGG1 operates as a monofunctional glycosylase *in vivo* and the mechanism suggested for this process involves the reaction proceeding through an oxocarbenium ion which is stabilised by Asp268. This oxocarbenium ion subsequently reacts with a water nucleophile to form an AP site which is incised by an AP endonuclease (Dalhus B. *et al.* 2011; Figure 1.13B).

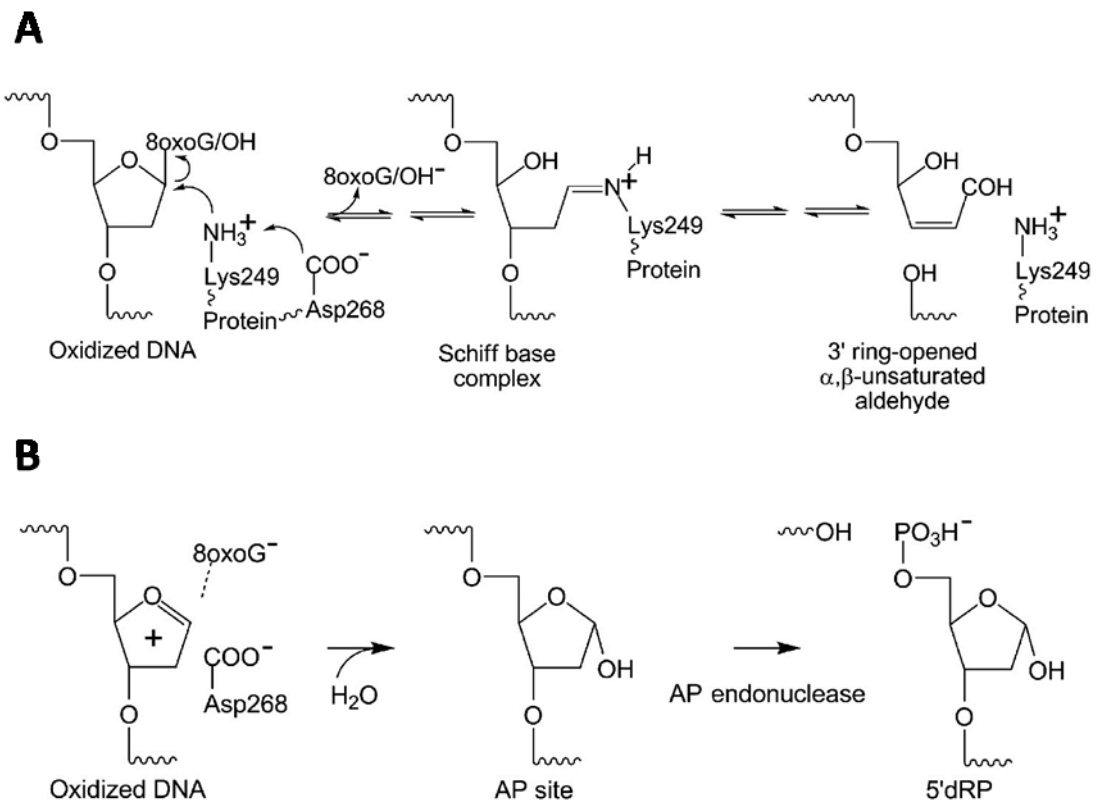

Figure 1.13: Reaction mechanisms of OGG1.

A: The acknowledged bifunctional mechanism of hOGG1 where Lys249 forms a covalent Schiff base intermediate and Asp268 activates Lys249. Hydrolysis with water results in beta-elimination and 3' strand incision.

B: Putative monofunctional mechanism of hOGG1 where the reaction proceeds via formation of an oxocarbenium ion charge-stabilised by Asp268. Subsequent reaction with a water nucleophile forms an AP site which is incised by AP endonuclease (Dalhus B. *et al.* 2011, Figure 1).

1.5.1 hOGG1 localisation, post-translational modification and protein interactions

It has been demonstrated that during S-phase of the cell cycle hOGG1 is localised within the nucleoli, and that this nuclear localisation is linked to transcription (Luna L. *et al.* 2005). During interphase wild-type α-hOGG1 has been shown to be associated with soluble chromatin and the nuclear matrix, and during mitosis with condensed chromatin (Dantzer F. *et al.* 2002).

Dantzer *et al.* (2002) performed western blot analysis of HeLa cells expressing enhanced green fluorescence protein (EGFP)-hOGG1 fusion protein fractions using an anti-phosphoserine antibody to examine hOGG1 phosphorylation *in vivo*. This showed that hOGG1 associated with the nuclear matrix is unphosphorylated but hOGG1 associated with chromatin is phosphorylated on a serine residue. Immunoprecipitation experiments revealed that *in vitro,* nuclear matrix-associated hOGG1 is phosphorylated by protein kinase C (PKC) and that chromatin-associated hOGG1 interacts with PKC but is not phosphorylated by it. No alteration in enzymatic function occurred following phosphorylation leading to the suggestion that the phosphorylation event may be involved in protein re-localisation rather than modulation of enzymatic function (Dantzer F. *et al.* 2002).

The first evidence that a post-translational modification of OGG1 could affect its activity was provided by Hu *et al.* (2005) who found that *in vitro* and *in vivo* OGG1 interacts with and is phosphorylated by Cdk4 and c-Abl kinases. The serine/threonine phosphorylation by Cdk4 was shown to stimulate 8-oxo dG incision and the authors suggest that this is due to phosphorylation mediated enhancement of the coupling

between the base release and strand cleavage steps. In contrast, tyrosine phosphorylation by c-Abl did not affect 8-oxo dG incision activity and its potential regulatory role remains to be determined (Hu J. *et al.* 2005).

As well as being phosphorylated OGG1 has also been shown to be acetylated by p300/CBP both *in vitro* and *in vivo* (Bhakat K.K. *et al.* 2006). The p300 and closely related CBP proteins are transcriptional co-activators with intrinsic histone acetylasetransferase activity which acetylate lysine residues in histones and a variety of transcription factors (Bannister A.J. and Kouzarides T 1996; Eckner R. *et al.* 1994; Goodman R.H. and Smolik S. 2000; Ogryzko V.V. *et al.* 1996). They have been shown to play a role in DNA replication and BER as they acetylate Fen1 and interact with proliferating cell nuclear antigen (PCNA) to stimulate Fen1 (Hasan S. *et al.* 2001; Hasan S. *et al.* 2001.2). Bhakat *et al.* (2006) show that acetylation of OGG1, predominantly at Lys338 and Lys341, increases its repair activity. They propose that this is due to the weakening of the interaction of OGG1 with the AP product; the rate limiting dissociation step in 8-oxo dG excision, resulting in OGG1 displacement by APE1. In agreement with this proposal, it has been shown that APE1 enhances OGG1 activity (Hill J.W. *et al.* 2001; Vidal A.E. *et al.* 2001.1) and that this is partly by active displacement of the protein from the nascent AP site (Sidorenko V.S. *et al.* 2007; Sidorenko V.S. *et al.* 2008). By a mechanism similar to that of APE1, NEIL1 has also been shown to stimulate OGG1 turnover and enhance its activity (Mokkapati S.K. *et al.* 2004). It is suggested that in some human cells NEIL1 serves as a backup to APE1 for stimulation of 8-oxo dG repair. OGG1 also interacts with p53, and *in vitro* p53 enhances 8-oxo dG excision by increasing OGG1 and APE1 activity (Achanta G. and Huang P. 2004).

The process of BER is highly coordinated and involves multiple interactions between the proteins of the pathway. One of the proteins which plays a central role in the coordination of BER is XRCC1 which interacts with all enzymes involved in BER downstream of the DNA glycosylase (Caldecott K.W. *et al.* 1994; Caldecott K.W. *et al.* 1996; Kubota Y. *et al.* 1996; Vidal A.E. *et al.* 2001.2) and serves as a scaffold to stimulate or stabilise the components. It has been shown to physically interact with and enhance the base excision activity of hOGG1 by stimulating the formation of the hOGG1 Schiff-base DNA intermediate (Marsin S. *et al.* 2003). The homologous recombination protein RAD52 has also been shown to physically interact with OGG1 (de Souza-Pinto N.C. *et al.* 2009). This interaction leads to stimulation of OGG1 incision activity, by increasing turnover, but to inhibition of RAD52 activity suggesting cooperation between the two proteins to repair oxidative damage. Interaction and cooperation between DNA repair proteins results in tight regulation of BER and could enhance cellular resistance to oxidative stress.

Proteins involved in other cellular pathways may also play a role in BER. One example of this is the human ribosomal protein S3 (hS3) which, as well as being a ribosomal subunit and involved in protein translation, has high binding affinity for 8-oxo dG (Hegde V. *et al.* 2004.1). Although hS3 shares 80% sequence homology with drosophila S3 (dS3) which has the ability to remove 8-oxo dG (Yacoub A. *et al.* 1996), hS3 has no glycosylase activity hence its function has been the subject of investigation. It was shown to interact with hOGG1 and APE1 and increase the activity of OGG1, but only when the purified proteins were mixed prior to exposure to DNA (Hegde V. *et al.* 2004.2). Further analysis showed that incubation of OGG1 with a hS3 mutant that

cannot bind 8-oxo dG resulted in OGG1 activity stimulation whereas incubation with wild-type hS3 resulted in OGG1 activity inhibition (Hegde V. *et al.* 2006). In support of the finding that hS3 can create an obstacle to OGG1 BER, a decrease in hS3 expression was shown to result in the increased survival of human embryonic kidney (HEK293) cells exposed to DNA damaging agents (Hegde V. *et al.* 2007). Following exposure to DNA damaging agents hS3 was found to translocate from the cytoplasm to the nucleus and co-localise with foci of nuclear 8-oxo dG DNA lesions *in vitro* (Yadavilli S. *et al.* 2007) and *in vivo* (Hegde V. *et al.* 2009). The significance of these findings and their relationship with OGG1 and other components of BER remain to be elucidated, but this serves as an example of cross-talk between BER proteins and proteins involved in alternate cellular pathways.

1.6 hOGG1 polymorphisms

The chromosomal location of the h*OGG1* gene is frequently subject to monoallelic deletion and loss of heterozygosity in various cancers (Audebert M. *et al.* 2000; Lu R. *et al.* 1997). Compared with wild-type mice m*Ogg1*$^{-/-}$ null (KO) mice have greater levels of 8-oxo dG, show increased G:C→T:A transversion mutations in their DNA, and are predisposed to lung adenocarcinoma and adenoma (Klungland A. *et al.* 1999; Minowa O. *et al.* 2000; Sakumi K. *et al.* 2003). OGG1 is therefore a candidate tumour suppressor gene, resulting in interest in identifying mutations in the h*OGG1* gene and investigating their effects on levels and activity of the protein (Kohno T. *et al.* 1998).

Although several polymorphisms of the h*OGG1* gene have been identified, the single nucleotide polymorphism (SNP) at codon 326 has received most attention because it is relatively common, and evidence suggests it is a possible genetic factor for increased

cancer risk (Yamane A. *et al.* 2004). This missense polymorphism, present at an allele frequency of 0.33 – 0.45 in Asian populations and 0.22 – 0.27 in Caucasian populations, occurs due to a C→G substitution at position 1245 in exon 7 and results in the exchange of a redox-sensitive cysteine for a serine in codon 326 (Weiss J.M. *et al.* 2005).

As large numbers of individuals possess this polymorphic variant, there is considerable justification for the numerous studies investigating both its links with cancers and its activity, to determine to what effect such individuals may be predisposed to certain cancers. The approaches used to evaluate the effect of the Ser326Cys (S326C) polymorphism have involved functional and epidemiologic studies, measuring the repair ability of Cys326-hOGG1 and the association between Cys326-hOGG1 and the risk of cancer respectively (Weiss J.M. *et al.* 2005).

1.6.1 Ser326Cys and cancer

Individuals homozygous for the S326C h*OGG1* allele have been shown to have an increased risk of cancers including nasopharyngeal, oesophageal, gallbladder and lung (Cho E.Y. *et al*. 2003; Kohno T. *et al.* 2006; Le Marchand L.L. *et al.* 2002; Park J. *et al.* 2004; Srivastava A. *et al.* 2009; Sugimura H. *et al.* 1999; Xing D.Y. *et al.* 2001) but to have no increased risk of breast, prostate or biliary tract cancers (Agalliu I. *et al.* 2010; Cai Q. *et al.* 2006; Choi J.Y. *et al.* 2003; Huang W.Y. *et al.* 2008; Sterpone S. *et al.* 2010; Vogel U. *et al.* 2003). Surprisingly, a recent meta-analysis of all available studies revealed that the S326C hOGG1 allele may play a protective role in the carcinogenesis of breast cancer in European women (Yuan W. *et al.* 2010). No association between colon cancer susceptibility and the S326C polymorphism was observed (Kim J.I. *et al.* 2003), even though the theoretical basis for such a link appeared strong as there is a clear role

for defects in DNA mismatch repair in colon carcinogenesis (de Wind N. *el al.* 1999). Although Kim *et al.* (2003) found no overall association between S326C and colon carcinogenesis, when external factors were evaluated they saw an increased risk associated with the CC genotype among smokers and those who ate more meat. As both exposures are known to increase DNA damage, this suggests that any functional deficit only becomes significant in stressed cells and only when two polymorphic alleles are present.

In support of this, no association between orolaryngeal or head and neck squamous cell carcinoma cancer risk and hOGG1 genotype was observed in individuals who abstained from drinking and smoking (Elahi A. *et al.* 2002; Zhang Z. *et al.* 2004). However, increased risk of orolaryngeal cancer was observed for CC homozygous individuals who smoked or drank alcohol (Elahi A. *et al.* 2002) and an association between the CC genotype and head and neck squamous cell carcinoma was observed in heavy cigarette smokers (Hashimoto T. *et al.* 2006). Interestingly, when factors including alcohol and meat consumption were evaluated an association between the S326C allele and increased risk of stomach cancer was observed (Takezaki T. *et al.* 2002). Furthermore, the risk of progression of *Helicobacter pylori*-induced gastric cancer, associated with oxygen free radical formation, was increased in CC homozygotes and this risk was significantly elevated in smokers (Li W.Q. *et al.* 2009). This evidence suggests that any defect of the Cys326-hOGG1 protein becomes more apparent in oxidising conditions.

Although the evidence for an association between S326C and increased cancer risk is conflicting, cancer is a complex disease and individual SNPs are too simple to be reliable predictors of cancer (Paz-Elizur T. *et al.* 2008). Current evidence supports the theory

that the impact of the S326C polymorphism is enhanced under conditions of oxidative stress. It is important however to consider that DNA repair genes do not act in isolation and that although the impact of a single SNP in a single repair gene such as OGG1 may not result in a clear association with carcinogenesis (Vineis P. *et al.* 2009), genetic variants in multiple repair pathways may have an additive effect in cancer risk (Klinchid J. *et al.* 2009; Sterpone S. *et al.* 2010). It is also important to consider the ethnic origins of the population studied when interpreting epidemiological data. This has been highlighted by a meta-analysis of published studies evaluating the association between S326C and lung cancer which found no association between SC or CC and susceptibility to lung cancer when analysing all subjects, but when analysed by ethnicity a significant association was observed in Asian but not Caucasian subjects (Li H. *et al.* 2008). As well as proposing the possibility of such an observation reflecting environmental exposures, the authors hypothesise that Asians may have a higher susceptibility to lung cancer due to having a higher frequency of the variant Cys326 allele.

1.6.2 Ser326Cys and hOGG1 functional activity

A range of functional assays have been used to assess the ability of polymorphic OGG1 protein to repair 8-oxo dG lesions. Indirect repair capacity has been assessed by measuring levels of 8-oxo dG in cultured cells, leukocytes, tumorous and non-tumorous tissues using high pressure liquid chromatography with electrochemical detection (HPLC-ECD) or flow cytometry, or by 8-oxo dG cleavage and lyase assays (Blons H. *et al.* 1999; Bravard A. *et al.* 2009; Chen S.K. *et al.* 2003; Kondo S. *et al.* 2000; Yamane A. *et al.* 2004). Direct repair capacity has been assessed using bacterial complementation assays (Kohno T. *et al.* 1998) and gas chromatography/isotope-dilution mass

spectrometry (GC/IDMS) quantification of 8-oxo dG following γ-irradiaton exposure and subsequent incubation with purified wild-type and polymorphic OGG1 proteins (Audebert M. *et al* 2000; Dherin C. *et al.* 1999).

The bacterial complementation assay involves transfection of mutant rifampicin resistant (Rif^R) *E.coli* strains, which are defective in the repair of 8-oxo dG and therefore have an extremely high G:C→T:A mutation rate, with plasmids that code for Ser326-h*OGG1* and Cys326-h*OGG1* protein products. Rifampicin resistance is then used as a marker for mutagenesis (Kohno T. *et al.* 1998). Using this approach Kohno *et al.* (1998) observed a significantly reduced repair activity of Cys326-hOGG1 compared with wild type, however other studies using the same approach found no reduction in repair capacity (Blons H. *et al.* 1999; Dherin C. *et al.* 1999), although the use of cleavage assays by Dherin *et al.* (1999) gave K_{cat}/K_m values for excision that were 1.6-fold lower for the GST-Cys326-α-hOGG1 protein. Using an *in vivo* version of the complementation system Yamane *et al.* (2004) compared the mutation suppressive ability between Ser326-OGG1 and Cys326-OGG1 under experimental conditions representing severe oxidative stress. They found that mutations caused by 8-oxo dG were more efficiently suppressed in Ser326-OGG1 transduced cells than in Cys326-OGG1 transduced cells. In agreement, Zielinska *et al.* (2011) observed a reduced repair rate of laser induced DNA damage by Cys326-hOGG1 compared with Ser326-hOGG1 in EGFP-OGG1-transfected cells.

Chen *et al.* (2003) obtained blood samples from healthy adult volunteers and using a cleavage assay, found a significant decrease in hOGG1 activity in those with the CC genotype and a minor decrease in those with the SC genotype. Bravard *et al.* (2009) also found, using homozygous Ser326- (SS) or Cys326-hOGG1 (CC) lymphoblastoid cell

lines, a two-fold lower basal glycosylase activity of CC cell extracts compared with SS cell extracts. Interestingly, significantly higher 8-oxo dG levels were detected by Tarng *et al.* (2001) in chronic haemodialysis patients with the CC genotype compared with those with the CS or SS genotype. This was not seen in healthy controls suggesting that any differences in repair ability between Ser326-hOGG1 and Cys326-hOGG1 only become apparent under conditions of stress. In contrast, no significant differences were observed using cleavage assays, measurement of 8-oxo dG levels or lyase assays by other groups (Hardie L.J. *et al.* 2000; Janssen K. *et al.* 2001; Kondo S. *et al.* 2000; Li D. *et al.* 2002; Park Y.J. *et al.* 2001; Shinmura K. *et al.* 1998).

The conventional comet assay and a modified version which uses fpg to specifically detect oxidised purines are recognised techniques for use in whole cells for the detection of DNA strand breaks and oxidative damage respectively (Figure 1.14) (Ostling O. and Johanson K.J. 1984; Duthie S.J. *et al.* 1996).

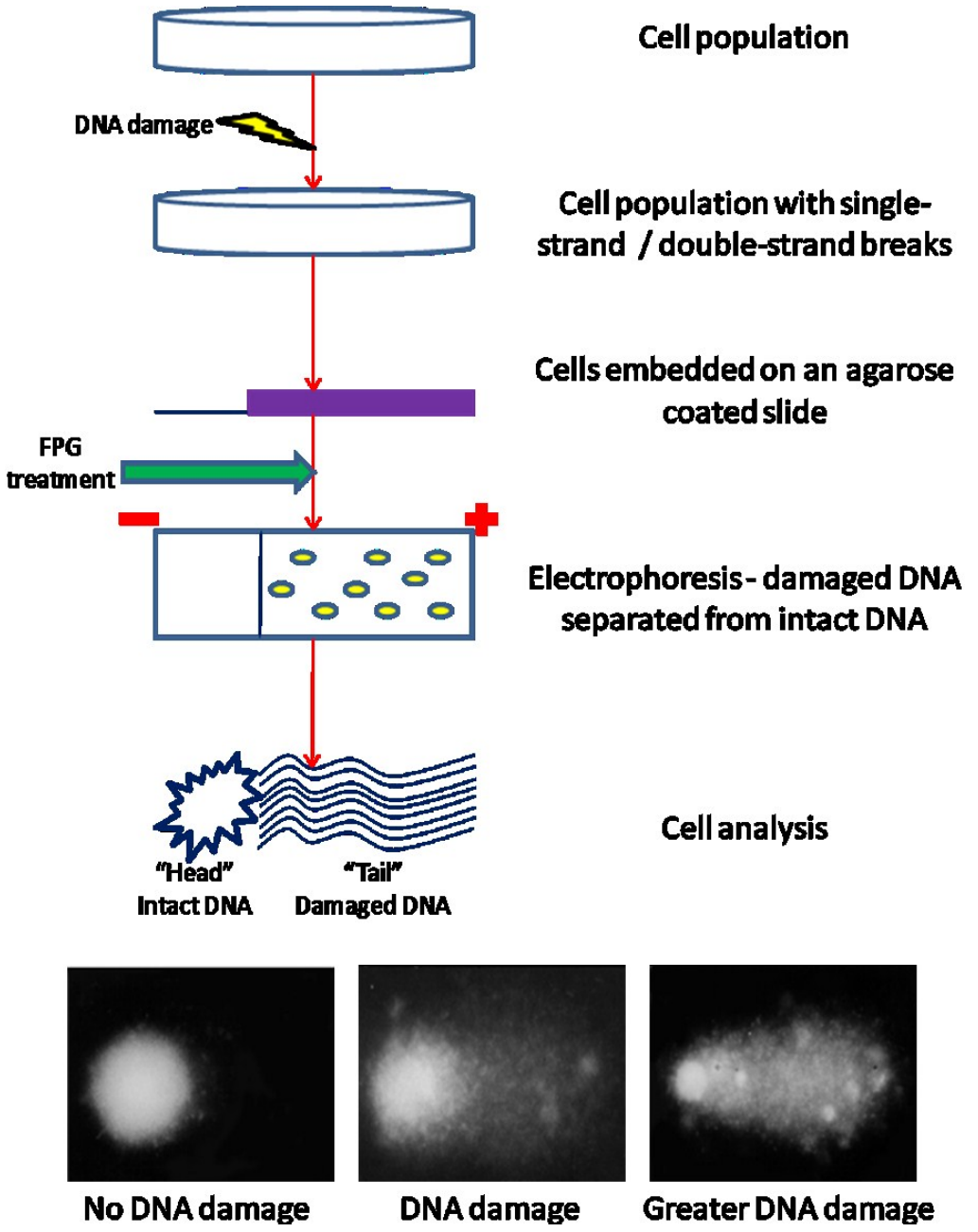

Figure 1.14: An overview of the conventional comet assay.
The FPG-modified comet assay involves all conventional steps plus treatment with FPG enzyme (green arrow).

Both versions have been used to assess wild-type and variant hOGG1 repair capacity in whole cells under conditions of oxidative stress (Lee A. *et al.* 2005; Smart D.J. *et al.* 2006). Lee *et al.* (2005) assessed the levels of DNA strand breaks in whole blood cells from healthy adult volunteers and found that treatment with sodium dichromate resulted in a significant increase in FPG-dependent oxidative DNA damage in CC individuals compared with SC and SS individuals. When divided on the basis of genotype, CC individuals also had a higher oxidative DNA damage: plasma antioxidant capacity ratio than SC or SS individuals. The difference in DNA damage was not observed without treatment suggesting that the Cys326-hOGG1 protein is deficient in repair ability only under conditions of cellular oxidative stress.

In support of this, Smart *et al.* (2006) found that the Cys326-hOGG1 variant had a significantly reduced repair capacity compared with Ser326-hOGG1 after treatment of mOGG1 $^{-/-}$ and mOGG1$^{+/+}$ MEF with the known 8-oxo dG inducing agents Ro19-8022 (+ light), sodium dichromate and potassium bromate. This reduced repair ability was observed at early time points, however longer periods allowed recovery of repair ability. The authors hypothesise that the substitution at position 326 results in either the loss of a regulatory serine phosphorylation site or the gain of a redox-sensitive cysteine residue, and that either or both of these events may be responsible for the reduced repair ability.

1.6.3 Ser326Cys and hOGG1 localisation

Luna *et al.* (2005) investigated the differences between wild-type and S326C mutant hOGG1 protein and found that the polymorphism affects association with the nuclear matrix and chromatin, localisation to the nucleoli during S-phase, and co-localisation to the condensed chromosomes during mitosis. As the S326C residue lies close to the

nuclear localisation signal (NLS) and within a predicted potential phosphorylation site, Luna *et al.* (2005) mimicked a hOGG1 protein phosphorylated at position 326 and demonstrated that S326C mutation-affected processes are mediated through phosphorylation of serine-326. They found that EGFP-hOGG1-Cys^{326} and EGFP-hOGG1-Ala^{326} proteins were excluded from the nucleoli, indicating that the presence of the serine residue is important for accurate hOGG1 localisation. Luna *et al.* (2005) suggest that phosphorylation of serine-326 is required for interaction with a protein during S-phase which will translocate hOGG1 to the nucleolus and to the condensed chromosomes during mitosis. They further suggest that the phosphorylation mediated subcellular localisation could explain any difference in mutational suppressive ability between the wild-type and S326C hOGG1 proteins.

1.6.4 Ser326Cys and hOGG1 dimer formation

The mechanistic basis underlying the observed reduced repair ability of Cys326-hOGG1 is currently unknown and as no crystal structures exist for OGG1 that include amino acids C-terminal to residue 325, no information can be gained from structural data. The loss of the Ser326 residue, a phosphorylation site important for the localisation of hOGG1, or the introduction of the redox-sensitive cysteine residue are two potential mechanisms, with recent evidence favouring the latter.

Evidence for redox state modulation of hOGG1 was presented by Bravard *et al.* (2006) who demonstrated that hOGG1 activity could be reversibly modulated by cadmium and inhibited using the cysteine-modifying agent *N*-ethylmaleimide or the thiol oxidant diamide. Bravard and colleagues then investigated the oxidation status effects on Ser326- and Cys326-hOGG1 in lymphoblastoid cell lines and observed reduced activity

of Cys326-hOGG1, which was recovered with the addition of reducing agents (Bravard *et al.* 2009). Incubation of cells with the cysteine oxidising agent diamide resulted in Cys326-hOGG1 cells showing only 20% of the activity of the untreated cells compared with 60% for the Ser326-hOGG1 cells.

A study using the electrophoretic mobility shift assay (EMSA) to investigate the DNA damage binding affinities of wild type and S326C mutant purified hOGG1 for 8-oxoguanine and abasic sites found that high molecular weight shifts consistent with a hOGG1 dimer were formed with Cys326-hOGG1 but not Ser326-hOGG1 (Hill J.W. and Evans M.K. 2006). Using an anti-FLAG western blot, Hill and Evans (2006) also observed this dimer in nuclear extracts from cells expressing both wild type and Cys326-hOGG1 following incubation with a chemical cross-linker. These findings suggest that Cys326-hOGG1 both exists as a dimer in solution and binds DNA as a dimer, and that Ser326-hOGG1 has the ability to form a dimer in the presence of cross-linker. In support of this, further analysis of the oxidation state of cysteine residues by Bravard *et al.* (2009) revealed that Cys326 can be easily involved in disulphide bond formation. Cross-linking experiments using GFP-hOGG1 and FLAG-hOGG1 fusion proteins expressed in HeLa cells showed that inactivation of Ser326-hOGG1 was associated with the oxidation of one cysteine residue whereas inactivation of Cys326-hOGG1 was associated with the oxidation of two. The authors conclude that this is likely to be the result of the formation of a disulphide bond and show that incubation with a reagent that specifically cross-links cysteines in close proximity resulted in an intramolecular cross-link such as that found with oxidative treatment.

The substitution of serine with cysteine at position 326 introduces a further redox active thiol group in addition to those of the eight other cysteine residues present in the hOGG1 protein. Thiol groups contain a labile proton which renders them subject to reversible oxidation to sulphenic acid in order to play a role in normal cellular redox regulation pathways. However, in the presence of oxidative stress and absence of GSH these thiol groups are susceptible to react readily with oxygen or other oxidants to produce sulphenic acid, sulphinic acid and irreversible sulfonic acid species. Sulphenic acid is relatively reactive and able to disulphide bond quickly with a nearby thiol (Biswas S. *et al.* 2006). The cys326 residue is present in a highly positively charged sequence environment (ADLRQ[ser326cys]RHAQ) and replaces the serine residue in a short disordered peptide segment at the C terminus of the hOGG1 protein (Bruner S.D. *et al.* 2000). Using C-terminally truncated hOGG1 proteins Hill and Evans (2006) found that the residues C-terminal to cys326 play roles in both the reduced activity and dimerisation of S326C hOGG1 and also showed that cys326 alone is sufficient to cause dimerisation and catalytic inhibition (Hill J.W. and Evans M.K. 2006).

1.7 Aims and objectives

The current study aimed to investigate the response of OGG1 to BSO-induced oxidative stress and further explore the hypothesis that a functional difference becomes more apparent between wild-type and variant hOGG1 under oxidative conditions.

Specifically:

- To investigate the effect of oxidative stress on OGG1 activity, gene and protein expression.
- To improve previous *in vitro* study models and generate mOGG1$^{-/-}$ MEF cells that stably express Ser326- and Cys326-hOGG1, then use these to investigate human OGG1 activity and gene expression following exposure to oxidative stress conditions.
- To investigate the mechanism underlying functional differences by studying Ser326- and Cys326-hOGG1 localisation and ability to form oligomeric complexes, and by assessing Ser326- and Cys326-hOGG1 retention within the insoluble nuclear fraction following oxidative stress.

Chapter 2 – Materials and Methods

2.1 Chemicals

All chemicals were obtained from Sigma-Aldrich (UK) unless otherwise statedMaterials and Methods

2.2 Cell culture

All cell culture work was conducted in sterile conditions in a class II tissue culture hood (Aura B4, Bio Air, Italy). All solutions used were obtained sterile or autoclaved as necessary before use.

2.2.1 Cell maintenance – mouse embryonic fibroblasts

Wild-type (WT) and m*Ogg1*$^{-/-}$ null (KO) mouse embryonic fibroblasts (MEFs) were a generous gift from T.Lindahl (Cancer Research U.K., Clare Hall Laboratories, South Mimms, Hertfordshire EN6 3LD, U.K.). Cells were cultured at 37°C in a humidified chamber (5% CO_2, 95% air; MCO-15AC, Sanyo, Japan) in 75cm^2 cell culture flasks (Greiner Bio-one, U.K.) containing Dulbecco's modified Eagle's medium (DMEM) supplemented with foetal bovine serum (10% v/v) (FBS), L-glutamine (2 mM), penicillin (100 U/ml) and streptomycin (100 µg/ml). Cells were seeded at approximately 1×10^5 cells per flask and passaged using a standard trypsin-EDTA (0.25%:0.02%) protocol when fully confluent.

2.2.2 Cell Cryopreservation

Resuspended trypsinised cells (10 ml) were transferred to sterile 15 ml centrifuge tubes (Falcon) and subjected to centrifugation at 1000 × g (Rotofix 32, Hettich Zentrifugen, Germany) at room temperature for 10 minutes. DMEM was removed and cells were resuspended in FBS (1 ml) containing cryoprotectant (10% v/v sterile dimethyl

sulphoxide DMSO). The suspension was transferred to 1 ml cryovials (Nalgene, U.S.A.) and stored at -80°C for 24 hours before transfer to liquid nitrogen.

2.3 Oxidative treatment

Cells seeded in 6, 12 or 24 well tissue culture plates (Greiner Bio-one, U.K.) were grown to confluence overnight. DMEM was removed and cells washed with phosphate buffered saline (PBS) (1 ml) prior to the addition of fresh DMEM containing L-buthionine-S-sulfoximine (BSO), or diamide at the appropriate concentrations. Cells were incubated at 37°C for 30 minutes (diamide) or 24 hours (BSO) as oxidative DNA modifications are formed following 24 hour BSO treatment (Green R.M. *et al.* 2006).

2.4 3-(4,5-Dimethyl-2-thiazolyl)-2,5-diphenyl-2H-tetrazolium bromide (MTT) reduction assay

The water soluble dye MTT is able to cross cell membranes and is reduced principally by mitochondrial succinate dehydrogenase yielding a blue insoluble formazan product. This product, when dissolved with DMSO, forms a purple solution allowing quantification of cell viability by measuring the absorbance of the solution between 500 and 570 nm (**Hussain et al 1993)**. The greater the absorbance reading, the greater the viable cell population.

2.4.1 Assay procedure

Cells were cultured in supplemented cell culture medium in 96 well cell culture plates (Greiner Bio-one, U.K.), grown to confluence and treated as described in 2.3. Cells were washed with PBS (200 µl) and fresh medium was added (200 µl) along with 3-(4,5-Dimethyl-2-thiazolyl)-2,5-diphenyl-2H-tetrazolium bromide (MTT) (0.5 mg/ml).

Following incubation at 37°C for 2 hours in a humidified chamber the medium was removed and DMSO was added (200 µl) to solubilise the blue formazan product. The plates were rocked gently for 2 hours at room temperature in the dark. The absorbance was determined at 570 nm using a Bio-Tek FL600 plate reader (Bio-Tek Instruments Inc. U.S.A.) against a DMSO blank.

2.5 Assay for the measurement of reactive oxygen species

This assay, based upon that described by Carini *et al.* (2000), uses the compound 2',7'-dichlorodihydrofluoroscein-diacetate (H_2DCF-DA) which is readily taken up by cells in culture and hydrolysed by intracellular esterases to yield 2',7'-dichlorodihydrofluoroscein (H_2DCF). H_2DCF is non-fluorescent but can be oxidised by intracellular reactive oxygen species (ROS) to yield the fluorophore DCF (Gomes A. *et al.* 2005; Bartosz G. 2006).

2.5.1 Assay procedure

Cells were seeded in 12 well tissue culture plates, grown to confluence and treated with BSO as described in section 2.3. Following treatment, DMEM was removed and cells were washed with PBS (1 ml). Fresh DMEM was added (3 ml) containing 10 µM H_2DCF-DA (Invitrogen U.K.) and cells were incubated for 45 minutes at 37°C prior to fluorescence analysis by flow cytometry (BD FACS Calibur) (emission wavelength 517 – 527 nm) as described previously (Hayden R.E. *et al.* 2009). Weasel software (Walter and Eliza hall institute of medical research, Australia) was used to generate histograms of the data and blank adjusted median values were used to compare fluorescence intensities.

2.6 Assay for the measurement of total reduced glutathione

Total reduced cellular glutathione (GSH) was measured using a fluorescence-based technique originally described by Cohn and Lyle (1966). This technique has been modified by Hissin and Hilf (1976) and Senft *et al.* (2000) and optimised for use in MEF cells by Green R.M. *et al.* (2006). The derivatising agent used in this assay; *o*-phthalaldehyde (OPA), is non-fluorescent until it reacts as a heterobifunctional reagent with a primary amine in the presence of a thiol, cyanide or sulphite and generates a fluorescent isoindole. GSH supplies both the amine and thiol moieties and therefore reacts with OPA (Senft A.P. 2000).

2.6.1 Buffers

Phosphate-EDTA assay buffer: NaH_2PO_4 (100 mM) and Na_2EDTA (5 mM), adjusted to pH 8

Cell lysis buffer: 0.1% Triton X-100 in phosphate-EDTA assay buffer

2.6.2 Sample preparation

Following treatment as described in section 2.3, DMEM was removed from confluent cells seeded in 6 well culture plates and cells were washed using PBS (1 ml). After removal of PBS, cells were scraped into 450 µl ice cold cell lysis buffer, transferred to 1.5 ml microcentrifuge tubes and an aliquot (2 µl) was taken and used for protein quantification as described in section 2.11.3. Ice cold 50% trichloroacetic acid (TCA) (50 µl) was added to each tube and GSH-containing protein-free supernatants were prepared by centrifugation of the samples at 15000 × g for 5 minutes at 4 °C.

2.6.3 Assay procedure

From the supernatants prepared, 100 µl was taken and added to 3 ml polystyrene fluorescence cuvettes containing 1.8 ml phosphate–EDTA assay buffer. A GSH standard curve was constructed by adding the required amount (0 – 20 µl, 0 – 2 µg) of a freshly prepared GSH stock (0.1 mg/ml in phosphate–EDTA assay buffer) to a cuvette containing 1.8 ml phosphate-EDTA assay buffer and 100 µl 5% TCA (w/v in phosphate-EDTA assay buffer). To each cuvette 100 µl OPA (1 mg/ml in methanol) was added. Cuvettes were left in the dark for 15 minutes on a rocking platform before fluorescence was read using a fluorimeter (Perkin Elmer LS 50B) with $\lambda_{excitation}$ = 340 nm (slit width 2.5 nm) and $\lambda_{emission}$ = 420 nm (slit width 4.0 nm). Using the standard curve total sample GSH was determined and normalised to protein as described in section 2.11.4.

2.7 Cloning

For the generation of hOGG1-expressing KO MEF cells, hOGG1 cDNA was cloned into mammalian expression vectors and used to transfect KO MEF cells. For the generation of yellow fluorescent protein (YFP)-hOGG1 bimolecular fluorescence complementation (BiFC) constructs YFP-hOGG1 cDNA was cloned into mammalian expression vectors and used for KO MEF cell transfection.

BiFC is a method for the visualisation of protein – protein interactions in live cells, as described in further detail in section 5.1. BiFC involves the reconstitution of the fluorescence of yellow fluorescent protein (YFP) by the association of two non-fluorescent YFP half molecules fused to proteins of interest, such as hOGG1 (Figure 2.1).

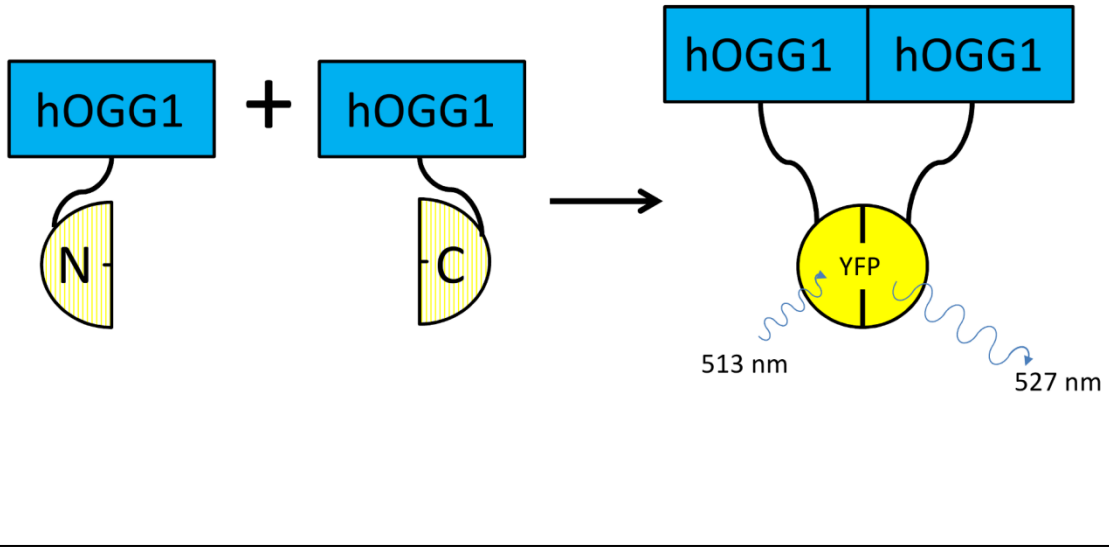

Figure 2.1: Principle of the BiFC assay.
The YFP-N and YFP-C fragments are fused to putative interaction partners. Upon interaction of these partners the non-fluorescent YFP halves will complement resulting in fluorescence.

2.7.1 hOGG1-expressing MEF cell vector preparation

pcDNA3© plasmids containing wild-type (Ser326-) and polymorphic (Cys326-) hOGG1 cDNA were a generous gift from J.Yokota (National Cancer Centre, Tokyo, Japan). These vectors had been previously sub-cloned in our laboratory into a pcDNA3.1/Hygro©(+) mammalian expression vector (Invitrogen, U.S.A.) (see appendix, pages 218-219). Following DNA isolation from frozen bacterial stocks, this was used for transient hOGG1 transfection of KO MEF cells.

The pcDNA3.1/Hygro©(+) plasmids had, in our laboratory, been previously used to sub-clone hOGG1 variant cDNA into a pIREShyg3 mammalian expression vector (B.D. Clontech, U.S.A.) (see appendix, page 220). Following DNA isolation from frozen bacterial stocks, this was used for stable hOGG1 transfection of KO MEF cells.

2.7.2 BiFC-construct vector preparation

pBluescript II KS(-) plasmids (see appendix, page 222) containing either the N- or C-terminus of yellow fluorescent protein, YFP-N and YFP-C respectively, were a generous gift from S. Brogna, (University of Birmingham, B15 2TT). Plasmid identities were confirmed by sequencing as described in section 2.7.6. Ser326- and Cys326-hOGG1 cDNA was amplified from pcDNA3© plasmids by polymerase chain reaction (PCR) (as described in section 2.10.4) using primers with BamHI sites, then cloned into pBluescript II vectors.

(Forward primer: 5'-GAGAGGATCCATGCCTGCCCGCGCGCTTCTG-3' Reverse primer: 5'-GGCAGGATCCTTACTAGCCTTCCGGCCCTTTG-3' see table 2.1 for conditions)

Next YFP-N and YFP-C-hOGG1 cDNA was subcloned first into a pEGFP-N1 mammalian expression vector (B.D. Clontech) (see appendix, page 221) then into a pcDNA3.1/Hygro©(+) mammalian expression vector (Invitrogen, U.S.A.) to generate: YFP-N-Ser326-hOGG1, YFP-C-Ser326-hOGG1, YFP-N-Cys326-hOGG1 and YFP-C-Cys326-hOGG1 constructs (Figure 2.2). To enable detection of background fluorescence arising from non-hOGG1 mediated YFP fragment association, controls were also generated without hOGG1: YFP-N and YFP-C.

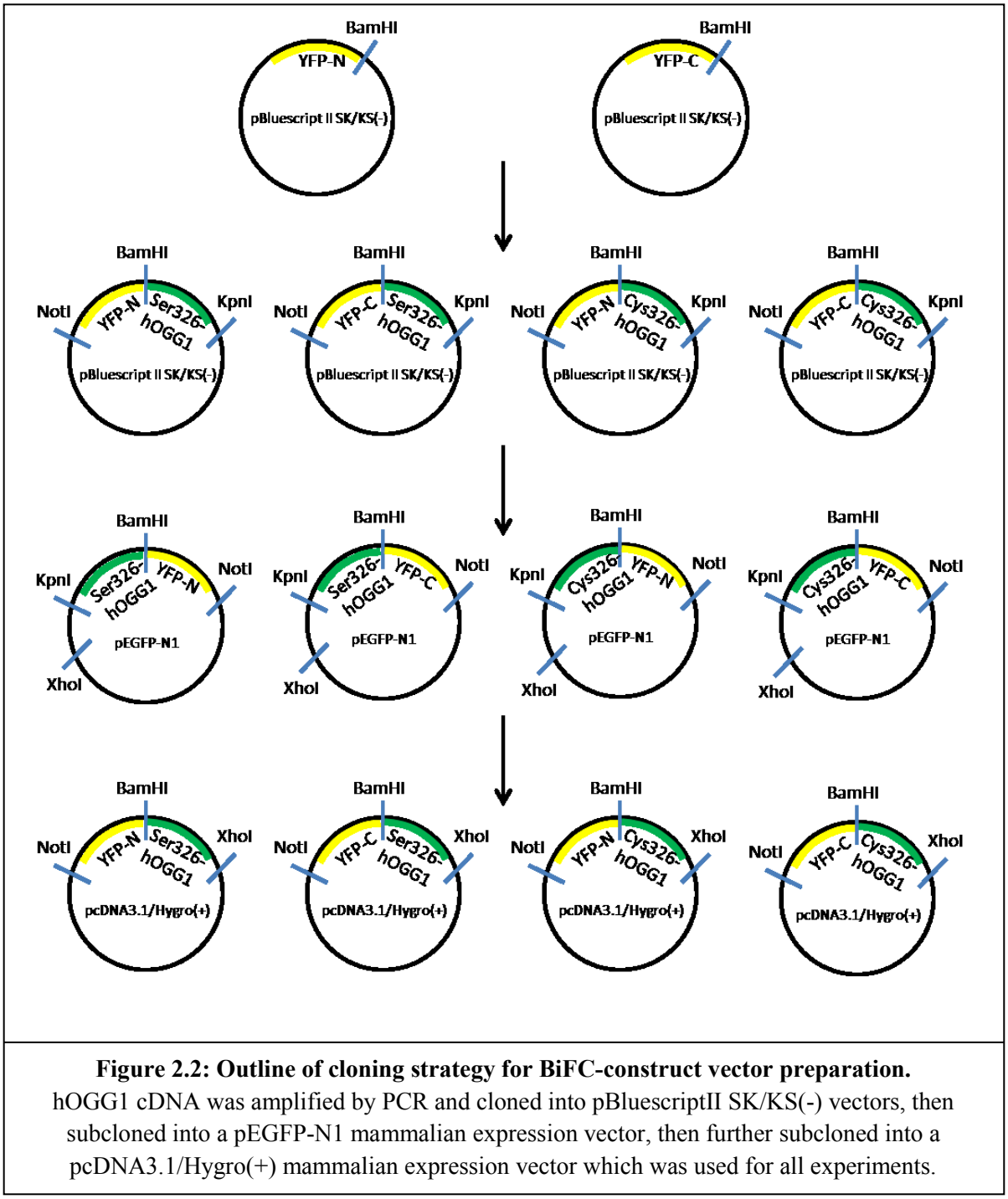

Figure 2.2: Outline of cloning strategy for BiFC-construct vector preparation. hOGG1 cDNA was amplified by PCR and cloned into pBluescriptII SK/KS(-) vectors, then subcloned into a pEGFP-N1 mammalian expression vector, then further subcloned into a pcDNA3.1/Hygro(+) mammalian expression vector which was used for all experiments.

This cloning strategy was undertaken as the work was initially intended to be done using a drosophila expression vector, with compatible NotI and KpnI restriction sites, for use in drosophila cells. As there were no compatible restriction sites which would allow direct cloning from the pBluescriptII SK/KS(-) plasmid into the mammalian pcDNA3.1 hygro

(+) expression vector, the approach detailed above was chosen. A more direct approach would be to use PCR to transfer the YFP-hOGG1 constructs.

2.7.2.1 Restriction digestion

1) pBluescript II KS(-) plasmids (5 µg) and Ser326- and Cys326-hOGG1 BamHI PCR products were combined with *BamHI* (5 units), 100X bovine serum albumin (BSA) (0.1 µl), NEBBuffer 3 (2 µl) (New England Biolabs, Hertfordshire, U.K.) and sterile water to 30 µl. Reactions were incubated for 16 hours at 37°C prior to gel purification, as described in section 2.10.7.
2) pBluescript II KS(-) plasmids (5 µg) containing Ser326- and Cys326-hOGG1 inserts and pEGFP-N1 plasmids (5 µg) were combined with *KpnI* (5 units), *NotI* (5 units), *BamHI*-buffer (2 µl) (Fermentas, U.K.) and sterile water to 20 µl. Reactions were incubated for 2 hours at 37°C prior to gel purification, as described in section 2.10.7.
3) pEGFP-N1 plasmids (5 µg) containing Ser326- and Cys326-hOGG1 inserts and pcDNA3.1/Hygro© (+) plasmids (5 µg) were combined with *NotI* (5 units), *XhoI* (5 units), 100X BSA (0.1 µl), NEBBuffer 3 (2 µl) (New England Biolabs, Hertfordshire, U.K.) and sterile water to 20 µl. Reactions were incubated for 2 hours at 37°C prior to gel purification, as described in section 2.10.7.

2.7.2.2 DNA ligation

1) Gel purified *BamHI*-digested pBluescript II KS(-) plasmids (15 µl) were incubated with calf intestinal alkaline phosphatase (10 units) and NEBBuffer 3 (1.5 µl) (New England Biolabs, Hertfordshire, U.K.) for 1 hour at 37°C prior to ligation with gel purified *BamHI*-digested Ser326- and Cys326-h*OGG1* using T4

DNA ligase (New England Biolabs, Hertfordshire, UK). Digested pBluescript II KS(-) plasmids (50 ng), digested h*OGG1* (50 ng), T4 DNA ligase (800 units), 10X ligation buffer (3 µl) were combined with sterile water to 30 µl and incubated at 12°C for 16 hours.

2) Gel purified *KpnI-NotI*-digested pEGFP-N1 plasmids (15 µl) were incubated with calf intestinal alkaline phosphatase (10 units) and NEBBuffer 3 (1.5 µl) (New England Biolabs, Hertfordshire, U.K.) for 1 hour at 37°C prior to ligation with gel purified *KpnI-NotI*-digested hOGG1-containing pBluescript II KS(-) plasmids as described above.
3) Gel purified *NotI-XhoI*-digested pcDNA3.1/Hygro© (+) plasmids (15 µl) were incubated with calf intestinal alkaline phosphatase (10 units) and NEBBuffer 3 (1.5 µl) (New England Biolabs, Hertfordshire, U.K.) for 1 hour at 37°C prior to ligation with gel purified *NotI-XhoI*-digested hOGG1-containing pEGFP-N1 plasmids as described above.

2.7.3 Bacterial transformation

High efficiency JM109 competent *E.coli* cells (>10^8 cfu/µg) (Promega, U.K.) were defrosted on ice. Ligated DNA (5 µl) was added to the cells and the suspension was mixed by gently flicking the tube. After incubating on ice for 30 minutes the cell suspension was incubated at 42°C for exactly 30 seconds before returning to ice for 2 minutes. Room temperature SOC medium (900 µl) was added and cells were incubated with shaking (225 rpm) at 37°C for 1 hour. Cells (10 µl) were spread onto Luria-Bertani (LB)-agar plates containing ampicillin (100 µg/ml) or kanamycin (30 µg/ml) which were inverted and incubated at 37°C for 16 hours. Colonies were selected at random using a

sterile pipette tip and used to inoculate 3 ml LB-broth containing ampicillin (100 μg/ml) or kanamycin (30 μg/ml). Bacterial cultures were shaken (225 rpm) at 37°C for 16 hours prior to insert screening by PCR, as described in section 2.10.4, using M13 primers or hOGG1 primers where appropriate (see table 2.1 for conditions and primer sequences) with an additional 10 minute initial denaturation step to lyse the bacteria.

2.7.4 Plasmid DNA mini-preparation

An aliquot of the appropriate stock of high efficiency JM109 competent *E.coli* cells transformed with the ligated expression vectors was added to LB-broth (15 ml) containing ampicillin (100 μg/ml) or kanamycin (30 μg/ml) using a sterile pipette tip. Bacterial cultures were shaken (225 rpm) at 37°C for 16 – 48 hours. Plasmid DNA was isolated from bacterial cultures using a QIAprep® spin miniprep kit (Qiagen) as per manufacturer's instructions. Briefly, bacterial cells were pelleted by centrifugation at 6000 × g for 10 minutes and resuspended in buffer P1 (500 μl), followed by vortexing. The cell suspension was transferred to a 1.5 ml microcentrifuge tube and buffer P2 (250 μl) added. Tubes were gently mixed and buffer N3 (350 μl) was added, followed by further gentle mixing. The tubes were centrifuged (8000 × g, 10 minutes) to remove precipitated bacterial cell debris. The supernatant was decanted and transferred to a QIAprep column with collecting tube. The column was centrifuged (8000 × g, 60 seconds). A second wash step was carried out using buffer PE (750 μl) and the column was subjected again to centrifugation at 8000 × g for 60 seconds. The flow through was discarded and the residual buffer removed by centrifugation at 8000 × g for 60 seconds. The column was transferred to a new 1.5 ml microcentrifuge tube and incubated with

buffer EB (100 µl) for 1 minute at room temperature, followed by centrifugation for 60 seconds at 8000 × g. Eluted plasmid DNA was stored at -20°C.

2.7.5 DNA quantification

Eluted plasmid DNA concentration expressed in micrograms per microlitre was determined using UV spectroscopy (UVIKON Spectrophotometer 922, Konton Instruments, U.K.) by measuring absorbance at 260 nm.

2.7.6 DNA sequencing

DNA was sequenced by The Genomics Laboratory, School of Biosciences, University of Birmingham, Edgbaston, Birmingham, B15 2TT, U.K.

2.8 Stable cell line generation

2.8.1 Linearisation of hOGG1 pIREShyg3

Vector linearisation prevents episomal replication and permits stable genomic integration. Linearisation of Ser326- and Cys326- pIREShyg3 expression vectors was achieved by restriction endonuclease digestion. Ser326- or Cys326-hOGG1 pIREShyg3 (15 µg) was incubated with 20 units of *SspI* restriction endonuclease (New England Biolabs, Hertfordshire, U.K.), 10X enzyme buffer (5 µl), 100X BSA (0.1 µl) and sterile water (to 50 µl) for 16 hours at 37°C prior to gel purification as described in section 2.10.7.

2.8.2 Selection of transfected cells; kill curve generation

KO MEF cells were seeded at 35 000 cells per well and cultured in 12-well cell culture plates (15 mm diameter, Greiner, Bio-one, U.K.). Hygromycin B, an aminocyclitol

compound that inhibits protein synthesis, was added to complete DMEM at final concentrations of 0, 25, 100, 200 and 250 µg/ml. Cells cultured with hygromycin B were trypsinised at 0, 24, 48, 72 and 120 hours and counted using a haemocytometer. These data were used to construct a KO MEF cell kill curve in order to determine the optimal concentration of hygromycin for selection and maintenance of stably-transfected clones.

2.8.3 Transient transfection of KO MEF cells

Cells were plated at 60% confluency in 60 mm cell culture dishes and incubated at 37°C for 4 hours to allow attachment, and growth to approximately 75% confluency. For each 60 mm cell culture dish TurboFect™ transfection reagent (Fermentas, U.K.) (10 µl) and Ser326- or Cys326-hOGG1 pcDNA3.1/Hygro©(+) (6 µg) were added to 500 µl serum-free DMEM in a sterile 1.5 ml microcentrifuge tube. Gentle pipetting was used to mix and the mixture incubated at room temperature for 20 minutes. The entire volume of DNA/TurboFect™/serum-free DMEM mixture was subsequently added drop-wise to cells and the dish was gently tilted several times to distribute evenly. Dishes were incubated for 24 hours prior to pro-oxidant treatment and/or harvesting.

2.8.4 Stable transfection of KO MEF cells

Cells were transfected as described in section 2.8.3 with either Ser326- or Cys326-pIREShyg3 (or empty vector as control) (6 µg) and incubated for 48 hours. Cells were washed with 5 ml PBS and fresh DMEM was added prior to a further 24 hour incubation to allow growth to confluence.

2.8.5 Selection and maintenance of stable cell lines

Confluent Ser326-, Cys326- or empty- pIREShyg3-transfected KO MEF cells were trypsinised and reseeded in 60 mm cell culture dishes (5 per transfection) prior to the addition of complete DMEM containing hygromycin B antibiotic (200 μg/ml). Cells were cultured for 14 days to allow growth. Healthy colonies (36 per transfection) were selected by trypsinisation and reseeded into 12 well cell culture plates and grown to confluence prior to reseeding into 6 well culture plates and finally 75 cm^2 cell culture flasks. All clones which grew to confluence were initially assessed for hOGG1 activity using the molecular beacon assay (as described in section 2.9). Total RNA/cDNA, genomic DNA and nuclear protein extract (as described in sections 2.10 and 2.11) were subsequently isolated from successful candidates to allow stable cell line characterisation.

2.9 Molecular beacon incision assay

The use of molecular beacon incision assays to allow measurement of DNA glycosylase activity in live cells has been previously described (Maksimenko *et al.* 2004) and further developed and optimised in our laboratory for the specific analysis of OGG1 activity (Mirbahai L. *et al.* 2010; Priestley C.C. *et al.* 2010). The molecular beacon (Figure 2.3A) is an oligonucleotide with a 5'-fluorophore (fluorescein isothiocyanate; FITC) and a 3'-quencher (4-dimethylaminophenylazobenzoic acid; DAB). The stem-loop conformation adopted due to the self-complementary regions brings the FITC fluorophore in close proximity with the DAB quencher which quenches the fluorescence by fluorescence resonance energy transfer (FRET). The oligonucleotide synthesised by Alta Biosciences (University of Birmingham, U.K.) contains an 8-oxo dG lesion which

pairs with a dC residue providing a lesion recognition site for OGG1. Once transfected into cells, the molecular beacon can be cleaved by OGG1, leading to separation of the fluorophore and quencher resulting in fluorescence (Figure 2.4). A positive control beacon was also synthesised (Figure 2.3B) and transfected into cells to assess and control for transfection efficiency.

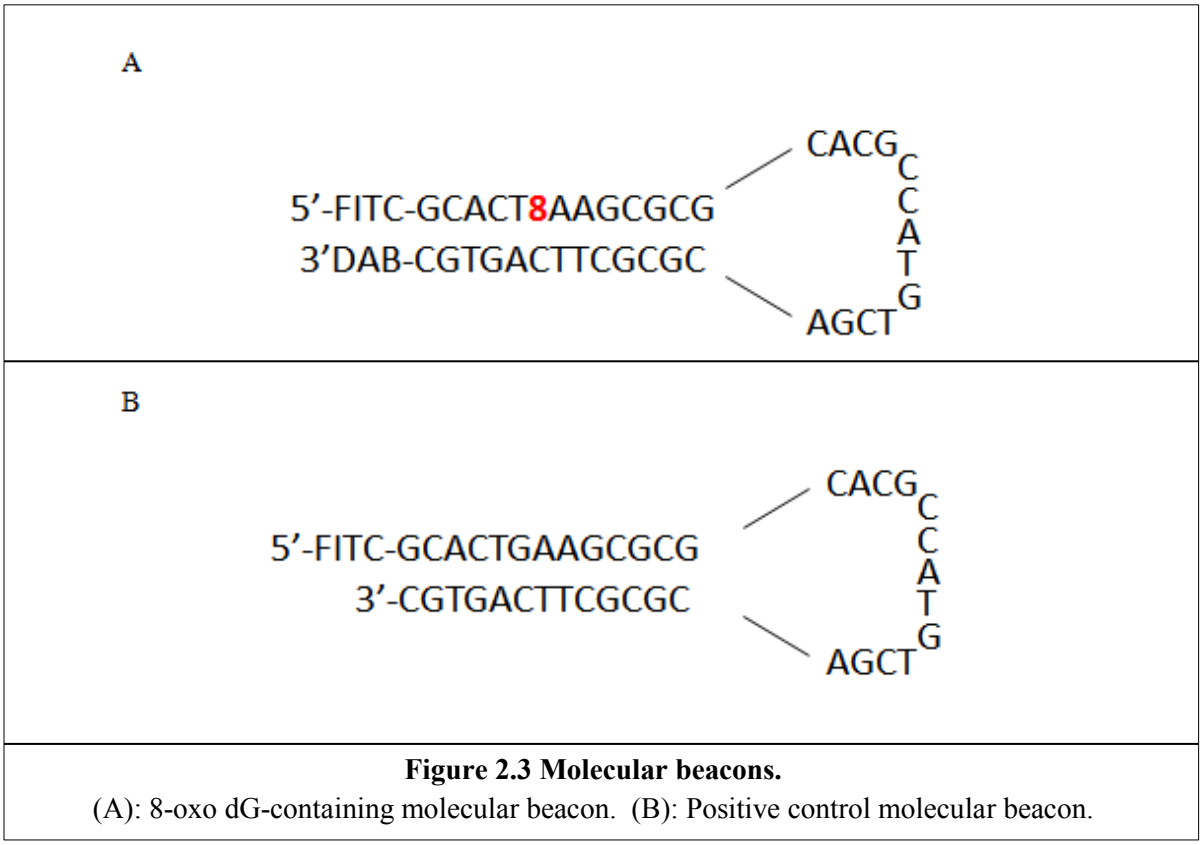

Figure 2.3 Molecular beacons.
(A): 8-oxo dG-containing molecular beacon. (B): Positive control molecular beacon.

2.9.1 Transfection with molecular beacons

The molecular beacon was dissolved in sterile H_2O to a final concentration of 10 pmol/µl, heated to 95°C for 3 minutes then allowed to anneal by cooling at room temperature for 3 hours. MEF cells were plated in 12 well cell culture dishes, allowed to grow to 75% confluence and either treated as described in section 2.3 or left as untreated controls. Per well, TurboFect™ transfection reagent (Fermentas, U.K.) (2 µl) was combined with beacon (140 pmol) and 67 µl serum free DMEM in a sterile 1.5 ml microcentrifuge tube. Gentle pipetting was used to mix and the mixture was incubated at room temperature for 20 minutes. The entire volume of beacon/TurboFect™/serum-free DMEM mixture was subsequently added drop-wise to cells and the dishes gently tilted several times to distribute evenly. Dishes were incubated at 37°C in a humidified chamber.

2.9.2 Flow cytometry analysis of FITC-derived fluorescence in MEF cells

Following treatment and transfection with molecular beacon DMEM was removed and cells were washed with PBS. Trypsin (500 µl) was used to detach cells which were centrifuged (1000 × g, 4 minutes, room temperature) and the resulting pellet resuspended in PBS (200 µl) and FACS fixative (200 µl) (1% (v/v) formaldehyde, 2% (v/v) FBS in PBS) with repeat pipetting to ensure a single cell suspension. Samples (10 000 live cells) were analysed using a BD FACScalibur™ flow cytometer (Becton Dickinson). CellQuestPro™ software and Weasel software (Walter and Eliza hall institute of medical research, Australia) were used to generate histograms of data, with an M-gate set at 10^1 on the FL1 (FITC) channel (Figure 2.5). This M-gate was applied to all of the data and

the percentage of positive events was compared (Figure 2.5). As controls, a mock-transfected population was analysed and BSO treated population without molecular beacon was also analysed.

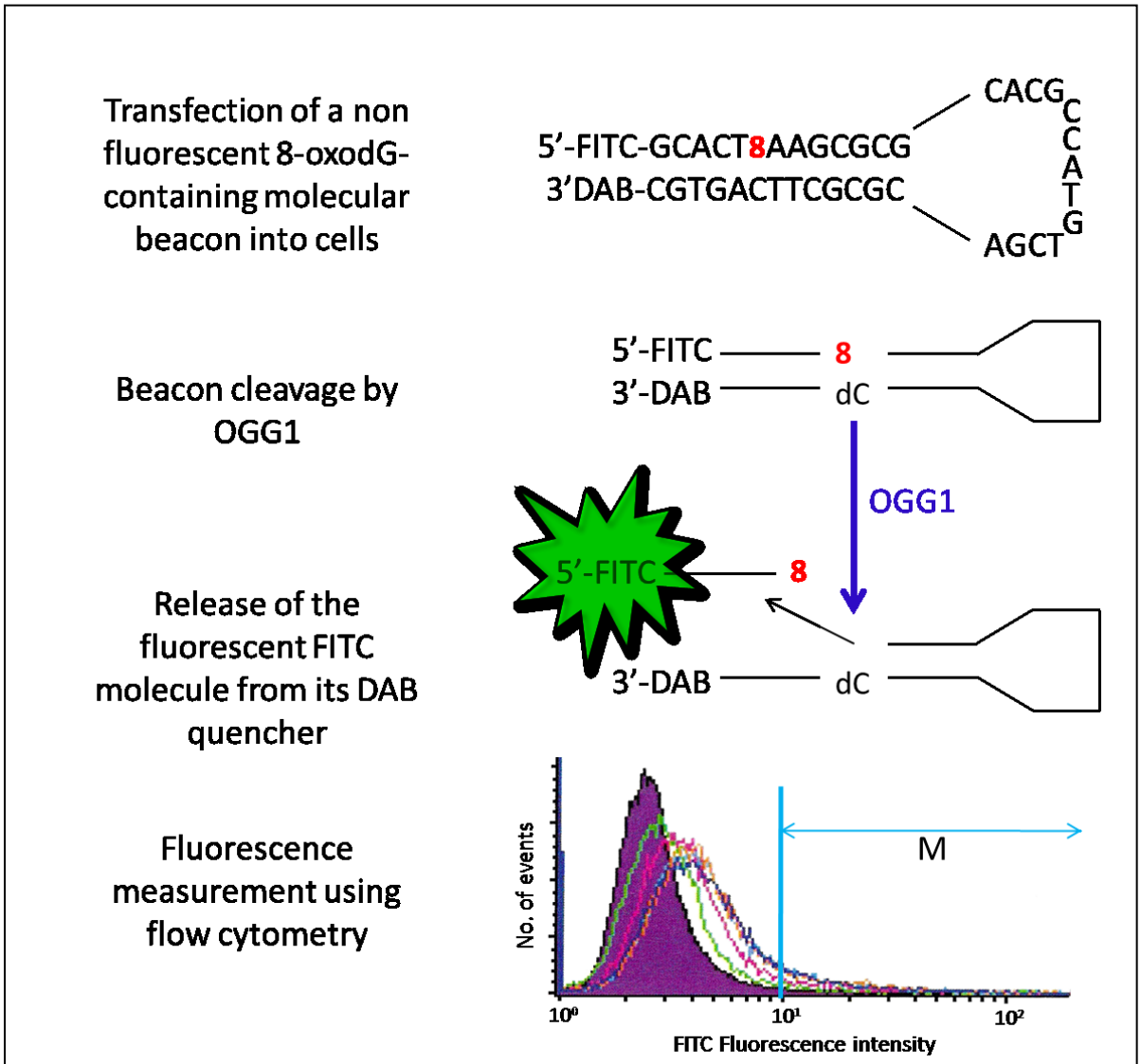

Figure 2.4: Measurement of OGG1 activity using 8-oxo dG-containing molecular beacon.

(1) A marker (M) gate was set at 10^1 fluorescence units on the FL1 (FITC) channel and the percentage of 8-oxo-dG beacon fluorescent events with intensity above this gate was calculated.

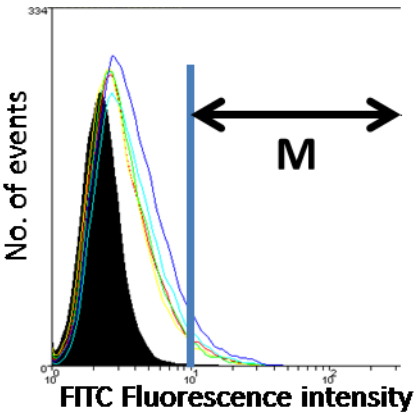

(2) The M gate was used to calculate the percentage of positive control beacon fluorescent events.

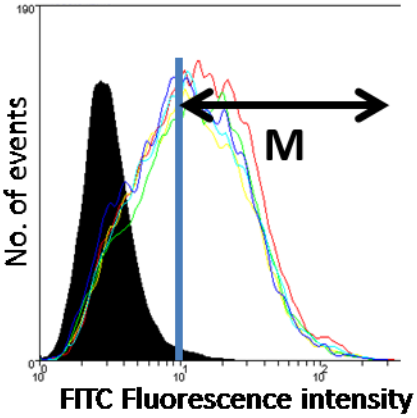

To normalise for transfection efficiency variation the number of 8-oxo-dG beacon fluorescent events (1) was divided by the number of positive control beacon fluorescent events (2). The number generated, expressed as a percentage, is termed the number of positive events.

Figure 2.5: Flow cytometry analysis of molecular beacon fluorescent events.

2.10 Nucleic acid purification and amplification

2.10.1 Isolation of total RNA from cultured cells

Total cellular RNA was isolated from cells as described by Chomczynski P. and Sacchi N. (1987) using an EZ-RNA kit (Geneflow, Staffordshire, U.K.) as per manufacturer's instructions. Briefly, cells grown to confluence in a 6 well culture plate (~5 × 10^6 cells) were washed with PBS prior to the addition of 500 µl guanidine thiocyanate detergent. The cell lysate was transferred to a 1.5 ml microcentrifuge tube and incubated at room temperature for 5 minutes. Phenol:chloroform extraction solution (500 µl) was added and following mixing by vortexing (15 seconds) left at room temperature for 10 minutes prior to centrifugation (12000 × g, 15 minutes, 4°C). The aqueous (RNA containing) phase (500 µl) was transferred to a fresh 1.5 ml microcentrifuge tube, isopropanol (500 µl) was added and the sample incubated for 16 hours at -20°C. Following centrifugation (12000 × g, 8 minutes, 4°C) and removal of the supernatant, the pellet was washed with 1 ml 75% ethanol and left to air dry (5 minutes) prior to resuspension in 20 µl DEPC-treated dH_2O. RNA was quantified by spectrophotometry using a Nanodrop ND1000 and stored at -80°C. DNA contamination was removed using a DNA-free treatment kit as per manufacturer's instructions (Ambion, Austin, U.S.A.).

2.10.2 Isolation of genomic DNA from cultured cells

Cells grown to confluence in a 6 well plate (~5 × 10^6 cells) were subjected to trypsinisation, centrifugation (1000 × g, 3 minutes) and resuspended in PBS (200 µl). Genomic DNA was isolated using the QIAamp® DNA Mini Kit as per manufacturer's instructions. Briefly, 20 µl Qiagen protease was added to the cell suspension and mixed

thoroughly. RNase A (4 µl, 100 ml/ml) was added, mixed, and the suspension was incubated for 2 minutes at room temperature. Buffer AL (200 µl) was added and mixed by pulse-vortexing prior to incubation at 56°C for 10 minutes to lyse cells. Ethanol (100%, 200 µl) was added and after mixing the sample was pipetted on to a QIAamp spin column and centrifuged (6000 × g, 1 minute). The column was transferred to a fresh collection tube and buffer AW1 (500 µl) was added prior to centrifugation (6000 × g, 1 minute). The column was transferred to a fresh collection tube and buffer AW2 (500 µl) was added prior to centrifugation (20000 × g, 3 minutes). Residual buffer AW2 was removed by a further centrifugation step in a new collection tube (8000 × g, 1 minute). The column was placed in a sterile 1.5 ml microcentrifuge tube and incubated with 50 µl buffer AE for 1 minute prior to centrifugation (6000 × g, 1 minute) to elute DNA. DNA was stored at -20°C.

2.10.3 First-strand cDNA synthesis from total RNA

Total RNA isolated as described in section 2.10.1 was used for first-strand cDNA synthesis using a SuperScript II Reverse Transcriptase kit as per manufacturer's instructions (Invitrogen, Paisley, U.K.). Briefly, RNA (1 µg) was combined with 1 µl random hexamers (50 ng) (Bioline, U.K.) and made up to a final volume of 15 µl with dH_2O prior to heating to 65°C for 5 minutes. 0.1 M DTT (2 µl), first strand buffer (5 µl), superscript II reverse transcriptase (0.5 µl), 25 mM dNTP mix (Bioline, U.K.) (0.4 µl) and dH_2O (2.1 µl) were added and first-strand cDNA synthesis completed by incubating at 25°C for 10 minutes and 42°C for 90 minutes followed by 70°C for 15 minutes. cDNA was quantified by spectrophotometry using a Nanodrop ND1000 and stored at -20°C.

2.10.4 Polymerase chain reaction (PCR)

cDNA was amplified by PCR using sequence specific primers synthesised by Alta Bioscience, Birmingham, U.K. (see table 2.1 for conditions and primer sequences). In a 200 µl microcentrifuge tube 0.625 units *Taq* DNA polymerase (Fermentas, U.K.), forward primer (10 pmol), reverse primer (10 pmol), 25 mM dNTPs (Bioline, U.K.) (0.2 µl), 10X *Taq* buffer (2.5 µl) and dH_2O up to a final volume of 25 µl were combined. PCR reaction mixtures were denatured at 95°C for 5 minutes then subjected to denaturation, annealing and extension steps in a PCR machine (Eppendorf Mastercycler Gradient). The PCR programme consisted of 34 cycles of denaturation at 95°C for 1 minute, annealing for 1 minute (at the required annealing temperature) and extension at 72°C for 1 minute, followed by a final extension step at 72°C for 5 minutes. The resulting products were analysed by DNA gel electrophoresis as described in section 2.10.6.

2.10.5 Quantitation of gene expression by real time PCR

Real time PCR with cDNA prepared as described in section 2.10.3 was performed using a Sensimix dT SYBR Green kit (Quantace, Finchley, U.K.) and the relevant sequence specific primers. Per well, cDNA (200 ng) was combined with Sensimix (13 µl), dH_2O (8 µl), SYBR Green (0.5 µl) and primers (0.2 pmol/µl) and made up to a final volume of 25 µl. Real time PCR was performed with all samples (n=3) in duplicate, using an Ambiprism 7000 sequence detection system with products amplified and detected, following a dissociation protocol, using a program of 35 cycles of 95°C for 30 seconds and 61.1°C for 30 seconds.

Sequence identity of PCR products was confirmed by sequencing (The Genomics Laboratory, University of Birmingham, U.K.). The melt curves for all samples were analysed and C_t values were recorded for each gene in the linear phase of amplification. Differences in sample C_t values (n=3) were assessed using a one-way ANOVA (SPSS v16). PCR reaction efficiencies were assessed using the LinRegPCR software (Ramakers et al 2003). Where differences in C_t values were significant, sample C_t values were normalised to β-actin mRNA levels, which were not affected by treatment, and fold change was calculated by the $2^{-\Delta\Delta C}{}_T$ method of relative quantification (Livak K.J. and Schmittgen T.D. 2001).

2.10.6 Nucleic acid gel electrophoresis

Powdered agarose (1.2 g) was dissolved by heating in 50 ml 1X TBE buffer (89 mM Tris base, 89 mM boric acid and 2 mM Na_2EDTA, adjusted to pH 8) containing ethidium bromide (0.5 μg/ml). The gel was cast, allowed to solidify at room temperature and immersed in 1X TBE buffer containing ethidium bromide (0.5 μg/ml). Nucleic acid samples were combined with 1 μl 6X gel loading dye (New England Biolabs, Hertfordshire, U.K.) and loaded into the sample wells. A DNA molecular weight marker (New England Biolabs, Hertfordshire, U.K.) was also loaded. Samples were subjected to electrophoresis at 80 V for 40 minutes and the gel visualised by UV transillumination.

2.10.7 Gel purification of DNA

Electrophoresis at 80 V for 40 minutes (1.2% w/v 1X TBE agarose gel containing 0.5 μg/ml ethidium bromide) was used to separate DNA fragments. Gels were visualised on a UV transilluminator and the appropriate band was excised. A QIAquick® gel extraction kit (Qiagen, U.K.) was used to extract DNA from the gel, according to the

manufacturer's instructions. Briefly, three volumes of buffer QG were added per volume of gel and the gel was dissolved by heating at 50°C for 10 minutes with regular vortexing. One gel volume of isopropanol was added and the sample mixed prior to loading onto a QIAquick spin column. Centrifugation (8000 × g, 1 minute) was followed by the addition of 500 µl buffer QG to remove traces of agarose and an additional centrifugation step (8000 × g, 1 minute). After discarding flow-through the column was washed with buffer PE (750 µl) followed by centrifugation (8000 × g, 1 minute). Residual buffer PE was removed by an additional centrifugation step (8000 × g, 1 minute). The column was transferred to a sterile 1.5 ml microcentrifuge tube and incubated with buffer EB (30 µl) for 2 minutes prior to DNA elution by centrifugation (8000 × g, 1 minute). DNA was stored at -20°C.

2.11 Isolation of protein extract from cultured cells

2.11.1 Isolation of nuclear protein extract

2.11.1.1 Buffers

Lysis buffer A: NP-40 (0.6% v/v), NaCl (150 mM), Tris-HCl pH 8.0 (10 mM), Na_2EDTA (1 mM) and mammalian protease cocktail inhibitor (10 µl/ml).

Lysis buffer B: Glycerol (25% v/v), NaCl (420 mM), Tris-HCl pH 8.0 (20 mM), Na_2EDTA (0.2 mM), MgCl (1.5 mM), mammalian protease cocktail inhibitor (10 µl/ml) and DTT (0.5 mM).

Dialysis buffer: Glycerol (20% v/v), KCl (0.1 mM), Tris-HCl pH 8.0 (20 mM), Na_2EDTA (0.2 mM) and DTT (0.5 mM).

2.11.1.2 Assay procedure

Following treatment as described in section 2.3, the growth medium was removed and cells washed in cold PBS (1 ml). Lysis buffer A was added (500 µl) and vigorous scraping was used to detach and resuspend cells. The cell suspension was transferred to a sterile 1.5 ml microcentrifuge tube and incubated at 4°C for 20 minutes prior to centrifugation (Hawk 15/05 refrigerated bench-top centrifuge, Sanyo, Japan) at 3000 × g, at 4°C, for 5 minutes. Following aspiration of the supernatant the pellet was resuspended in lysis buffer B (50 µl) and cells were incubated at 4°C for 30 minutes with regular gentle vortexing. The supernatant was subjected to centrifugation at 15 000 × g for 20 minutes at 4°C and then aspirated and transferred into the lumen of sterile dialysis tubing. The supernatant was dialysed at 4°C against 1000 volumes of dialysis buffer for 16 hours, with stirring. The nuclear protein extract was transferred to a sterile 1.5 ml microcentrifuge tube and used immediately in the oligonucleotide incision assay or stored at -80°C.

2.11.2 Isolation of whole protein extract

2.11.2.1 Buffers

RIPA buffer: Tris-HCl pH 7.6 (25 mM), NaCl (150 mM), NP-40 (1% v/v), sodium deoxycholate (1%), sodium dodecyle sulphate (SDS) (0.1% w/v) and mammalian protease cocktail inhibitor (10 µl/ml).

2.11.2.2 Assay procedure

Following treatment as described in section 2.3, the growth medium was removed and cells washed in cold PBS (1 ml). Trypsin (500 µl) was used to detach cells which were

then subjected to centrifugation (1000 × g; 4 minutes, room temp). Cell pellets (~ 5 × 10^6 cells) were incubated with RIPA buffer on ice for 20 minutes with regular vortexing. Cell debris was pelleted by centrifugation at 14 000 × g for 15 minutes at 4°C. The supernatant was transferred to a sterile 1.5 ml microcentrifuge tube and used immediately or stored at -80°C.

2.11.3 Isolation of soluble and insoluble nuclear protein

Cytoskeleton (CSK) buffer: NaCl (100 mM), sucrose (300 mM), PIPES (10 mM) pH 6.8, $MgCl_2$ (3 mM), 0.5% Triton X-100 and mammalian protease cocktail inhibitor (10 µl/ml).

Following treatment as described in section 2.3, the growth medium was removed and cells washed in cold PBS (1 ml). Cells were incubated with CSK buffer (300 µl) for 5 min on ice which was then removed and retained as the soluble protein-containing (S1) fraction. Next, cells were scraped into RIPA buffer (150 µl) and incubated on ice with regular vortexing for 20 minutes. Cell debris was pelleted by centrifugation at 14 000 × g for 15 minutes at 4°C. The supernatant was transferred to a sterile 1.5 ml microcentrifuge tube and retained as the insoluble protein-containing (P1) fraction. Fractions were used immediately or stored at -80°C.

2.11.4 Bradford assay

Protein concentrations were determined using the Bradford method (Bradford M. M. 1976) using BSA (1 – 10 µg) as a standard.

2.12 Oligonucleotide incision assay (Figure 2.6)

2.12.1 Buffers

1.8X REC buffer: Tris-HCl pH 7.5 (18 mM), KCl (180 mM), Na_2EDTA (18 mM) and BSA (0.18 mg/ml).

Formamide loading buffer: Na_2EDTA (0.5 mM), SDS (2.5% w/v), xylene cyanol (XC) / bromophenol blue (BPB) (46.5 µl) made up to 1 ml with formamide.

2.12.2 Labelling of probe

A single-stranded oligonucleotide (24 mer) containing a single 8-oxo dG residue (**8**) at position 10 (5'-GAACTAGTG**8**ATCCCCCGGGCTGC-3') (Trevigen, U.S.A.) (10 pmol) was combined with 2.5 µl of 10X T4 polynucleotide kinase (T4 PNK) buffer (Promega, U.S.A.) and dH_2O up to a final volume of 25 µl. The oligonucleotide was end-labelled with ^{32}phosphorus (^{32}P) via incubation with T4 PNK (Promega) (7.5 units) (1.5 µl) and 225 µCi of γ-^{32}P-ATP (Perkin Elmer, U.S.A.) (5 µl) for 10 minutes at 37°C. The addition of 0.5 M Na_2EDTA (2 µl) followed by heating to 78°C for 60 seconds terminated the end-labelling reaction.

Annealing of the labelled oligonucleotide to a complimentary oligonucleotide (3'-CTTGATCACCTAGGGGGCCCGACG-5') (24 mer Trevigen, U.S.A.) was achieved via the addition of a 1.5 fold excess of complimentary oligonucleotide. The mixture was heated to 95°C for 10 minutes and allowed to cool slowly to room temperature. The resulting ^{32}P-labelled double-stranded oligonucleotide was purified using the QIAquick® nucleotide removal kit (Qiagen, U.K.).

2.12.3 Sample preparation and visualisation

Nuclear protein extract, extracted as described in section 2.11.1 (5 µg) was added to a sterile 1.5 ml microcentrifuge tube and combined with 1.8X REC buffer (5.5 µl) and the ^{32}P-labelled double-stranded 8-oxo dG oligonucleotide (3.5 µl) in a final volume of 20 µl. Following vortexing the reaction mixture was incubated at 37°C for 1 hour. Formamide loading buffer (10 µl) was added and the sample was denatured by heating to 95°C for 5 minutes, then cooling on ice for 3 minutes. The entire sample was loaded onto a polyacrylamide gel (20% acrylamide, 8 M urea, 1X TBE) and electrophoresed at 300V for 120 minutes. After electrophoresis the gel was placed onto blotting paper and wrapped in SaranWrap™. Exposure of the gel to radiation sensitive film (Amersham, U.K.) for 3.5 hours at -80°C was followed by development using an X-ograph machine (AGFA Curix60).

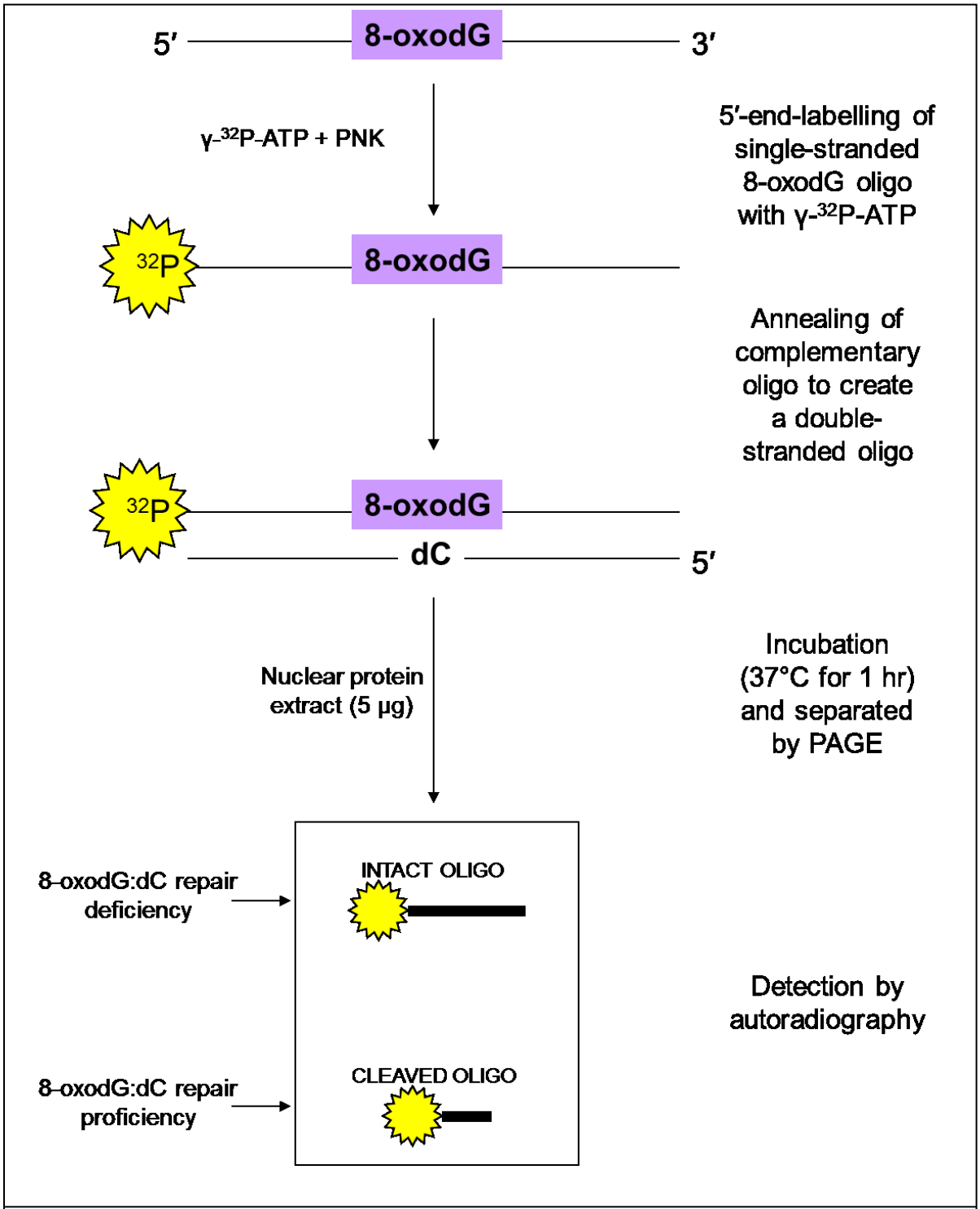

Figure 2.6: Oligonucleotide incision assay.
Adapted from Smart (2006) Activity of OGG1 in the repair of pro-oxidant-induced 8-oxo-2′-deoxyguanosine 2002-2006 PhD Thesis, University of Birmingham

2.13 Western blotting

2.13.1 Buffers

1X TBS: Tris base (0.1 M) and NaCl (0.15 M), adjusted to pH 8.0.

1X TBS-0.05% Tween 20: Tris base (0.1 M), NaCl (0.15 M) and Tween 20 (0.05%), adjusted to pH 8.0.

SDS-PAGE running buffer: Tris base (25 mM), glycine (192 mM), and SDS (0.1% w/v).

Transfer buffer: Tris base (20 mM), glycine (150 mM) and methanol (20% v/v).

Blocking buffer: Low-fat powdered milk (Marvel, U.K.) (5%) in 1X TBS-0.05% Tween 20

2.13.2 Gels

12.5% Resolving gel: Acrylamide:bisacrylamide 30% solution (12.5%), Tris-HCl pH 8.8 (375 mM), SDS (0.1% w/v). Immediately prior to casting N,N,N,N-tetramethylethylenediamine (TEMED) (15 µl per 10 ml) and 10% w/v ammonium persulphate (APS) (150 µl per 10 ml) were added.

4% Stacking gel: Acrylamide:bisacrylamide 30% solution (4%), Tris-HCl pH 6.8 (125 mM), SDS (0.1% w/v). Immediately prior to casting N,N,N,N-tetramethylethylenediamine (TEMED) (15 µl per 10 ml) and 10% w/v ammonium persulphate (APS) (150 µl per 10 ml) were added.

2.13.3 Assay procedure

Nuclear protein extracts (15 μg for hOGG1, 70 μg for rOGG1) or whole cell extracts (20 μg) were mixed with Laemmli 2X loading buffer and heated at 95°C for 5 minutes. Samples were resolved on a 12.5% SDS-polyacrylamide gel at 120V for 90 minutes then transferred to a nitrocellulose membrane (Amersham Biosciences) using a mini trans-blot electrophoretic transfer cell (Bio-Rad) at 100V for 120 minutes at 4°C. Blocking was achieved by incubating the nitrocellulose membrane with blocking buffer for 16 hours at 4°C on a rocking platform (Stuart Scientific STR9, U.K.). The nitrocellulose membrane was then incubated with either (hOGG1 blotting): mouse anti-hOGG1 polyclonal IgG primary antibody (1 μg/ml, clone 7E2, Assay Designs Inc., U.S.A.), (rOGG1 blotting): goat anti-Ogg1 polyclonal IgG primary antibody (0.3 μg/ml, Abcam, Cambridge, U.K.) or (EGFP blotting): rabbit polyclonal anti-GFP primary antibody (1:2000 dilution, Abcam, Cambridge, U.K.) in blocking buffer for 1 hour on a rocking platform at room temperature. 1X TBS-0.05% Tween 20 solution was used to wash the membrane (3 × 10 minutes), which was subsequently incubated with a horseradish peroxidase (HRP)-conjugated (hOGG1 blotting): anti-mouse secondary antibody (1:750 dilution, DAKO, U.K.), (rOGG1 blotting): anti-goat secondary antibody (1:10000 dilution, DAKO, U.K.) or (EGFP blotting): anti-rabbit secondary antibody (1:5000 dilution, DAKO, U.K.) in blocking buffer at room temperature for 1 hour. 1X TBS-0.05% Tween 20 solution was used to wash again (2 × 10 minutes), followed by a final wash in 1X TBS (1 × 10 minutes). The membrane was incubated with SuperSignal West Pico chemiluminescent detection reagent (Thermo Fisher Scientific, U.K.), prepared as per manufacturer's instructions. Protein bands were visualised via exposure to ECL hyperfilm (Amersham

Biosciences) and development in an X-ograph machine (AGFA Curix60). Where appropriate, the intensity of each band was quantified by densitometry (ImageJ) and normalised to a beta actin loading control.

2.14 Confocal microscopy

Cells were grown on coverslips and counterstained by incubation with 0.5 μg/ml Hoechst-34580 (Invitrogen, U.K.) for 20 minutes at 37°C. All images were collected using live cells, except when cells were incubated with CSK buffer (as described in section 2.11.3) prior to fixation with 4 % para-formaldehyde, pH 7.4, for 20 minutes at room temperature.

Image acquisition was performed with a Leica TCS SP2 confocal microscope (Leica Microsystems), using a 63x oil immersion objective NA 1.32. Fluorochromes were excited using an argon laser at 488 nm for FITC, EGFP and YFP and 405 nm for Hoechst. Images were collected sequentially then merged using Adobe Photoshop CS5 (Adobe Systems Inc.).

2.15 Statistical analysis of data

All statistical analysis was performed using SPSS version 16 software. Data which was normally distributed (as assessed by Shapiro-Wilk test) and displayed homogeneity of variance (as assessed by Levene's test) was analysed by one-way ANOVA followed by a 2-tailed or paired Student's *t*-test. Data which was not normally distributed or did not display homogeneity of variance was analysed by Kruskal-Wallis test or Mann-Whitney U test.

Table 2.1: PCR primers and conditions

Name	Primer Sequence	Predicted Annealing Temperature	Primer pair PCR conditions
mOGG1 F	5'-GTAACTACGGCTGGCATCC-3'	55.5	95°C (5 min), 95°C (1 min), 61°C (1 min), 72°C (5 min)
mOGG1 R	5'-AGGCTTGGTTGGCGAAGG-3'	60.9	
Hygromycin F	5'-GATGTAGGAGGGCGTGGATA-3'	57.4	95°C (5 min), 95°C (1 min), 60°C (1 min), 72°C (5 min)
Hygromycin R	5'-GATGTTGGCGACCTCGTATT-3'	57.5	
mBeta actin F	5'-AGCCATGTACGTAGCCATCC-3'	57.6	95°C (5 min), 95°C (1 min), 61°C (1 min), 72°C (5 min)
mBeta actin R	5'-CTCTCAGCTGTGGTGGTGAA-3'	56.3	
BamHI F	5'-GAGAGGATCCATGCCTGCCCGCGCGCTTCTG-3'	86.5	98°C (30 s), 98°C (30 s), 65°C (30 s), 72°C (30 s)*
BamHI R	5'-GGCAGGATCCTTACTAGCCTTCCGGCCCTTTG-3'	79.7	
M13 F	5'-GTAAAACGACGGCCAGT-3	50.8	95°C (5 min), 95°C (1 min), 55°C (1 min), 72°C (5 min)
M13 R	5'-AACAGCTATGACCATG-3'	38.5	
hOGG1 F	5' -GAGGTGGAGGCTCATCTCAG-3'	56.7	95°C (5 min), 95°C (1 min), 61°C (1 min), 72°C (5 min)
hOGG1 R	5' -AGGGTGCCAGCTGTAGTCAC-3'	57.4	
hOGG1 F	5' -GAGGTGGAGGCTCATCTCAG-3'	56.7	95°C (5 min), 95°C (1 min), 63°C (1 min), 72°C (5 min)
Hygromycin R	5'-GATGTTGGCGACCTCGTATT-3'	57.5	
			All with a final extension step at 72°C for 10 min

* Instead of Fermentas Taq DNA polymerase, Phusion ® High Fidelity DNA polymerase was used

Chapter 3 – Response of mouse and rat OGG1 to oxidative stress

3.1 Introduction

Normal cellular processes generate approximately 10^3 8-oxo dG lesions per cell per day (Lindahl T. and Barnes D.E. 2000) which are repaired primarily by the OGG1 BER protein. As 8-oxo dG can exist in the *syn* conformation in DNA and mimic thymine it can mispair with adenine during DNA replication and lead to G:C→T:A transversion mutations (Wang D. *et al.* 1998). An increase in ROS results in cellular oxidative stress. Reduction of OGG1 activity under such conditions could result in reduced DNA repair capacity and sensitivity to oxidative DNA damage. The response of the OGG1 protein to oxidative stress conditions has therefore been the subject of investigation with gene expression, protein levels and activity measured following exposure to a variety of compounds implicated in ROS production including cadmium, sodium dichromate and potassium bromate.

Many studies report compound-specific induction or inhibition of OGG1 activity associated with altered mRNA expression. The response of mouse OGG1 (Zharkov D.O and Rosenquist T.A. 2002), rat OGG1 (Potts R.J. *et al.* 2003) and human OGG1 (Bravard 2006; Youn C.K. *et al.* 2005) to cadmium was a reduction in glycosylase activity associated with decreased levels of protein and mRNA expression. Reduced hOGG1 activity associated with decreased levels of protein and mRNA expression was also observed in human A549 lung carcinoma cells following treatment with sodium dichromate (Hodges N.J. and Chipman J.K. 2002). In contrast, an increase in rOGG1 activity, associated with an increase in mRNA expression, was observed following exposure of male Sprague-Dawley rats to aniline (Ma H. *et al.* 2008).

The increase in rOGG1 activity observed in neuronal cells treated with synthetic nitrogen compounds previously shown to have elevated ROS scavenging activity, was not linked with an increase in mRNA expression (Silva J.P. *et al.* 2009). Furthermore, we observed an increase in mOGG1 activity following treatment of mouse embryonic fibroblast (MEF) cells with potassium bromate which was not associated with any change in mRNA levels (Mirbahai L. *et al.* 2010). Such non-transcriptional regulation of OGG1 activity suggests that in these cells any observed ROS-mediated alteration in OGG1 activity is a result of protein or mRNA stabilisation, alteration in localisation, post-translational modification and/or protein interactions. In support of this, treatment of MEF cells with glucose oxidase, which induces cellular oxidative stress by generation of $O_2^{\bullet-}$, resulted in a transient increase in OGG1 acetylation and OGG1 activity, with no change at the polypeptide level (Bhakat K.K. *et al.* 2006).

The work presented in this chapter aimed to build on previous data showing induction of mOGG1 activity following treatment of MEF cells with potassium bromate (Mirbahai L. *et al.* 2010) and used the glutathione synthesis inhibitor BSO to assess the effect of ROS on OGG1 activity, mRNA expression and protein levels. The response of mOGG1 was investigated using wild-type MEF cells however OGG1 protein could not be detected in these cells with any commercially available antibody. Rat OGG1 shows extensive homology with the human and mouse protein (Prieto Alamo M.J. *et al.* 1998; For sequence alignment see appendix, page 223) and was easily detected in rat hepatoma (MH1C1) cells by western blotting hence MH1C1 cells were employed to investigate potential BSO-mediated OGG1 protein level alteration.

3.2 Results

3.2.1 Cell viability following BSO treatment

To investigate BSO mediated cytotoxcity, MEF and MH1C1 cells were cultured in 96 well cell culture plates and treated for 24 h with BSO (0, 1, 10, 100, 1000 μM) prior to analysis by the MTT reduction assay, as described in section 2.4. No significant difference in absorbance was observed between untreated and BSO treated cells ($P > 0.05$ as determined by one-way ANOVA) indicating that 24 h treatment with up to 1000 μM BSO does not affect the viability of these cells (Figure 3.1).

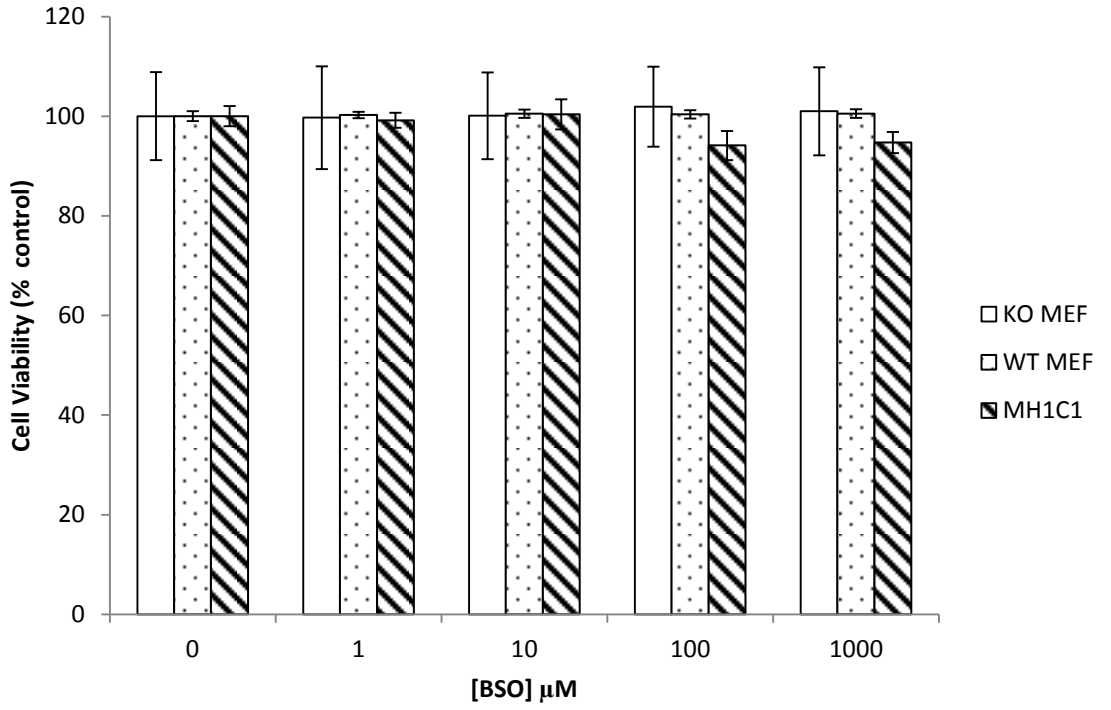

Figure 3.1: Viability of MEF and MH1C1 cells after 24 h BSO treatment as assessed using the MTT reduction assay.

Data are displayed as percentage of untreated control ±SEM from 3 independent experiments. No statistically significant change in MTT reduction was observed, as determined by one-way ANOVA.

3.2.2 Total cellular reduced glutathione following BSO treatment

Treatment with BSO for 24 h at concentrations ≥ 1 μM has been shown to deplete cytoplasmic GSH in KO and WT MEF cells, with nuclear depletion occurring following treatment with 1000 μM BSO (Green R.M. *et al.* 2006). To determine and compare the levels of total GSH in MEF and MH1C1 cells after BSO treatment (0, 1, 10, 100, 1000 μM, 24 h), cells were treated and total GSH measured as described in section 2.6.

Statistically significant depletion of total GSH occurred following treatment with ≥ 1 μM BSO in KO MEF cells. In WT MEF and MH1C1 cells statistically significant depletion of total GSH occurred following treatment with ≥ 10 μM BSO. No significant difference in total GSH was observed between KO and WT MEF cells following treatment with any concentration ($P > 0.05$ as determined by one-way ANOVA), however MH1C1 cells had significantly more total GSH than KO MEF cells following treatment with 1, 10 and 100 μM BSO and significantly more total GSH than WT MEF cells following treatment with 1 and 10 μM BSO (Figure 3.2).

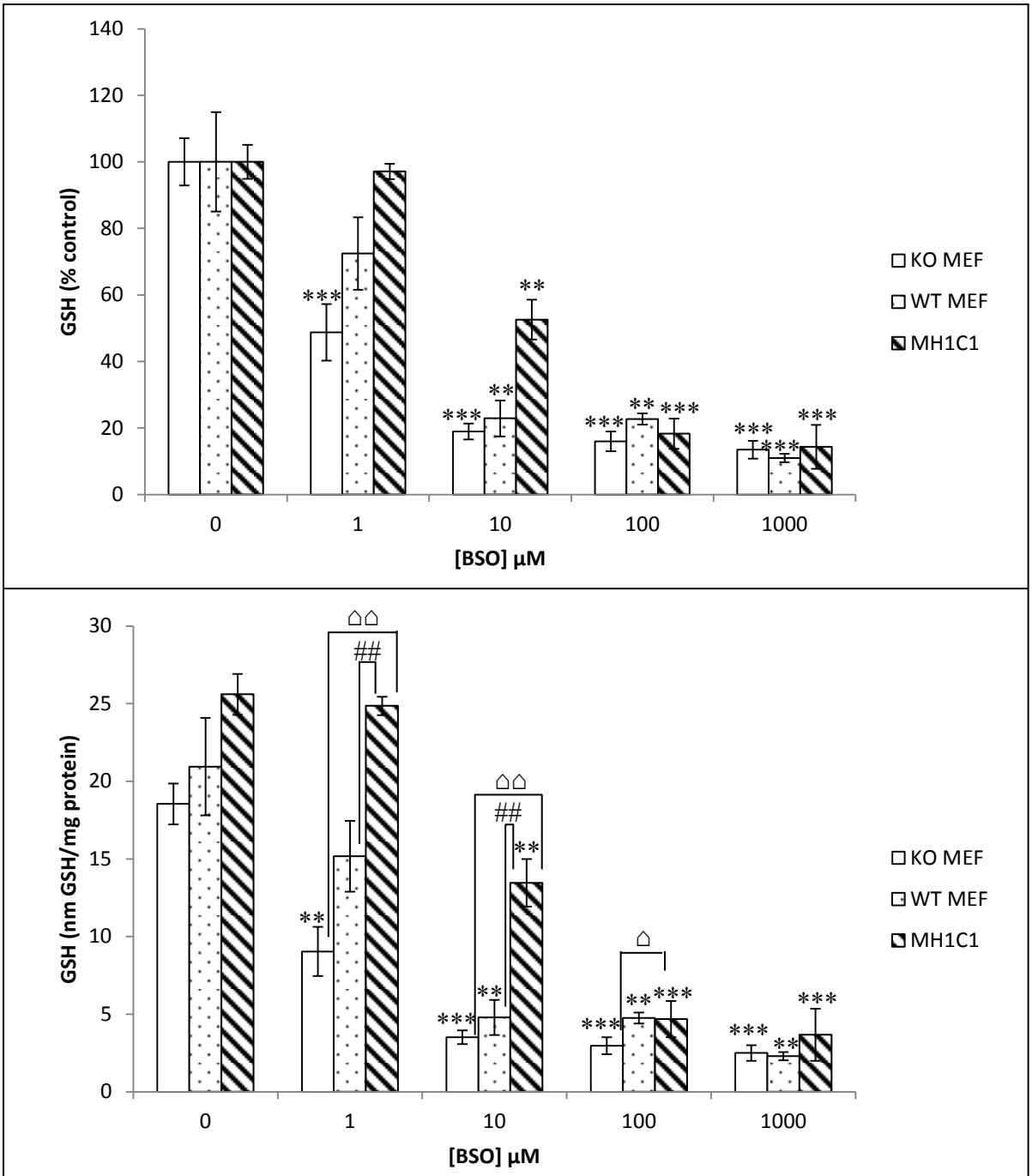

Figure 3.2: Total GSH in MEF and MH1C1 cells after 24 h BSO treatment.
Data are displayed as percentage of untreated control (nm GSH/mg protein KO MEF: 18.54 ± 1.32, WT MEF: 20.94 ± 3.13, MH1C1: 25.6 ± 1.32) and as nm GSH/mg protein ±SEM from 3 independent experiments. **,***: Significantly different from control (**$P < 0.01$ ***$P < 0.001$), #: significantly different from WT MEF (##$P < 0.01$), ⌂: significantly different from KO MEF ($^{⌂}P < 0.05$ $^{⌂⌂}P < 0.01$) as determined by 2-tailed Student's *t*-test.

3.2.3 Intracellular ROS following BSO treatment

Using the fluorescent dye dichlorofluorescein, intracellular ROS have been shown to be induced in KO and WT MEF cells with 24 h BSO treatment at concentrations ≥ 100 μM (Green R.M. *et al.* 2006). The current study modified the technique used by Green *et al.* and employed the use of flow cytometry to measure intracellular ROS levels, as described in section 2.5.

Fluorescence was statistically significantly increased in a concentration dependent manner compared with control in all cells following treatment with ≥ 10 μM BSO. There was no statistically significant difference in response between WT and KO MEF cells, however fluorescence was significantly lower in MH1C1 cells than KO MEF following treatment with 10, 100 and 1000 μM BSO. Fluorescence was significantly lower in MH1C1 cells than WT MEF cells without treatment and following treatment with all concentrations of BSO (Figures 3.3 and 3.4).

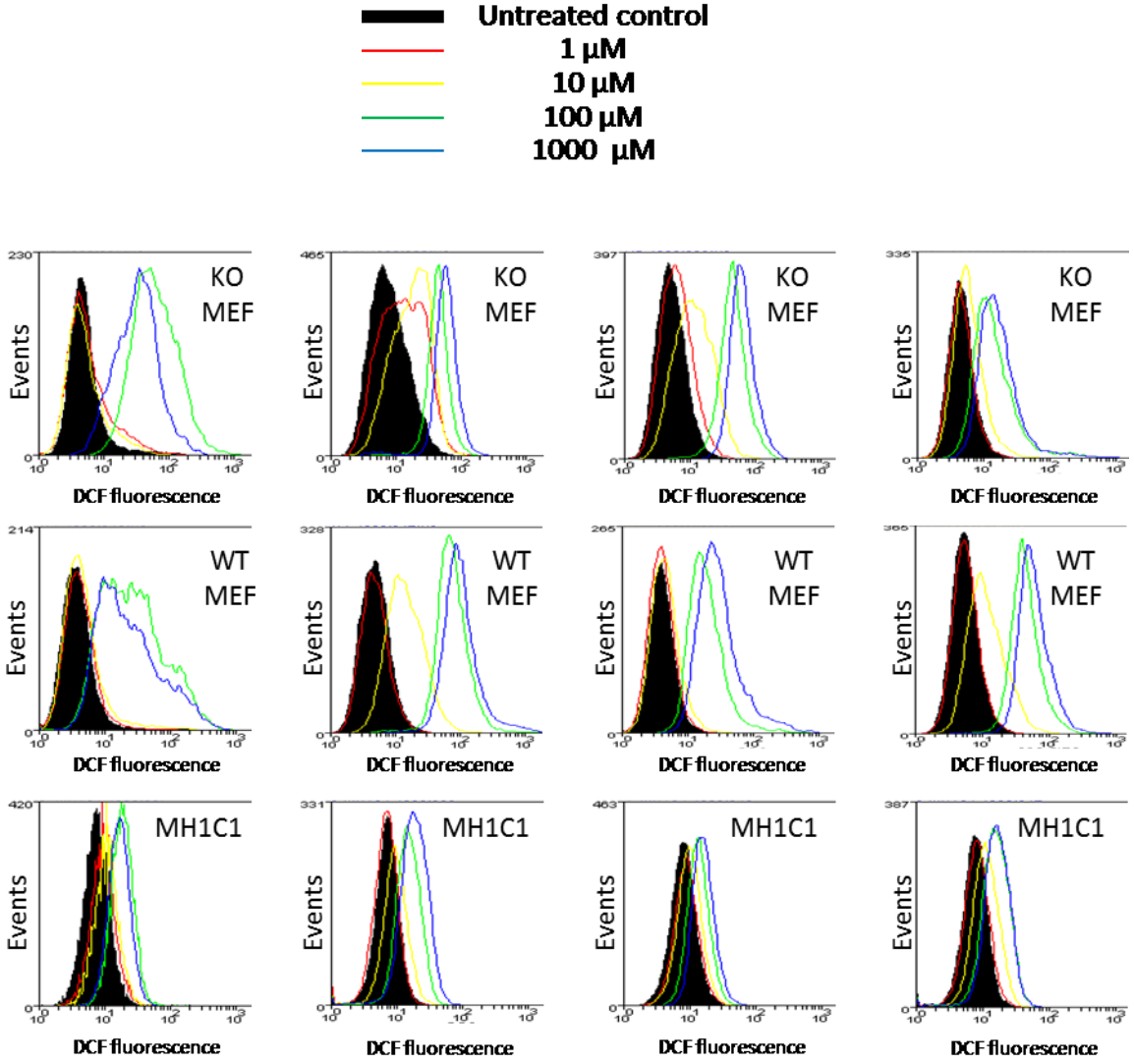

Figure 3.3: ROS levels as assessed by DCF fluorescence in MEF and MH1C1 cells after 24 h BSO treatment.

Individual replicates are displayed (n=4).

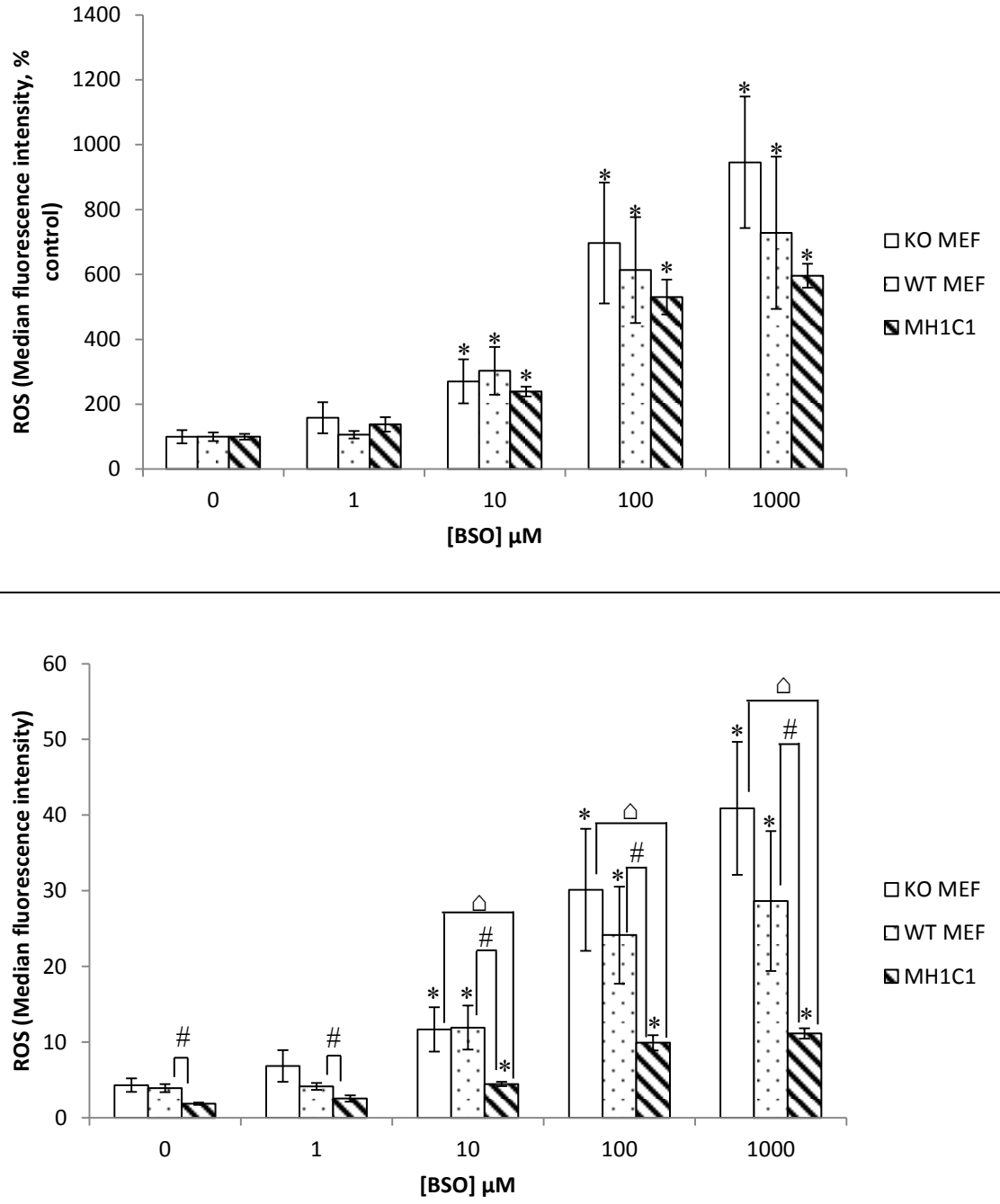

Figure 3.4: ROS levels in MEF and MH1C1 cells after 24 h BSO treatment.
Data are displayed as median fluorescence intensity as percentage of untreated control (KO MEF: 4.33 ± 0.88, WT MEF: 3.94 ± 0.52, MH1C1: 1.87 ± 0.32) and as median fluorescence intensity ±SEM from 4 independent experiments. *: Significantly different from control (*$P < 0.05$), #: significantly different from WT MEF (#$P < 0.05$), ⌂: significantly different from KO MEF (⌂$P < 0.05$) as determined by Mann-Whitney *U* test.

3.2.4 Mouse OGG1 activity following BSO treatment

To determine the effect of increased cellular ROS on mOGG1 activity WT MEF cells were treated with BSO (0, 1, 5, 10, 50, 100 and 1000 μM, 24 h) then transfected with an 8-oxo dG-containing molecular beacon prior to fluorescence analysis by flow cytometry as described in section 2.9. Data are displayed as the number of positive events (as described in section 2.9.2) as a percentage of untreated control. A statistically significant concentration dependent increase in fluorescence was observed following treatment with BSO at concentrations ≥ 5 μM (Figure 3.5).

Transfection of WT MEF cells with a positive control molecular beacon after BSO treatment (0, 1, 5, 10, 50, 100, 1000 μM, 24 h) allowed the assessment of transfection efficiency. No statistically significant difference in fluorescence was observed at any BSO concentration ($P > 0.05$ as determined by one-way ANOVA) (Bottom panel, figure 3.5), confirming that BSO treatment did not affect transfection efficiency of cells.

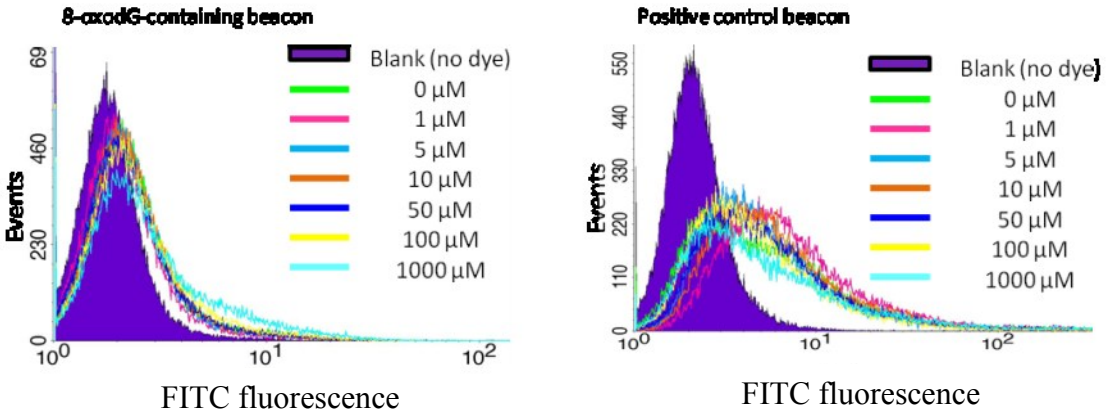

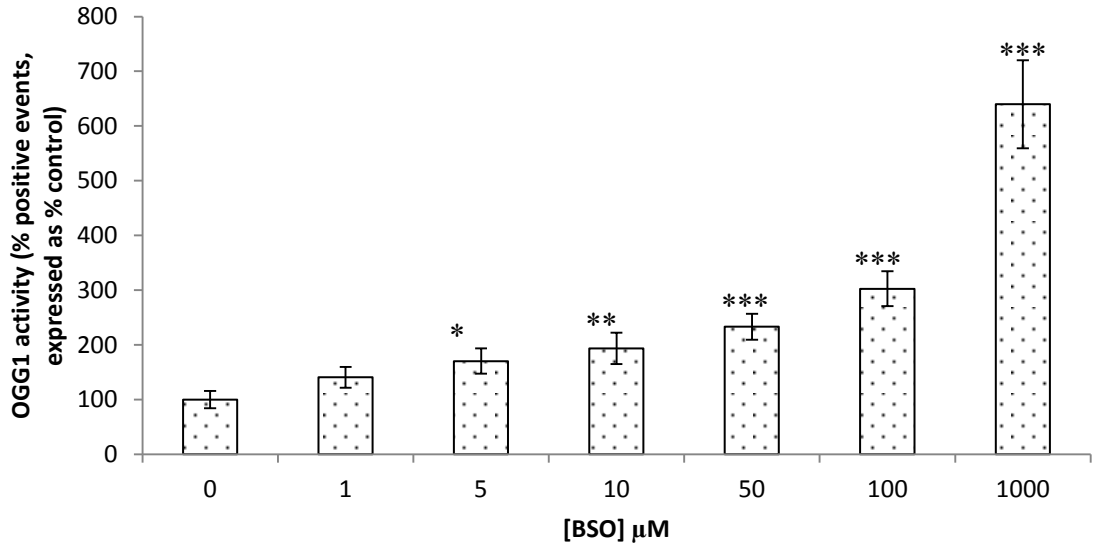

[BSO] µM	Number of positive control beacon events (WT MEF) ± SEM
0	33.91±6.78
1	25.63±3.55
5	22.31±2.96
10	23.58±2.92
50	23.46±4.05
100	24.57±5.73
1000	26.61±1.99

Figure 3.5: mOGG1 activity, as assessed by beacon fluorescence following 24 h BSO treatment.

Data are displayed as the number of positive events as percentage of untreated control (3.32±0.53), ±SEM from 3 independent experiments. *,**,***: Significantly different from control (*$P < 0.05$ **$P < 0.01$ ***$P < 0.001$) as determined by 2-tailed Student's *t*-test.

3.2.5 Mouse OGG1 activity controls

To confirm the specificity of the beacon, KO MEF cells were transfected with 8-oxo dG-containing molecular beacon. Fluorescence levels were significantly lower than in WT MEF cells ($P < 0.05$ as determined by 2-tailed Student's *t*-test) (Tables 3.1 and 3.2) and not affected by BSO treatment.

To confirm that the fluorescence was a result of BSO-induced OGG1 activity and not BSO alone, KO MEF cells were transfected with 8-oxo dG-containing molecular beacon. No increase in fluorescence was observed with BSO treatment ($P > 0.05$ as determined by 2-tailed Student's *t*-test) (Table 3.1). To determine whether differences in transfection efficiency could account for the reduced fluorescence in KO MEF cells compared with WT MEF cells, KO MEF cells were treated with BSO (0, 10, 1000 μM, 24 h) then transfected with positive control molecular beacon. No statistically significant difference in fluorescence was observed at any BSO concentration investigated ($P > 0.05$ as determined by one-way ANOVA) (Table 3.2).

Table 3.1: Beacon cutting activity in MEF cells following BSO treatment

[BSO] μM	Number of positive events (KO MEF) ± SEM	Number of positive events (WT MEF) ± SEM
0	0.52±0.13	1.07±0.11
100	0.68±0.29	2.34±0.31

Table 3.2: Positive control beacon events in KO MEF cells

[BSO] µM	Number of positive events (KO MEF) ± SEM
0	53.48±4.12
10	49.48±0.80
1000	53.50±1.35

3.2.6 Mouse OGG1 mRNA expression following BSO treatment

To assess whether levels of OGG1 mRNA changed following treatment with BSO, RNA was extracted from WT MEF cells then used to synthesise cDNA. Levels of OGG1 mRNA were measured using real time PCR as described in section 2.10. To determine time-dependent changes in OGG1 expression during the 24 h BSO treatment period RNA was extracted from control and BSO treated (1000 µM) WT MEF cells 0, 6, 12, 18 and 24 h post treatment. Analysis by real time PCR revealed that there was no significant difference in Ct values between any control and treated samples ($P > 0.05$ as determined by one-way ANOVA) however there was a significant change in Ct values in control samples between 0 and 24 h. Therefore Ct values were normalised to a beta-actin loading control and expressed as fold change relative to untreated control (t=0). There was a time dependent increase in OGG1 mRNA levels which became statistically significant after 24 h in untreated samples. There was no difference between control and treated samples at any time point investigated (Figure 3.6).

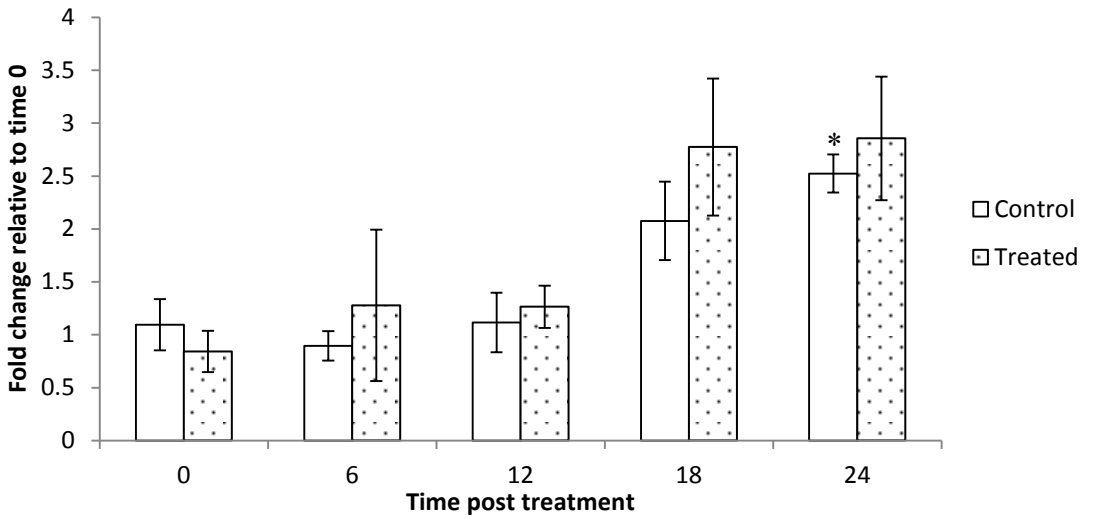

Figure 3.6: mOGG1 mRNA levels following BSO treatment.
WT MEF cells were treated with BSO (1000 μM) then OGG1 mRNA levels were measured at various times post treatment (0, 6, 12, 18, 24 h) by real time PCR (n = 3, performed in duplicate), normalised to a beta-actin control and expressed as fold change relative to untreated control at time 0 ±S.E.M. No significant difference between treated and untreated samples was observed. A significant increase in OGG1 mRNA levels was observed at 24 h. *: Significantly different from control at time 0 (*$P < 0.05$) as determined by 2-tailed Student's t-test.

3.2.7 OGG1 protein levels following BSO treatment

To determine the effect of BSO treatment on OGG1 protein levels several commercial antibodies specific to mouse OGG1 were tried, however OGG1 could not be detected in MEF cells. Mouse and rat OGG1 proteins show significant sequence homology and the rOGG1 protein was detectable in MH1C1 cells. For this reason, MH1C1 cells were used to investigate OGG1 protein levels following BSO treatment (24 h, 0, 1, 10, 100, 1000 μM) prior to nuclear protein extraction as described in section 2.11.1. OGG1 protein levels were determined by western blot as described in section 2.13 and normalised to a beta-actin loading control. A representative blot is shown (Figure 3.7A). Densitometry analysis was performed using ImageJ. Absorbance units (AU) after correction for beta-actin loading controls are plotted, with values displayed as percentage of untreated control. A significant increase in OGG1 protein levels was observed compared with control following 1 and 10 μM BSO treatment ($P > 0.05$ as determined by paired Student's *t*-test) (Figure 3.7B), but not following treatment with 100 and 1000 μM.

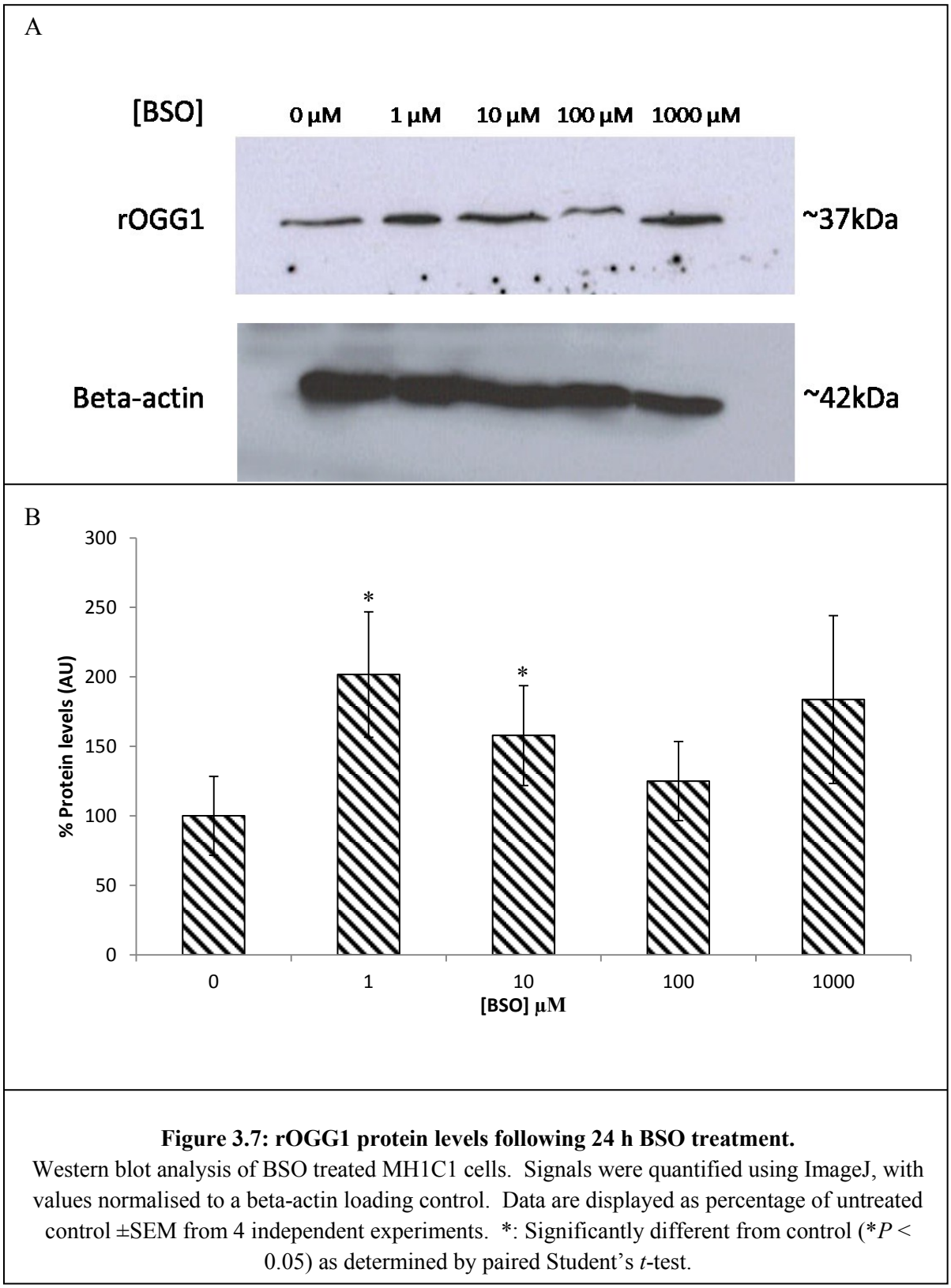

Figure 3.7: rOGG1 protein levels following 24 h BSO treatment.
Western blot analysis of BSO treated MH1C1 cells. Signals were quantified using ImageJ, with values normalised to a beta-actin loading control. Data are displayed as percentage of untreated control ±SEM from 4 independent experiments. *: Significantly different from control (*$P <$ 0.05) as determined by paired Student's *t*-test.

3.2.8 Rat OGG1 activity following BSO treatment

To determine the effect of reactive oxygen species on rOGG1 activity MH1C1 cells were treated with BSO (0, 1, 10, 100 and 1000 μM, 24 h) then transfected with an 8-oxo dG-containing molecular beacon prior to analysis by flow cytometry as described in section 2.9. Data are displayed as the number of positive events, as described in section 2.9.2. No statistically significant difference in fluorescence was observed following treatment with any concentration of BSO ($P > 0.05$ as determined by one way ANOVA) (Figure 3.8).

Transfection of MH1C1 cells with a positive control molecular beacon after BSO treatment (0, 1, 10, 100, 1000 μM, 24 h) allowed the assessment of transfection efficiency. No statistically significant difference in fluorescence was observed following treatment with BSO at any concentration ($P > 0.05$ as determined by one way ANOVA) (Bottom panel, figure 3.8).

The activities of mOGG1 and rOGG1 in MEF and MH1C1 cells following BSO treatment were compared, with data displayed as the number of positive events, as described in section 2.9.2. A statistically significant difference between fluorescence in WT MEF and MH1C1 cells was observed in untreated and low dose (1 μM) BSO treated cells (Figure 3.9).

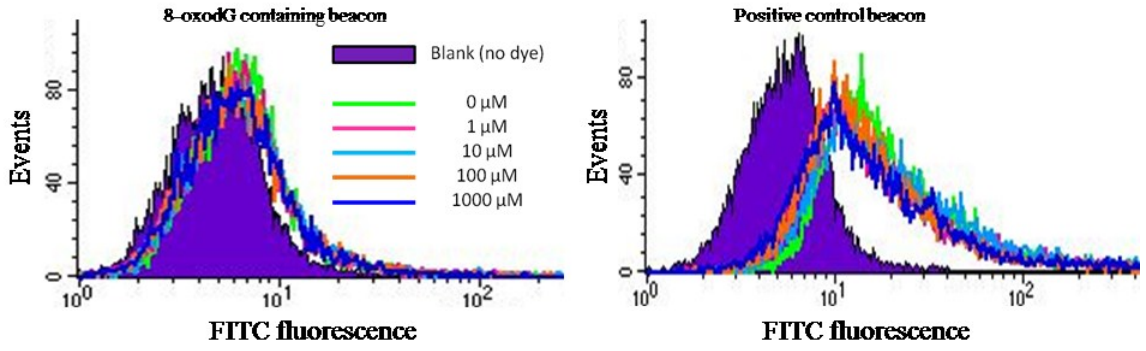

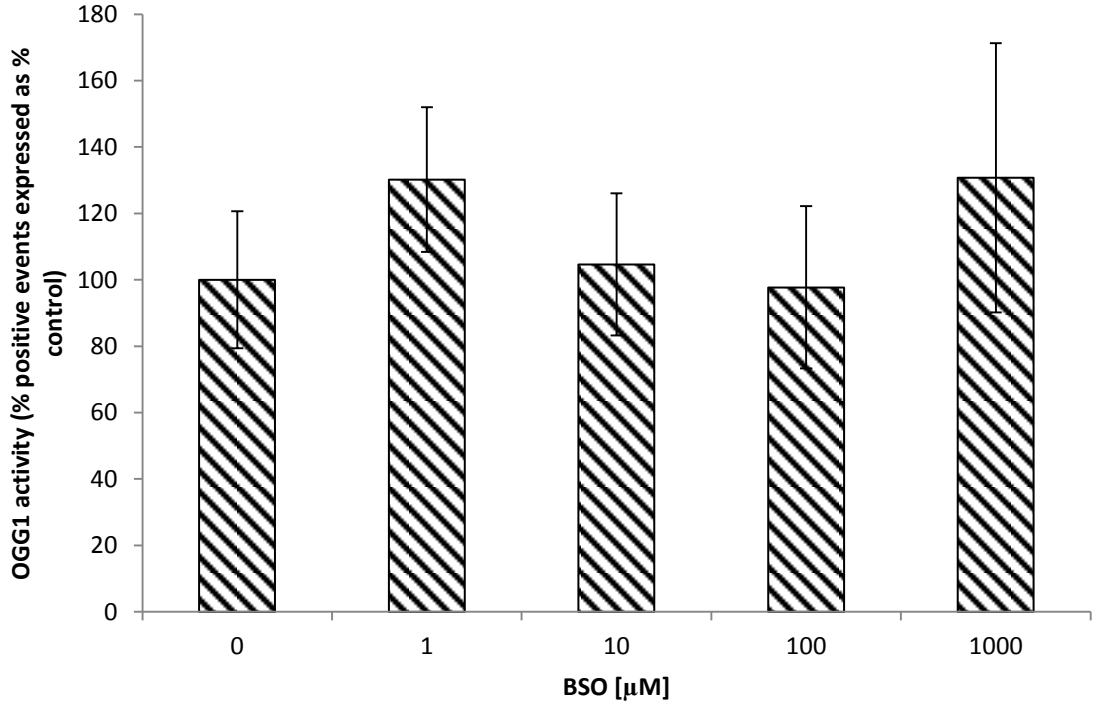

[BSO] µM	Number of positive control beacon events ±SEM
0	62.90±5.95
1	62.94±1.38
10	63.08±5.54
100	65.22±2.64
1000	56.80±1.65

Figure 3.8: rOGG1 glycosylase activity, as assessed by beacon fluorescence following 24 h BSO treatment.

Data are displayed as the number of positive events as percentage of untreated control (12.49±2.50), ±SEM from 4 independent experiments.

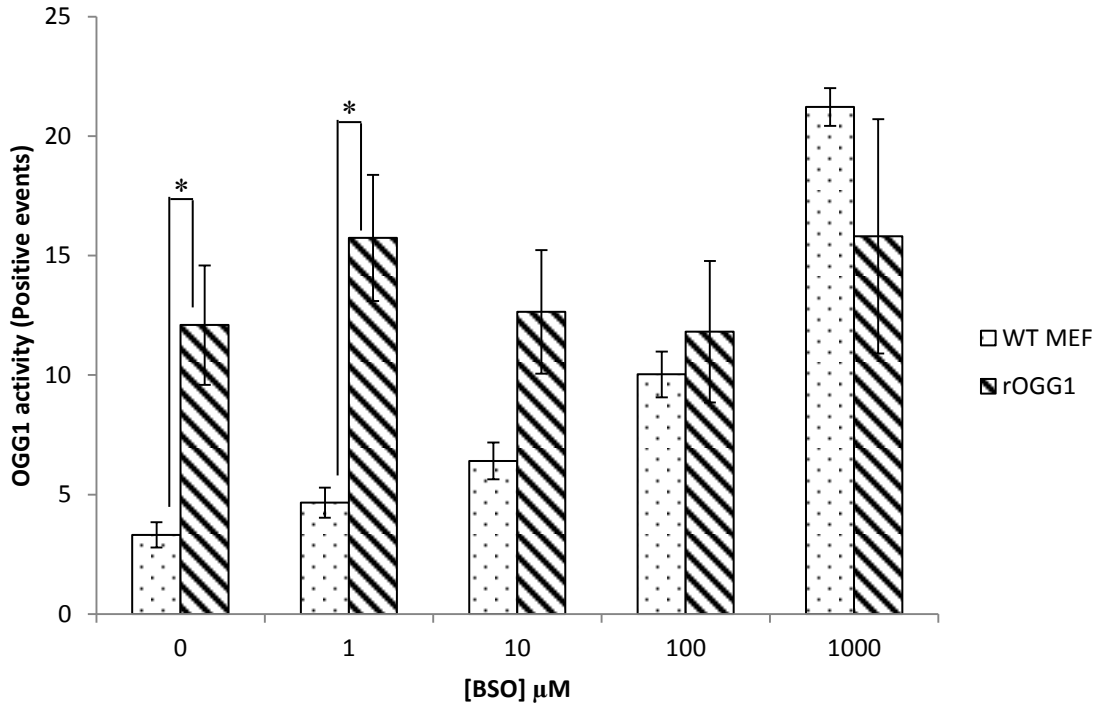

Figure 3.9: mOGG1 and rOGG1 glycosylase activity, as assessed by beacon fluorescence following 24 h BSO treatment.

Data are displayed as the number of positive events ±SEM from 3 (mOGG1) or 4 (rOGG1) independent experiments. *: Significantly different between cell types (*$P < 0.05$) as determined by 2-tailed Student's *t*-test.

3.3 Discussion

Intracellular ROS, which can oxidise DNA, are increased in a variety of pathological conditions including cancer, Alzheimer's disease and diabetes (Halliwell B. 2007; Reddy V.P. *et al.* 2009). An understanding of the mechanism of regulation of OGG1 activity following induction of oxidative stress is important as OGG1 is the only enzyme able to eliminate the potentially mutagenic 8-oxo dG lesion from genomic DNA. Previous studies have shown both OGG1 activity inhibition (Bravard A. *et al.* 2006; Hodges N.J. and Chipman J.K. 2002; Potts R.J. *et al.* 2003; Youn C.K. *et al.* 2005; Zharkov D.O and Rosenquist T.A. 2002) and induction (Ma H. *et al.* 2008; Mirbahai L. *et al.* 2010; Silva J.P. *et al.* 2009) following exposure to pro-oxidant compounds and the response appears to be cell and compound specific. In order to further investigate the response of OGG1 to cellular oxidative stress this study used the glutathione synthesis inhibitor BSO to induce oxidative stress conditions and investigate OGG1 activity, mRNA expression and protein levels.

Treatment of MEF and MH1C1 cells with BSO depleted glutathione and increased ROS in a concentration dependent manner with no effect on cell viability at the concentrations investigated. The highest BSO concentration used was selected based on its ability to deplete nuclear GSH in MEF cells (Green R.M. *et al.* 2006) however its effect on nuclear GSH in MH1C1 cells was not investigated. BSO treatment resulted in concentration dependent induction of ROS and mOGG1 activity. An increase in mOGG1 activity following an increase in ROS is easily rationalised as a response to the requirement of the cell to repair oxidatively damaged DNA, as an inability to rapidly repair 8-oxo dG lesions could result in the accumulation of G:C→T:A transversion mutations.

Interestingly, the activity increase in MEF cells was not a result of any change in mRNA levels because although OGG1 mRNA levels increased in culture over time, possibly as a result of stress in culture, this was not affected by BSO. This is in agreement with previous work in our laboratory using the same cells treated with potassium bromate (Mirbahai L. *et al.* 2010) and several other studies which demonstrate that the activity of OGG1 is modulated post-transcriptionally (Bhakat K.K. *et al.* 2006; Conlon K.A. *et al.* 2003; Silva J.P. *et al.* 2009).

It is possible that this activity increase could be due in part to an increased level of protein, however despite extensive testing no commercial mouse OGG1 antibody was found that could consistently detect mOGG1 in this cell line. As rat OGG1 shows extensive homology to mouse OGG1 and the rat OGG1 protein was very easily detected, this hypothesis was instead tested using MH1C1 cells to measure rat OGG1 protein levels following treatment with BSO. Interestingly, rOGG1 protein levels were significantly increased following treatment with low concentrations of BSO and appeared increased, although not statistically significantly, following treatment with very high concentrations of BSO. There was no significant change in rOGG1 activity following BSO treatment although, as with the protein levels, activity appeared greater following treatment with very low concentrations and very high concentrations of BSO.

Oxidative stress conditions are induced by BSO by depletion of GSH, which serves to deactivate ROS either by direct interaction or by the indirect activity of GSH peroxidases, to levels low enough to result in increased ROS. Both WT MEF cells and MH1C1 cells had similar levels of GSH prior to BSO treatment however higher BSO concentrations were required to deplete GSH in MH1C1 cells. All mammalian cells are

able to synthesise GSH but the major site of synthesis is the liver (Morand C. *et al.* 1997) and in hepatocytes, which export GSH, concentrations can reach 10 mM (Forman H.J. *et al.* 2009). It is therefore possible that in MH1C1 cells, which are derived from rat liver hepatomas, there is increased GCL therefore greater inhibition of GCL is required for GSH depletion, hence the requirement for increased concentrations of BSO.

Basal levels of ROS were lower in MH1C1 cells and were increased by BSO treatment to a lesser extent than in WT MEF cells, in agreement with the reduced decrease in GSH. It has been demonstrated that levels of oxidised purines show a positive linear correlation with levels of ROS and a negative linear correlation with levels of GSH (Green R.M. *et al*. 2006). It is therefore likely that fewer oxidised guanine residues were generated following BSO treatment in MH1C1 cells hence the requirement for OGG1-mediated repair was lower compared with MEF cells. A direct comparison between mOGG1 activity in WT MEF cells and rOGG1 activity in MH1C1 cells revealed that the basal rOGG1 activity was roughly four times greater than that of mOGG1 and comparable to the activity observed following 1000 μM BSO treatment in WT MEF cells. This suggests that the lack of induction of rOGG1 activity following increased ROS in these cells could be explained by the basal activity levels being great enough to repair any oxidatively damaged DNA arising as a result of modestly increased ROS. It is possible that increased concentrations of BSO or prolonged BSO exposure may further increase ROS and may result in an alteration of rOGG1 repair activity.

An improvement to our study would be the use of a mOGG1 antibody to detect mOGG1 protein following BSO treatment however we failed to find a suitable commercially available antibody and due to time and financial restrictions were unable to generate our

own. An increase in mOGG1 protein levels in MEF cells has however been previously shown following 2 hours of nutrient deprivation (Conlon K.A. *et al.* 2003). In agreement with our data, Conlon *et al.* (2003) note that the short time frame of their experiment suggests that the newly appearing mOGG1 is not the result of transcription. A study showing increased rOGG1 protein expression in photoreceptor synaptic terminals following bright light treatment in rats (Cortina M.S. *et al.* 2005) provides further evidence of oxidative stress induced modification of rOGG1 protein levels. However the low concentration BSO-initiated increase followed by high concentration decrease we observed in rOGG1 protein levels is difficult to interpret. There is evidence that low levels of oxidative stress induces cellular proliferation (Burden R. H. 1995), for example by activation of epidermal growth factor receptor (EGFR), and that rOGG1 mRNA expression is increased in foetal tissue during periods of rapid cellular proliferation (Riis B. *et al.* 2002).

The assessment of OGG1 cutting activity using the molecular beacon provides a measurement of overall cellular OGG1 activity. In contrast, this study measured nuclear rOGG1 protein levels. It is possible that nuclear rOGG1 protein levels increased in response to low levels of ROS but at higher BSO concentrations rOGG1 protein was relocated to the mitochondria. Mitochondrial DNA, which lacks protective histones and other DNA associated proteins are susceptible to ROS-induced damage and it is thought that OGG1 may represent the only 8-oxo dG repair pathway in mitochondria (de Souza-Pinto N.C. *et al.* 2001). Studies have shown that targeting OGG1 to mitochondria protects against this oxidative damage by enhancing mitochondrial DNA repair (Dobson A.W. *et al.* 2002; LeDoux S.P. *et al.* 2007; Rachek L.I. *et al.* 2002). There is some

evidence to support BER enzyme relocalisation in response to oxidative stress. For example, APE1, the major hydrolytic AP endonuclease responsible for cleavage of AP sites in mammalian cells, has been shown to re-localise from the nucleus to the mitochondria in the B-lymphocyte Raji cell line in response to oxidative stress induced by H_2O_2 (Frossi B. *et al.* 2002).

The response of OGG1 to oxidative stress conditions appears to be damage and cell specific (as noted recently by van Loon B. *et al.* 2010) and this study provides further evidence to support this. The data support evidence that the activity of OGG1 can be modulated in response to increased cellular ROS. Interestingly, the absence of any change in rOGG1 activity in MH1C1 cells, where ROS levels were lower, further supports this. It would be interesting to investigate the ROS response in a non-tumour rOGG1 expressing cell, as the contrasting MH1C1 and MEF responses could be related to the tumorous origin of the MH1C1 cells which may have altered DNA repair capacity and a greater tolerance for oxidative DNA damage.

The effect of oxidative stress induced by BSO on human OGG1 is of paramount interest as reduction of OGG1 activity under conditions of oxidative stress would result in reduced DNA repair capacity and sensitivity to chemically-induced oxidative DNA damage. The data presented here demonstrate that the activity of mouse OGG1 in MEF cells is modified post-transcriptionally following induction of oxidative stress by BSO. This justifies the use of transgenic cell lines expressing human OGG1 under the control of the cytomegalovirus (CMV) promoter (Chapter 4) to investigate the effect of ROS on human OGG1 and investigate any difference in response between the wild-type Ser326- and variant Cys326-hOGG1 proteins (Chapter 5).

Chapter 4 – Development of hOGG1 stably expressing cells to study Ser326- and Cys326-hOGG1 repair activity

4.1 Introduction

There is evidence that the Cys326-hOGG1 protein variant has a reduced repair ability compared with the wild-type Ser326-hOGG1, particularly under conditions of oxidative stress, as described in detail in section 1.6.2. To investigate such repair differences a variety of techniques have been employed including the use of the comet assay, bacterial complementation assays, cleavage assays, gel shift assays and more recently laser directed damage using multi-photon microscopy (Zielinska A.E. *et al.* 2011). Extensive use has been made of purified hOGG1 proteins and this has yielded both detailed structural information revealing the mechanistic basis for recognition and catalytic excision of 8-oxo dG, and important repair activity information (Bruner S.D. *et al.* 2000; Hill J.W. and Evans M.K. 2006). Human blood and tissue samples from individuals expressing either Ser326- or Cys326-hOGG1 have also been used to investigate activity differences *in vivo* and to establish cell lines (Bravard A. *et al.* 2009; Chen S.K. *et al.* 2003; Kondo S. *et al.* 2000; Lee A.J. *et al.* 2005).

Cultured mammalian cells provide a powerful tool for relatively large scale, inexpensive and fast investigations into DNA-repair activity of proteins and are advantageous to bacterial overexpression systems and studying purified protein as proteins are maintained in their cellular environment. This is particularly useful when observing the effect of oxidising cellular conditions. The overexpression of hOGG1 has been achieved by transient and stable transfection in a variety of cultured cells including AS52 and AA8 Chinese hamster ovary cells (Dahle J. *et al.* 2008; Hollenbach S. *et al.* 1999), HeLa cells (Bravard A. *et al.* 2009), human fibroblast GM00637 cells (Jeong H.G. *et al.* 2004) and mouse embryonic fibroblast cells (Oka S. *et al.* 2008).

Homozygous *Ogg1*$^{-/-}$ null mice have been generated by replacing approximately 4.6 kilo bases (kb) of genomic DNA, including the helix-hairpin-helix required for catalytic activity, with a targeting construct containing the neomycin (*neo)* resistance gene (Klungland A. *et al.* 1999). These knock-out mice are viable and have allowed the derivation of m*Ogg1*$^{-/-}$ embryonic fibroblast (KO MEF) cells which have been used to investigate the consequences of OGG1 deficiency and the role of OGG1 in 8-oxodG repair and prevention of mutagenesis (Klungland A. *et al.* 1999; Osterod M. *et al.* 2001).

Transiently transfected KO MEF provide an excellent model for the *in vitro* study of wild-type and mutant hOGG1 as they allow overexpression of hOGG1 proteins whilst eliminating background OGG1 activity levels. In our laboratory transiently transfected KO MEF cells have been successfully used to assess differences between Ser326- and Cys326-hOGG1 using the comet assay (Smart D. *et al.* 2006). Whilst useful, the process of transfection is variable and, as discussed further in section 4.3, limits the techniques that can be used to investigate activity. To extend our research into differences between wild-type and Cys326-hOGG1 this study generated KO MEF cells stably expressing Ser326- and Cys326-hOGG1.

4.2 Results

4.2.1 Hygromycin B selection optimisation

Hygromycin B resistance is conferred by the hygromycin B phosphotransferase (*hph*) gene encoded by the pIREShyg3 mammalian expression vector. In order to optimise colony selection conditions a KO MEF cell kill curve was constructed following treatment with hygromycin B (0, 25, 100, 200, 250 µg/ml) at 0 h, 24 h, 48 h, 72 h and 120 h (Figure 4.1). The results showed that 200 µg/ml Hygromycin B (120 h) was 100% lethal to non-transfected cells and this concentration was therefore used for selection of OGG1 expressing clones.

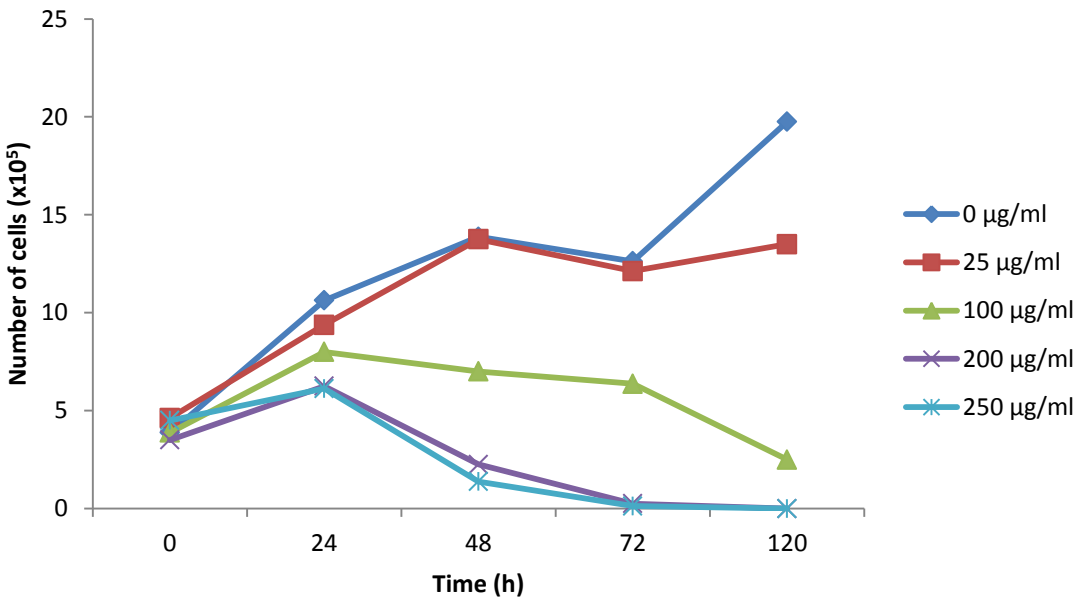

Figure 4.1: Hygromycin B kill curve.
KO MEF cells were cultured in 12 well plates then treated with hygromycin B (0, 25, 100, 200, 250 µg/ml). Live cells were counted at 0, 24, 48, 72 and 120 h post treatment. Data are displayed as numbers of live cells at each time point.

4.2.2 Initial hOGG1 activity screen

To generate stable transgenic cell lines KO MEF cells were transfected with Ser326- and Cys326-hOGG1 pIREShyg3 mammalian expression vectors and empty expression vector as a control, as described in section 2.8. After selection in hygromycin B (200 μg/ml, 120 h) colonies were picked and expanded then putative Ser326- and Cys326-hOGG1 MEF cell clones were assessed for OGG1 activity by transfection with an 8-oxo dG-containing molecular beacon prior to fluorescence analysis 48 h later by flow cytometry, as described in section 2.9. Cleaved beacon fluorescence, expressed as the percentage of fluorescent events greater than 10^1 on the FITC channel, was compared with that of 8-oxo dG-containing molecular beacon-transfected KO MEF cells. Ser326-hOGG1 transfected cells (S) and Cys326-hOGG1 transfected cells (C) were analysed separately with their own controls (Table 4.1).

Background (Blank) KO and WT MEF cell fluorescence was measured in the absence of transfection reagent and molecular beacon. To ensure the transfection reagent did not fluoresce, fluorescence was measured in KO and WT MEF cells after 48 h transfection with Turbofect™ alone, no fluorescence was observed (Table 4.1).

Table 4.1: OGG1 activity in putative Ser326- and Cys326-hOGG1 MEF cell clones.
Data are displayed as number of positive events and compared with KO MEF cells (fluorescence > than KO MEF cells = red, fluorescence < KO MEF cells = green). All samples were transfected with 8-oxo dG-containing molecular beacon for 48 h.

Sample	Positive events	Sample	Positive events
mOGG1$^{-/-}$ Blank	0.53	mOGG1$^{-/-}$ Blank	0.07
mOGG1$^{+/+}$ Blank	0.57	mOGG1$^{+/+}$ Blank	0.18
mOGG1$^{-/-}$ + Turbofect™	0.56	mOGG1$^{-/-}$ + Turbofect™	0.05
mOGG1$^{+/+}$ + Turbofect™	0.62	mOGG1$^{+/+}$ + Turbofect™	0.19
mOGG1$^{-/-}$	1.60	mOGG1$^{-/-}$	1.76
mOGG1$^{+/+}$	2.86	mOGG1$^{+/+}$	11.35
S1	4.29	C1	19.57
S2	6.35	C2	7.21
S3	5.50	C3	11.45
S4	1.48	C4	29.12
S5	8.76	C5	37.26
S6	11.02	C6	29.18
S7	1.25	C7	29.49
S8	2.01	C8	29.66
S9	5.38	C9	15.62
S10	1.93	C11	10.34
S11	1.52	C12	11.97
S12	2.29	C13	12.72
S13	0.66	C19	4.48
S14	4.62	C20	8.99
S15	3.48	C22	3.62
S16	3.16	C23	4.01
S17	10.06	C24	9.68
S18	3.71	C25	6.62
S19	8.27	C26	4.39
S20	1.99	C27	3.44
S21	6.71	C28	7.95
S22	3.94	C29	11.23
S23	3.14	C30	9.88
S24	9.81	C31	8.61
S25	5.93	C32	2.99
S26	2.97	C33	11.8
S28	5.35	C34	12.03
S29	2.68	C35	3.39
S30	4.72	C36	9.31
S31	2.27		
S32	1.99		
S33	2.05		

4.2.3 Human OGG1 protein expression

Cell lines which grew well and had high activity based on the 8-oxo dG-molecular beacon assay were selected and analysed for protein expression by western blot, as described in section 2.13. Transiently transfected Ser326- and Cys326-hOGG1 MEF cells and KO MEF cells were included as controls. hOGG1 protein was detected in S5, C8, C5 and C4 MEF cells, with S5 and C4 having the greatest levels as determined by densitometry using ImageJ (Integrated Density, S5:57307, C4:63471, C5:42881, C8:60164) (Figure 4.2). Based on this finding S5 and C4 MEF cells were selected.

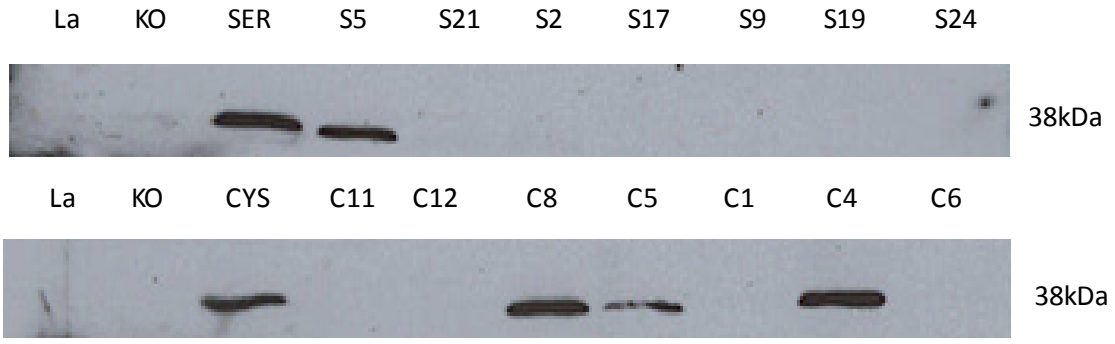

La	Ladder
KO (-ve control)	mOGG1 $^{-/-}$ null (KO) cells
SER (+ve control)	Transiently transfected Ser326-hOGG1 KO cells
CYS (+ve control)	Transiently transfected Cys326-hOGG1 KO cells
S-	Putative stable transgenic Ser326-hOGG1 cell line, no. -
C-	Putative stable transgenic Cys326-hOGG1 cell line, no. -

Figure 4.2: hOGG1 protein expression in putative Ser326- and Cys326-hOGG1 MEF cells. Protein expression was confirmed in S5, C8, C5 and C4 MEF.

4.2.4 Human OGG1 gene expression

To further confirm and characterise OGG1 expression RNA was extracted from KO, WT, Ser326-hOGG1 (S5), Cys326-hOGG1 (C4) and vector control-transfected MEF cells and used to synthesise cDNA to detect *hph* (hygromycin B) and h*OGG1* gene expression by PCR, as described in section 2.10. *hph* Gene expression was confirmed by the amplification of a 579 base pair (bp) product in S5, C4 and vector control-transfected MEF cells and absent in KO and WT MEF cells. h*OGG1* gene expression was confirmed by the amplification of a 279bp product in S5 and C4 MEF, and absent in KO MEF, WT MEF and vector control-transfected MEF cells (Figure 4.3).

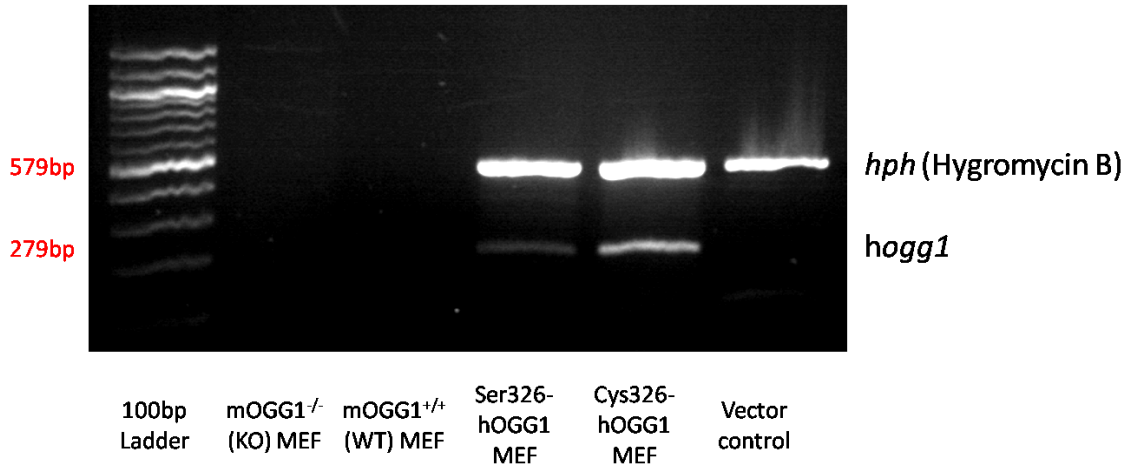

Figure 4.3: *hph* and h*OGG1* gene expression in Ser326- and Cys326-hOGG1 MEF cells. *hph* mRNA expression is indicated by the presence of a 579bp product in Ser326-hOGG1, Cys326-hOGG1 and vector control-transfected MEF. h*OGG1* mRNA expression is indicated by the presence of a 279 bp product in Ser326- and Cys326-hOGG1 MEF cells.

4.2.5 Quant ification of hOGG1 mRNA expression

Real-time PCR was used to quantify relative Ser326-hOGG1 and Cys326-hOGG1 expression in cell lines S5 and C4, as described in section 2.10. There was no significant difference in mRNA expression between the cell lines (Figure 4.4).

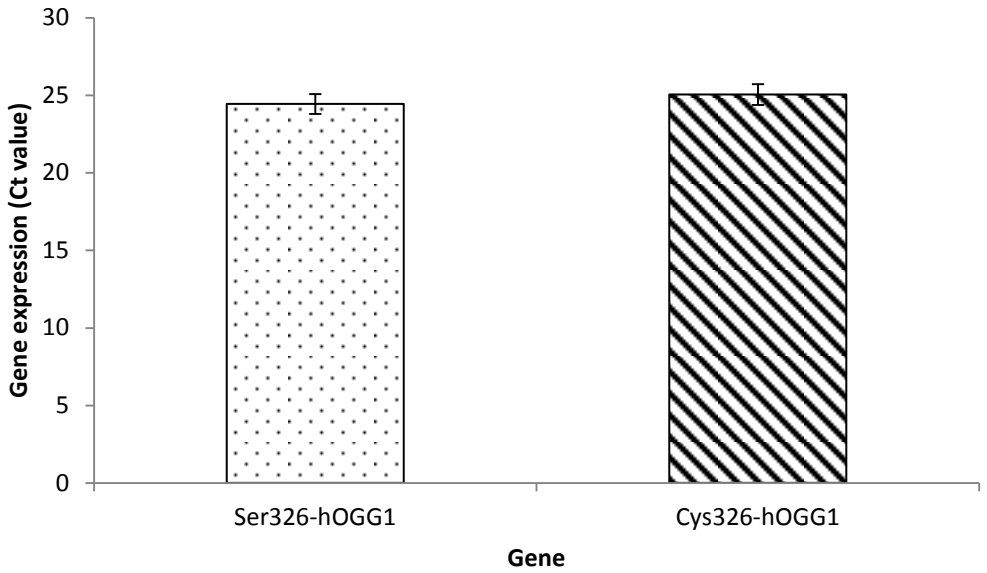

Figure 4.4: Relative *Ogg1* mRNA expression in Ser326- and Cys326-hOGG1 MEF cells. Ct values are plotted ±SEM. No significant difference in Ct values was observed ($P > 0.05$ as determined by one-way ANOVA).

4.2.6 Quantification of hOGG1 activity

Similar basal OGG1 activity was required for these cell lines to be a suitable model to investigate differences between Ser326- and Cys326-hOGG1. The relative activities of Ser326- and Cys326-hOGG1 were determined by transfecting MEF cells with an 8-oxo dG-containing molecular beacon prior to fluorescence analysis by flow cytometry as described in section 2.9. The number of Ser326- and Cys326-hOGG1 positive events (as described in section 2.9.2) are expressed as a percentage of mOGG1 positive events.

Ser326-hOGG1 and Cys326-hOGG1 both exhibited greater activity than mOGG1 but there was no statistically significant difference in activity between Ser326- and Cys326-hOGG1, as determined by 2-tailed Student's *t*-test (Figure 4.5). This is in agreement with the similar levels of expression detected by western blot and confirmed the suitability of the cells as a model system for the study of OGG1 repair.

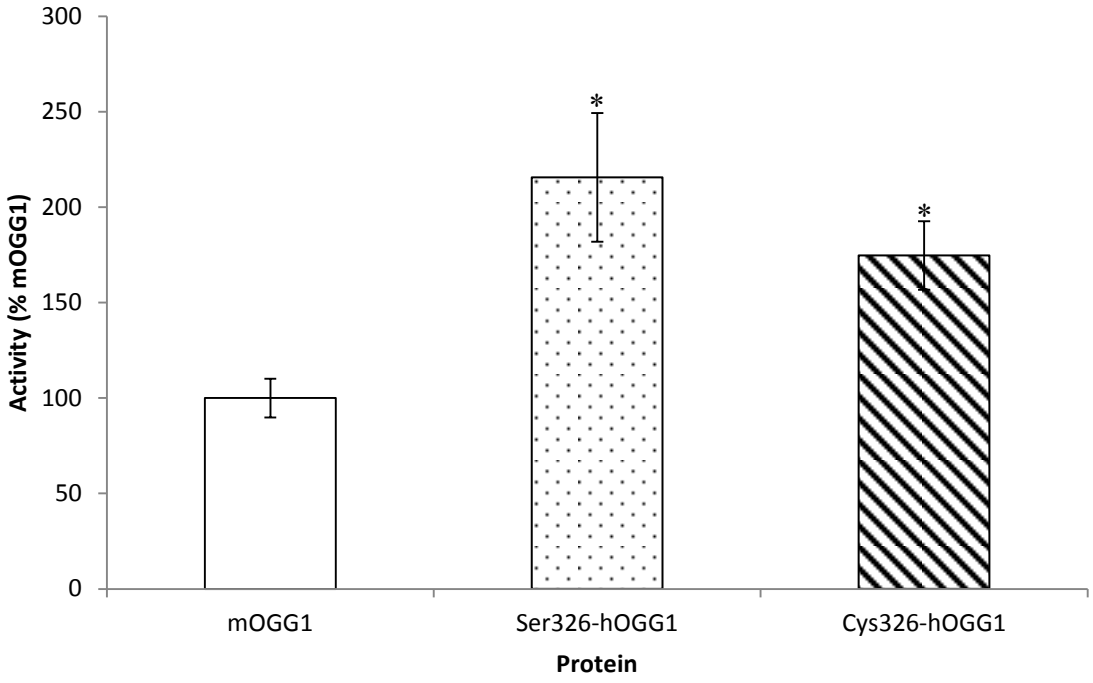

Figure 4.5: Relative OGG1 activity in Ser326- and Cys326-hOGG1 MEF cells
Data are displayed as percentage glycoslyase activity relative to mOGG1. *: Significantly different from mOGG1 ($P < 0.05$) as determined by 2-tailed Student's *t*-test.

4.2.6 Genomic incorporation of the OGG1 transgene

Genomic DNA was extracted from KO, WT, Ser326-hOGG1 (S5), Cys326-hOGG1 (C4) and vector control-transfected MEF cells and used to detect *hph* (hygromycin B) and h*OGG1* by PCR as described in section 2.10. *hph* Genomic DNA incorporation was confirmed by the amplification of a 579 bp product in S5, C4 and vector control-transfected MEF cells and shown to be absent in KO and WT MEF cells. h*OGG1* genomic DNA incorporation was confirmed by the amplification of a 279 bp product in S5 and C4 MEF cells and shown to be absent in KO, WT and vector control-transfected MEF cells (Figure 4.6).

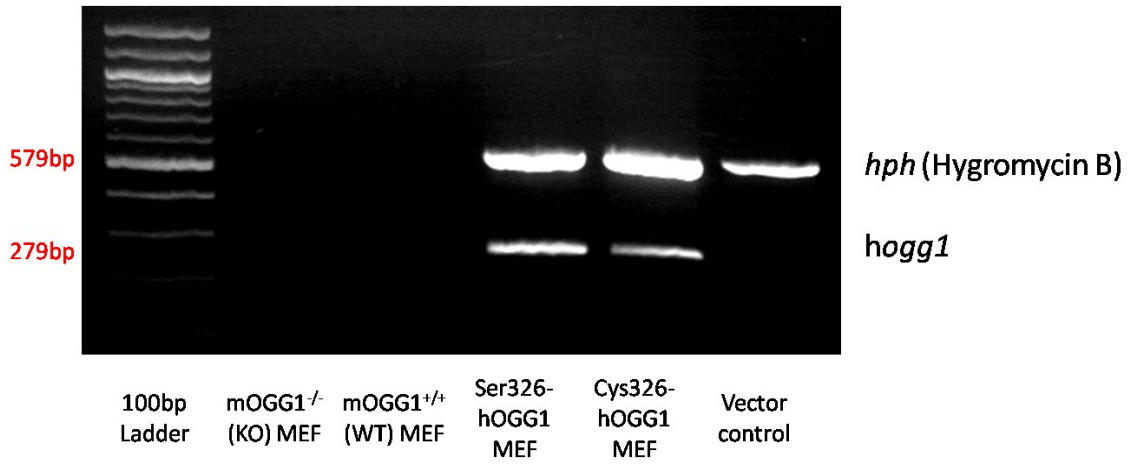

Figure 4.6: *hph* and h*OGG1* Genomic DNA incorporation in Ser326- and Cys326-hOGG1 MEF cells.

hph Genomic DNA incorporation is indicated by the presence of a 579bp product in Ser326-hOGG1, Cys326-hOGG1 and vector control-transfected MEF. h*OGG1* Genomic DNA incorporation is indicated by the presence of a 279 bp product in Ser326- and Cys326-hOGG1 MEF cells.

4.2.7 Confirmation of hOGG1 genotype by sequencing

The genotype of the S5 and C4 clones was confirmed by sequencing as described in section 2.10.5 (Figure 4.7).

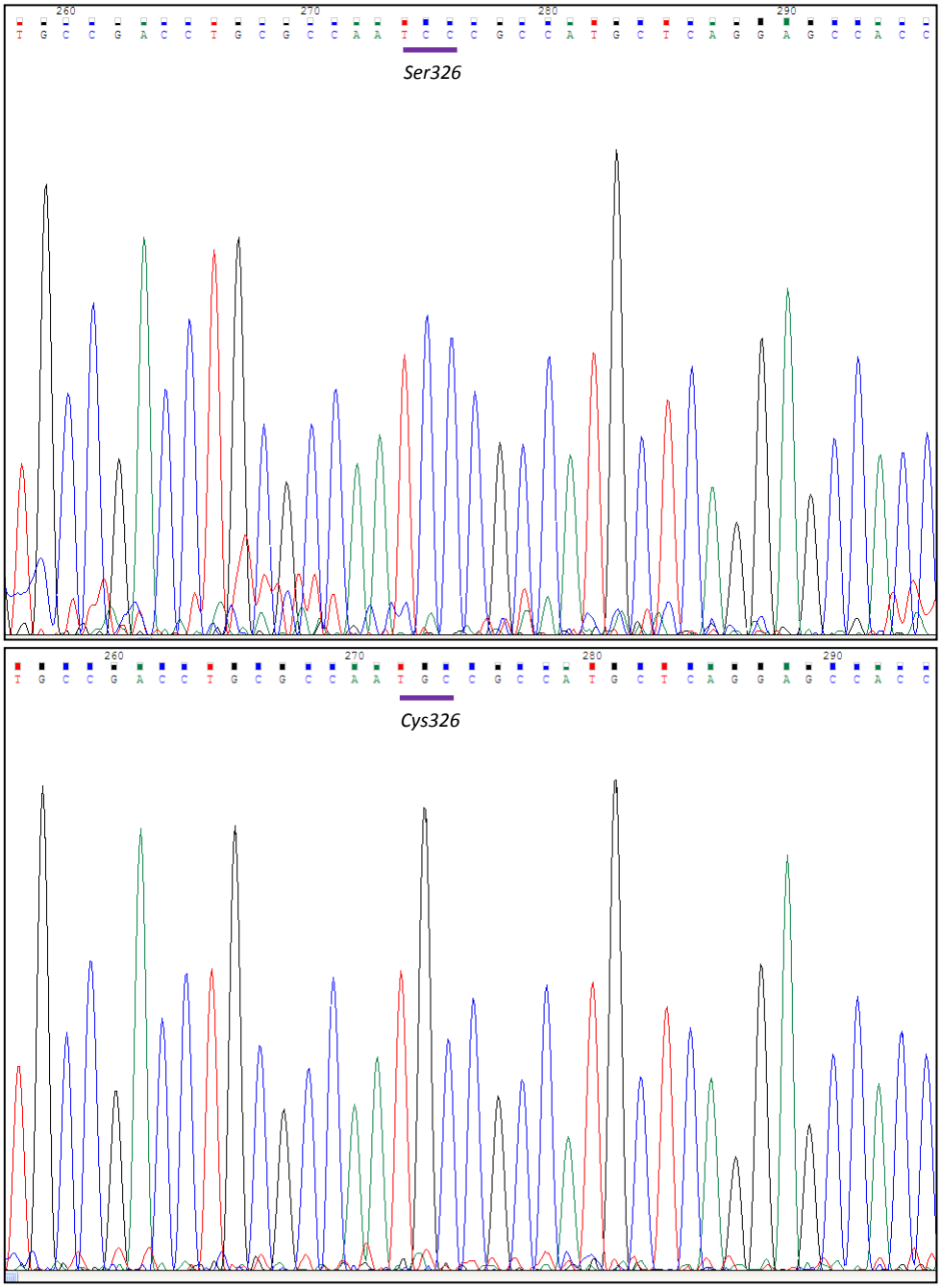

Figure 4.7: Confirmation of Ser326- and Cys326-hOGG1 sequence identity in Ser326- and Cys326-hOGG1 MEF cells.

4.2.8 Confirmation of hOGG1 activity

An oligonucleotide incision assay was used as an established method with an alternative measurement end-point to confirm hOGG1 activity in Ser326- and Cys326-hOGG1 MEF cells as described in section 2.12, n=1. Cleavage of the 8-oxo dG-containing oligonucleotide was observed in nuclear protein extract from WT, Ser326-hOGG1 (S5) and Cys326-hOGG1 (C4) MEF cells. Cleavage was not observed in nuclear protein extract from KO MEF cells. The oligonucleotide was incubated with lysis buffer B as a negative control and with formamidopyrimidine glycosylase (Fpg) (1 unit) as a positive control (Figure 4.8).

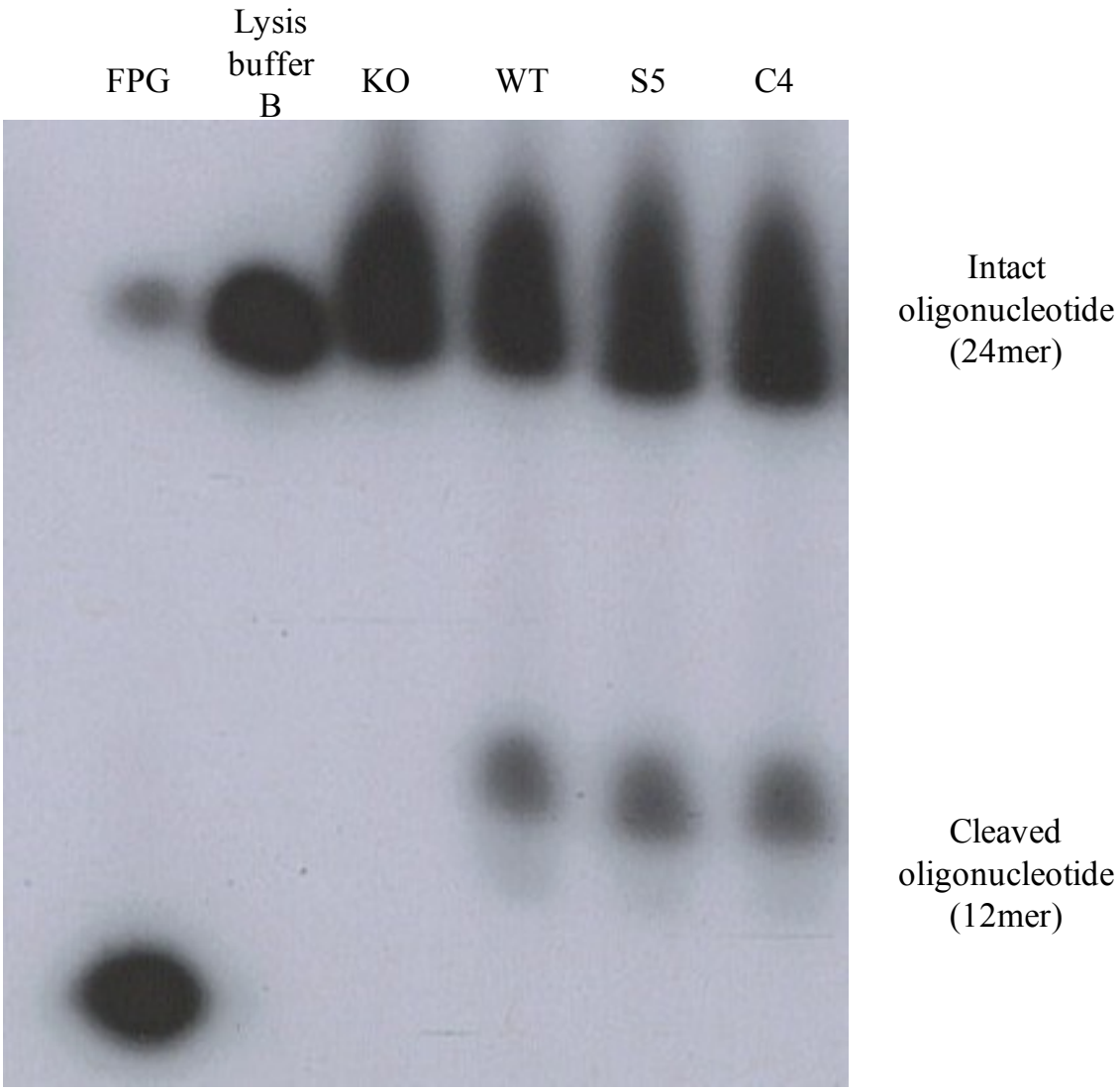

Figure 4.8: hOGG1 activity in WT, Ser326- and Cys326-hOGG1 MEF cells.
Cutting activity was detected in WT, Ser326-hOGG1 (S5) and Cys326-hOGG1 (C4) MEF cells (n=1). No cleavage was detected following incubation with extracts from KO MEF or with lysis buffer B.

4.3 Discussion

Many researchers have used OGG1-overexpressing transgenic cell lines to study the OGG1 protein. These studies have yielded important information about the protein including its localisation, post-translational modification and response to oxidative stress and DNA damage (Dahle J. *et al.* 2008; Dantzer F. *et al.* 2002; Hollenbach S. *et al.* 1999; Jeong H.G. *et al.* 2004; Luna L. *et al.* 2005; Oka S. *et al.* 2008). The substitution of serine 326 for cysteine has been linked with increased risk of various cancers (Cho E.Y. *et al*. 2003; Elahi A. *et al.* 2002; Kohno T. *et al.* 2006; Le Marchand L.L. *et al.* 2002; Park J. *et al.* 2004; Srivastava A. *et al.* 2009; Sugimura H. *et al.* 1999; Xing D.Y. *et al.* 2001) and transgenic cell lines have been successfully used to focus on possible differences in repair abilities between Ser326- and Cys326-hOGG1 (Bravard A. *et al.* 2009; Hill J.W. and Evans M.K. 2006; Smart D.J. *et al.* 2006).

The efficient removal of 8-oxo dG:C pairs is catalysed by mammalian OGG1 which has been shown to be the only DNA glycosylase that efficiently removes 8-oxo dG:C from DNA (Klungland A. *et al.* 1999). KO MEF cells do not express m*Ogg1* and as a result are unable to undergo OGG1-mediated BER. They are therefore extremely well suited to stably over-express the human OGG1 protein to address the objectives of this study. Previously, HeLa cells have commonly been used to overexpress hOGG1 (e.g. Dantzer F. *et al.* 2002; Luna L. *et al.* 2005) however these express low levels of endogenous hOGG1 and are a rapidly dividing cancer cell line. The MEF cells generated in the current study, in contrast to HeLa cells, have no background OGG1 expression and are karyotypically normal therefore, even allowing for the accumulation of mutations in culture, they offer a significant improvement to previous models.

This study used a pIREShyg3 bicistronic expression vector to enable the translation of two open reading frames from a single mRNA species. Translation of h*OGG1* and *hph*, which confers resistance to hygromycin B, occurs from the same mRNA molecule therefore cells resistant to treatment with hygromycin B should express h*OGG1*. An additional modification to the IRES sequence results in the attenuation of the efficiency of initiation of the *hph* resistance gene relative to that of h*OGG1*, resulting in the preferential selection of hygromycin B resistant cells with high h*OGG1* gene expression. Following transfection of KO MEF cells with Ser326-hOGG1-, Cys326-hOGG1- and empty pIREShyg3 vector, thirty six hygromycin B resistant clones were selected from both Ser326- and Cys326-hOGG1 pIREShyg3 transfected cells and those that grew to confluence were assessed for hOGG1 activity. Seven of those clones with the greatest hOGG1 activity were screened for protein expression and of those, the Ser326-hOGG1 and Cys326-hOGG1 clones with the greatest protein expression were further characterised.

This study successfully generated nuclear and functional Ser326- and Cys326-hOGG1 expressing KO MEF cells and confirmed hOGG1 genomic incorporation, protein expression and activity. The expression of both genes, under the control of the cytomegalovirus (CMV) promoter, was greater than that of mOGG1 and this was reflected in the OGG1 glycosylase activity, however there was no significant difference in their activities or protein expression therefore they provide a suitable model system for investigating relative repair differences between Ser326- and Cys326-hOGG1.

The generation of these cell lines has also allowed the use of a novel molecular beacon assay optimised in our laboratory which, coupled with either flow cytometry or confocal

microscopy, allows the specific measurement of OGG1 activity in live cells (Mirbahai L. *et al.* 2010; Priestley C.C. *et al.* 2010). This assay, which involves the transfection of an 8-oxo dG-containing molecular beacon into cultured cells, was previously impractical using a transient transfection model as it involved a poorly tolerated double transfection (data not shown). Following the successful generation of these cell lines this technique has been employed to investigate Ser326-hOGG1 and Cys326-hOGG1 repair ability differences following induction of oxidative stress conditions (Chapter 5).

Chapter 5 – Response of Ser326- and Cys326-hOGG1 to oxidative stress

5.1 Introduction

Inflammation and exposure to cigarette smoke, ionising radiation, environmental pollution, toxic food ingredients and sunlight can all result in increased cellular ROS and increased 8-oxo dG formation (Ma Q. 2009). Efficient repair of 8-oxo dG by hOGG1 is required to prevent errors during DNA replication and elevated frequency of mutation and cancer. Epidemiological evidence suggests that under normoxic conditions risk of cancers including nasopharyngeal, oesophageal, gallbladder and lung is increased in individuals homozygous for the S326C h*OGG1* allele (Cho E.Y. *et al*. 2003; Kohno T. *et al.* 2006; Le Marchand L.L. *et al.* 2002; Park J. *et al.* 2004; Srivastava A. *et al.* 2009; Sugimura H. *et al.* 1999; Xing D.Y. *et al.* 2001). When external factors are evaluated such as smoking, alcohol or meat consumption the risk of head and neck squamous cell carcinoma, colon, orolaryngeal and stomach cancer is increased in CC homozygotes (Elahi A. *et al.* 2002; Hashimoto T. *et al.* 2006; Kim J.I. *et al.* 2003; Lan Q. *et al.* 2004; Li W.Q. *et al.* 2009; Takezaki T. *et al.* 2002; Zhang Z. *et al.* 2004).

It is accepted that in addition to the separate contributions of genetic differences and environmental factors, interactions between the two are important in disease development (Hunter D.J. 2005) and epidemiological evidence supports an interaction between the Cys326-h*OGG1* allele and environmental exposure to ROS resulting in increased risk of cancer. In support of this, whilst evidence for reduced repair activity of Cys326-hOGG1 under normoxic conditions is conflicting, with reduced repair observed by some (Bravard A. *et al.* 2009; Kohno T. *et al.* 1998) but not others (Blons H. *et al.* 1999; Dherin C. *et al.* 1999; Hardie L.J. *et al.* 2000; Janssen K. *et al.* 2001; Kondo S. *et al.* 2000; Li D. *et al.* 2002; Park Y.J. *et al.* 2001; Shinmura K. *et al.* 1998), it is becoming

increasingly clear that reduced repair ability of Cys326-hOGG1 becomes more apparent under oxidising conditions (Bravard A. *et al.* 2009; Chen S.K. *et al.* 2003; Hill J.W. and Evans M.K. 2006; Lee A. *et al.* 2005; Smart D. *et al.* 2006; Yamane A. *et al.* 2004).

The mechanism underlying any difference in repair ability is poorly understood. It is possible that the loss of a potential regulatory serine residue could affect activity as the phosphorylation of Ser326 has been shown to be important in hOGG1 localisation, with Cys326-hOGG1 excluded from the nucleoli during S-phase (Luna L. *et al.* 2005). An increasing body of evidence supports the alternative possibility that repair activity could be affected by the introduction of a redox-sensitive cysteine residue, as repair defects are more marked under oxidising conditions. Redox state modulation of hOGG1 activity has previously been demonstrated, with recovery of decreased Cys326-hOGG1 activity following the addition of reducing agents (Bravard A. *et al.* 2006; Bravard A. *et al.* 2009). The additional cysteine thiol group is susceptible to the formation of sulphenic acid under conditions of oxidative stress which can disulphide bond with a nearby thiol (Biswas S. *et al.* 2006). There is evidence that Cys326 can be easily involved in disulphide bond formation (Bravard A. *et al.* 2009) and purified Cys326-hOGG1 has been shown to exist as a dimer that is dependent on residues C-terminal to Cys326 (Hill J.W. and Evans M.K. 2006).

To extend the work of Hill and Evans (2006) and investigate hOGG1 dimer formation in live cells, a relatively new fluorescence based technique; bimolecular fluorescence complementation (BiFC) was employed in the current study. This assay is useful for investigating protein-protein interactions in living cells (Hu C.D. *et al.* 2002; Kerppola T.K. 2008; Kerppola T.K. 2009) and involves the reconstitution of fluorescence of

yellow fluorescent protein (YFP) by the association of two non-fluorescent YFP half molecules fused to proteins of interest, such as hOGG1 (Figure 2.1). The fluorescence resulting from this association can be quantified by flow cytometry and visualised by confocal microscopy. Using BiFC to study hOGG1 dimer formation rather than EMSA allows investigation of dimer formation in live cells, without the removal of the OGG1 protein from its native environment. Additionally, the technique could reveal important information about the intracellular localisation of any dimer products.

In addition to investigation of possible OGG1 dimer formation by BiFC, results are presented in this chapter of Ser326- and Cys326-hOGG1 activity, gene expression, protein levels and protein localisation following oxidative stress induction by BSO treatment using stably expressing cells described in chapter 4.

5.2 Results

5.2.1 Cell viability following BSO treatment

To investigate BSO mediated cytotoxcity, MEF cells were cultured in 96 well cell culture plates and treated for 24 h with BSO (0, 1, 10, 100, 1000 μM) prior to analysis by the MTT reduction assay, as described in section 2.4. No statistically significant difference in absorbance was observed between untreated and BSO treated cells ($P > 0.05$ as determined by one-way ANOVA) indicating that 24 h treatment with up to 1000 μM BSO does not affect the viability of these cells (Figure 5.1).

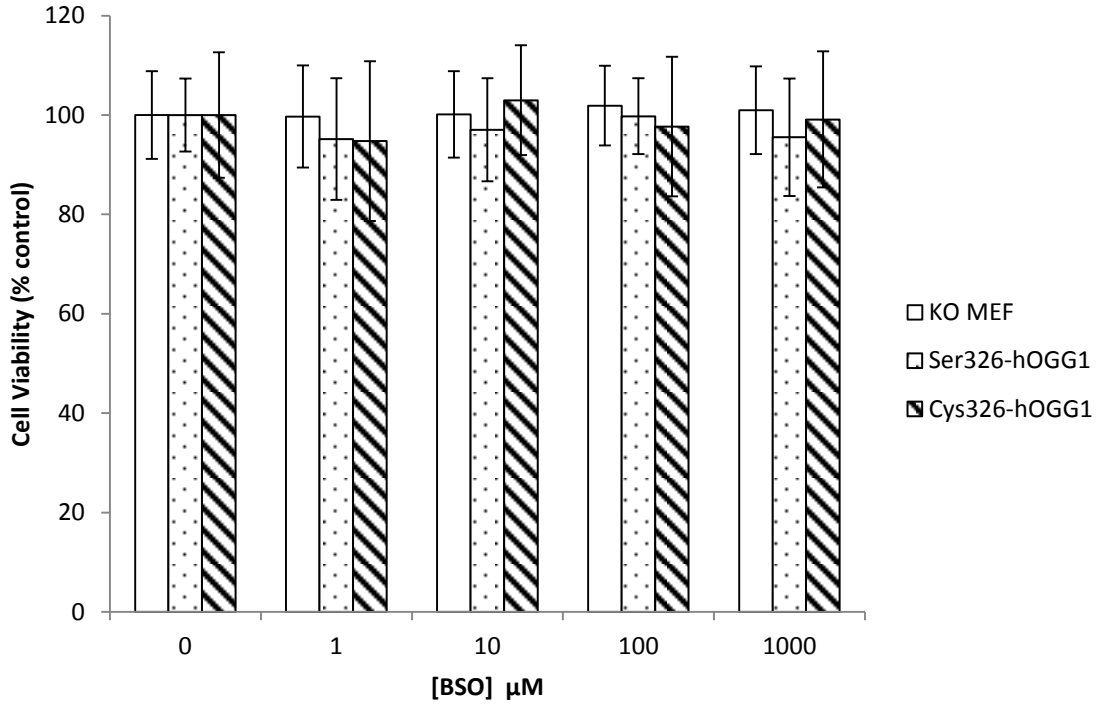

Figure 5.1: Viability of MEF cells after 24 h BSO treatment as assessed using the MTT reduction assay.

Data are displayed as percentage of untreated control ±SEM from 3 independent experiments.

5.2.2 Total cellular reduced glutathione following BSO treatment

Treatment with BSO for 24 h at concentrations ≥ 1 μM has been shown to deplete cytoplasmic GSH in KO MEF cells, with nuclear depletion occurring following treatment with 1000 μM BSO (Green R.M. *et al.* 2006). To determine and compare the levels of total GSH in Ser326-hOGG1 MEF and Cys326-hOGG1 MEF after BSO treatment (0, 1, 10, 100, 1000 μM, 24 h), cells were treated then total GSH was measured as described in section 2.6.

Statistically significant depletion of total cellular GSH occurred following treatment with ≥ 1 μM BSO in KO and Ser326-hOGG1 MEF cells. In Cys326-hOGG1 MEF cells statistically significant depletion of total GSH occurred following treatment with ≥ 10 μM BSO. No significant difference in total GSH was observed between any of the MEF cell lines following treatment with any concentration of BSO ($P > 0.05$ as determined by one-way ANOVA) (Figure 5.2).

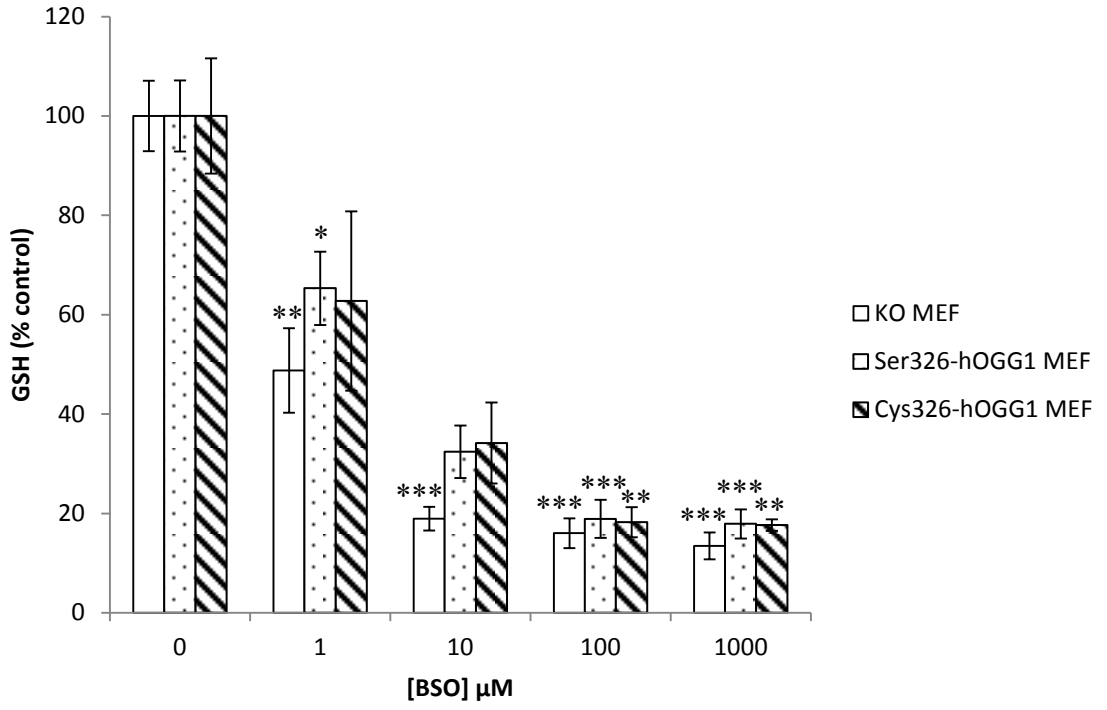

Figure 5.2: Total GSH in MEF cells after 24 h BSO treatment.
Data are displayed as percentage of untreated control (nm GSH/mg protein. KO MEF: 18.54 ± 1.32, Ser326-hOGG1 MEF: 24.77 ± 1.77, Cys326-hOGG1 MEF: 19.88 ± 2.30) ±SEM from 3 independent experiments. *,**,***: Significantly different from control (*$P < 0.05$ **$P < 0.01$ ***$P < 0.001$) as determined by 2-tailed Student's *t*-test.

5.2.3 Intracellular ROS following BSO treatment

Using the fluorescent dye dichlorofluorescein, intracellular ROS have been shown to be induced in KO MEF cells with 24 h BSO treatment at concentrations ≥ 100 μM (Green R.M. *et al.* 2006). The current study modified the technique used by Green *et al.* and employed the use of flow cytometry to measure intracellular ROS levels, as described in section 2.5.

Fluorescein fluorescence was statistically significantly increased compared with untreated control in all cell lines following treatment with ≥ 10 μM BSO. There was no statistically significant difference in response between any of the cell lines (Figures 5.3 and 5.4).

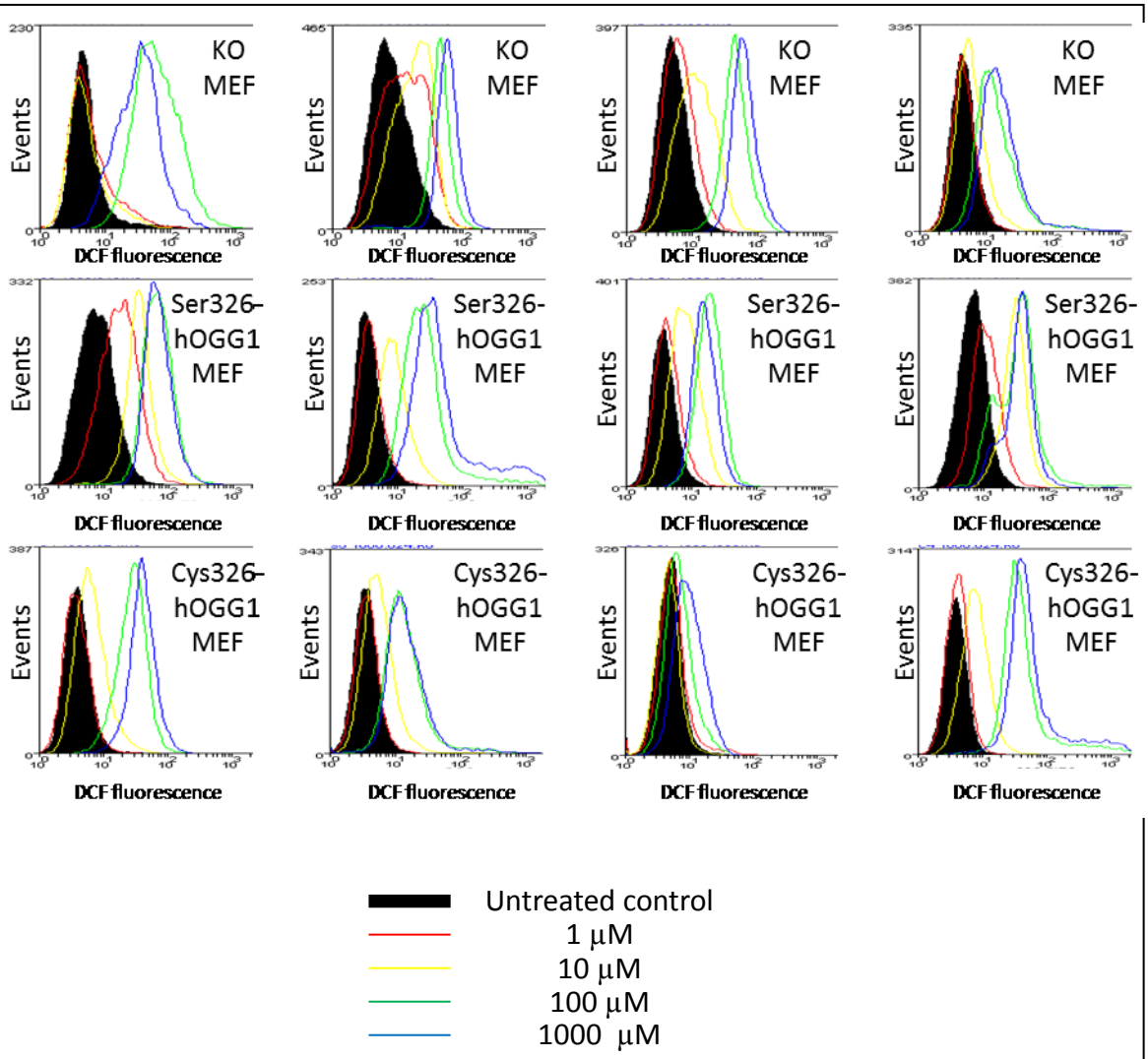

Figure 5.3: ROS levels, as assessed by DCF fluorescence in MEF cells after 24 h BSO treatment.

Individual replicates are displayed (n = 4).

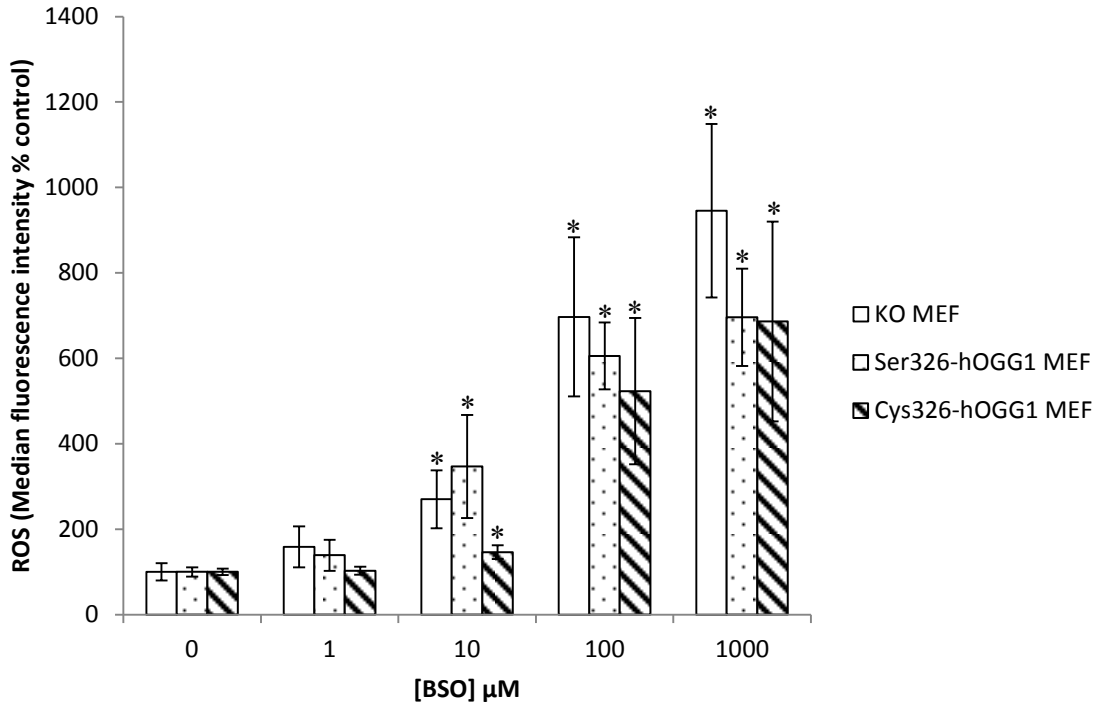

Figure 5.4: ROS levels in MEF cells after 24 h BSO treatment.
Data are displayed as median fluorescence intensity as percentage of untreated control ±SEM from 4 independent experiments. *: Significantly different from control ($P < 0.05$) as determined by Mann-Whitney U test.

5.2.4 hOGG1 activity following BSO treatment

To determine the effect of BSO on Ser326- and Cys326-hOGG1 repair activity, Ser326- and Cys326-hOGG1 MEF were treated with BSO (0, 1, 10, 100, 1000 μM, 24 h) then transfected with an 8-oxo dG-containing molecular beacon prior to fluorescence analysis by flow cytometry as described in section 2.9 and confocal microscopy as described in section 2.14.

Data are expressed as the number of positive events (as described in section 2.9.2) as a percentage of time matched untreated control (Figure 5.6A) or as a percentage of untreated control (Figure 5.6B and C). Following treatment with 1000 μM BSO, a peak in beacon fluorescence was observed after 12 h in Ser326-hOGG1 MEF cells and after 24 h in Cys326-hOGG1 MEF cells (Figure 5.5 and 5.6A). Beacon fluorescence in both Ser326- and Cys326-hOGG1 expressing cells increased in a concentration dependent manner following BSO treatment (Figure 5.5 and Figure 5.6B and C).

Beacon fluorescence was visualised using confocal microscopy 12 hours (Figures 5.7 and 5.8) and 24 hours (Figures 5.9 and 5.10) post BSO treatment. This confirmed the increase in fluorescence and indicated that although there is some faint cytoplasmic staining, the majority of the cleaved beacon appeared to be in the nucleus of the cells.

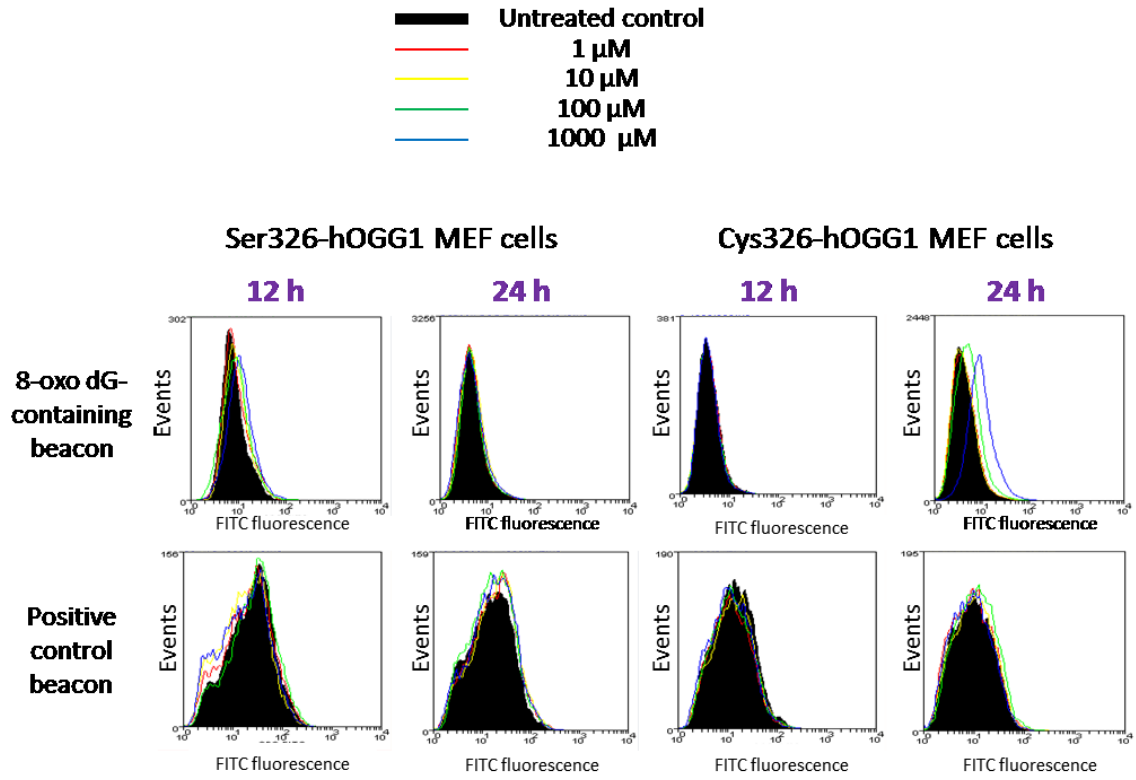

Figure 5.5: Ser326- and Cys326-hOGG1 activity, as assessed by beacon fluorescence following BSO treatment.

Representative histograms are displayed.

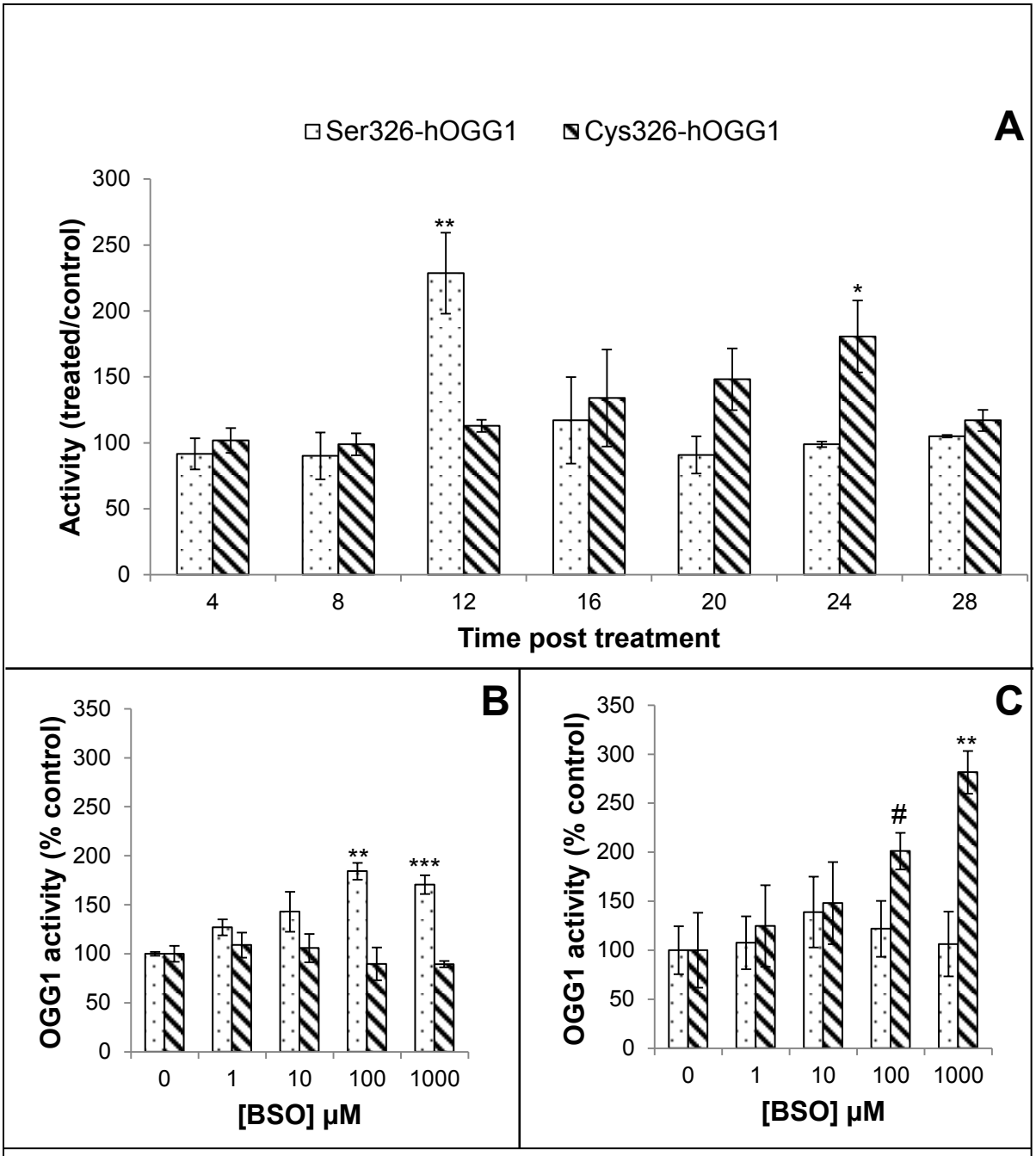

Figure 5.6: Ser326- and Cys326-hOGG1 activity following BSO treatment.
A: Time-dependent increase in hOGG1 activity, with each bar representing the number of positive beacon events of treated cells (1000 µM BSO) as a percentage of time-matched untreated cells. **B:** Concentration-dependent increase in activity in Ser326-hOGG1 MEF cells 12 h post BSO treatment. **C:** Concentration-dependent increase in activity in Cys326-hOGG1 MEF cells 24 h post BSO treatment. Data are expressed as the number of positive beacon events as a percentage of untreated control, ±SEM from 4 independent experiments. Significantly different from untreated control (#$P = 0.05$ *$P < 0.05$ **$P < 0.01$ ***$P < 0.001$) as determined by 2-tailed Student's *t*-test.

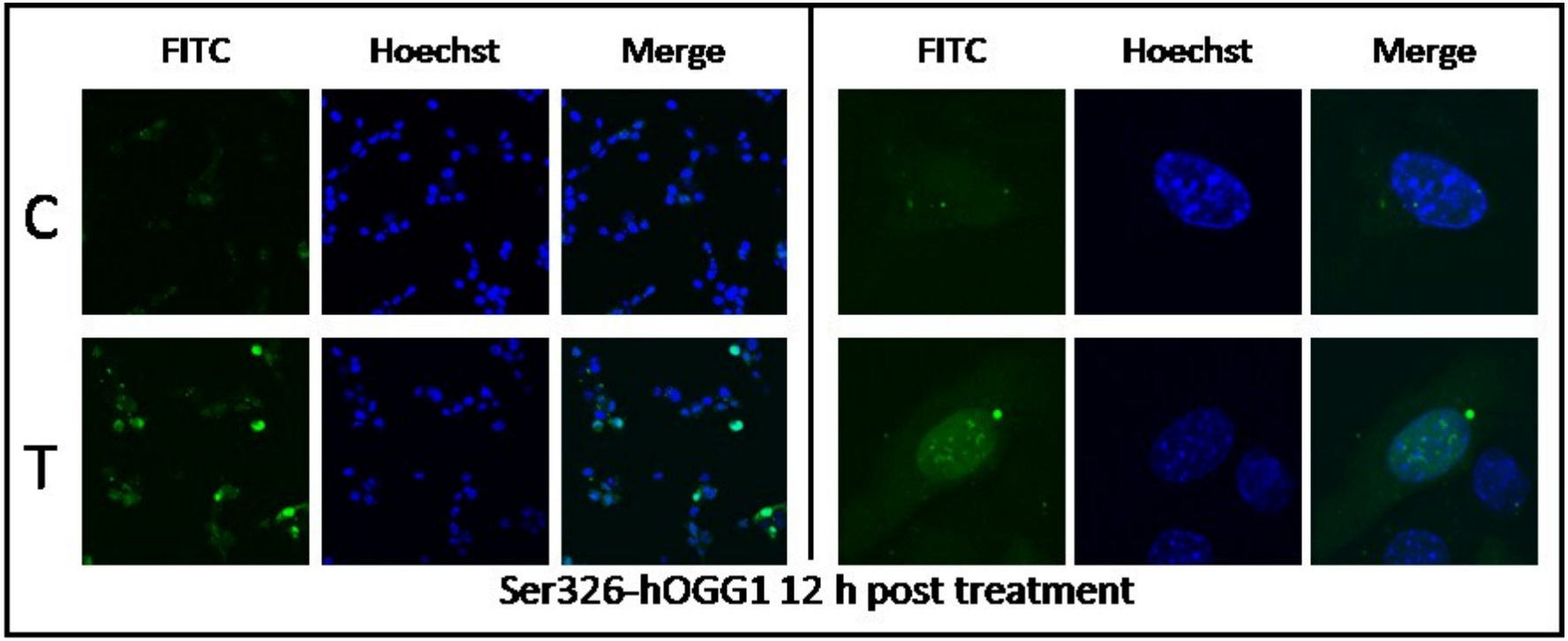

Figure 5.7: Confocal microscopy analysis of cleaved 8-oxo dG-molecular beacon in Ser326-hOGG1 MEF cells 12 hours post BSO treatment (1000 µM).

OGG1 activity was visualised by the FITC fluorescence (green channel) of cleaved beacon. The nucleus was visualised by Hoechst stain (blue channel). C = control, T = treated.

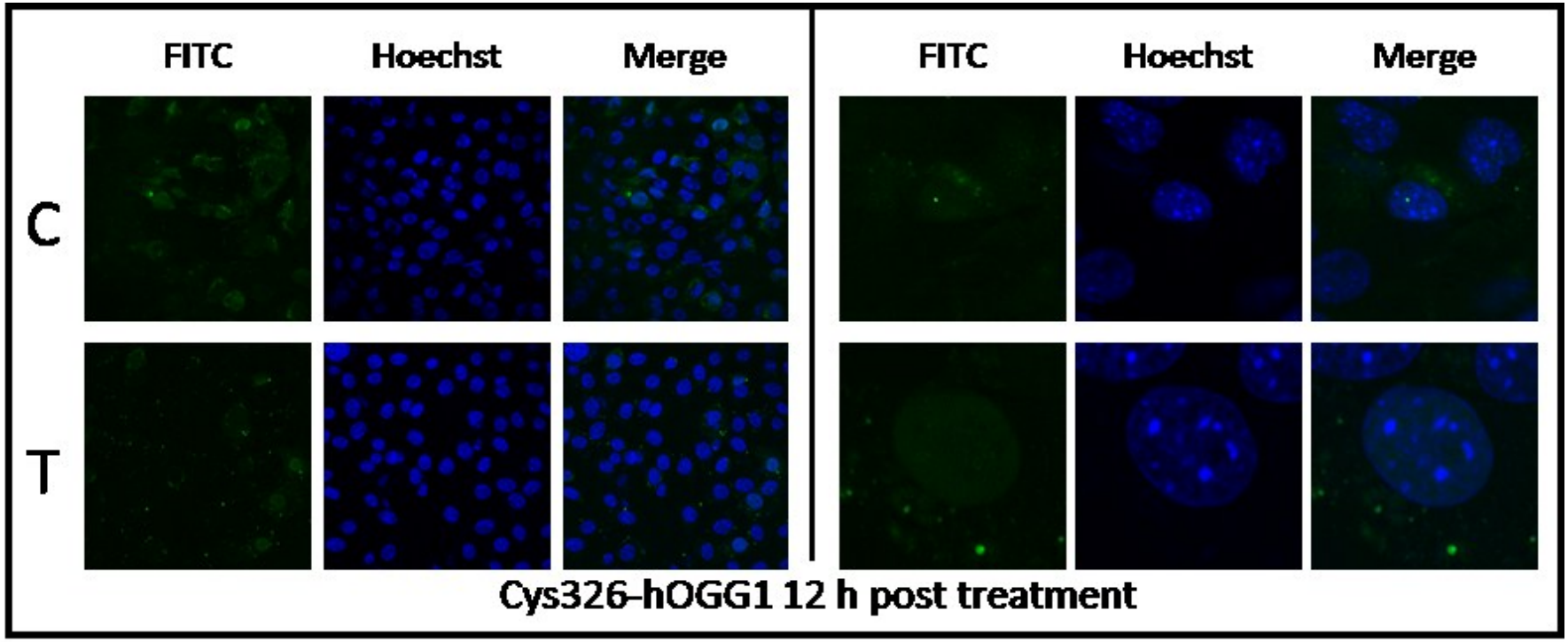

Figure 5.8: Confocal microscopy analysis of cleaved 8-oxo dG-molecular beacon in Cys326-hOGG1 MEF cells 12 hours post BSO treatment (1000 μM).

OGG1 activity was visualised by the FITC fluorescence (green channel) of cleaved beacon. The nucleus was visualised by Hoechst stain (blue channel). C = control, T = treated.

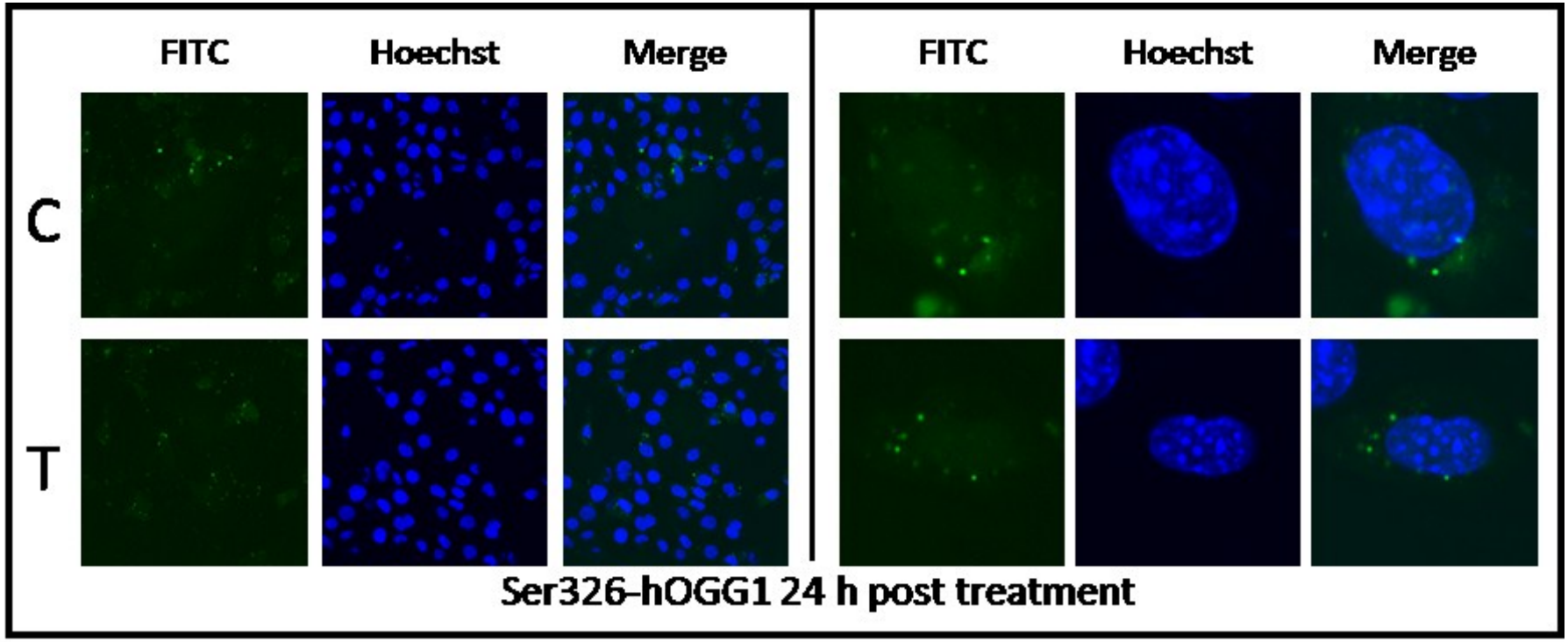

Figure 5.9: Confocal microscopy analysis of cleaved 8-oxo dG-molecular beacon in Ser326-hOGG1 MEF cells 24 hours post BSO treatment (1000 µM).

OGG1 activity was visualised by the FITC fluorescence (green channel) of cleaved beacon. The nucleus was visualised by Hoechst stain (blue channel). C = control, T = treated.

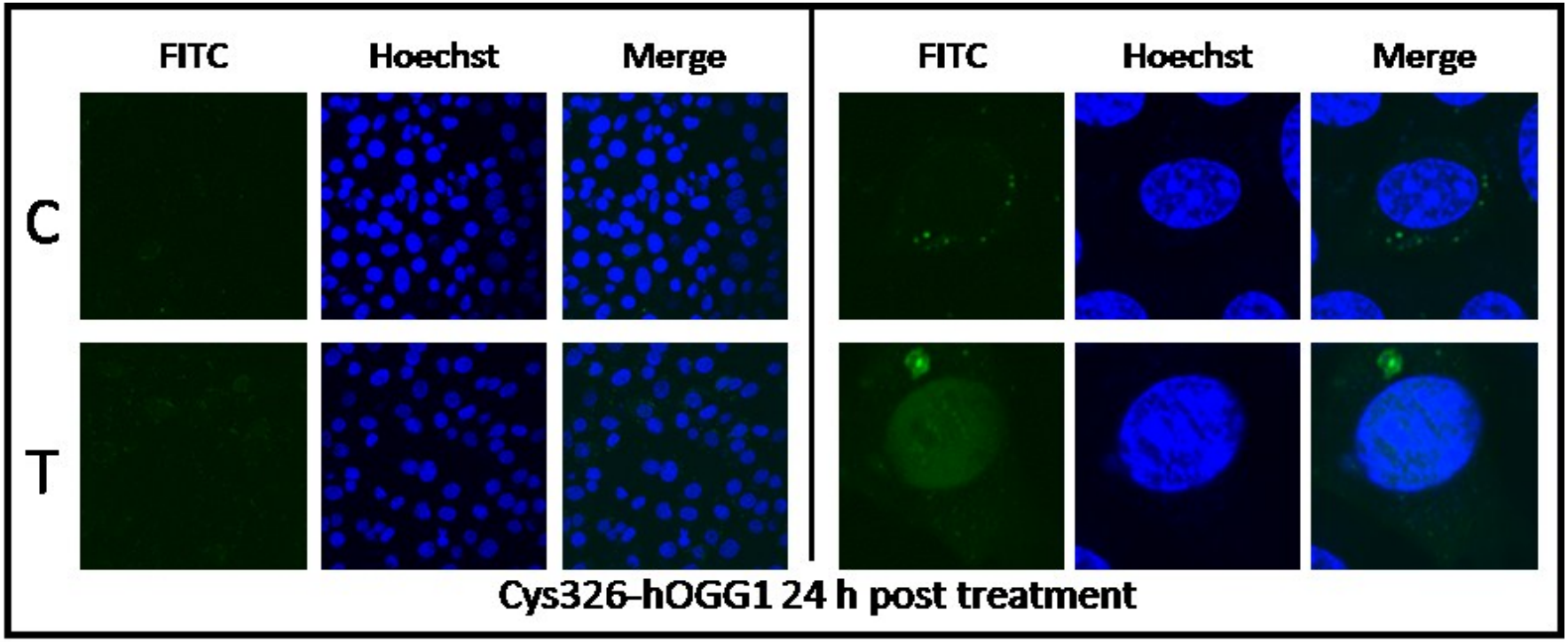

Figure 5.10: Confocal microscopy analysis of cleaved 8-oxo dG-molecular beacon in Cys326-hOGG1 MEF cells 24 hours post BSO treatment (1000 µM).

OGG1 activity was visualised by the FITC fluorescence (green channel) of cleaved beacon. The nucleus was visualised by Hoechst stain (blue channel). C = control, T = treated.

Transfection of Ser326-hOGG1 and Cys326-hOGG1 MEF cells with a positive control molecular beacon after BSO treatment (0, 1, 10, 100, 1000 μM, 24 h) allowed the assessment of transfection efficiency. Using flow cytometry no statistically significant difference in fluorescence was observed following treatment with BSO at any concentration investigated ($P > 0.05$ as determined by Kruskal-Wallis test) (Table 5.1). Using confocal microscopy, fluorescence was detected 12 hours (Figures 5.11 and 5.12) and 24 hours (Figures 5.13 and 5.14) post BSO treatment, with no difference in localisation observed between the cell types of following BSO treatment. Positive control beacon fluorescence was present in the nucleus and cytoplasm.

Table 5.1: Ser326- and Cys326-hOGG1 positive control beacon events

[BSO] μM	Ser326-hOGG1 MEFs (12 h post treatment)	Cys326-hOGG1 MEFs (12 h post treatment)	Ser326-hOGG1 MEFs (24 h post treatment)	Cys326-hOGG1 MEFs (24 h post treatment)
0	72.03±3.19	74.11±5.10	78.31±8.05	73.63±7.71
1	71.86±4.47	71.44±6.70	69.51±12.14	71.74±10.27
10	70.10±2.53	69.73±5.37	69.36±17.27	64.45±16.06
100	72.90±5.67	70.58±5.67	66.41±18.81	64.72±15.44
1000	69.37±4.81	67.83±8.62	67.98±16.67	68.89±16.09

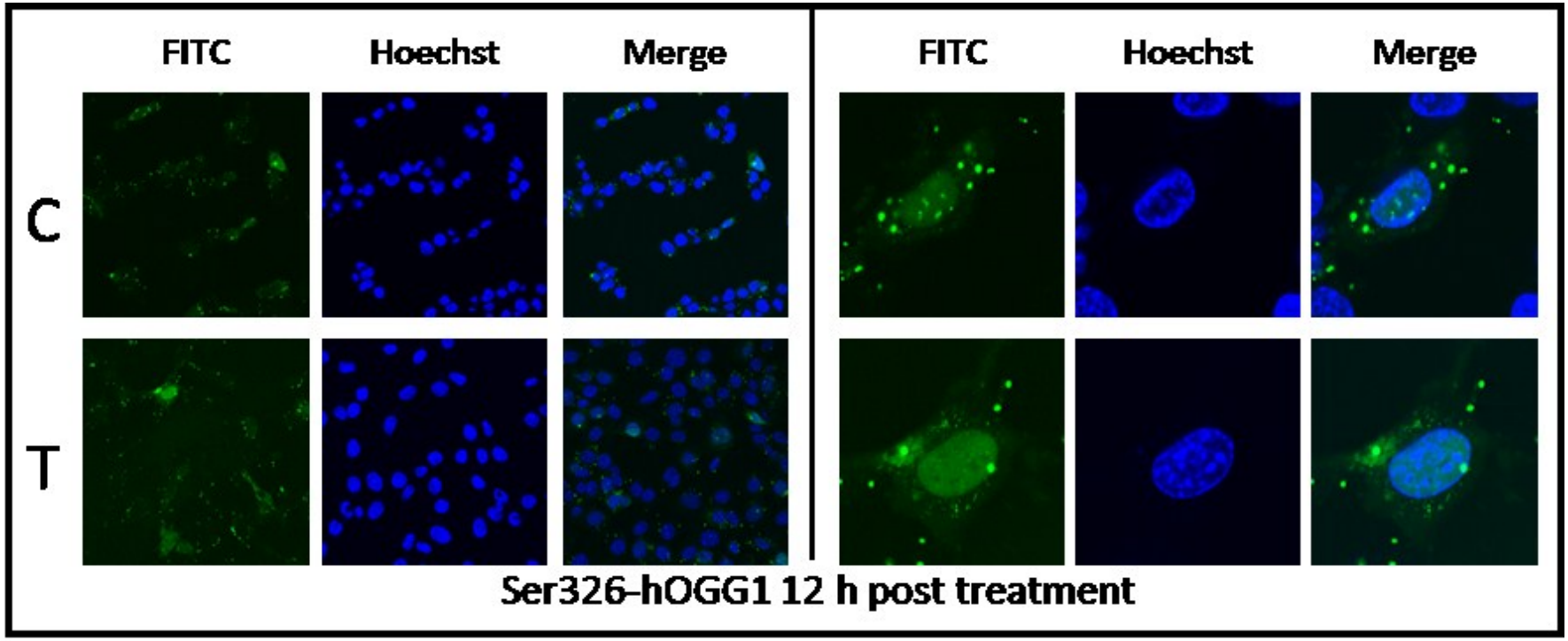

Figure 5.11: Confocal microscopy analysis of positive control beacon in Ser326-hOGG1 MEF cells 12 hours post BSO treatment (1000 µM). Positive control molecular beacon fluorescence was visualised by FITC fluorescence (green channel). The nucleus was visualised by Hoechst stain (blue channel). C = control, T = treated.

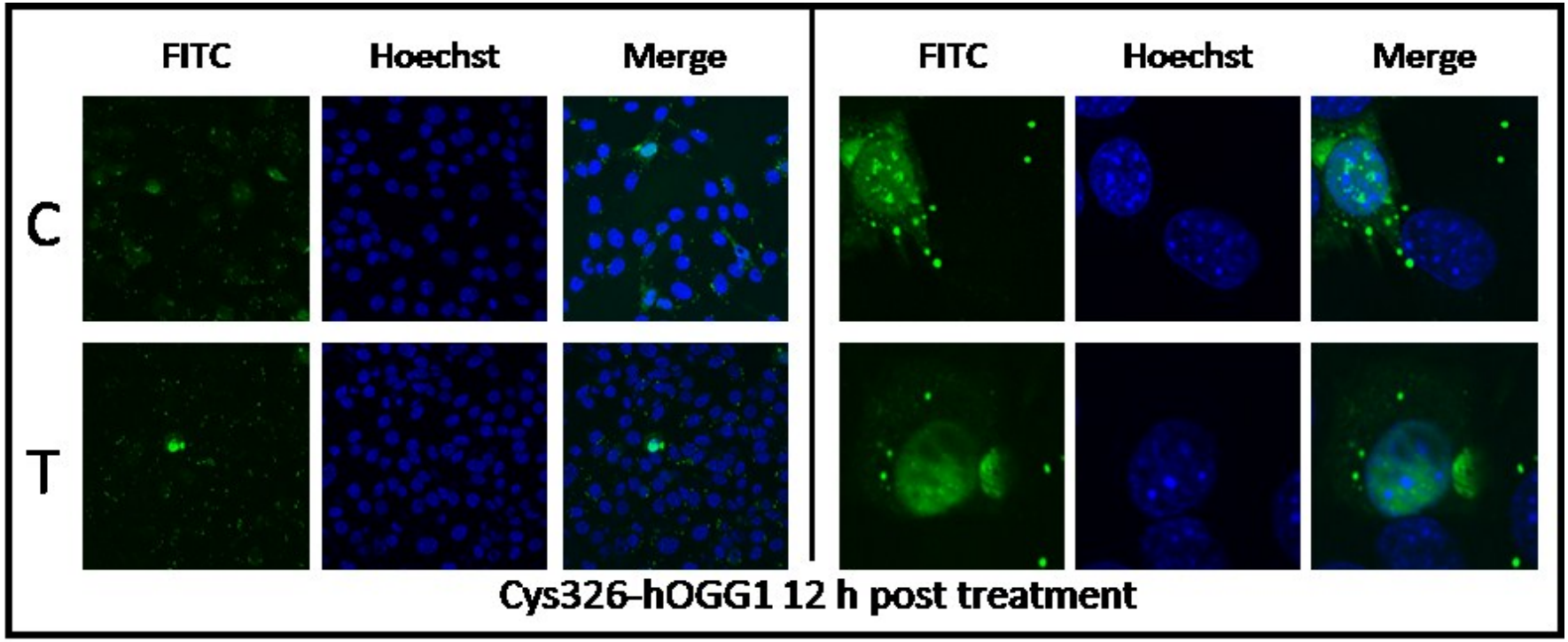

Figure 5.12: Confocal microscopy analysis of positive control beacon in Cys326-hOGG1 MEF cells 12 hours post BSO treatment (1000 µM). Positive control molecular beacon fluorescence was visualised by FITC fluorescence (green channel). The nucleus was visualised by Hoechst stain (blue channel). C = control, T = treated.

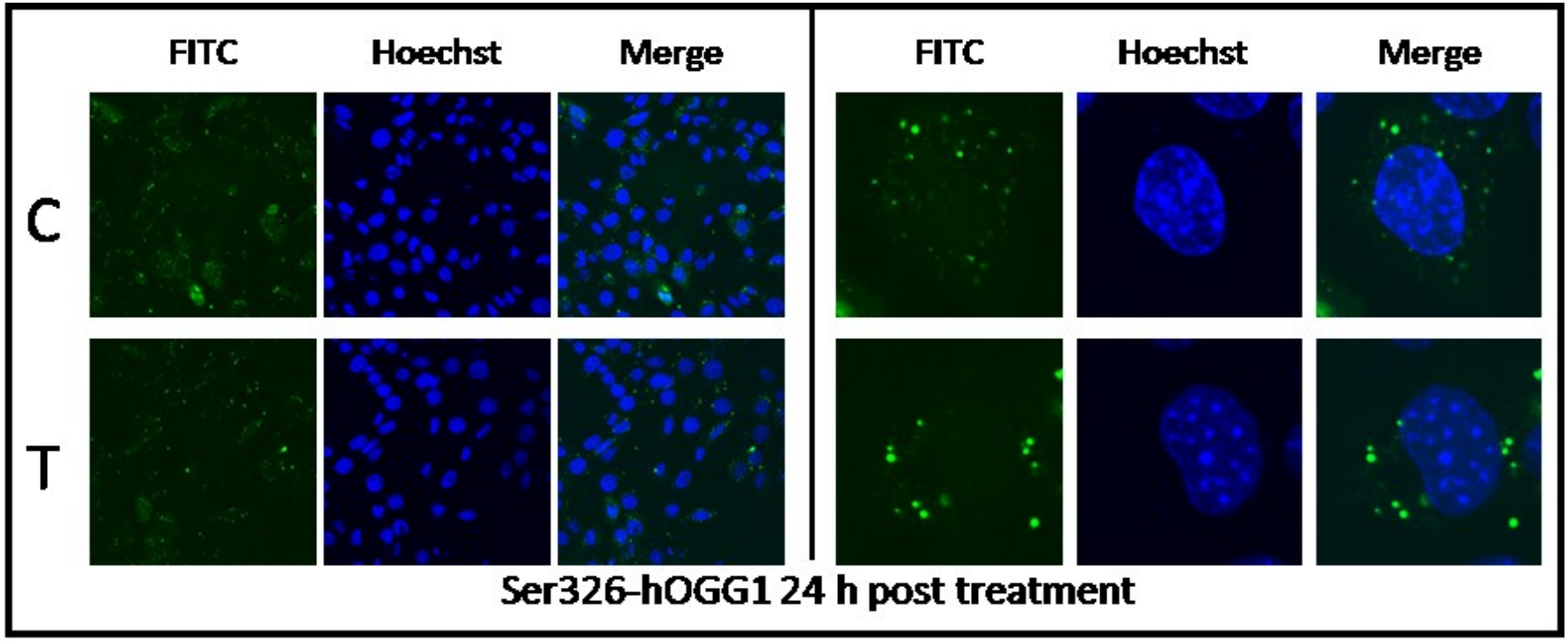

Figure 5.13: Confocal microscopy analysis of positive control beacon in Ser326-hOGG1 MEF cells 24 hours post BSO treatment (1000 µM). Positive control molecular beacon fluorescence was visualised by FITC fluorescence (green channel). The nucleus was visualised by Hoechst stain (blue channel). C = control, T = treated.

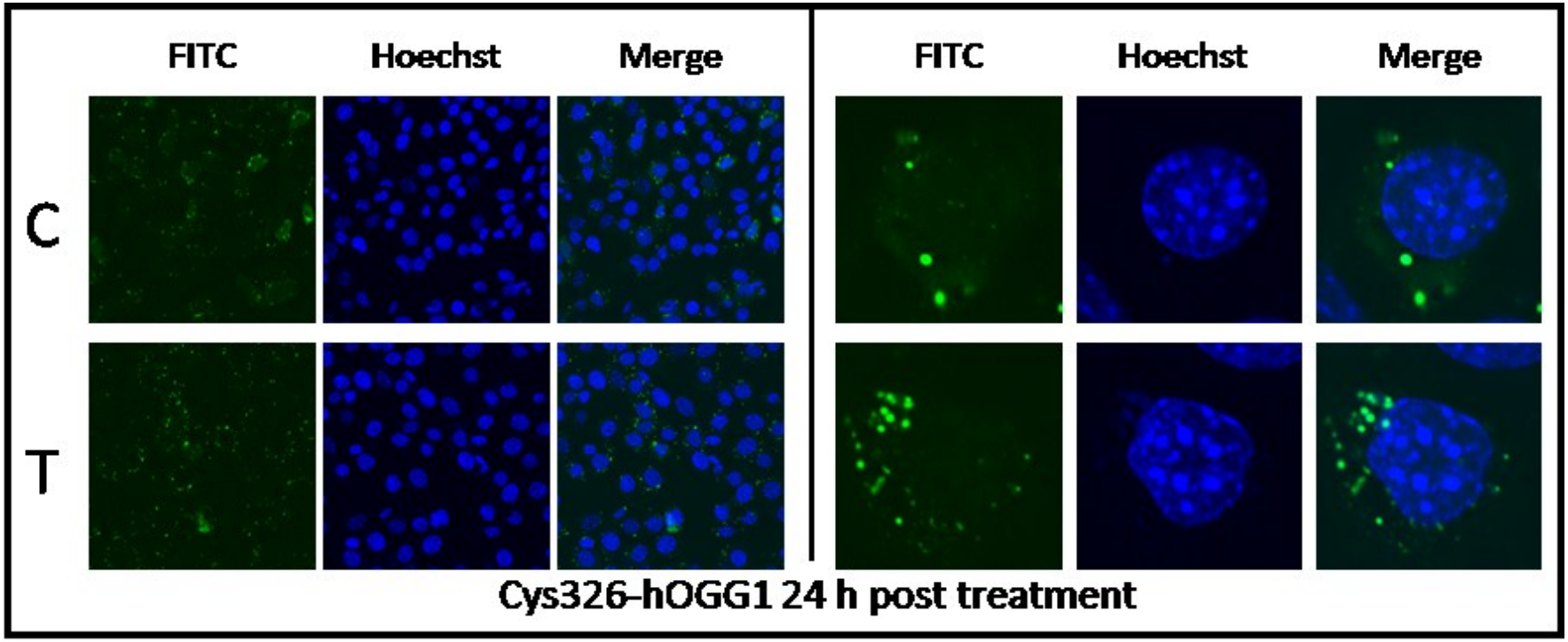

Figure 5.14: Confocal microscopy analysis of positive control beacon in Cys326-hOGG1 MEF cells 24 hours post BSO treatment (1000 µM). Positive control molecular beacon fluorescence was visualised by FITC fluorescence (green channel). The nucleus was visualised by Hoechst stain (blue channel). C = control, T = treated.

5.2.5 hOGG1 mRNA expression following BSO treatment

In this experimental model the CMV promoter controls the expression of ser326- and cys326-hOGG1. It was therefore important to test that BSO treatment had no effect on the CMV driven transcription of hOGG1. Levels of hOGG1 mRNA were measured using real time PCR as described in section 2.10. To determine whether there was any change in hOGG1 expression during the 24 h BSO treatment period RNA was extracted from control and BSO treated (1000 μM) Ser326- and Cys326-hOGG1 MEF at 0, 6, 12, 18 and 24 h post treatment. Analysis by real time PCR revealed that there was no significant difference in Ct values between control and treated samples at any time point investigated (Figure 5.15) ($P > 0.05$ as determined by one-way ANOVA).

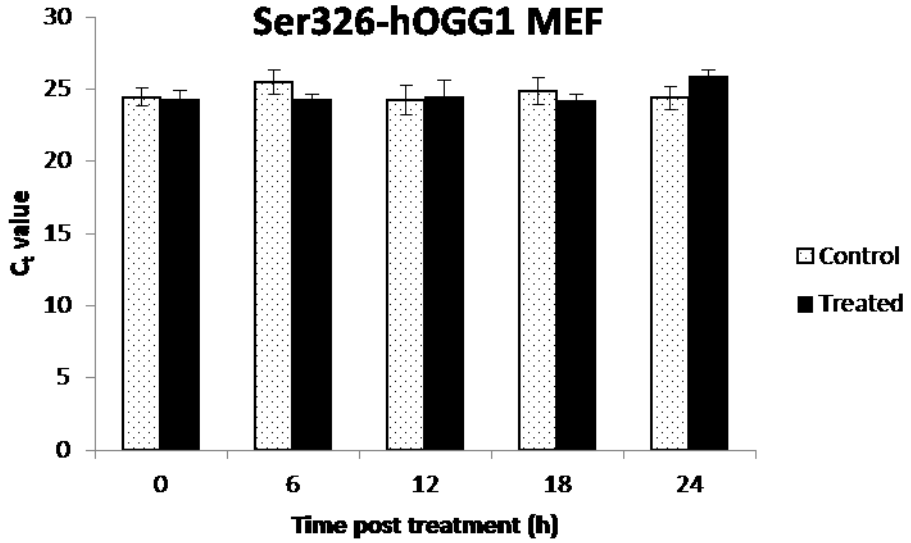

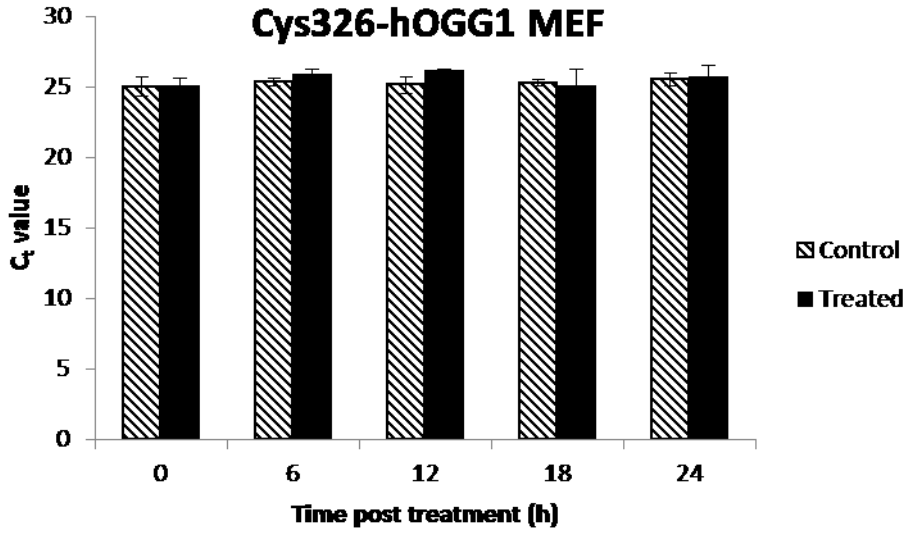

Figure 5.15: hOGG1 mRNA levels following BSO treatment.
Ser326- and Cys326-hOGG1 MEF cells were treated with 1000 μM BSO for 24 h then OGG1 mRNA levels were assessed by real time PCR (n = 3, performed in duplicate). Ct values are plotted ±SEM. No significant difference between Ct values was observed with oxidative treatment or over time ($P > 0.05$ as determined by one-way ANOVA).

5.2.6 hOGG1 protein levels following BSO treatment

To determine any effect of BSO treatment on Ser326- and Cys326-hOGG1 protein levels, KO MEF cells transfected with EGFP-Ser326- and EGFP-Cys326-hOGG1 were treated with BSO for 24 h (1000 μM), washed, then total protein was extracted (as described in section 2.11.2) 0 h, 8 h and 24 h after treatment. hOGG1 protein levels were measured by western blot as described in section 2.13 and normalised to a beta-actin loading control. A representative blot is shown (Figure 5.16). No significant difference in levels of hOGG1 protein was observed compared with time-normalised control following treatment ($P > 0.05$ as determined by one-way ANOVA).

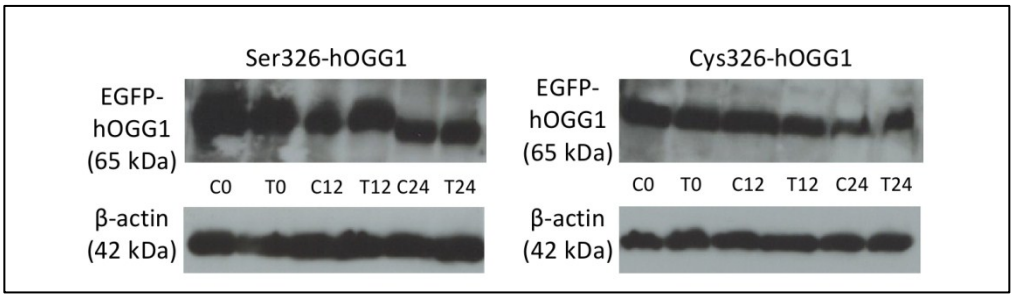

Figure 5.16: hOGG1 protein levels following 24 h BSO treatment (1000 µM).
Western blot analysis of BSO treated EGFP-Ser326-hOGG1 and EGFP-Cys326-hOGG1 expressing MEF cells. Signals were quantified using ImageJ, with values normalised to the beta actin loading control. Each value represents a treated sample as a ratio of time-matched control ±SEM. No significant difference in protein levels was observed ($P > 0.05$ as determined by one-way ANOVA).

5.2.7 EGFP-Ser326- and EGFP-Cys326-hOGG1 protein localisation following BSO treatment

To investigate intracellular localisation of hOGG1 following BSO treatment KO MEF cells transfected with EGFP-Ser326- and EGFP-Cys326-hOGG1 were treated with BSO for 24 h (1000 μM) then imaged by confocal microscopy (as described in section 2.14) 0 h, 12 h and 24 h after treatment. Diffuse staining of both EGFP-Ser326- and EGFP-Cys326-hOGG1 was observed throughout the entire nucleus with stronger staining observed on regions corresponding to heterochromatin, as indicated by Hoechst staining of condensed foci. No difference in protein localisation was observed between Ser326- and Cys326-hOGG1 and no change in protein localisation was observed following BSO treatment at any time point investigated (Figure 5.17).

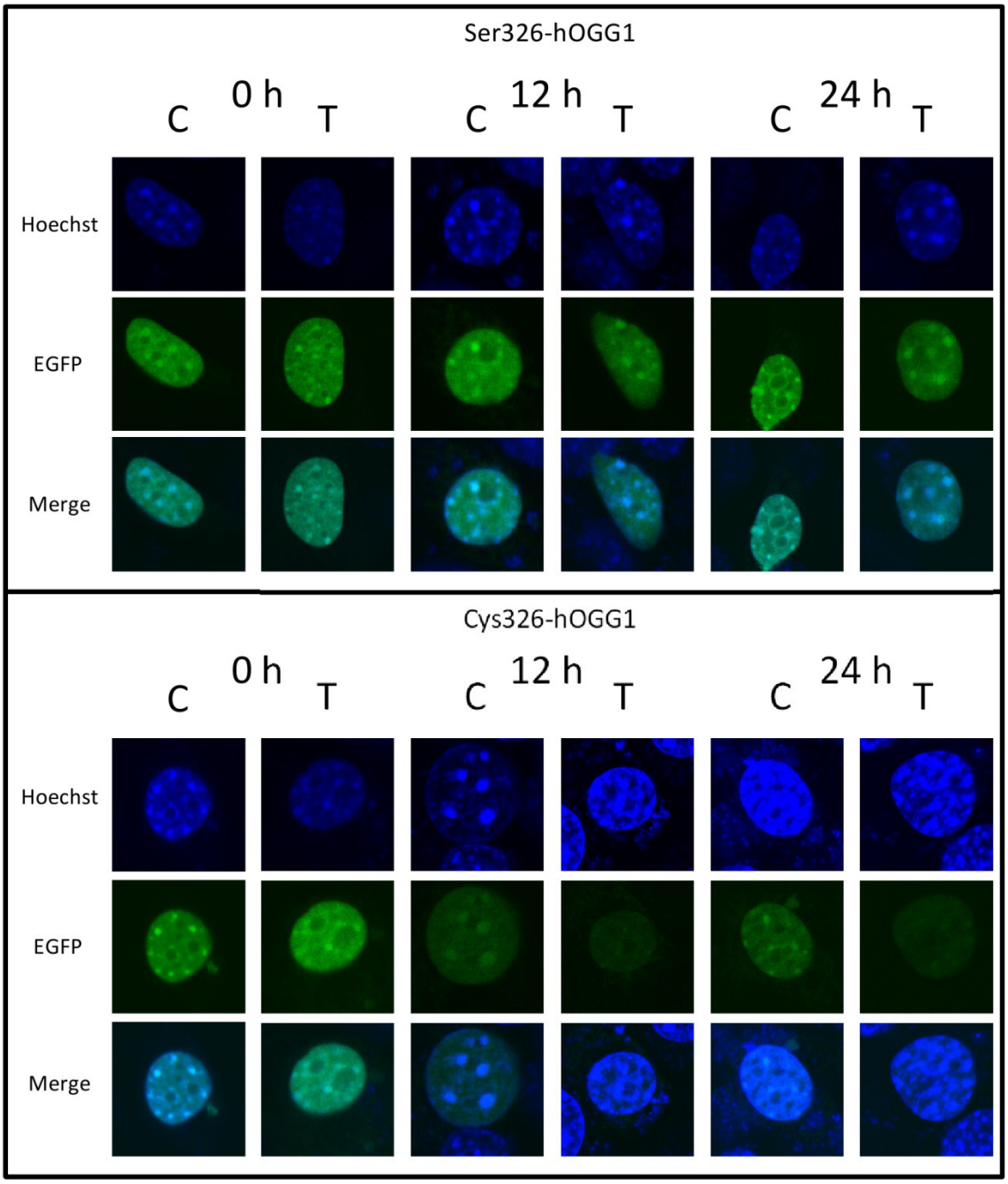

Figure 5.17: Confocal microscopy analysis of EGFP-Ser326- and EGFP-Cys326-hOGG1 localisation in BSO treated (1000 µM) KO MEF cells.

EGFP-tagged proteins were visualised by EGFP fluorescence (green channel). The nucleus was visualised by Hoechst stain (blue channel). C = control, T = treated. Top panel: EGFP-Ser326-hOGG1 transfected KO MEF cells. Bottom panel: EGFP-Cys326-hOGG1 transfected KO MEF cells.

5.2.8 Bimolecular fluorescence complementation (BiFC) analysis of hOGG1-hOGG1 interactions in MEF cells

Purified Cys326-hOGG1 has been shown to exist as a homo-dimer that is dependent on residues including and C-terminal to cys326 (Hill J.W. and Evans M.K. 2006). Using BiFC the ability of hOGG1 proteins to interact in MEF cells in the presence and absence of oxidants was investigated. As described in section 2.7, hOGG1 cDNA was fused to the N-terminal and C-terminal fragments of YFP and the expression plasmids were transiently co-transfected into KO MEF cells. Following treatment with 1000 μM BSO and 250 μM diamide, which oxidises thiols, any fluorescence resulting from the reconstitution of the two YFP half molecules was quantified by flow cytometry (exactly as for FITC-derived fluorescence as described in section 2.9.2) and imaged by confocal microscopy (as described in section 2.14). To detect background fluorescence arising from non-specific association of the two YFP half molecules, cells were co-transfected with plasmids expressing untagged YFP-N and YFP-C.

Fluorescence above background was detected in all cells transfected with YFP-containing vectors, including those transfected with the YFP-N and YFP-C control vectors (Figure 5.18A and B). Data are displayed as the number of cells with fluorescence above 10^1. There was no statistically significant difference between fluorescence detected in cells transfected with YFP-N and YFP-C control vectors and those transfected with YFP-hOGG1 vectors, or following treatment with 1000 μM BSO or 250 μM diamide ($P > 0.05$ as determined by 2-tailed student's *t*-test).

Confocal microscopy analysis confirmed the absence of fluorescence in untransfected MEF cells (Figure 5.19) and the presence of faint fluorescence in YFP-N and YFP-C

(Figure 5.20), YFP-N-Ser326-hOGG1 and YFP-C-Ser326-hOGG1 transfected MEF cells (Figure 5.21). Fluorescence appeared greater in YFP-N-Cys326-hOGG1 and YFP-C-Cys326-hOGG1 transfected MEF cells (Figure 5.22) however the staining pattern was not nuclear, as expected, but instead appeared to be dispersed throughout the cytoplasm with no evidence of fluorescent foci, suggesting it may just be background fluorescence.

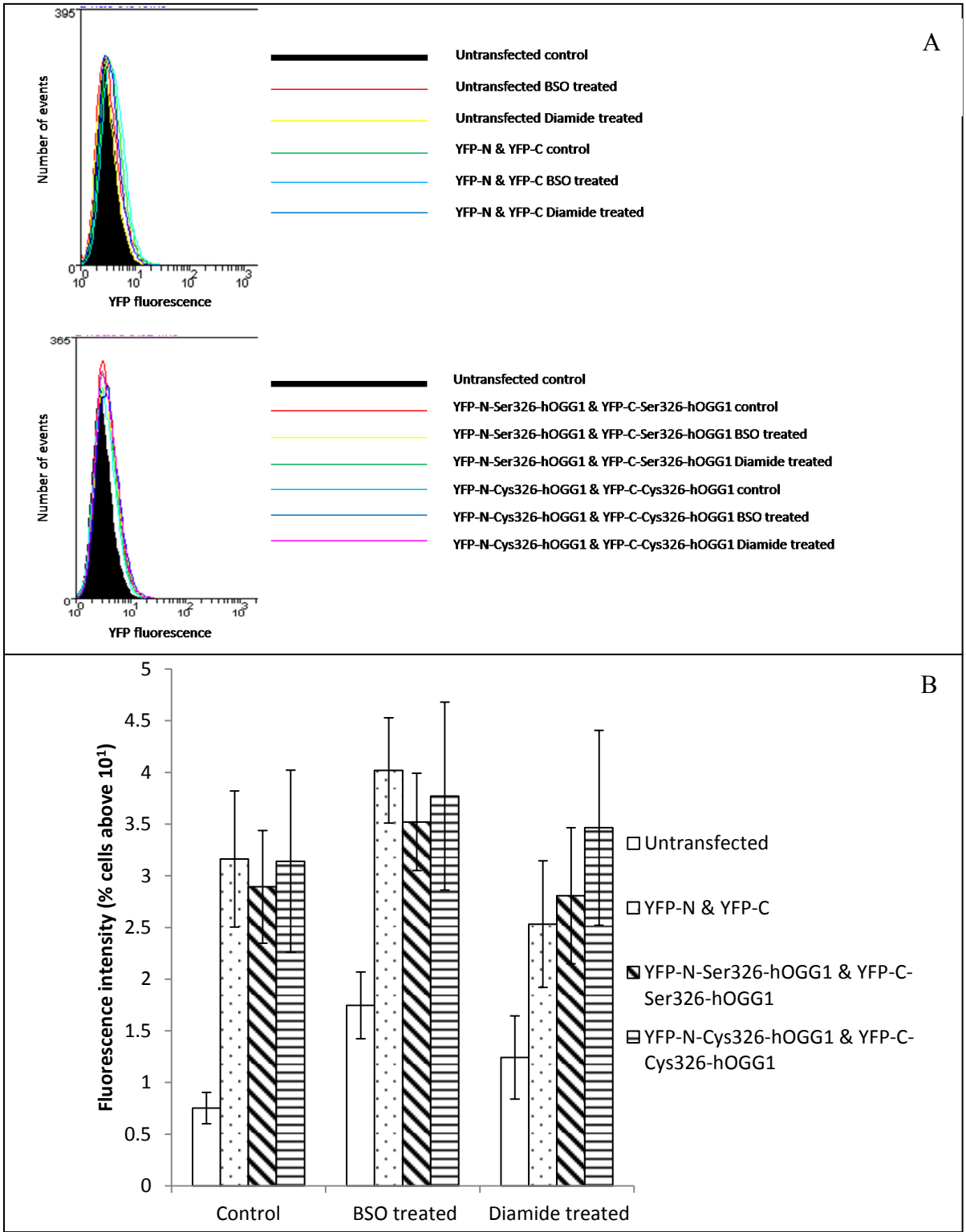

Figure 5.18: hOGG1 protein interactions following 24 h BSO treatment (1000 µM) and 30 minute diamide treatment (250 µM).

A: Representative histograms are displayed. B: Data are plotted as fluorescence intensity ±SEM from 3 independent experiments.

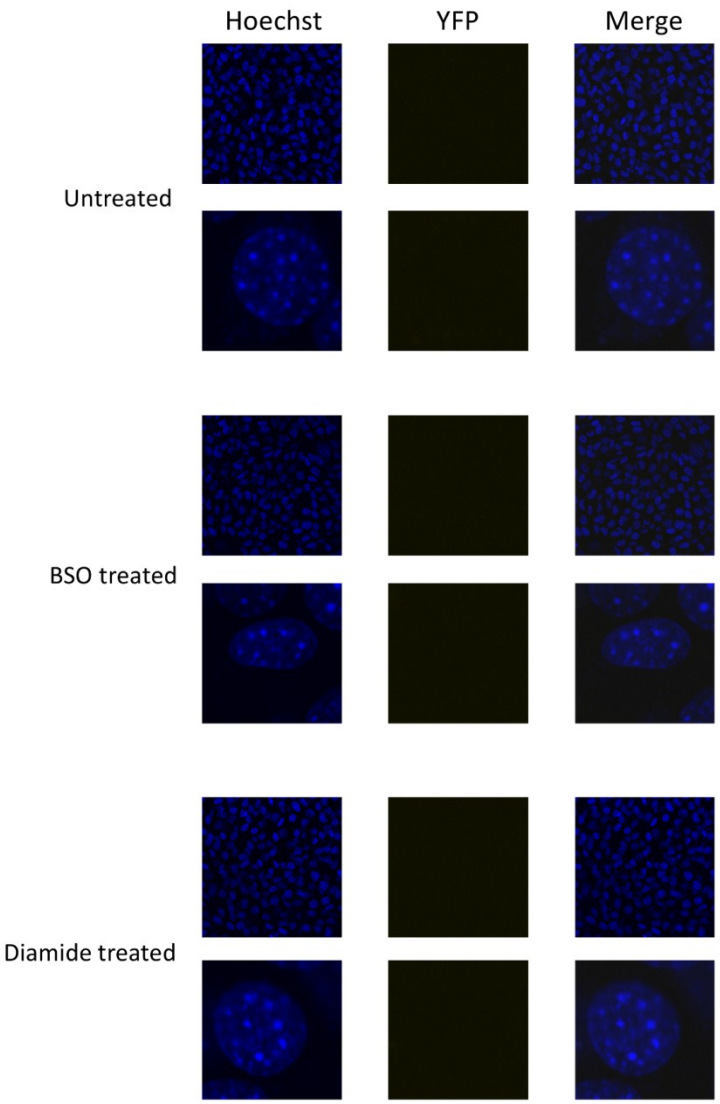

Figure 5.19: Confocal microscopy analysis of background YFP fluorescence in untransfected KO MEF cells following 24 h BSO treatment (1000 µM) and 30 minute diamide treatment (250 µM).

Background fluorescence was visualised by YFP fluorescence (yellow channel). The nucleus was visualised by Hoechst stain (blue channel).

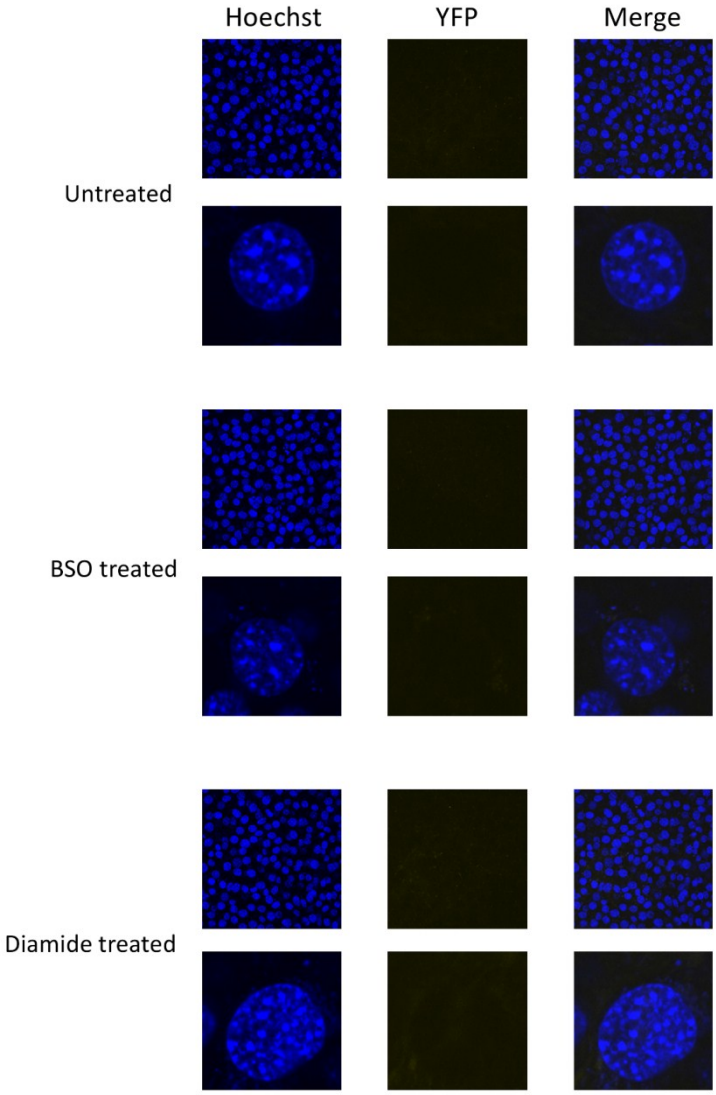

Figure 5.20: Confocal microscopy analysis of non-specific YFP fluorescence in YFP-N and YFP-C transfected KO MEF cells following 24 h BSO treatment (1000 µM) and 30 minute diamide treatment (250 µM).

YFP-N and YFP-C interactions were visualised by YFP fluorescence (yellow channel). The nucleus was visualised by Hoechst stain (blue channel).

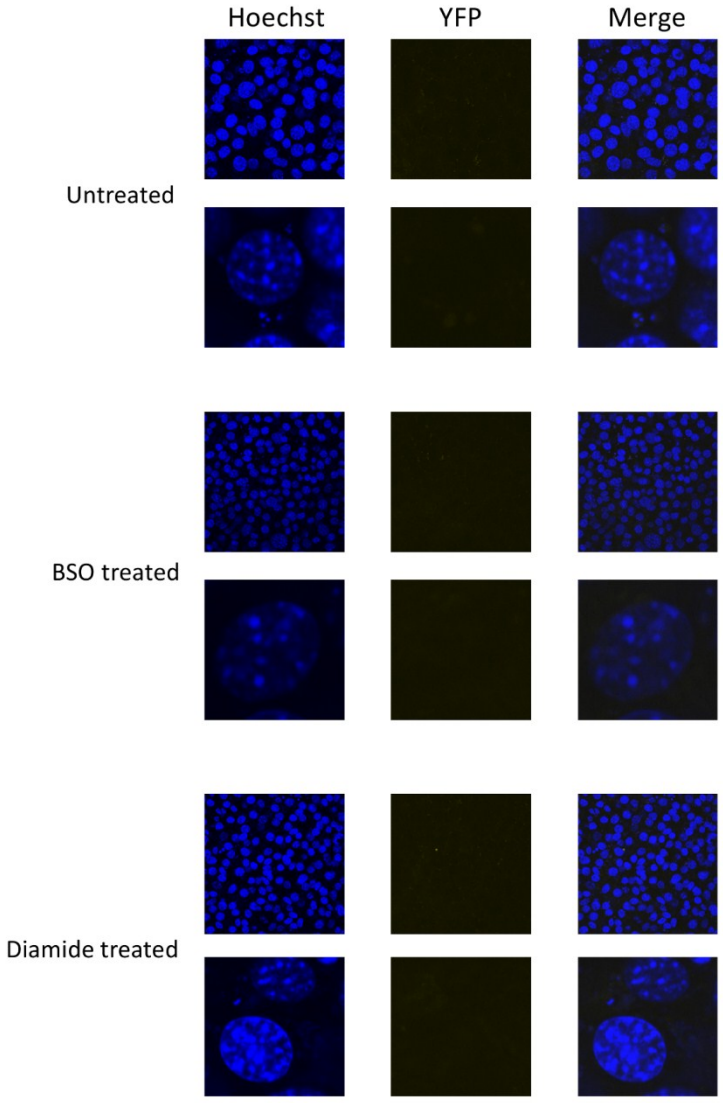

Figure 5.21: Confocal microscopy analysis of YFP fluorescence in YFP-N-Ser326-hOGG1 and YFP-C-Ser326-hOGG1 transfected KO MEF cells following 24 h BSO treatment (1000 µM) and 30 minute diamide treatment (250 µM).

YFP-N-Ser326-hOGG1 and YFP-C-Ser326-hOGG1 interactions were visualised by YFP fluorescence (yellow channel). The nucleus was visualised by Hoechst stain (blue channel).

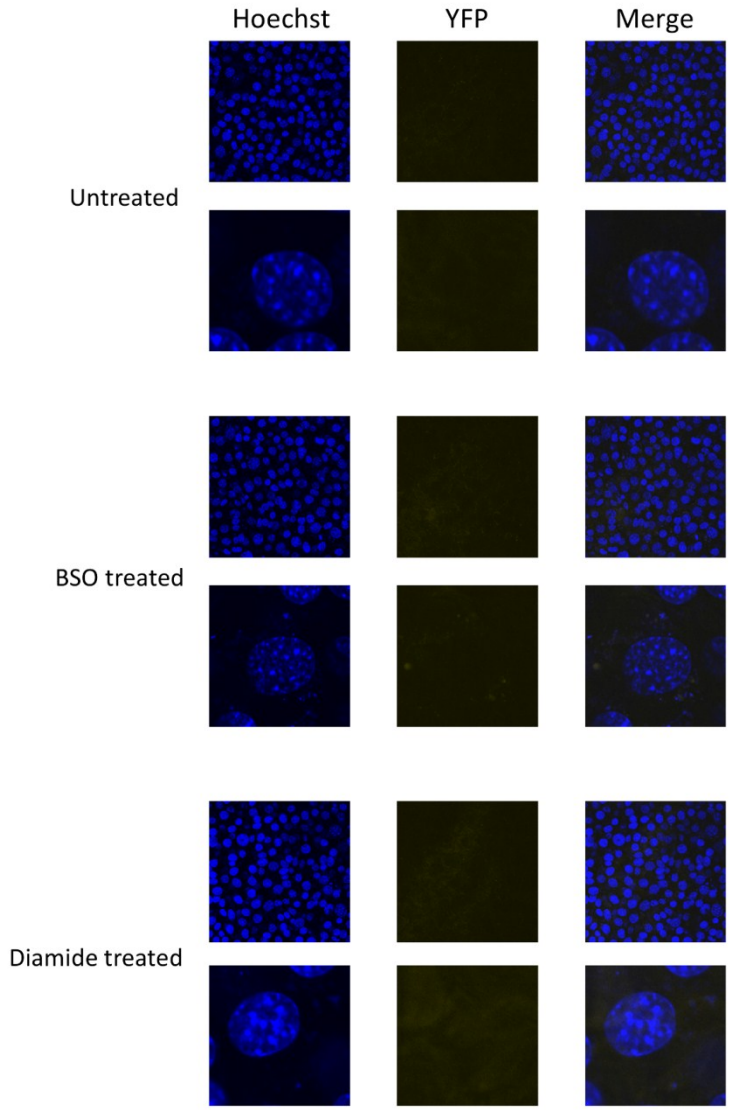

Figure 5.22: Confocal microscopy analysis of YFP fluorescence in YFP-N-Cys326-hOGG1 and YFP-C-Cys326-hOGG1 transfected KO MEF cells following 24 h BSO treatment (1000 µM) and 30 minute diamide treatment (250 µM).

YFP-N-Cys326-hOGG1 and YFP-C-Cys326-hOGG1 interactions were visualised by YFP fluorescence (yellow channel). The nucleus was visualised by Hoechst stain (blue channel).

5.2.9 Ser326- and Cys326-hOGG1 retention within an insoluble nuclear fraction

As nuclear localisation of hOGG1 was found to be unaffected by BSO treatment, retention within the nucleus following BSO treatment was investigated. Wild-type hOGG1-GFP protein has previously been shown to remain soluble in the nucleus of untreated cells but to be retained in an insoluble nuclear fraction, containing chromatin- and matrix-associated proteins, following treatment with the pro-oxidant potassium bromate (Amouroux R. *et al.* 2010). To investigate whether there was a difference between retention of Ser326- and Cys326-hOGG1 in this insoluble nuclear fraction following BSO treatment, KO MEF cells were transiently transfected with plasmids expressing EGFP-Ser326-hOGG1 or EGFP-Cys326-hOGG1. Following BSO treatment (1000 μM, 24 h) cells were incubated with CSK buffer to remove soluble proteins, washed, then fixed with paraformaldehyde (as described in sections 2.11.3 and 2.14). Any remaining insoluble EGFP-hOGG1 was observed by confocal microscopy 8 h, 16 h and 24 h post treatment.

There was no difference between nuclear expression of Ser326- and Cys326-EGFP-hOGG1 prior to the CSK wash, indicating similar transfection efficiency (Figure 5.23). Following the CSK wash, very little EGFP-hOGG1 remained in the nucleus in untreated cells. However, BSO treatment resulted in retention of EGFP-hOGG1 in the insoluble fraction (Figure 5.24). Interestingly, EGFP-Ser326-hOGG1 was retained within the insoluble fraction to a far greater extent than EGFP-Cys326-hOGG1, particularly 8 h post treatment.

To further investigate this, soluble and insoluble protein fractions from KO MEF cells transiently transfected with plasmids expressing EGFP-Ser326-hOGG1 or EGFP-Cys326-hOGG1 were analysed by western blotting (as described in section 2.13). EGFP-Ser326-hOGG1 protein was detected in both insoluble and soluble fractions in control and treated cells at all time points investigated. EGFP-Cys326-hOGG1 protein was also detected in soluble fractions in control and treated cells at all time points investigated but was not detected in insoluble fractions in any sample (Figure 5.25).

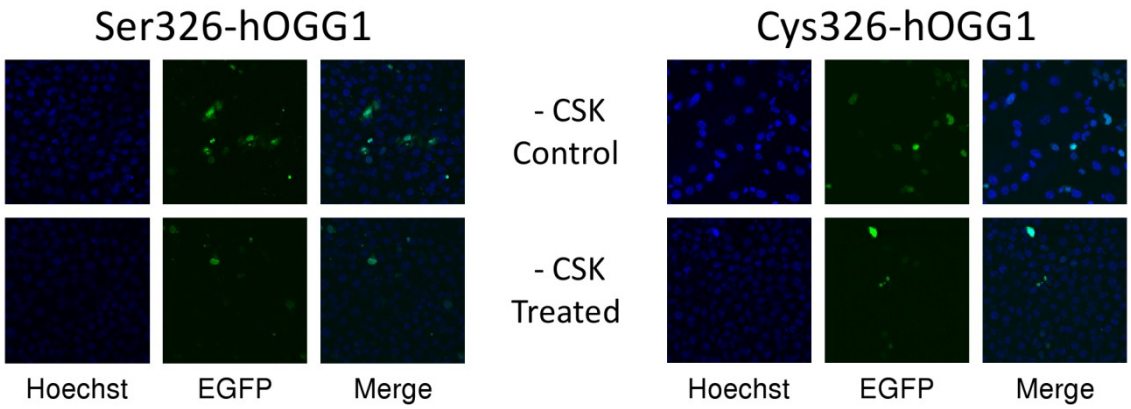

Figure 5.23: Confocal microscopy analysis of total (soluble and insoluble, -CSK wash) EGFP-Ser326- and EGFP-Cys326-hOGG1 in control and BSO treated (1000 µM) KO MEF cells.

EGFP-hOGG1 proteins were visualised by EGFP fluorescence (green channel). The nucleus was visualised by Hoechst stain (blue channel).

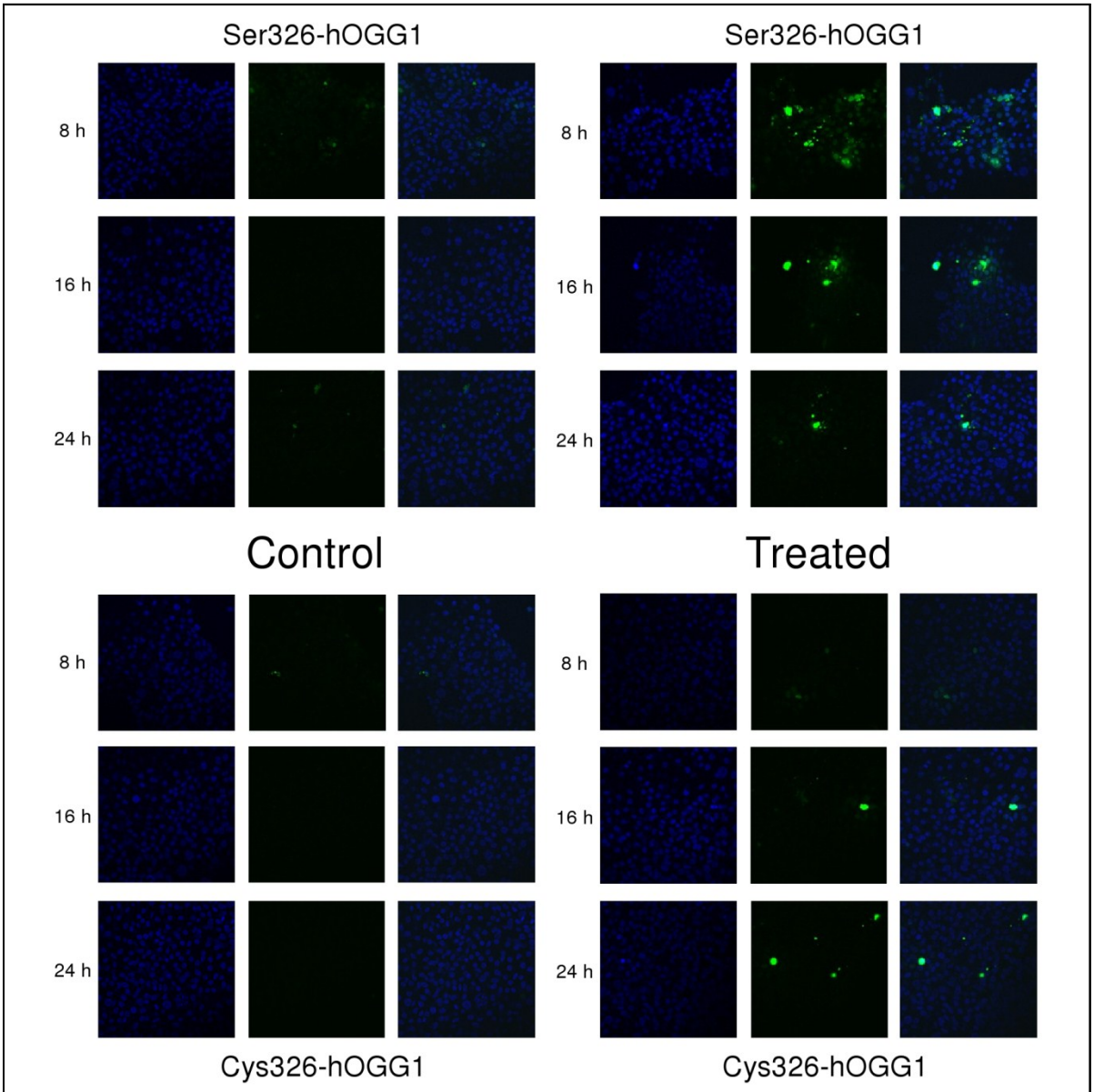

Figure 5.24: Confocal microscopy analysis of insoluble (+CSK wash) EGFP-Ser326- and EGFP-Cys326-hOGG1 8 h, 16 h and 24 h post treatment in control and BSO treated (1000 µM) KO MEF cells.

EGFP-hOGG1 proteins were visualised by EGFP fluorescence (green channel). The nucleus was visualised by Hoechst stain (blue channel).

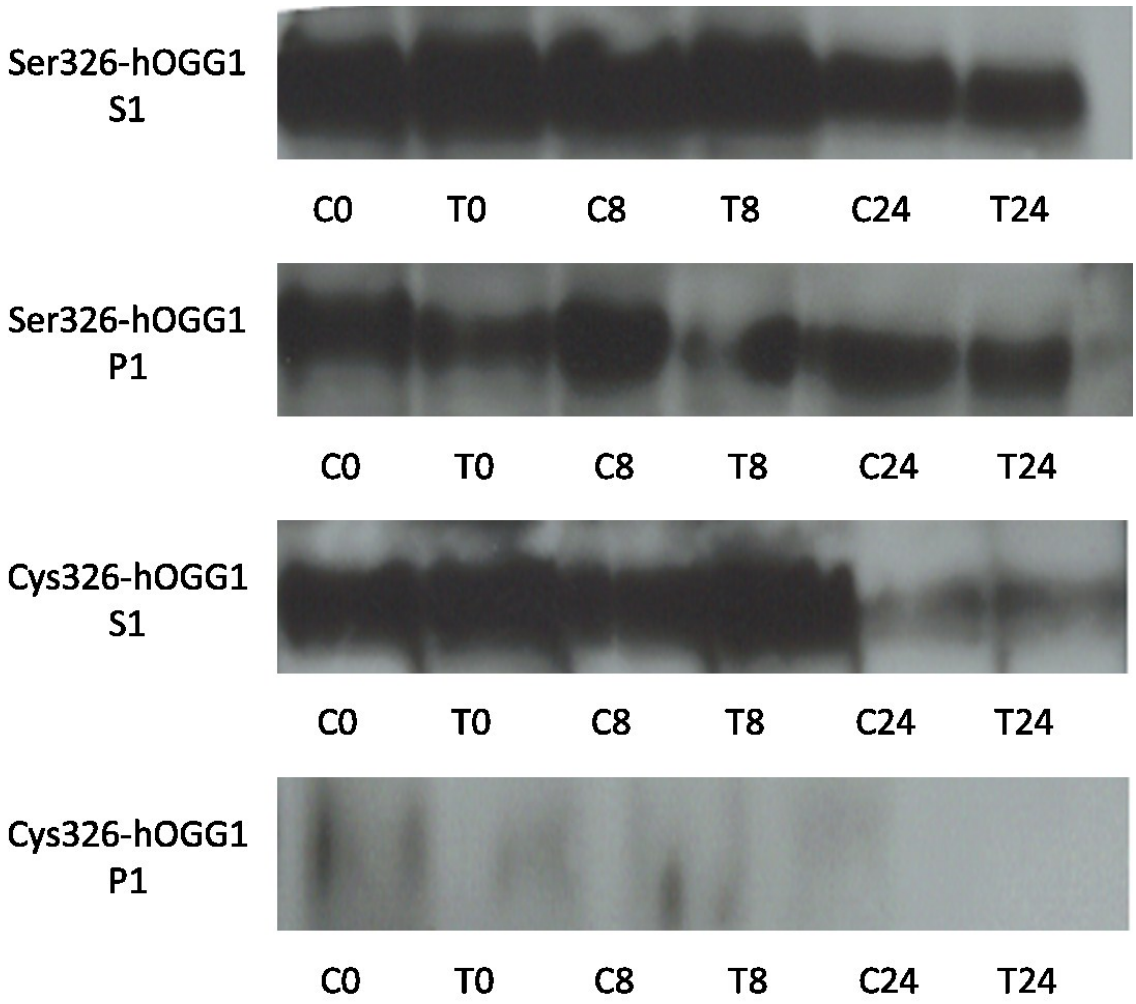

Figure 5.25: Ser326- and Cys326-hOGG1 protein in soluble (S1) and insoluble (P1) fractions following 24 h BSO treatment (1000 μM).

5.3 Discussion

Epidemiological evidence indicates increased cancer risk in individuals that are Cys326-hOGG1 homozygotes and it is becoming increasingly clear from functional studies that any reduced repair ability of Cys326-hOGG1 becomes most apparent under conditions of cellular oxidative stress. The work described in chapter 3 showed that oxidative stress induced by BSO resulted in increased mOGG1 activity which was not related to increased gene expression. To investigate wild-type and variant hOGG1 regulation and activity under oxidising conditions MEF cells expressing Ser326- and Cys326-hOGG1 were generated (chapter 4). Human OGG1 activity, gene expression, protein expression, protein localisation and ability to form dimers following BSO treatment were measured.

Treatment of Ser326- and Cys326-hOGG1 MEF cells with BSO resulted in a concentration-dependent depletion of glutathione and increase in ROS with no effect on cell viability at any concentration investigated. As observed for mouse OGG1 (chapter 3), treatment with BSO resulted in a concentration dependent increase in Ser326- and Cys326-hOGG1 activity, with no change in gene expression or protein levels. The expression of h*OGG1* is not believed to vary during the cell cycle and this, combined with the lack of TATA or CAAT boxes within the promoter, indicates that it is a constitutively expressed gene (Dhénaut A. et al 2000). The OGG1 promoter does however contain SP1 transcription factor binding sites and a Nrf2 antioxidant response element and expression of *OGG1* can be modulated by a range of cellular stresses (Cortina M.S. *et al.* 2005; Hodges N.J. and Chipman J.C. 2002; Imai K. *et al.* 2005; Lee A. *et al.* 2004; Potts R.J. *et al.* 2003; Youn C.K. *et al.* 2005). In this study, expression of ser326- and cys326-h*OGG1* were under the control of the CMV promoter and not subject

to regulation at the transcriptional level, as shown in section 5.2.5. The data presented here support other studies which show that oxidative stress has the ability to modulate OGG1 activity post-transcriptionally (Mirbahai L. *et al.* 2010; Conlon K.A. *et al.* 2003; Silva J.P. *et al.* 2009; Bhakat K.K. *et al.* 2006).

Although Ser326- and Cys326-hOGG1 protein levels increased slightly 12 and 24 hours post BSO treatment, no statistically significant change in protein levels was observed between BSO treated and untreated control samples at any time point investigated. It seems likely therefore that post-translational modifications are responsible for the activity modulation observed in this study. It has been shown that OGG1 activity can be stimulated by phosphorylation (Hu J. *et al.* 2005) and acetylation (Bhakat K.K. *et al.* 2006). Further work remains to be done to investigate the phosphorylation and acetylation status of the hOGG1 protein following oxidative stress. The process of BER is highly coordinated and involves multiple interactions between the proteins of the pathway. The activity of OGG1 has previously been shown to be enhanced by apurinic/apyrimidinic endonuclease 1 (APE1) (Hill J.W. *et al.* 2001; Vidal A.E. *et al.* 2001), Nei-like glycosylase 1 (NEIL1) (Mokkapati S.K. *et al.* 2004), X-ray cross complementing protein 1 (XRCC1) (Marsin S. *et al.* 2003) and RAD52 (de Souza-Pinto N.C. *et al.* 2009). It is therefore also possible that oxidative stress induced by BSO treatment could affect the interaction with one of these protein partners.

In the current study BSO treatment resulted in an increased activity response of Cys326-hOGG1 which was delayed relative to that of Ser326-hOGG1. To ensure this was not a clone-specific effect we repeated the activity measurements using two independent MEF cell lines expressing Ser326- and Cys326-hOGG1 and observed the same trend (see

appendix, page 224). The data suggests altered kinetics of Ser326- and Cys326-hOGG1 in response to the same oxidative stress. Cys326-hOGG1 has previously been shown to have decreased 8-oxo dG binding affinity and reduced 8-oxo dG excision catalytic efficiency (Dherin C. *et al.* 1999; Hill J.W. and Evans M. K. 2006). Interestingly, although Cys326-hOGG1 was shown to be less efficient than wild-type hOGG1 removing 8-oxo dG:C from oligodeoxynucleotide substrates, the effect was far more pronounced when removing 8-oxo dG from high molecular weight DNA (Sidorenko V.S. *et al.* 2009). The data presented in this study are in agreement with functional studies observing reduced rate of repair of Cys326-hOGG1 and thus support epidemiological evidence suggesting increased risk of cancer in individuals homozygous for the Cys326-h*OGG1* allele.

The human *OGG1* gene undergoes alternative splicing generating two major isoforms; α-hOGG1 (hOGG1-1a) and β-hOGG1 (hOGG1-2a). The first 316 amino acids are identical and contain a mitochondrial targeting sequence however the carboxy-terminal ends differ extensively, with that of α-hOGG1 containing a C-terminal nuclear localisation sequence absent from β-hOGG1 (Boiteux S. and Radicella J.P. 2000) which targets it to the nucleus (Takao M. *et al.* 1998) and suppresses the mitochondrial targeting sequence which targets β-hOGG1 to the mitochondria (Nishioka K. *et al.* 1999). Little is known about the function of the β-form as surprisingly, it has been shown to lack repair activity (Hashiguchi K. *et al.* 2004) but to have an effect on the mechanism of cell death in MEF cells (Oka S. *et al.* 2008). Although mainly located in the nucleus, it is thought that the alpha form is responsible for both nuclear and mitochondrial 8-oxo dG repair. The current study used MEF cells expressing the α-

hOGG1 isoform and analysis by confocal microscopy revealed that, as expected, in both Ser326- and Cys326-hOGG1 MEF cells the cleaved beacon was mainly located in the nucleus. Furthermore, fluorescence of nuclear localised beacon increased in intensity in a concentration dependent manner following BSO treatment. Interestingly, this is in contrast to previous observations which showed mitochondrial beacon localisation following treatment of MEF cells expressing endogenous mOGG1 with potassium bromate (Mirbahai L. *et al.* 2010). Mouse OGG1 exists as only a single isoform responsible for both nuclear and mitochondrial BER. The staining pattern observed using the positive control beacon shows that in the current study the beacon is present in the nucleus and cytoplasm, as well as in mitochondrial sized organelles. Based on these observations we propose that the localisation difference may either be a species specific response or a result of hOGG1 overexpression. Alternatively, it is possible that in these cells, in contrast to potassium bromate treatment, it is genomic rather than mitochondrial DNA that is preferentially oxidatively damaged following BSO treatment, resulting in an accumulation of cleaved beacon in the nucleus; the site of greatest damage.

The mechanism underlying the repair difference between Ser326- and Cys326-hOGG1 observed is unknown and as no crystal structure exists that includes amino acids beyond position 325 no information can be obtained from structural studies. Two major hypotheses have been proposed to explain repair differences; the introduction of a redox-sensitive cysteine residue, or the loss of a serine residue whose phosphorylation may be important for OGG1 localisation or activity. An increasing body of evidence supports the theory that the Cys326 residue, present in a highly positively charged sequence environment (ADLRQ[ser326cys]RHAQ), is redox sensitive and susceptible to the

formation of a reactive thiolate anion (Giustarini D. *et al.* 2004) which can be oxidatively modified and form disulphide bonds (Bravard A. *et al.* 2009). The Cys326 residue is present in a disordered and highly mobile region (Bruner S.D. *et al.* 2000) suggesting that this residue may be located in an accessible part of the molecule, rendering it a likely target for redox modification. Hill and Evans (2006) used purified hOGG1 protein to show Cys326-hOGG1 exists as a homo-dimer, which may explain a reduction in activity, however no clear evidence of hOGG1 homo-dimer formation was detected in the current study using BiFC in MEF cells following treatment with either BSO or diamide.

It is possible that homo-dimer formation was observed by Hill and Evans (2006) and not in the current study because hOGG1 does not form a dimer in its native cellular environment. hOGG1 may form a dimer with other proteins *in vivo* which would not have been detected using BiFC, or limitations of the BiFC technique may have prevented the visualisation of any hOGG1 protein interactions. The BiFC technique was used to measure hOGG1 protein interactions in live cells as it has been successfully used to investigate a variety of protein – protein interactions in mammalian cells (Hu C.D. *et al.* 2002; de Virgilio M. *et al.* 2004; Shaffer J.M. *et al.* 2009). Dimer formation could also be further investigated using Förster resonance energy transfer (FRET). In contrast to FRET techniques, where changes in existing fluorescence are measured, the complementation process of BiFC produces a new fluorescent signal, hence it is a more sensitive method (Ciruela F. 2008). However, non-specific interactions and spontaneous association of the YFP half molecules, such as those observed in the current study, are a limitation (Cabantous S. *et al.* 2005; Zhang S. *et al.* 2004) and may mask any true fluorescence due to hOGG1 protein interaction. For the current study, although not

possible during the time available, the generation of a positive control using two proteins known to interact within mammalian cells would have allowed easy differentiation between non-specific YFP fluorescence and fluorescence resulting from a specific protein – protein interaction.

A further limitation of BiFC using YFP half molecules is that the maturation of the YN-YC complex to produce an active fluorophore is enhanced by temperatures below 30°C. As mammalian cells are cultured at 37°C initial trial experiments using Drosophila Schneider 2 (S2) cells, which are cultured at 27°C, were conducted however no fluorescence above background could be detected following YFP-hOGG1 transfection in these cells (data not shown). Furthermore, the cells did not respond well to BSO, showing reduced viability at low concentrations without significantly increased ROS. These studies were not pursued further and the technique was optimised in MEF cells by incubating cells for 5 hours at 27°C prior to fluorescence detection. This allowed the detection of some YFP fluorescence however it is possible that this incubation time was too short for maturation which may explain the low fluorescence observed. Unfortunately longer incubation times reduced cell viability and were therefore not possible. To overcome this barrier a modified version of YFP such as the Venus protein for which the maturation process occurs at a higher temperature could be used (Shyu Y.J. *et al.* 2006). This was not possible in the current study due to time constraints.

Previous studies have shown that the localisation of OGG1 varies throughout the cell cycle (Dantzer F. *et al.* 2002; Luna L. *et al.* 2005). During interphase hOGG1 is associated with the soluble chromatin and nuclear matrix, whereas during mitosis it associates with condensed chromosomes and relocalises to the nucleoli during S-phase.

All of these relocalisation processes have been shown to be mediated through the phosphorylation of serine326, with the subcellular localisation of Cys326-hOGG1 disrupted by exclusion from the nucleoli during S-phase (Luna L. *et al.* 2005). As expected, the localisation of both EGFP-Ser326- and EGFP-Cys326-hOGG1 in MEF cells was predominantly nuclear and concentrated on regions of heterochromatin. The nuclear, heterochromatin concentrated localisation of the proteins did not change either 12 or 24 hours post BSO treatment, when the activity difference was detected, suggesting that BSO treatment does not affect the localisation of Ser326- or Cys326-hOGG1 and that the activity induction was not as a result of any change in hOGG1 cellular localisation. There is increasing interest in the sub nuclear distribution of BER proteins following oxidative stress but our data do not support any difference in hOGG1 localisation to the nucleus or nucleoli between the two proteins or following BSO treatment.

Interestingly, hOGG1 has been shown to be recruited to nuclear speckles via a ROS-mediated mechanism (Campalans A. *et al.* 2007) and to rapidly accumulate at sites of laser irradiation induced-DNA damage (Zielinska A.E. *et al.* 2011). A recent report also demonstrated that hOGG1 is recruited to regions of open chromatin following exposure to high concentrations of potassium bromate. The study showed that in unstressed cells hOGG1 exists in a soluble cellular fraction containing the cytoplasm and nucleoplasm. Following treatment with high concentrations of potassium bromate, hOGG1, along with APE1 and XRCC1, was recruited to and retained within an insoluble cellular fraction containing chromatin- and matrix-associated proteins (Amouroux R. *et al.* 2010). This recruitment was not cell-cycle dependent. The data presented in the current study are in

agreement with Amouroux *et al*. (2010), showing that following treatment with high dose BSO a fraction of the hOGG1-EGFP protein is retained within a nuclear fraction resistant to the detergent wash. The confocal microscopy images further suggest that there may be a difference in the retention of hOGG1 in this insoluble fraction between the wild-type and variant protein, with Ser326-hOGG1 retained to a much greater extent than Cys326-hOGG1. Western blotting analysis indicated that Ser326-hOGG1 was present in both soluble and insoluble fractions before and after BSO treatment. It is possible that this is due to contamination of the fractions during the extraction process or the combination of over-expression of the OGG1 protein and the high sensitivity of the EGFP antibody. Interestingly, no Cys326-hOGG1 could be detected in the insoluble fraction. Although further confirmation is required, both the microscopy images and western blotting data suggest that there is a difference in the retention of wild type and variant hOGG1 in the insoluble nuclear fraction. It is possible that this difference could play a role in the delayed repair of Cys326-hOGG1 observed in this study.

In conclusion, the data presented here provide further evidence for impaired Cys326-hOGG1 repair ability under conditions of oxidative stress and suggest a potential mechanism underlying this repair difference.

Chapter 6 –General discussion

6.1 General Discussion

Many normal cellular processes such as gene regulation, cell mediated immunity and cell signalling require low levels of reactive oxygen species which are generated by intracellular components and exogenous sources (as described in section 1.1.3). A variety of physiological reactive species are produced, including $O_2^{\bullet-}$ which can dismutate to form H_2O_2 which easily diffuses across membranes and can function as a second messenger. However, in the presence of transition metals H_2O_2 can generate highly reactive $HO^{\bullet}$ radicals, with the potential for toxicity. An increase above physiological levels of intracellular ROS, for example via inflammation or exposure to environmental toxicants, is normally counter-balanced by various antioxidant defence mechanisms. However, if these defences become overwhelmed, disruption of the critical redox balance results in cellular oxidative stress where ROS can react with and damage cellular components including DNA (as described in section 1.1.4).

A range of DNA base lesions are induced by ROS but due to its low oxidation potential guanine is the most commonly oxidised base yielding fapyG and 8-oxo dG (Steenken S. and Jovanovic S.V. 1997). As 8-oxo dG can mispair with adenine during DNA replication it is a potentially mutagenic lesion and its repair is essential to maintain genomic stability (as described in section 1.3). Its relative abundance, potential for mutation and ease of detection make 8-oxo dG the best studied oxidative DNA lesion (David S.S. *et al.* 2007). The repair of 8-oxo dG by the base excision repair pathway is mediated primarily by OGG1 which is the only known enzyme that recognises oxoG:C pairs and catalyses the removal of 8-oxo dG prior to nucleotide replacement by β-

polymerase and DNA ligation by DNA ligase III and XRCC1 (Boiteux S. and Guillet M. 2004; Hazra T.K. *et al.* 2007) (as described in section 1.5).

Increased oxidative stress occurs in a variety of pathological conditions including cancer (Halliwell B. 2007), although it is unclear whether this is causative or a consequence of these conditions. Regulation of OGG1 enzyme under conditions of oxidative stress is important as impaired 8-oxo dG removal could have implications for disease development and progression. The work presented in this thesis investigated the response of OGG1 to oxidative stress and differences between the wild-type and common human variant Cys326-hOGG1. Previous work in our laboratory (Mirbahai L. *et al.* 2010) and work presented in chapters three and five demonstrates that OGG1 activity is modulated following treatment with the pro-oxidant potassium bromate and the glutathione depleting agent BSO in MEF cells. Using MEF cells, for which we have a negative control m*Ogg1*$^{-/-}$ KO cell line, we showed that the activity of both mouse and human OGG1 increased following induction of cellular oxidative stress via treatment with BSO. In contrast, no effect on rat OGG1 activity following identical treatment of MH1C1 cells was observed. This may be related to the low ROS levels and high basal OGG1 activity we observed in this cell line (sections 3.2.3 and 3.2.9). Our and other groups have shown OGG1 activity inhibition (Bravard A. *et al.* 2006; Hodges N.J. and Chipman J.K. 2002; Potts R.J. *et al.* 2003; Youn C.K. *et al.* 2005; Zharkov D.O. and Rosenquist T.A. 2002) and induction (Ma H. *et al.* 2008; Silva J.P. *et al.* 2009) in various cellular models following treatment with a range of pro-oxidants. Our findings confirm that the OGG1 response is complex and dependent on the pro-oxidant and study model chosen, as noted by van Loon *et al.* (2010).

Regulation of OGG1 activity under conditions of oxidative stress represents an important adaptive response to the increased requirement of a cell to repair 8-oxo dG lesions. Our data indicate that the increased repair activity in MEF cells following BSO treatment is not due to any alteration of gene transcription. This suggests that the change in activity is mediated by post-translational modification, interaction with other protein partners, protein stabilisation or altered protein localisation. Work presented in chapter five shows that no detectable change in human OGG1 protein levels was observed following BSO treatment, suggesting increased repair activity was not the result of OGG1 protein stabilisation (section 5.2.6). The OGG1 protein is known to be post-translationally modified, and both acetylation (Bhakat K.K. *et al.* 2006) and phosphorylation (Hu J. *et al.* 2005) have been shown to modify activity. Further studies are required to determine the nature of OGG1 post-translational modifications in oxidative stress conditions, however it is possible that when an immediate increase in 8-oxo dG repair is required, post-translational modification could be favoured over increased gene expression. It is also possible that interaction with other proteins could modulate OGG1 activity as enhanced activity has been shown by OGG1 interaction with APE1, NEIL1, XRCC1 and RAD52 (de Souza-Pinto N.C. *et al.* 2009; Hill J.W. *et al.* 2001; Marsin S. *et al.* 2003; Mokkapati S.K. *et al.* 2004; Vidal A.E. *et al.* 2001.2).

Data presented in chapter three showing post transcriptional activation of OGG1 following BSO treatment, justified the generation and use of transgenic MEF cells constitutively expressing hOGG1 under the control of the CMV promoter for the investigation into potential differences between wild-type and variant hOGG1 repair acitivity. As described in detail in section 1.6, the S326C hOGG1 variant, which arises

due to a C→G substitution at position 1245 in exon 7, has been linked with increased cancer susceptibility (Cho E.Y. *et al*. 2003; Elahi A. *et al.* 2002; Kohno T. *et al.* 2006; Le Marchand L.L. *et al.* 2002; Park J. *et al.* 2004; Sugimura H. *et al.* 1999; Xing D.Y. *et al.* 2001) and reduced functional activity, particularly in oxidising conditions (Bravard A. *et al.* 2009; Chen S.K. *et al.* 2003; Hill J.W. and Evans M.K. 2006; Lee A. *et al.* 2005; Smart D.J. *et al.* 2006; Yamane A. *et al.* 2004).

Previous work in our laboratory investigated the effect of oxidative stress on the human OGG1 protein using transiently transfected KO MEF cells (Smart D.J. *et al.* 2006). In order to eliminate transfection efficiency variability, data presented in chapter four shows that we have improved this model and successfully generated KO MEF cells which stably express both wild-type (Ser326) and variant (Cys326) hOGG1. Our transgenic cell model has advantages compared with previous models as KO MEF cells exhibit no background OGG1 expression and are karyotypically normal. The generation of Ser326- and Cys326-hOGG1-expressing MEF cells with similar OGG1 repair activities allowed us to investigate any differences in response to oxidative stress, as presented in chapter five.

Interestingly, following BSO treatment, we did not observe reduced repair activity in Cys326-hOGG1 MEF, but a delay in the increased activity response to oxidative treatment (section 5.2.4). This is in agreement with other functional studies which show decreased 8-oxo dG binding affinity and reduced excision efficiency for Cys326-hOGG1 (Dherin C. *et al.* 1999; Hill J.W. and Evans M.K. 2006; Sidorenko V.S. *et al.* 2009). The 8-oxo dG-containing molecular beacon assay, recently optimised in our laboratory, offers several advantages over traditional activity assays as the OGG1 protein is retained within

its intracellular environment and activity and location can be monitored in real time. As expected, the repair activity increase observed was not a result of increased hOGG1 gene expression and further supports evidence for post-transcriptional OGG1 activity modulation following acute oxidative stress.

Recent evidence suggests that any difference between Ser326- and Cys326-hOGG1 activity is due to the additional redox sensitive cysteine residue (Bravard A. *et al.* 2006; Bravard A. *et al.* 2009; Smart D.J. *et al.* 2006) and may be as a result of OGG1 dimer formation (Hill J.W. and Evans M.K. 2006; Simonelli V. *et al.* 2011). However, as shown in chapter five, we failed to demonstrate conclusive evidence for hOGG1 homo-dimer formation in live cells following BSO or diamide treatment (section 5.2.8). Whilst this could be due to limitations of the BiFC technique employed, it is also possible that hOGG1 does not form a dimer in native intracellular conditions. In support of our data, other groups have also been unable to demonstrate OGG1 dimer formation in live cells (Anne Bravard, *pers. comm.*). Indeed it seems more likely that a heterodimer with another protein could form and this could be investigated by immunoprecipitation coupled with mass spectrometry or by a yeast two hybrid assay.

Recent research by Amouroux *et al.* (2010) has demonstrated that following exposure to the pro-oxidant potassium bromate, hOGG1 is recruited to sites of repair in insoluble nuclear structures containing chromatin- and matrix-associated proteins. This prompted us to investigate hOGG1 retention in this insoluble nuclear fraction following BSO treatment. In agreement with Amouroux *et al.* (2010), we also found that Ser326- and Cys326-hOGG1 proteins were present in the soluble fraction in untreated cells and that wild-type hOGG1 was retained in the insoluble fraction following BSO treatment.

However, in contrast, the Cys326-hOGG1 protein was retained to a much lesser extent than the wild-type protein (section 5.2.9). This localisation difference is supported by previous studies showing impaired localisation of Cys326-hOGG1 (Dantzer F. *et al.* 2002; Luna L. *et al.* 2005). Although further work remains to be done to confirm these findings, we hypothesise that this difference in retention in the insoluble nuclear fraction may in part underlie the difference in repair activity we observed.

Our data, in agreement with many other studies, are strongly supportive of reduced repair ability of Cys326-hOGG1 compared with wild-type under conditions of oxidative stress. As the evidence for a repair difference is less convincing in the absence of oxidative stress, the relationship between possession of the cys326 allele and the ability of OGG1 to repair 8-oxo dG is complicated by interactions with the environment. Lifestyle choices such as smoking status and diet, or exposure to environmental toxicants could have an impact on mutation frequency in individuals who possess the variant protein. Therefore risk of cancer development does not simply depend on the possession of the variant allele, but on a variety of factors including the individual's exposure to carcinogens.

Our data suggest that although the OGG1 protein is required to respond to 8-oxo dG arising from a variety of cellular stresses during an individual's lifetime, in cell culture models the regulation of OGG1 is complex, cell type and compound specific. The repair of damaged DNA takes place in a complex cellular environment and is associated with many other cellular processes. In such an environment any dramatic change in gene expression or protein activity could have profound effects on other vital cellular processes and must therefore be tightly regulated. The viability of the OGG1 KO mouse

and the prevalence of the Cys326-hOGG1 variant highlight the potential redundancy in the base excision repair system and suggest that there is a degree of compensation in DNA repair mechanisms. In support of this there is slow removal of 8-oxo dG from genomic DNA in proliferating KO MEF cells (Klungland A. *et al.* 1999). Whilst glycosylase enzymes have substrate preference, they do not have absolute specificity, for example the NEILs are known to repair oxidised bases during transcription and DNA replication (Dou H. *et al.* 2003). There is also integration between different DNA repair pathways and DNA glycosylases interact with components from MMR and NER as well as BER pathways (reviewed by Kovtun I.V. and McMurray C.T. 2007). It has been shown that Msh2 defective mouse embryonic stem cells accumulate 8-oxo dG more than wild-type cells (Colussi C. *et al.* 2002) and that exposure to γ-irradiation in MSH2 or MutL homologue (MLH1) deficient tumour cell lines or MEF cells resulted in increased 8-oxo dG levels (DeWeese T.L. *et al.* 1998) suggesting that interaction of MMR with BER plays a role in the reduction of 8-oxo dG levels in mammalian cells.

Evidence for such cross-talk and intracellular communication emphasises that although studies investigating polymorphisms in a single gene are important, DNA repair does not occur by a single enzyme in isolation. Polymorphisms exist in a variety of other BER repair proteins including XRCC1 and APE1 (Hung R.J. *et al.* 2005) and an individual with a combination of mutant, potentially deficient, repair proteins could be more at risk of disease development. This may explain why there is conflicting epidemiological evidence linking possession of the cys326 allele with increased cancer risk. Increasingly, epidemiology studies are addressing this issue by investigating the risk of cancer in

individuals with multiple BER protein polymorphic variants (e.g. Klinchid J. *et al.* 2009; Stanczyk M. *et al.* 2011).

In summary, the data presented in this thesis provide further evidence of modulation of OGG1 activity, not due to transcriptional change, following exposure to oxidative stress. We have successfully developed Ser326-hOGG1 and Cys326-hOGG1 expressing MEF cells which provide a useful tool for the continued study of the hOGG1 protein. Our data further support the growing evidence for impaired Cys326-hOGG1 repair activity under conditions of oxidative stress which may have important implications for individual susceptibility to diseases including cancer.

6.2 Future work

The work presented in chapter three using MH1C1 cells could be extended to determine what underlies the differential response of mOGG1 and rOGG1 to BSO treatment. Using MH1C1 cells, the concentration of BSO could be increased or alternative oxidants could be used to attempt to induce greater levels of ROS. Additionally, the experiments described in chapter three could be conducted with non-tumorous rOGG1-expressing cells and/or rOGG1-expressing cells with lower basal OGG1 activity.

The work presented in chapter five reveals three major areas which could be further investigated; hOGG1 dimer formation, hOGG1 retention within the insoluble nuclear fraction and hOGG1 post translational modification following oxidative stress. As described in section 5.3 there are several modifications required for a successful study into OGG1 dimerisation using BiFC. The current model using YFP could be improved by the use of positive control vectors and cross linking agents. Alternatively, the study could be completely modified to use a different version of YFP such as the Venus protein, which is better suited to the mammalian cell system. The formation of a hetero-dimer with other cellular proteins could be investigated using immunoprecipitation coupled with mass spectrometry or a yeast two hybrid assay.

The difference in retention of Ser326- and Cys326-hOGG1 within the insoluble nuclear fraction is potentially very interesting but due to time restraints it was not possible to fully complete the western blotting section of the investigation. A combination of optimised western blotting and more advanced use of confocal microscopy imaging would allow quantification of hOGG1 fluorescence in each fraction. Western blotting

could also be used to investigate hOGG1 post translational modifications such as acetylation and phosphorylation status following BSO treatment.

Finally, as described in chapter five, we found that following BSO treatment of Ser326- and Cys326-hOGG1 MEF cells the cleaved beacon localised in the nucleus, in contrast to previously observed mitochondrial beacon localisation following potassium bromate treatment of WT MEF cells (Mirbahai L. *et al.* 2010). This interesting observation is currently the subject of investigation within our laboratory.

Chapter 7 – References

Aburatani H., Hippo Y., Ishida T., Takashima R., Matsuba C., Kodama T., Takao M., Yasui A., Yamamoto K., Asano M., Fukasawa K., Yoshinari T., Inoue H., Ohtsuka E. and Nishimura S. **(1997)** *Cloning and characterization of mammalian 8-hydroxyguanine-specific DNA glycosylase/apurinic, apyridimic lyase, a functional mutM homologue* Cancer Research 57:2151-2156

Achanta G. and Huang P. **(2004)** *Role of p53 in sensing oxidative DNA damage in response to reactive oxygen species-generating agents* Cancer Research 64:6233–6239

Adler V., Yin Z., Tew K.D. and Ronai Z. **(1999)** *Role of redox potential and reactive oxygen species in stress signaling* Oncogene 18:6104-6111

Agalliu I., Kwon E.M., Salinas C.A., Koopmeiners J.S., Ostrander E.A. and Stanford J.L. **(2010)** *Genetic variation in DNA repair genes and prostate cancer risk: results from a population-based study* Cancer Causes Control 21:289-300

Alam Z.I., Jenner A., Daniel S.E., Lees A.J., Cairns N., Marsden C.D., Jenner P. and Halliwell B. **(1997)** *Oxidative DNA damage in the parkinsonian brain: An apparent selective increase in 8-hydroxyguanine levels in substantia nigra* Journal of Neurochemistry 69:1196-1203

Alexeyev M.F., LeDoux S.P. and Wilson G.L. **(2004)** *Mitochondrial DNA and aging* Clinical Science 107:355-364

Almeida K.H. and Sobol R.W. **(2007)** *A unified view of base excision repair: Lesion-dependent protein complexes regulated by post-translational modification* DNA Repair 6:695-711

Ames B.N., Shigenaga M.K. and Hagen T.M. **(1993)** *Oxidants, antioxidants, and the degenerative diseases of aging* Proceedings of the National Academy of Sciences U.S.A. 90:7915-7922

Amouroux R., Campalans A., Epe B. and Radicella J.P. **(2010)** *Oxidative stress triggers the preferential assembly of base excision repair complexes on open chromatin regions* Nucleic Acids Research 38:2878-2890

Anderson M.E. **(1998)** *Glutathione: an overview of biosynthesis and modulation* Chemico-Biological Interactions 111-112:1-14

Arai K., Morishita K., Shinmura K., Kohno T., Kim S.R., Nohmi T., Taniwaki M., Ohwada S. and Yokota J. **(1997)** *Cloning of a human homolog of the yeast OGG1 gene that is involved in the repair of oxidative DNA damage* Oncogene 14:2857-2861

Audebert M., Radicella J.P. and Dizdaroglu M. **(2000)** *Effect of single mutations in the OGG1 gene found in human tumours on the substrate specificity of the Ogg1 protein* Nucleic Acids Research 28:2672-2678

Bagchi D., Hassoun E.A., Bagchi M., Muldoon D.F. and Stohs S.J. **(1995)** *Oxidative stress induced by chronic administration of sodium dichromate [Cr(VI)] to rats*

Comparative biochemistry and physiology, Part C, Pharmacology, Toxicology and Endocrinology 110:281-287

Balendiran G.K., Dabur R. and Fraser D. **(2004)** *The role of glutathione in cancer* Cell Biochemistry and Function 22:343-352

Ballatori N., Hammond C.L., Cunningham J.B., Krance S.M. and Marchan R. **(2005)** *Molecular mechanisms of reduced glutathione transport: role of the MRP/CFTR/ABCC and OATP/SLC21A families of membrane proteins* Toxicology and Applied Pharmacology 204:238-255

Bannister A.J. and Kouzarides T. **(1996)** *The CBP co-activator is a histone acetyltransferase* Nature 384:641-643

Bartosz G. **(2006)** *Use of spectroscopic probes for detection of reactive oxygen species* Clinica Chimica Acta 368:53-76

Beckman J.S., Beckman T.W., Chen J., Marshall P.A. and Freeman B.A. **(1990)** *Apparent hydroxyl radical production by peroxynitrite: Implications for endothelial injury from nitric oxide and superoxide* Proceedings of the National Academy of Sciences U.S.A. 87:1620-1624

Bedard K. and Krause K.H. **(2007)** *The NOX family of ROS-generating NADPH oxidases: physiology and pathophysiology* Physiological Reviews 87:245-313

Bhakat K.K., Mokkapati S.K., Boldogh I., Hazra T.K. and Mitra S. **(2006)** *Acetylation of human 8-oxoguanine-DNA glycosylase by p300 and its role in 8-oxoguanine repair in vivo* Molecular and Cellular Biology 26:1654-1665

Biswas S., Chida A.S. and Rahman I. **(2006)** *Redox modifications of protein-thiols: Emerging roles in cell signalling* Biochemical Pharmacology 71:551-564

Bjørås M., Seeberg E., Luna L., Pearl L.H. and Barrett T.E. **(2002)** *Reciprocal "flipping" underlies substrate recognition and catalytic activation by the human 8-oxo-guanine DNA glycosylase* Journal of Molecular Biology 317:171-177

Black H.S. **(1987)** *Potential involvement of free radical reactions in ultraviolet light-mediated cutaneous damage* Photochemistry and Photobiology 46:213-221

Blons H., Radicella J.P., Laccourreye O., Brasnu D., Beaune P., Boiteux S. and Laurent-Puig P. **(1999)** *Frequent allelic loss at chromosome 3p distinct from genetic alterations of the 8-oxoguanine DNA glycosylase 1 gene in head and neck cancer* Molecular Carcinogenesis 26:254-260

Boiteux S. and Guillet M. **(2004)** *Abasic sites in DNA: repair and biological consequences in Saccharomyces cerevisiae* DNA Repair 3:1-12

Boiteux S. and Radicella J.P. **(2000)** *The human OGG1 gene: structure, functions, and its implication in the process of carcinogenesis* Archives of Biochemistry and Biophysics 377:1-8

Bokara K.K., Brown E., McCormick R., Yallapragada P.R., Rajanna S. and Bettaiya R. **(2008)** *Lead-induced increase in antioxidant enzymes and lipid peroxidation products in developing rat brain* Biometals 21:9-16

Borgaonkar D.S. **(1973)** *Philadelphia-chromosome translocation and chronic myeloid leukaemia* Lancet 1(7814)1250

Boyce R.P. and Howard-Flanders P. **(1964)** *Release of ultraviolet light-induced thymine dimers from DNA in E.coli K1-12* Proceedings of the National Academy of Sciences U.S.A. 51:293-300

Bradford M.M. **(1976)** *A rapid and sensitive method for the quantification of microgram quantities of protein utilizing the principle of protein-dye binding.* Analytical Biochemistry 72:248-254

Bravard A., Vacher M., Gouget B., Coutant A., de Boisferon F.H., Marsin S., Chevillard S. and Radicella J.P. **(2006)** *Redox regulation of human OGG1 activity in response to cellular oxidative stress* Molecular and Cellular Biology 26:7430-7436

Bravard A., Vacher M., Moritz E., Vaslin L., Hall J., Epe B. and Radicella J.P. **(2009)** *Oxidation status of human OGG1-S326C polymorphic variant determines cellular DNA repair capacity* Cancer Research 69:3642-3649

Breen A.P. and Murphy J.A. **(1995)** *Reactions of oxyl radicals with DNA* Free Radical Biology and Medicine 18:1033-1077

Brown G.C. and Borutaite V. **(2004)** *Inhibition of mitochondrial respiratory complex I by nitric oxide, peroxynitrite and S-nitrothiols* Biochimica et Biophysica Acta 1658:44-49

Browne S.E., Bowling A.C., MacGarvey U., Baik M.J., Berger S.C., Muqit M.M., Bird E.D. and Beal M.F. **(1997)** *Oxidative damage and metabolic dysfunction in Huntington's disease: selective vulnerability of the basal ganglia* Annals of Neurology 41:646-653

Bruner S.D., Norman D.P.G. and Verdine G.L. **(2000)** *Structural basis for recognition and repair of the endogenous mutagen 8-oxoguanine in DNA* Nature 403:859-866

Burden R.H. **(1995)** *Superoxide and hydrogen peroxide in relation to mammalian cell proliferation* Free Radical Biology and Medicine 18:775-794

Cabantous S., Terwilliger T.C. and Waldo G.S. **(2005)** *Protein tagging and detection with engineered self-assembly fragments of green fluorescent protein* Nature Biotechnology 23:102-107

Cadet J., Douki T., Ravanat J.L. **(2008)** *Oxidatively generated damage to the guanine moiety of DNA: mechanistic aspects and formation in cells* Accounts of Chemical Research 41:1075-1083

Cai Q., Shu X.O., Wen W., Courtney R., Dai Q., Gao Y.T. and Zheng W. **(2006)** *Functional Ser326Cys polymorphism in the hOGG1 gene is not associated with breast cancer risk* Cancer Epidemiology Biomarkers and Prevention 15:403-404

Caldecott K.W., Aoufouchi S., Johnson P. and Shall S. **(1996)** *XRCC1 polypeptide interacts with DNA polymerase β and possibly poly (ADP-ribose) polymerase, and DNA ligase III is a novel molecular 'nick-sensor' in vitro* Nucleic Acids Research 24:4387-4394

Caldecott K.W., McKeown C.K., Tucker J.D., Ljungquist S. and Thompson L.H. **(1994)** *An interaction between the mammalian DNA repair protein XRCC1 and DNA ligase III* Molecular and Cellular Biology 14:68-76

Campalans A., Amouroux R., Bravard A., Epe B. and Radicella J.P. **(2007)** *UVA irradiation induces relocalisation of the DNA repair protein hOGG1 to nuclear speckles* Journal of Cell Science 120:23-32

Carini M., Aldini G., Piccone M. and Facino R.M. **(2000)** *Fluorescent probes as markers of oxidative stress in keratinocyte cell lines following UVB exposure* Il Farmaco 55:526-534

Caro A.A. and Cederbaum A.I. **(2004)** *Oxidative stress, toxicology, and pharmacology of CYP2E1* Annual Reviews in Pharmacology and Toxicology 44:27-42

Chen S.K., Hsieh W.A., Tsai M.H., Chen C.C., Hong A.I., Wei Y.H. and Chang W.P. **(2003)** *Age-associated decrease of oxidative repair enzymes, human 8-oxoguanine DNA glycosylases (hOGG1), in human aging* Journal of Radiation Research 44:31-35

Chenna, Ramu, Sugawara, Hideaki, Koike,Tadashi, Lopez, Rodrigo, Gibson, Toby J, Higgins, Desmond G, Thompson and Julie D. **(2003)** Nucleic Acids Research 31:3497-34500

Cheng K.C., Cahill D.S., Kasai H., Nishimura S. and Loeb L.A. **(1992)** *8-Hydroxyguanine, an abundant form of oxidative DNA damage, causes G→T and A→C substitutions* Journal of Biological Chemistry 267:166-172

Chinta S.J. and Anderson J.K. **(2008)** *Redox imbalance in Parkinson's disease* Biochimica et Biophysica Acta 1780:1362-1367

Cho E.Y., Hildesheim A., Chen C.J., Hsu M.M., Chen I.H., Mittl B.F., Levine P.H., Liu M.Y., Chen J.Y., Brinton L.A., Cheng Y.J. and Yang C.S. **(2003)** *Nasopharyngeal carcinoma and genetic polymorphisms of DNA repair enzymes XRCC1 and hOGG1* Cancer Epidemiology Biomarkers and Prevention 12:1100-1104

Choi J.Y., Hamajima N., Tajima K., Yoo K.Y., Yoon K.S., Kyunk Park S., Kim S.U., Lee K.M., Noh D.Y., Ahn S.H., Choe K.J., Han W., Hirvonen A. and Kang D. **(2003)** *hOGG1 Ser326Cys polymorphism and breast cancer risk among Asian women* Breast Cancer Research and Treatment 79:59-62

Chomczynski P. and Sacchi N. **(1987)** *Single-step method of RNA isolation by acid guanidinium thiocyanate-phenol-chloroform extraction* 162:156-159

Christmann M., Tomicic M.T., Roos W.P. and Kaina B. **(2003)** *Mechanisms of human DNA repair: an update* Toxicology 193:3-34

Ciruela F. **(2008)** *Fluorescence-based methods in the study of protein-protein interactions in living cells* Current Opinion in Biotechnology 19:338-343

Cohn V.H. and Lyle J. **(1966)** *A fluorometric assay for glutathione* Analytical Biochemistry 14:434-440

Colussi C., Parlanti E., Degan P., Aquilina G., Barnes D., Macpherson P., Karran P., Crescenzi M., Dogliotti E. and Bignami M. **(2002)** *The mammalian mismatch repair pathway removes DNA 8-oxodGMP incorporated from the oxidized dNTP pool* Current Biology 12:912-918

Conlon K.A., Zharkov D.O. and Berrios M. **(2003)** *Immunofluorescent localization of the murine 8-oxoguanine DNA glycosylase (mOGG1) in cells growing under normal and nutrient deprivation conditions* DNA Repair 2:1337-1352

Cooke M.S., Olinski R. and Evans M.D. **(2006)** *Does measurement of oxidative damage to DNA have clinical significance?* Clinica Chimica Acta 365:30-49

Cortina M.S., Gordon W.C., Lukiw W.J. and Bazan N.G. **(2005)** *Oxidative stress-induced retinal damage up-regulates DNA polymerase gamma and 8-oxoguanine-DNA-glycosylase in photoreceptor synaptic mitochondria* Experimental Eye Research 81:742-750

Costa R.M.A., Chigançcas V., da Silva Galhardo R., Carvalho H., Menck C.F.M. **(2003)** *The eukaryotic nucleotide excision repair pathway* Biochimie 85:1083-1099

Dahle J., Brunborg G., Svendsrud D.H., Stokke T. and Kvam E. **(2008)** *Overexpression of human OGG1 in mammalian cells decreases ultraviolet A induced mutagenesis* Cancer Letters 267:18-25

Dalhus B., Forsbring M., Helle I.H., Vik E.S., Forstrøm R.J., Backe P.H., Alseth I. and Bjøras M. **(2011)** *Separation-of-function mutants unravel the dual-reaction mode of human 8-oxoguanine DNA glycosylase* Structure 19:117-127

Dantzer F., Luna L., Bjørås M. and Seeberg E. **(2002)** *Human OGG1 undergoes serine phosphorylation and associates with the nuclear matrix and mitotic chromatin in vivo* Nucleic Acids Research 30:2349-2357

David S.S., O'Shea V.L. and Kundu S. **(2007)** *Base-excision repair of oxidative DNA damage* Nature 447:941-950

de Souza-Pinto N.C., Eide L., Hogue B.A., Thybo T., Stevnsner T., Seeberg E., Klungland A. and Bohr V.A. **(2001)** *Repair of 8-oxodeoxyguanosine lesions in mitochondrial DNA depends on the oxoguanine DNA glycosylase (OGG1) gene and 8-*

oxoguanine accumulates in the mitochondrial DNA of OGG1-defective mice Cancer Research 61:5378-5381

de Souza-Pinto N.C., Maynard S., Hashiguchi K., Hu J., Muftuoglu M. and Bohr V.A. **(2009)** *The recombination protein RAD52 cooperates with the excision repair protein OGG1 for the repair of oxidative lesions in mammalian cells* Molecular and Cellular Biology 29:4441-4454

de Souza-Pinto N.C., Wilson D.M.III, Stevnsner T.V. and Bohr V.A. **(2008)** *Mitochondrial DNA, base excision repair and neurodegeneration* DNA Repair 7:1098-1109

de Virgilio M., Kiosses W.B. and Shattil S.J. **(2004)** *Proximal, selective, and dynamic interactions between integrin αIIbβ3 and protein tyrosine kinases in living cells* The Journal of Cell Biology 165:305-311

de Wind N., Dekker M., Claij N., Jansen L., van Klink Y., Radman M., Riggins G., van der Valk M., van't Wout K. and te Riele H. **(1999)** *HNPCC-like cancer predisposition in mice through simultaneous loss of Msh3 and Msh6 mismatch-repair protein functions* Nature Genetics 23:359-362

Demple B. and Harrison L. **(1994)** *Repair of oxidative damage to DNA: Enzymology and Biology* Annual Reviews Biochemistry 63:915-948

DeWeese T.L., Shipman J.M., Larrier N.A., Buckley N.M., Kidd L.R., Groopman J.D., Cutler R.G., Te Riele H., Nelson W.G. **(1998)** *Mouse embryonic stem cells carrying one or two defective Msh2 alleles respond abnormally to oxidative stress inflicted by low-level radiation* Proceedings of the National Academy of Sciences U.S.A. 95:11915-11920

Dhakshinamoorthy S., Long D.J. 2nd. and Jaiswal A.K. **(2000)** *Antioxidant regulation of genes encoding enzymes that detoxify xenobiotics and carcinogens* Current Topics in Cellular Regulation 36:201-216

Dhénaut A., Boiteux S. and Radicella J.P. **(2000)** *Characterization of the hOGG1 promoter and its expression during the cell cycle* Mutation Research 461:109-118

Dherin C., Radicella J.P., Dizdaroglu M. and Boiteux S. **(1999)** *Excision of oxidatively damaged DNA bases by the human α-hOgg1 protein and the polymorphic α-hOgg1(Ser326Cys) protein which is frequently found in human populations* Nucleic Acids Research 27:4001-4007

Dobson A.W., Kelley M.R., Wilson G.L. and LeDoux S.P. **(2002)** *Targeting DNA repair proteins to mitochondria* Methods in Molecular Biology 197:351-362

Dou H., Mitra S. and Hazra T.K. **(2003)** *Repair of oxidized bases in DNA bubble structures by human DNA glycosylases NEIL1 and NEIL2* The Journal of Biological Chemistry 278:49679-49684

Dröge W. **(2002)** *Free radicals in the physiological control of cell function* Physiological Reviews 82:47-95

Duthie S.J., Ma A., Ross M.A. and Collins A.R. **(1996)** *Antioxidant supplementation decreases oxidative DNA damage in human lymphocytes* Cancer Research 15:1291-1295

Eckner R., Ewen M.E., Newsome D., Gerdes M., DeCaprio J.A., Lawrence J.B. and Livingston D.M. **(1994)** *Molecular cloning and functional analysis of the adenovirus E1A-associated 300-kD protein (p300) reveals a protein with properties of a transcriptional adaptor* Genes and Development 8:869-884

Elahi A., Zheng Z., Park J., Eyring K., McCaffrey T. and Lazarus P. **(2002)** *The human OGG1 DNA repair enzyme and its association with orolaryngeal cancer risk* Carcinogenesis 23:1229-1234

Erhola M., Toyokuni S., Okada K., Tanaka T., Hiai H., Ochi H., Uchida K., Osawa T., Nieminen M.M., Alho H. and Kellokumpu-Lehtinen P. **(1997)** *Biomarker evidence of DNA oxidation in lung cancer patients: association of urinary 8-hydroxy-2'-deoxyguanosine excretion with radiotherapy, chemotherapy, and response to treatment* Federation of European Biochemical Societies Letters 409:287-291

Evans M.D., Dizdaroglu M. and Cooke M.S. **(2004)** *Oxidative DNA damage and disease: induction, repair and significance* Mutation Research 567:1-61

Floyd R.A. **(1990)** *The role of 8-hydroxyguanine in carcinogenesis* Carcinogenesis 11:1447-1450

Forman H.J., Zhang H. and Rinna A. **(2009)** *Glutathione: overview of its protective roles, measurement, and biosynthesis* Molecular Aspects of Medicine 30:1-12

Fousteri M. and Mullenders L.H.F. **(2008)** *Transcription-coupled nucleotide excision repair in mammalian cells: molecular mechanisms and biological effects* Cell Research 18:73-84

Fridovich I. **(1978)** *The Biology of Oxygen Radicals* Science 201:875-880

Frossi B., Tell G., Spessotto P., Colombatti A., Vitale G. and Pucillo C. **(2002)** *H_2O_2 induces translocation of APE/Ref-1 to mitochondria in the Raji B-cell line* Journal of Cellular Physiology 193:180-186

Gackowski D., Banaszkiewicz Z., Rozalski R., Jawien A. and Olinski R. **(2002)** *Persistent oxidative stress in colorected carcinoma patients* International Journal of Cancer 101:395-397

Genestra M. **(2007)** *Oxyl radicals, redox-sensitive signalling cascades and antioxidants* Cellular Signalling 19:1807-1819

Ghosh R. and Mitchell D.L. **(1999)** *Effect of oxidative DNA damage in promoter elements on transcription factor binding* Nucleic Acids Research 27:3213-3218

Giulivi C., Poderoso J.J. and Boveris A. **(1998)** *Production of nitric oxide by mitochondria* The Journal of Biological Chemistry 273:11038-11043

Giustarini D., Rossi R., Milzani A., Colombo R. and Dalle-Donne I. **(2004)** *S-glutathionylation: from redox regulation of protein functions to human diseases* Journal of Cellular and Molecular Medicine 8:201-212

Gomes A., Fernandes E. and Lima J.L.F.C. **(2005)** *Fluorescence probes used for detection of reactive oxygen species* Journal of Biochemical and Biophysical Methods 65:45-80

Goodman R.H. and Smolik S. **(2000)** *CBP/p300 in cell growth, transformation, and development* Genes and Development 14:1553-1577

Green R.M., Graham M., O'Donovan M.R., Chipman J.K. and Hodges N.J. **(2006)** *Subcellular compartmentalization of glutathione: correlations with parameters of oxidative stress related to genotoxicity* Mutagenesis 21:383-390

Greenman C., Stephens P., Smith R., Dalgliesh G.L., Hunter C., Bignell G., Davies H., Teague J., Butler A., Stevens C., Edkins S., O'Meara S., Vastrik I., Schmidt E.E., Avis T., Barthorpe S., Bhamra G., Buck G., Choudhury B., Clements J., Cole J., Dicks E., Forbes S., Gray K., Halliday K., Harrison R., Hills K., Hinton J., Jenkinson A., Jones D., Menzies A., Mironenko T., Perry J., Raine K., Richardson D., Shepherd R., Small A., Tofts C., Varian J., Webb T., West S., Widaa S., Yates A., Cahill D.P. Louis D.N., Goldstraw P., Nicholson A.G., Brasseur F., Looijjenga L., Weber B.L., Chiew Y.E., Chenevix-Trench G., Tan M.H., Khoo S.K., Teh B.T., Yuen S.T., Leung S.Y., Wooster R., Futreal P.A. and Strattor M.R. **(2007)** *Patterns of somatic mutation in cancer genomes* Nature 446:153-158

Griffith O.W. **(1982)** *Mechanism of action, metabolism, and toxicity of buthionine sulphoximine and its higher homologues, potent inhibitors of glutathione synthesis* Journal of Biological Chemistry 257:13704-13712

Griffith O.W., Anderson M.E. and Meister A. **(1979)** *Inhibition of glutathione biosynthesis by prothionine sulfoximine (S-n-propyl-homocysteine sulfoximine), a selective inhibitor of γ-glutamylcysteine synthetase* The Journal of Biological Chemistry 254:1205-1210

Griffith O.W. and Meister A. **(1979)** *Glutathione, interorgan translocation, turnover and metabolism* Proceedings of the National Academy of Sciences U.S.A. 76:5606-5610

Gruber J., Schaffer S. and Halliwell B. **(2008)** *The mitochondrial free radical theory of ageing – where do we stand?* Frontiers in Bioscience 13:6554-6579

Guyton K.Z. and Kensler T.W. **(1993)** *Oxidative mechanisms in carcinogenesis* British Medical Bulletin 49:523-544

Hailer M.K., Slade P.G., Martin B.D., Rosenquist T.A. and Sugden K.D. **(2005)** *Recognition of the oxidised lesions spiroiminodihydantoin and guanidinohydantoin in*

DNA by the mammalian base excision repair glycosylases NEIL1 and NEIL2 DNA Repair 4:41-50

Halliwell B. **(2007)** *Oxidative stress and cancer: have we moved forward?* Biochemical Journal 401:1-11

Hardie L.J., Briggs J.A., Davidson L.A., Allan J.M., King R.F.G.J., Williams G.I. and Wild C.P. **(2000)** *The effect of hOGG1 and glutathione peroxidase I genotypes and 3p chromosomal loss on 8-hydroxydeoxyuanosine levels in lung cancer* Carcinogenesis 21:167-172

Harman D. **(1956)** *Aging: a theory based on free radical and radiation chemistry* Journal of Gerontology 11:298-300

Harrison R. **(2002)** *Structure and function of xanthine oxidoreductase: Where are we now?* Free Radical Biology and Medicine 33:774-797

Hasan S., Hassa P.O., Imhof R. and Hottiger M.O. **(2001)** *Transcription coactivator p300 binds PCNA and may have a role in DNA repair synthesis* Nature 410:387-391

Hasan S., Stucki M., Hassa P.O., Imhof R., Gehrig P., Hunziker P., Hübscher U. and Hottiger M.O. **(2001.2)** *Regulation of human flap endonuclease-1 activity by acetylation through the transcriptional coactivator p300* Molecular Cell 7:1221-1231

Hashiguchi K., Stuart J.A., de Souza-Pinto N.C. and Bohr V.A. **(2004)** *The C-terminal αO helix of human Ogg1 is essential for 8-oxoguanine DNA glycosylase activity: the mitochondrial β-Ogg1 lacks this domain and does not have glycosylase activity* Nucleic Acids Research 32:5596-5608

Hashimoto T., Uchida K., Okayama N., Imate Y., Suehiro Y., Hamanaka Y., Ueyama Y., Yamashita H. and Hinoda Y. **(2006)** *Interaction of OGG1 Ser326Cys polymorphism with cigarette smoking in head and neck squamous cell carcinoma* Molecular Carcinogenesis 45:344-348

Hayden R.E., Pratt G., Davies N.J., Khanim F.L., Birtwistle J., Delgado J., Pearce C., Sant T., Drayson M.T. and Bunce C.M. **(2009)** *Treatment of primary CLL cells with bezafibrate and medroxyprogesterone acetate induces apoptosis and represses the pro-proliferative signal of CD40-ligand, in part through increased* $15d\Delta^{12,14,}PGJ_2$ Leukemia 23:292-304

Haynes V., Elfering S., Traaseth N. and Giulivi C. **(2004)** *Mitochondrial nitric-oxide synthase: enzyme expression, characterization, and regulation* Journal of Bioenergetics and Biomembranes 36:341-346

Hazra T.K., Das A., Das S., Choudhury S., Kow Y.W. and Roy R. **(2007)** *Oxidative DNA damage repair in mammalian cells: A new perspective* DNA Repair 6:470-480

Hegde M.L., Hazra T.K. and Mitra S. **(2008)** *Early steps in the DNA base excision/single-strand interuption repair pathway in mammalian cells* Cell Research 18:27-47

Hegde V., Wang M. and Deutsch W.A. **(2004.1)** *Characterization of human ribosomal protein S3 binding to 7,8-dihydro-8-oxoguanine and abasic sites by surface plasmon resonance* DNA Repair 3:121-126

Hegde V., Wang M. and Deutsch W.A. **(2004.2)** *Human ribosomal protein S3 interacts with DNA base excision repair proteins hAPE/Ref-1 and hOGG1* Biochemistry 43:14211-14217

Hegde V., Wang M., Mian S., Spyres L. and Deutsch W.A. **(2006)** *The high binding affinity of human ribosomal protein S3 to 7,8-dihydro-8-oxoguanine is abrogated by a single amino acid change* DNA Repair 5:810-815

Hegde V., Yadavilli S. and Deutsch W.A. **(2007)** *Knockdown of ribosomal protein S3 protects human cells from genotoxic stress* DNA Repair 6:94-99

Hegde V., Yadavilli S., McLaughlin L.D. and Deutsch W.A. **(2009)** *DNA repair efficiency in transgenic mice over expressing ribosomal protein S3* Mutation Research 666:16-22

Hill J.W. and Evans M.K. **(2006)** *Dimerization and opposite base-dependent catalytic impairment of polymorphic S326C OGG1 glycosylase* Nucleic Acids Research 34:1620-1632

Hill J.W., Hazra T.K., Izumi T. and Mitra S. **(2001)** *Stimulation of human 8-oxoguanine-DNA glycosylase by AP-endonuclease: potential coordination of the initial steps in base excision repair* Nucleic Acids Research 29:430-438

Hissin P.J. and Hilf R. **(1976)** *A fluorometric method for determination of oxidised and reduced glutathione in tissues* Analytical Biochemistry 74:214-226

Hodges N.J. and Chipman J.K. **(2002)** *Down-regulation of the DNA-repair endonuclease 8-oxo-guanine DNA glycosylase 1 (hOGG1) by sodium dichromate in cultured human A549 lung carcinoma cells* Carcinogenesis 23:55-60

Hoeijmakers J.H. **(2001)** *Genome maintenance mechanisms for preventing cancer* Nature 411:366-374

Hollenbach S., Dhénaut A., Eckert I., Radicella J.P. and Epe B. **(1999)** *Overexpression of ogg1 in mammalian cells: effects on induced and spontaneous oxidative DNA damage and mutagenesis* Carcinogenesis 20:1863-1868

Hollstein M., Shomer B., Greenblatt M., Soussi T., Hovig E., Montesano R. and Harris C.C. **(1996)** *Somatic point mutations in the p53 gene of human tumours and cell lines: updated compilation* Nucleic Acids Research 24:141-146

Horton T.M., Petros J.A., Heddi A., Shoffner J., Kaufman A.E., Graham S.D. Jr., Gramlich T. and Wallace D.C. **(1996)** *Novel mitochondrial DNA deletion found in renal cell carcinoma* Genes, Chromosomes and Cancer 15:95-101

Hu C.D., Chinenov Y. and Kerppola T.K. **(2002)** *Visualization of interactions among bZIP and Rel family proteins in living cells using bimolecular fluorescence complementation* Molecular Cell 9:789-798

Hu J., Imam S.Z., Hashiguchi K., de Souza-Pinto N.C. and Bohr V.A. **(2005)** *Phosphorylation of human oxoguanine DNA glycosylase (α-OGG1) modulates its function* Nucleic Acids Research 33:3271-3282

Huang W.Y., Gao Y.T., Rashid A., Sakoda L.C., Deng J., Shen M.C., Wang B.S., Han T.Q., Zhang B.H., Chen B.E., Rosenberg P.S., Chanock S.J. and Hsing A.W. **(2008)** *Selected base excision repair gene polymorphisms and susceptibility to biliary tract cancer and biliary stones: a population-based case-control study in China* Carcinogenesis 29:100-105

Hung R.J., Hall J., Brennan P. and Boffetta P. **(2005)** *Genetic polymorphisms in the base excision repair pathway and cancer risk: a HuGE review* Americal Journal of Epidemiology 162:925-942

Hunter D.J. **(2005)** *Gene-environment interactions in human diseases* Nature Reviews Genetics 6:287-298

Hussain R.F., Nouri A.M. and Oliver R.T. **(1993)** *A new approach for measurement of cytotoxicity using colorimetric assay* Journal of immunological methods 160:89-96

Ikediobi C.O., Badisa V.L., Ayuk-Takem L.T., Latinwo L.M. and West J. **(2004)** *Response of antioxidant enzymes and redox metabolites to cadmium-induced oxidative stress in CRL-1439 normal rat liver cells* International Journal of Molecular Medicine 14:87-92

Imai K., Nakata K., Kawai K., Hamano T., Mei N., Kasai H. and Okamoto T. **(2005)** *Induction of OGG1 gene expression by HIV-1 Tat* The Journal of Biological Chemistry 250:26701-26713

Inoue M., Osaki T., Noguchi M., Hirohashi S., Yasumoto K. and Kasai H. **(1998)** *Lung cancer patients have increased 8-hydroxydeoxyguanosine levels in peripheral lung tissue DNA* Japanese Journal of Cancer Research 89:691-695

Janssen K., Schlink K., Götte W., Hippler B., Kaina B. and Oesch F. **(2001)** *DNA repair activity of 8-oxoguanine DNA glycosylase 1 (OGG1) in human lymphocytes is not dependent on genetic polymorphism Ser326/Cys326* Mutation Research 486:207-216

Jeong H.G., Youn C.K., Cho H.J., Kim S.H., Kim M.H., Kim H.B., Chang I.Y., Lee Y.S., Chung M.H. and You H.J. **(2004)** *Metallothionein-III prevents γ-ray-induced 8-oxoguanine accumulation in normal and hOGG1-depleted cells* The Journal of Biological Chemistry 279:34138-34149

Ježek P. and Hlavatá L. **(2005)** *Mitochondria in homeostasis of reactive oxygen species in cell, tissues, and organism* The International Journal of Biochemistry and Cell Biology 37:2478-2503

Kalinina E.V., Chernov N.N. and Saprin A.N. **(2008)** *Involvement of Thio-, Peroxi-, and Glutaredoxins in cellular redox-dependent processes* Biochemistry (Moscow) 73:1493-1510

Kamata H. and Hirata H. **(1999)** *Redox regulation of cellular signalling* Cellular Signalling 11:1-14

Kasai H. and Nishimura S. **(1984)** *Hydroxylation of deoxyguanosine at the C-8 position by ascorbic acid and other reducing agents* Nucleic Acids Research 12:2137-2145

Kerppola T.K. **(2008)** *Bimolecular fluorescence complementation (BiFC) analysis as a probe of protein interactions in living cells* Annual Review of Biophysics 37:465-487

Kerppola T.K. **(2009)** *Visualization of molecular interactions using bimolecular fluorescence complementation analysis: Characteristics of protein fragment complementation* Chemical Society Reviews 38:2876-2886

Kim K.B. and Lee B.M. **(1997)** *Oxidative stress to DNA, protein, and antioxidant enzymes (superoxide dismutase and catalase) in rats treated with benzo(a) pyrene* Cancer Letters 113:205-212

Kim J.I., Park Y.J., Kim K.H., Kim J.I., Song B.J., Lee M.S., Kim C.N. and Chang S.H. **(2003)** *hOGG1 Ser326Cys polymorphism modifies the significance of the environmental risk factor for colon cancer* World Journal of Gastroenterology 9:956-960

Klein J.C., Bleeker M.J., Saris C.P., Roelen H.C.P.F., Brugghe H.F., van den Elst H., van der Marel G.A., van Boom J.H., Westra J.G., Kriek E. and Berns A.J.M. **(1992)** *Repair and replication of plasmids with site-specific 8-oxo-dG and 8-AAF-dG residues in normal and repair-deficient human cells* Nucleic Acids Research 20:4437-4443

Klinchid J., Chewaskulyoung B., Saeteng S., Lertprasertsuke N., Kasinrerk W. and Cressey R. **(2009)** *Effect of combined genetic polymorphisms on lung cancer risk in northern Thai women* Cancer Genetics and Cytogenetics 195:143-149

Klungland A. and Bjelland S. **(2007)** *Oxidative damage to purines in DNA: Role of mammalian OGG1* DNA Repair 6:481-488

Klungland A., Rosewell I., Hollenbach S., Larsen E., Daly G.K., Epe B., Lindahl T. and Barnes D.E. **(1999)** *Accumulation of premutagenic DNA lesions in mice defective in removal of oxidative base damage* Proceedings of the National Academy of Sciences U.S.A. 96:13300-13305

Kohen R. and Nyska A. **(2002)** *Oxidation of biological systems: Oxidative stress phenomena, antioxidants, redox reactions, and methods for their quantification* Toxicologic Pathology 30:620-650

Kohno T., Shinmura K., Tosaka M., Tani M., Kim S.R., Sugimura H., Nohmi T., Kasai H. And Yokota J. **(1998)** *Genetic polymorphisms and alternative splicing of the hOGG1 gene, that is involved in the repair of 8-hydroxyguanine in damaged DNA* Oncogene 16:3219-3225

Kohno T., Kunitoh H., Toyama K., Yamamoto S., Kuchiba A., Saito D., Yanagitani N., Ishihara S.I., Saito R., and Yokota J. **(2006)** *Association of the OGG1-Ser326Cys polymorphism with lung adenocarcinoma risk* Cancer Science 97:724–728

Kondo S., Toyokuni S., Tanaka T., Hiai H., Onodera H., Kasai H. and Imamura M. **(2000)** *Overexpression of the hOGG1 gene and high 8-hydroxy-2'-deoxyguanosine (8-OHdG) lyase activity in human colorectal carcinoma: regulation mechanism of the 8-OHdG level in DNA* Clinical Cancer Research 6:1394-1400

Kovtun I.V. and McMurray C.T. **(2007)** *Crosstalk of DNA glycosylases with pathways other than base excision repair* DNA Repair 6:517-529

Krokan H.E., Drabløs F. and Slupphaug G. **(2002)** *Uracil in DNA - occurrance, consequences and repair* Oncogene 21:8935-8948

Kubota Y., Nash R.A., Klungland A., Schär P., Barnes D.E. and Lindahl T. **(1996)** *Reconstitution of DNA base excision-repair with purified human proteins: interaction between DNA polymerase β and the XRCC1 protein* The EMBO Journal 15:6662-6670

Kuchino Y., Mori F., Kasai H., Inoue H., Iwai S., Miura K., Ohtsuka E. and Nishimura S. **(1987)** *Misreading of DNA templates containing 8-hydroxydeoxyguanosine at the modified base and at adjacent residues* Nature 327:77-79

Lacza Z., Puskar M., Figueroa J.P., Zhang J., Rajapaske N. and Busika D.W. **(2001)** *Mitochondrial nitric oxide synthase is constitutively active and is functionally upregulated in hypoxia* Free Radical Biology and Medicine 31:1609-1615

Lan Q. Mumford J.L., Shen M., DeMarini D.M., Bonner M.R., He X., Yeager M., Welch R., Chanock S., Tian L., Chapman R.S., Zheng T., Keohavong P., Caporaso N. and Rothman N. **(2004)** *Oxidative damage-related genes AKR1C3 and OGG1 modulate risks for lung cancer due to exposure to PAH-rich coal combustion emissions* Carcinogenesis 25:2177-2181

LeDoux S.P., Druzhyna N.M., Hollensworth S.B., Harrison J.F. and Wilson G.L. **(2007)** *Mitochondrial DNA repair: a critical player in the response of cells of the CNS to genotoxic insults* Neuroscience 145:1249-1259

Lee A.J., Hodges N.J. and Chipman J.K. **(2005)** *Interindividual variability in response to sodium dichromate-induced oxidative DNA damage: Role of the Ser^{326}Cys polymorphism in the DNA-repair protein of 8-oxo-7,8-dihydro-2'-deoxyguanosine DNA glycosylase 1* Cancer Epidemiology, Biomarkers and Prevention 14:497-505

Lee M.R., Kim S.H., Cho H.J., Lee K.Y., Moon A.R., Jeong H.G., Lee J.S., Hyun J.W., Chung M.H. and You H.J. **(2004)** *Transcription factors NF-YA regulate the induction of human OGG1 following DNA-alkylating agent methylmethane sulfonate (MMS) treatment* The Journal of Biological Chemistry 279:9857-9866

Le Marchand L.L., Donlon T., Lum-Jones A., Seifried A. and Wilkens L.R. **(2002)** *Association of the hOGG1 Ser326Cys polymorphism with lung cancer risk* Cancer Epidemiology, Biomarkers and Prevention 11:409-412

Li D., Firozi P.F., Zhang W., Shen J., DiGiovanni J., Lau S., Evans D., Friess H., Hassan M. and Abbruzzese J.L. **(2002)** *DNA adducts, genetic polymorphisms, and K-ras mutation in human pancreatic cancer* Mutation Research 513:37-48

Li H., Hao X., Zhang W., Wei Q. and Chen K. **(2008)** *The hOGG1 Ser326Cys polymorphism and lung cancer risk: a meta-analysis* Cancer Epidemiology Biomarkers and Prevention 17:1739-1745

Li W.Q., Zhang L., Ma J.L., Zhang Y., Li J.Y., Pan K.F. and You W.C. **(2009)** *Association between genetic polymorphisms of DNA base excision repair genes and evolution of precancerous gastric lesions in a Chinese population* Carcinogenesis 30:500-505

Limón-Pacheco J. and Gonsebatt M.E. **(2009)** *The role of antioxidants and antioxidant-related enzymes in protective responses to environmentally induced oxidative stress* Mutation Research 674:137-147

Lindahl T. **(1974)** *An N-Glycosidase form Escherichia coli that releases free uracil from DNA containing deaminated cytosine residues* Proceedings of the National Academy of Sciences U.S.A. 71:3649-3653

Lindahl T. and Barnes D.E. **(2000)** *Repair of endogenous DNA damage* Cold Springs Harbor symposia on quantitative biology 65:127-133

Lindahl T. and Wood R.D. **(1999)** *Quality control by DNA repair* Science 286:1897-1905

Liu P. and Demple B. **(2010)** *DNA repair in mammalian mitochondria: much more than we thought?* Environmental and Molecular Mutagenesis 51:417-426

Livak K.J. and Schmittgen T.D. **(2001)** *Analysis of relative gene expression data using real-time quantitative PCR and the* $2^{-\Delta\Delta C}{}_T$ *method* Methods 25:402-408

Lovell M.A., Gabbita S.P. and Markesbery W.R. **(1999)** *Increased DNA oxidation and decreased levels of repair products in Alzheimer's disease ventricular CSF* Journal of Neurochemistry 72:771-776

Lovell M.A. and Markesbery W.R. **(2007)** *Oxidative DNA damage in mild cognitive impairment and late-stage Alzheimer's disease* Nucleic Acids Research 35:7497-7504

Lu R., Nash H.M. and Verdine G.L. **(1997)** *A mammalian DNA repair enzyme that excises oxidatively damaged guanines maps to a locus frequently lost in lung cancer* Current Biology 7:397-407

Luna L., Rolseth V., Hildrestrand G.A., Otterlei M., Dantzer F., Bjørås M. and Seeberg E. **(2005)** *Dynamic relocalization of hOGG1 during the cell cycle is disrupted in cells*

harboring the hOGG1-Cys^{326} polymorphic variant Nucleic Acids Research 33:1813-1824

Ma H., Wang J., Abdel-Rahman S.Z., Boor P.J. and Khan M.F. **(2008)** *Oxidative DNA damage and its repair in rat spleen following subchronic exposure to aniline* Toxicology and Applied Pharmacology 233:247-253

Ma Q. **(2009)** *Transcriptional responses to oxidative stress: Pathological and toxicological implications* Pharmacology and Therapeutics 125:376-393

Maksimenko A., Ishchenko A.A., Sanz G., Laval J., Elder R.H. and Saparbaev M.K. **(2004)** *A molecular beacon assay for measuring base excision repair activities* Biochemical and Biophysical Research Communications 319:240-246

Malayappan B., Garrett T.J., Segal M. and Leeuwenburgh C. **(2007)** *Urinary analysis of 8-oxoguanine, 8-oxoguanosine, fapy-guanine and 8-oxo-2'-deoxyguanosine by high-performance liquid chromatography-electrospray tandem mass spectrometry as a measure of oxidative stress* Journal of Chromatography 1167:54-62

Marnett L.J. **(1999)** *Lipid peroxidation - DNA damage by malondialdehyde* Mutation Research 424:83-95

Martinet W., Knaapen M.W.M., De Meyer G.R.Y., Herman A.G. and Kockx M.M. **(2001)** *Oxidative DNA damage and repair in experimental atherosclerosis are reversed by dietary lipid lowering* Circulation Research 88:733-739

Marsin S., Vidal A.E., Sossou M., Ménissier-de Murcia J., Le Page F., Boiteux S., de Murcia G. and Radicella J.P. **(2003)** *Role of XRCC1 in the coordination and stimulation of oxidative DNA damage repair initiated by the DNA glycosylase hOGG1* The Journal of Biological Chemistry 278:44068-44074

Matés J.M., Segura J.A., Alonso F.J. and Márquez J. **(2008)** *Intracellular redox status and oxidative stress: implications for cell proliferation, apoptosis, and carcinogenesis* Archives of Toxicology 82:273-299

Matsui A., Ikeda T., Enomoto K., Hosoda K., Nakashima H., Omae K., Watanabe M., Hibi T. and Kitajima M. **(2000)** *Increased formation of oxidative DNA damage, 8-hydroxy-2'-deoxyguanosine, in human breast cancer tissue and its relationship to GSTP1 and COMT genotypes* Cancer Letters 151:87-95

McNally J.S., Saxena A., Cai H., Dikalov S. and Harrison D.G. **(2005)** *Regulation of xanthine oxidoreductase protein expression by hydrogen peroxide and calcium* Arteriosclerosis, Thrombosis, and Vascular Biology 25:1623-1628

Mecocci P., Polidori M.C., Ingegni T., Cherubini A., Chionne F., Cecchetti R. and Senin U. **(1998)** *Oxidative damage to DNA in lymphocytes from AD patients* Neurology 51:1014-1017

Meister A. and Anderson M.E. **(1983)** *Glutathione* Annual Reviews in Biochemistry 52:711-760

Minowa O., Arai T., Hirano M., Monden Y., Nakai S., Fukufa M., Itoh M., Takano H., Hippou Y., Aburatani H., Masumura K., Nohmi T., Nishimura S. and Noda T. **(2000)** *Mmh/Ogg1 gene inactivation results in accumulation of 8-hydroxyguanine in mice* Proceedings of the National Academy of Sciences U.S.A. 97:4156-4161

Mirbahai L., Kershaw R.M., Green R.M., Hayden R.E., Meldrum R.A. and Hodges N.J. **(2010)** *Use of a molecular beacon to track the activity of base excision repair protein OGG1 in live cells* DNA Repair 9:144-152

Modrich P. and Lahue R. **(1996)** *Mismatch repair in replication fidelity, genetic recombination, and cancer biology* Annual Review of Biochemistry 65:101-133

Mokkapati S.K., Wiederhold L., Hazra T.K. and Mitra S. **(2004)** *Stimulation of DNA glycosylase activity of OGG1 by NEIL1: Functional collaboration between two human DNA glycosylases* Biochemistry 43:11596-11604

Morand C., Rios L., Moundras C., Besson C., Remesy C. and Demigne C. **(1997)** *Influence of methionine availability on glutathione synthesis and delivery by the liver* The Journal of Nutritional Biochemistry 8:246-255

Moriya M. **(1993)** *Single-stranded shuttle phagemid for mutagenesis studies in mammalian cells: 8-oxoguanine in DNA induces targeted GC→TA transversions in simian kidney cells* Proceedings of the National Academy of Sciences U.S.A. 90:1122-1126

Moriya M., Ou C., Bodepudi V., Johnson F., Takeshita M. and Grollman A.P. **(1991)** *Site-specific mutagenesis using a gapped duplex vector: a study of translesion synthesis past 8-oxodeoxyguanosine in E.coli* Mutation Research 254:281-288

Murphy M.P. **(2009)** *How mitochondria produce reactive oxygen species* The Biochemical Journal 417:1-13

Niesink R.J.M., de Vries J. and Hollinger M.A. **(1996)** *Toxicology Principles and Applications* 1st Edition; CRC press, Inc.; U.S.A. p307

Nishioka K., Ohtsubo T., Oda H., Fujiwara T., Kang D., Sugimachi K. and Nakabeppu Y. **(1999)** *Expression and differential intracellular localization of two major forms of human 8-oxodGuanine DNA glycosylase encoded by alternatively spliced OGG1 mRNAs* Molecular Biology of the Cell 10:1637-1652

Nguyen T., Nioi P. and Pickett C.B. **(2009)** *The Nrf2-antioxidant response element signalling pathway and its activation by oxidative stress* The Journal of Biological Chemistry 284:13291-13295

Oka S., Ohno M., Tsuchimoto D., Sakumi K., Furuichi M. and Nakabeppu Y. **(2008)** *Two distinct pathways of cell death triggered by oxidative damage to nuclear and mitochondrial DNAs* The EMBO Journal 27:421-432

Ogryzko V.V., Schiltz R.L., Russanova V., Howard B.H. and Nakatani Y. **(1996)** *The transcriptional coactivators p300 and CBP are histone acetyltransferases* Cell 87:953-959

Osterod M., Hollenbach S., Hengstler J.G., Barnes D.E., Lindahl T. and Epe B. **(2001)** *Age-related and tissue-specific accumulation of oxidative DNA base damage in 7,8-dihydro-8-oxoguanine-DNA glycosylase (Ogg1) deficient mice* Carcinogenesis 22:1459-1463

Ostling O. and Johnson K.J. **(1984)** *Microelectrophoretic study of radiation-induced DNA damages in individual mammalian cells* Biochemical and Biophysical Research Communications 123:291-298

Palmer R.M.J., Rees D.D., Ashton D.S. and Moncada S. **(1988)** *L-arginine is the physiological precursor for the formation of nitric oxide in endothelium-dependent relaxation* Biochemical and Biophysical Research Communications 153:1251-1256

Papanikolaou G. and Pantopoulos K. **(2005)** *Iron metabolism and toxicity* Toxicology and Applied Pharmacology 202:199-211

Pardo L., Osman R., Banfelder J., Mazurek A.P. and Weinstein H. **(1991)** *Molecular mechanisms of radiation induced DNA damage: HO-abstraction and β-cleavage* Free Radical Research Communications 12-13: Pt 2: 461-463

Park Y.J., Choi E.Y., Choi J.Y., Park J.G., You H.J. and Chung M.H. **(2001)** *Genetic changes of hOGG1 and the activity of oh8Gua glycosylase in colon cancer* European Journal of Cancer 37:340-346

Park J., Chen L., Tockman M.S., Elahi A. and Lazarus P. **(2004)** *The human 8-oxoguanine DNA N-glycosylase 1 (hOGG1) DNA repair enzyme and its association with lung cancer risk* Pharmacogenetics 14:103-109

Paulsen C.E. and Carroll K.S. **(2009)** *Orchestrating redox signaling networks through regulatory cysteine switches* ACS Chemical Biology 5:47-62

Paz-Elizur T., Sevilya Z., Leitner-Dagan Y., Elinger D., Roisman L.C. and Livneh Z. **(2008)** *DNA repair of oxidative DNA damage in human carcinogenesis: Potential application for cancer risk assessment and prevention* Cancer Letters 266:60-72

Peak M.J. and Peak J.G. **(1989)** *Solar-ultraviolet-induced damage to DNA* Photo-dermatology 6:1-15

Phillips E.R. and McKinnon P.J. **(2007)** *DNA double-strand break repair and development* Oncogene 26:7799-7808

Potts R.J., Watkin R.D. and Hart B.A. **(2003)** *Cadmium exposure down-regulates 8-oxoguanine DNA glycosylase expression in rat lung and alveolar epithelial cells* Toxicology 184:189-202

Priestley C.C., Green R.M., Fellows M.D., Doherty A.T., Hodges N.J. and O'Donovan M.R. **(2010)** *Anomalous genotoxic responses induced in mouse lymphoma L5178Y cells by potassium bromate* Toxicology 267:45-53

Prieto Alamo M.J., Jurado J., Francastel E. and Laval F. **(1998)** *Rat 7,8-dihydro-8-oxoguanine DNA glycosylase: substrate specificity, kinetics and cleavage mechanism at an apurinic site* Nucleic Acids Research 26:5199-5202

Pourahmad J. and O'Brien P.J. **(2000)** *A comparison of hepatocyte cytotoxic mechanisms for Cu^{2+} and Cd^{2+}* Toxicology 143:263-273

Rachek L.I., Grishko V.I., Musiyenko S.I., Kelley M.R., LeDoux S.P. and Wilson G.L. **(2002)** *Conditional targeting of the DNA repair enzyme hOGG1 into mitochondria* The Journal of Biological Chemistry 277:44932-44937

Ramakers C., Ruijter J.M., Lekanne Deprez R.H. and Moorman A.F.M. **(2003)** *Assumption-free analysis of quantitative real-time polymerase reaction (PCR) data* Neuroscience Letters 339:62-66

Ramon O., Sauvaigo S., Gasparutto D., Faure P., Favier A. and Cadet J. **(1999)** *Effects of 8-oxo-7,8-dihydro-2'-deoxyguanosine on the binding of the transcription factor Sp1 to its cognitive target DNA sequence (GC box)* Free Radical Research 31:217-229

Reddy V.P., Zhu X., Perry G. and Smith M.A. **(2009)** *Oxidative stress in diabetes and Alzheimer's disease* Journal of Alzheimer's Disease 16:763-774

Riis B., Rison L., Loft S., Poulsen H.E. **(2002)** *OGG1 mRNA expression and excision activity in rats are higher in foetal tissue than in adult liver tissue while 8-oxo-2'-deoxyguanosine levels are unchanged* DNA Repair 1:709-717

Romano G., Sgambato A., Mancini R., Capelli G., Giovagnoli M.R., Flamini G., Boninsegna A., Vecchione A. and Cittadini A. **(2000)** *8-Hygroxy-2'-deoxyguanosine in cervical cells: correllation with grade of dysplasia and human papillomavirus infection* Carcinogenesis 21:1143-1147

Rosenquist T.A., Zharkov D.O. and Grollman A.P. **(1997)** *Cloning and characterization of a mammalian 8-oxoguanine DNA glycosylase* Proceedings of the National Academy of Sciences of the U.S.A. 94:7429-7434

Rushmore T.H. and Pickett C.B. **(1990)** *Transcriptional regulation of the rat glutathione-S-transferase Ya subunit gene* The Journal of Biological Chemistry 265:14648-14653

Sakumi K., Tominaga Y., Furuichi M., Xu P., Tsuzuki T., Sekiguchi M. and Nakabeppu Y. **(2003)** *Ogg knockout-associated lung tumorigenesis and its suppression by Mth1 gene disruption* Cancer Research 63:902-905

Salsbury Jr. F.R., Knutson S.T., Poole L.B. and Fetrow J.S. **(2008)** *Functional site profiling and electrostatic analysis of cysteines modifiable to cyteine sulfenic acid* Protein Science 17:299-312

Sampson J.R., Jones S., Dolwani S. and Cheadle J.P. **(2005)** *MutYH (MYH) and colorectal cancer* The Molecular Biology of Colorectal Cancer 33:679-683

Sastre J., Pallardó F.V. and Viña J. **(2000)** *Mitochondrial oxidative stress plays a key role in aging and apoptosis* Life 49:427-435

Schrader M. and Fahimi H.D. **(2006)** *Peroxisomes and oxidative stress* Biochimica et Biophysica Acta 1763:1755-1766

Sedgwick B., Bates P.A., Paik J., Jacobs S.C. and Lindahl T. **(2007)** *Repair of alkylated DNA: recent advances* DNA Repair 6:429-442

Senft A.P., Dalton T.P. and Shertzer H.G. **(2000)** *Determining glutathione and glutathione disulphide using the fluorescence probe o-phthalaldehyde* Analytical Biochemistry 280:80-86

Sentürker S., Karahalil B., Inal M., Yilmaz H., Müslümanoglu H., Gedikoglu G. and Dizdaroglu M. **(1997)** *Oxidative DNA base damage and antioxidant enzyme levels in childhood acute lymphoblastic leukemia* Federation of European Biochemical Societies Letters 416:286-290

Setlow R.B. and Carrier W.L. **(1964)** *The disappearance of thymine dimers from DNA: an error-correcting mechanism* Proceedings of the National Academy of Sciences U.S.A. 51:226-231

Shaffer J.M., Hellwig S. and Smithgall T.E. **(2009)** *Bimolecular fluorescence complementation demonstrates that the c-Fes protein-tyrosine kinase forms constitutive oligomers in living cells* Biochemistry 48:4780-4788

Shibutani S., Takeshita M. and Grollman A.P. **(1991)** *Insertion of specific bases during DNA synthesis past the oxidation-damaged base 8-oxodG* Nature 349:431-434

Shinmura K., Kohno T., Kasai H., Koda K., Sugimura H. and Yokata J. **(1998)** *Infrequent mutations of the hOGG1 gene, that is involved in the excision of 8-hydroxyguanine in damaged DNA, in human gastric cancer* Japanese Journal of Cancer Research 89:825-828

Shuck S.C., Short E.A. and Turchi J.J. **(2008)** *Eukaryotic nucleotide excision repair: from understanding mechanisms to influencing biology* Cell Research 18:64-72

Shyu Y.J., Liu H., Deng X. and Hu C.D. **(2006)** *Identification of new fluorescent protein fragments for bimolecular fluorescence complementation analysis under physiological conditions* BioTechniques 40:61-66

Sidorenko V.S., Grollman A.P., Jaruga P., Dizdaroglu M. and Zharkov D.O. **(2009)** *Substrate specificity and excision kinetics of natural polymorphic variants and phosphomimetic mutants of human 8-oxoguanine-DNA glycosylase* The FEBS journal 276:5149-5162

Sidorenko V.S., Nevinsky G.A. and Zharkov D.O. **(2007)** *Mechanism of interaction between human 8-oxoguanine-DNA glycosylase and AP endonuclease* DNA Repair 6:317-328

Sidorenko V.S., Nevinsky G.A. and Zharkov D.O. **(2008)** *Specificity of stimulation of human 8-oxoguanine-DNA glycosylase by AP endonuclease* Biochemical and Biophysical Research Communications 368:175-179

Silva J.P., Gomes A.C., Proença F. and Coutinho O.P. **(2009)** *Novel nitrogen compounds enhance protection and repair of oxidative DNA damage in a neuronal cell model: Comparison with quercetin* Chemico-Biological Interactions 181:328-337

Simonelli V., Mazzei F., D'errico M., Camerini S., Guarrera S., Barone F., Allione A., Minoprio A., Bjoras M., Matullo G. and Dogliotti E. **(2011)** *OGG1-S326C variant is associated with lower repair activity: effects of gene expression and oxidation status* Conference proceedings, Responses to DNA damage from molecular mechanism to human disease conference, Egmond aan Zee, Netherlands, April 3-8

Smart D.J., Chipman J.K. and Hodges N.J. **(2006)** *Activity of OGG1 variants in the repair of pro-oxidant-induced 8-oxo-2'-deoxyguanosine* DNA Repair 5:1337-1345

Speina E., Cieśla J.M., Wojcik J., Bajek M., Kuśmierek J.T. and Tudek B. **(2001)** *The pyrimidine ring-opened derivative of 1,N^6-Ethenoadenine is excised from DNA by the Escherichia coli Fpg and Nth proteins* The Journal of Biological Chemistry 276:21821-21827

Srivastava A., Srivastava K., Pandey S.N., Choudhuri G. and Mittal B. **(2009)** *Single-nucleotide polymorphisms of DNA repair genes OGG1 and XRCC1: association with gallbladder cancer in North Indian population* Annals of Surgical Oncology 16:1695-1703

Stadtman E.R. **(1992)** *Protein oxidation and aging* Science 257:220-224

Stamler J.S., Singel D.J. and Loscalzo J. **(1992)** *Biochemistry of nitric oxide and its redox-activated forms* Science 258:1898-1902

Stanczyk M., Sliwinski T., Cuchra M., Zubowska M., Bielecka-Kowalska A., Kowalski M., Szemraj J., Mlynarski W. and Majsterek I. **(2011)** *The association of polymorphisms in DNA base excision repair genes XRCC1, OGG1 and MUTYH with the risk of childhood acute lymphoblastic leukemia* Molecular Biology Reports 38:445-451

Steenken S. **(1989)** *Purine bases, nucleosides and nucleotides: Aqueous solution redox chemistry and transformation reactions of their radical cations and e^- and OH adducts* Chemical Reviews 89:503-520

Steenken S. And Jovanovic S.V. **(1997)** *How easily oxidizable is DNA? One-electron reduction potentials of adenosine and guanosine radicals in aqueous solution* Journal of the American Chemical Society 119(3):617-618

Sterpone S., Mastellone V., Padua L., Novelli F., Patrono C., Cornetta T., Giammarine D., Donato V., Testa A. and Cozzi R. **(2010)** *Single-nucleotide polymorphisms in BER and HRR genes, XRCC1 haplotypes and breast cancer risk in Caucasian women* Journal of Cancer Research and Clinical Oncology 136:631-636

Sugimura H., Kohno T., Wakai K., Nagura K., Genka K., Igarashi H., Morris B.J., Baba S., Ohno Y., Gao C., Li Z., Wang J., Takezaki T., Tajima K., Varga T., Sawaguchi T., Lum J.K., Martinson J.J., Tsugane S., Iwamasa T., Shinmura K. and Yokota J. **(1999)** *hOGG1 Ser326Cys polymorphism and lung cancer susceptibility* Cancer Epidemiology Biomarkers and Prevention 8:669-674

Tagesson C., Källberg M., Klintenberg C. and Starkhammar H. **(1995)** *Determination of urinary 8-hydroxydeoxyguanosine by automated coupled-column high performance liquid chromatography: a powerful technique for assaying in vivo oxidative DNA damage in cancer patients* Eurpoean Journal of Cancer 31A:934-940

Takao M., Aburatani H., Kobayashi K. and Yasui A. **(1998)** *Mitochondrial targeting of human DNA glycosylases for repair of oxidative DNA damage* Nucleic Acids Research 26:2917-2922

Takezaki T., Gao C.M., Wu J.Z., Li Z.Y., Wang J.D., Ding J.H., Liu Y.T., Hu X., Xu T.L., Tajima K. and Sugimura H. **(2002)** *hOGG1 SER326CYS polymorphism and modification by environmental factors of stomach cancer risk in Chinese* International Journal of Cancer 99:624-627

Tamura G., Nishizuka S., Maesawa C., Suzuki Y., Iwaya T., Sakata K., Endoh Y. and Motoyama T. **(1999)** *Mutations in mitochondrial control region DNA in gastric tumours of Japanese patients* European Journal of Cancer 35:316-319

Tarng D.C., Tsai T.J., Chen W.T., Liu T.Y. and Wei Y.H. **(2001)** *Effect of human OGG1 1245C→G gene polymorphism on 8-hydroxy-2'-deoxyguanosine levels of leukocyte DNA among patients undergoing chronic hemodialysis* Journal of the American Society of Nephrology 12:2338-2347

Thiviyanathan V., Somasunderam A., Hazra T.K., Mitra S. and Gorenstein D.G. **(2003)** *Solution structure of a DNA duplex containing 8-hydroxy-2'-deoxyguanosine opposite deoxyguanosine* Journal of Molecular Biology 325:433-442

Umar A. and Kunkel T.A. **(1996)** *DNA-replication fidelity, mismatch repair and genome instability in cancer cells* European Journal of Biochemistry 238:297-307

Valinluck V., Tsai H.H., Rogstad D.K., Burdzy A., Bird A. and Sowers L.C. **(2004)** *Oxidative damage to methyl-CpG sequences inhibits the binding of the methyl-CpG binding domain (MBD) of methyl-CpG binding protein 2 (MeCP2)* Nucleic Acids Research 32:4100-4108

Valko M., Leibfritz D., Moncol J., Cronin M.T.D., Mazur M. and Telser J. **(2007)** *Free radicals and antioxidants in normal physiological functions and human disease* The International Journal of Biochemistry and Cell Biology 39:44-84

van Gent D.C., Hoeijmakers J.H.J. and Kanaar R. **(2001)** *Chromosomal stability and the DNA double-stranded break connection* Nature Reviews Genetics 2:196-206

van Loon B., Markkanen E. and Hübscher U. **(2010)** *Oxygen as a friend and enemy: How to combat the mutational potential of 8-oxo-guanine* DNA Repair 9:604-616

Vidal A.E., Hickson I.D., Boiteux S. and Radicella J.P. **(2001.1)** *Mechanism of stimulation of the DNA glycosylase activity of hOGG1 by the major human AP endonuclease: bypass of the AP lyase activity step* Nucleic Acids Research 29:1285-1292

Vidal A.E., Boiteux S., Hickson I.D. and Radicella J.P. **(2001.2)** *XRCC1 coordinates the initial and late stages of DNA abasic site repair through protein-protein interactions* The EMBO Journal 20:6530-6539

Vineis P., Manuguerra M., Kavvoura F.K., Guarrera S., Allione A., Rosa F., Di Gregorio A., Polidoro S., Saletta F., Ionnidis J.P.A. and Matullo G. **(2009)** *A field synopsis on low-penetrance variants in DNA repair genes and cancer susceptibility* Journal of the National Cancer Institute 101:24-36

Vladimirova O., O'Connor J., Cahill A., Alder H., Butunoi C. and Kalman B. **(1998)** *Oxidative damage to DNA in plaques of MS brains* Multiple Sclerosis 4:413-418

Vogel U., Nexø B., Olsen A., Thomsen B., Jacobsen N.R., Wallin H., Overvad K. and Tjønneland A. **(2003)** *No association between OGG1 Ser326Cys polymorphism and breast cancer risk* Cancer Epidemiology, Biomarkers and Prevention 12:170-171

von Sonntag C. **(1987)** *The chemical basis of radiation biology* Taylor and Francis: London: pp116-166

Wallace S.S. **(1998)** *Enzymatic processing of radiation-induced free radical damage in DNA* Radiation Research 150:S60-S79

Wang D., Kreutzer D.A. and Essigmann J.M. **(1998)** *Mutagenicity and repair of oxidative DNA damage: insights from studies using defined lesions* Mutation Research 400:99-11

Weiss J.M., Goode E.L., Ladiges W.C. and Ulrich C.M. **(2005)** *Polymorphic variation in hOGG1 and risk of cancer: A review of the functional and epidemiologic literature* Molecular Carcinogenesis 42:127-141

Weterings E. and Chen D.J. **(2008)** *The endless tale of non-homologous end-joining* Cell Research 18:114-124

Wood M.L., Dizdaroglu M., Gajewski E. and Essigmann J.M. **(1990)** *Mechanistic studies of ionizing radiation and oxidative mutagenesis: genetic effects of a single 8-hydroxyguanine (7-hydro-8-oxodGuanine) residue inserted at a unique site in a viral genome* Biochemistry 29:7024-7032

Xing D.Y., Tan W., Song N. And Lin D.X. **(2001)** *Ser326Cys polymorphism in hOGG1 gene and risk of esophageal cancer in a chinese population* International Journal of Cancer (Pred. Oncol.) 95:140-143

Yacoub A., Augeri L., Kelley M.R., Doetsch P.W. and Deutsch W.A. **(1996)** *A Drosophila ribosomal protein contains 8-oxoguanine and abasic site DNA repair activities* The EMBO Journal 15:2306-2312

Yadavilli S., Hegde V. and Deutsch W.A. **(2007)** *Translocation of human ribosomal protein S3 to sites of DNA damage is dependent on ERK-mediated phosphorylation following genotoxic stress* DNA Repair 6:1453-1462

Yamamoto T., Hosokawa K., Tamura T., Kanno H., Urabe M. and Honjo H. **(1996)** *Urinary 8-hydroxy-2'-deoxyguanosine (8-OHdG) levels in women with or without gynecologic cancer* The Journal of Obstetrics and Gynaecology Research 22:359-363

Yamane A., Takashi K., Ito K., Sunaga N., Aoki K., Yoshimura K., Murakami H., Nojima Y. and Yokota J. **(2004)** *Differential ability of polymorphic OGG1 proteins to suppress mutagenesis induced by 8-hydroxyguanine in human cell in vivo* Carcinogenesis 25:1689-1694

Youn C.K., Kim S.H., Lee D.Y., Song S.H., Chang I.Y., Hyun J.W., Chung M.H. and You H.J. **(2005)** *Cadmium down-regulates human OGG1 through suppression of Sp1 activity* The Journal of Biological Chemistry 280:25185-25195

Yuan W., Xu L., Feng Y., Yang Y., Chen W., Wang J., Pang D. and Li D. **(2010)** *The hOGG1 Ser326Cys polymorphism and breast cancer risk: a meta-analysis* Breast Cancer Research and Treatment 122:835-842

Zielinska A.E., Davies O.T., Meldrum R.A. and Hodges N.J. **(2011)** *Direct visualization of repair of oxidative damage by OGG1 in the nuclei of live cells* Journal of Biochemical and Molecular Toxicology 25:1-7

Zhang Z., Ma C. and Chalfie M. **(2004)** *Combinatorial marking of cells and organelles with reconstituted fluorescent proteins* Cell 119:137-144

Zhang J., Perry G., Smith M.A., Robertson D., Olson S.J., Graham D.G. and Motine T.J. **(1999)** *Parkinson's disease in associated with oxidative damage to cytoplasmic DNA and RNA in substantia nigra neurons* American Journal of Pathology 154:1423-1429

Zharkov D.O. and Rosenquist T.A. **(2002)** *Inactivation of mammalian 8-oxoguanine-DNA glycosylase by cadmium(II): implications for cadmium genotoxicity* DNA Repair 1:661-670

Appendix

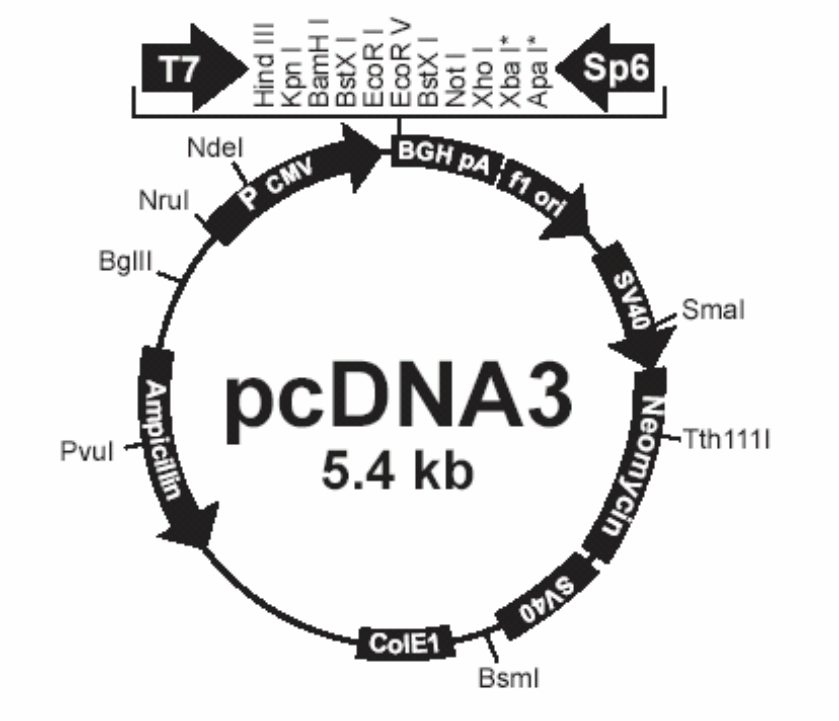

Vector map of pcDNA3© (Invitrogen).
Ser326- and Cys326-hOGG1 cDNA molecules were cloned into the BamHI and EcoRI sites of the multiple cloning site.

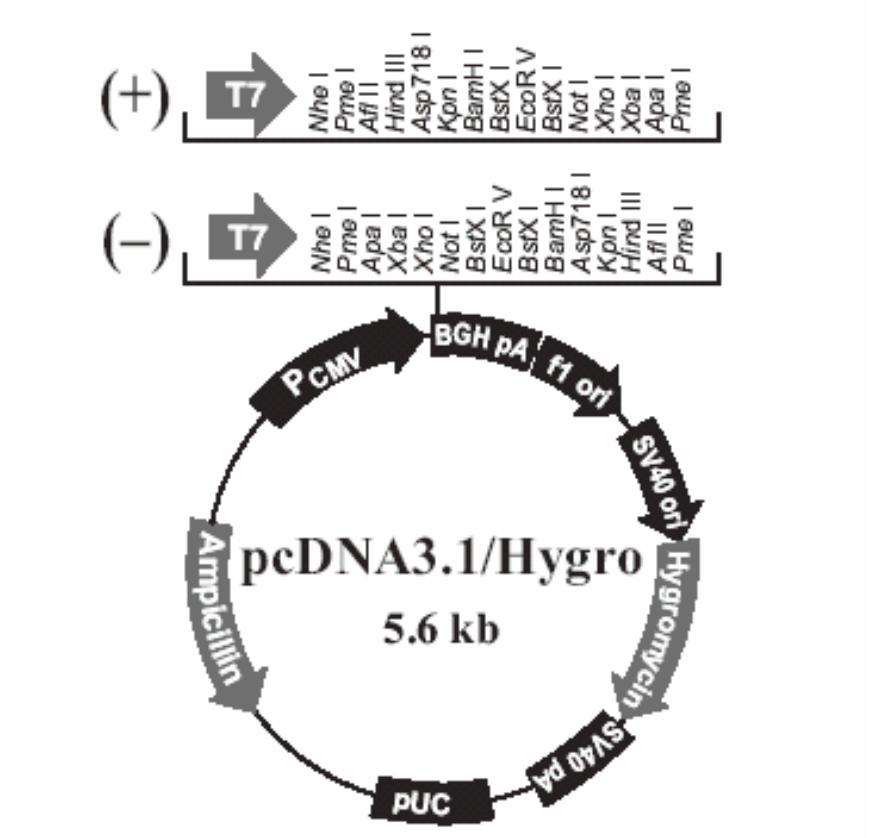

Vector map of pcDNA3.1/Hygro©(+) (Invitrogen).
Ser326- and Cys326-hOGG1 cDNA molecules were sub-cloned from pcDNA3© into the BamHI and XhoI sites of the multiple cloning site.

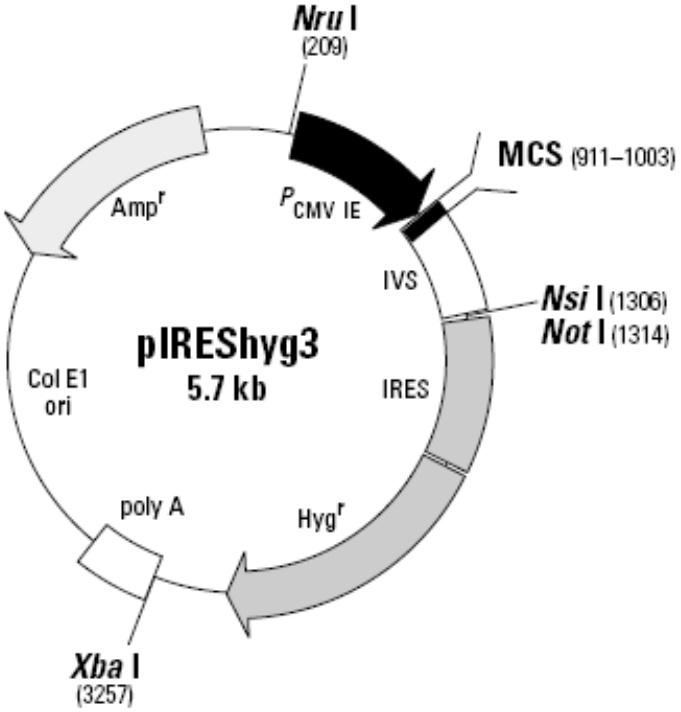

Vector map of pIREShyg3 (B.D. Clontech).
Ser326- and Cys326-hOGG1 cDNA molecules were sub-cloned from pcDNA3.1/Hygro(+)© into the AflII and BamHI sites of the multiple cloning sites.

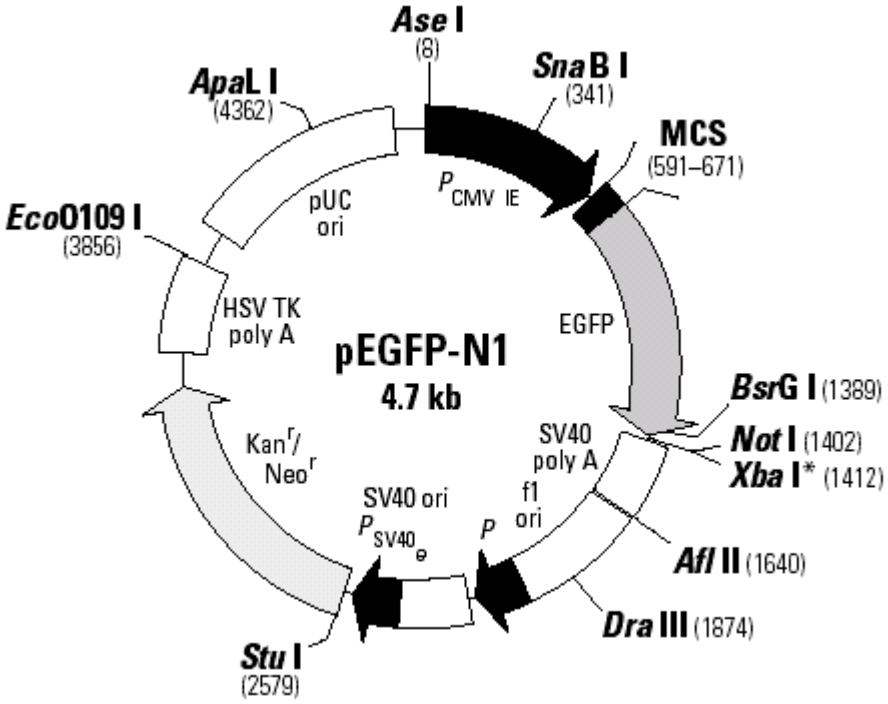

Vector map of pEGFP-N1 (B.D. Clontech).
Ser326- and Cys326-hOGG1 cDNA molecules were inserted into the KpnI and AgeI sites of the multiple cloning site.

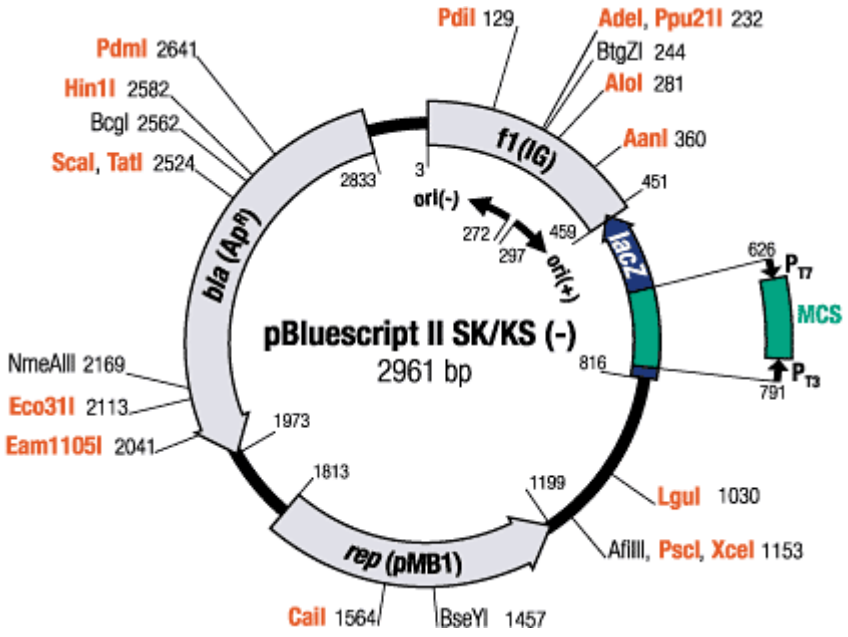

Vector map of pBluescript II KS(-).

The N and C terminal cDNA of YFP had previously been cloned into the BamHI site of the multiple cloning site. Ser326- and Cys326-hOGG1 cDNA molecules were cloned into the BamHI sites of the same multiple cloning site, C-terminal to the YFP cDNA.

```
Mouse MLFRSWLPSSMRHRTLSSSPALWASIPCPRSELRLDLVLASGQSFRWKEQSPAHWSGVLA 60
Rat   MLFSSSLSSSMRHRTLTSSPALWASIPCPRSELRLDLVLASGQSFRWREQSPAHWSGVLA 60
      *** * *.********:******************************:************

Mouse DQVWTLTQTEDQLYCTVYRGDDSQVSRPTLEELETLHKYFQLDVSLAQLYSHWASVDSHF 120
Rat   DQVWTLTQTEDQLYCTVYRGDKGQVGRPTLEELETLHKYFQLDVSLTQLYSHWASVDSHF 120
      **********************..**.********************:*************

Mouse QRVAQKFQGVRLLRQDPTECLFSFICSSNNNIARITGMVERLCQAFGPRLIQLDDVTYHG 180
Rat   QSVAQKFQGVRLLRQDPTECLFSFICSSNNNIARITGMVERLCQAFGPRLVQLDDVTYHG 180
      * ************************************************:*********

Mouse FPNLHALAGPEAETHLRKLGLGYRARYVRASAKAILEEQGGPAWLQQLRVAPYEEAHKAL 240
Rat   FPNLHALAGPEVETHLRKLGLGXRARYVCASAKAILEEQGGPAWLQQLRVASYEEAHKAL 240
      ***********.********** ***** **********************.********

Mouse CTLPGVGAKVADCICLMALDKPQAVPVDVHVWQIAHRDYGWHPKTSQAKGPSPLANKELG 300
Rat   CTLPGVGTKVADCICLMALDKPQAVPVDIHVWQIAHRDYGWQPKTSQTKGPSPLANKELG 300
      *******:********************:************:*****:************

Mouse NFFRNLWGPYAGWAQAVLFSADLRQPSLSREPPAKRKKGSKRPEG 345
Rat   NFFRNLWGPYAGWAQAVLFSADLRQQNLSREPPAKRKKGSKKTEG 345
      ************************ .**************:.**
```

Multiple sequence alignment with the Clustal series of programs.
Multiple alignment score = 93 (Chenna *et al.* 2003).

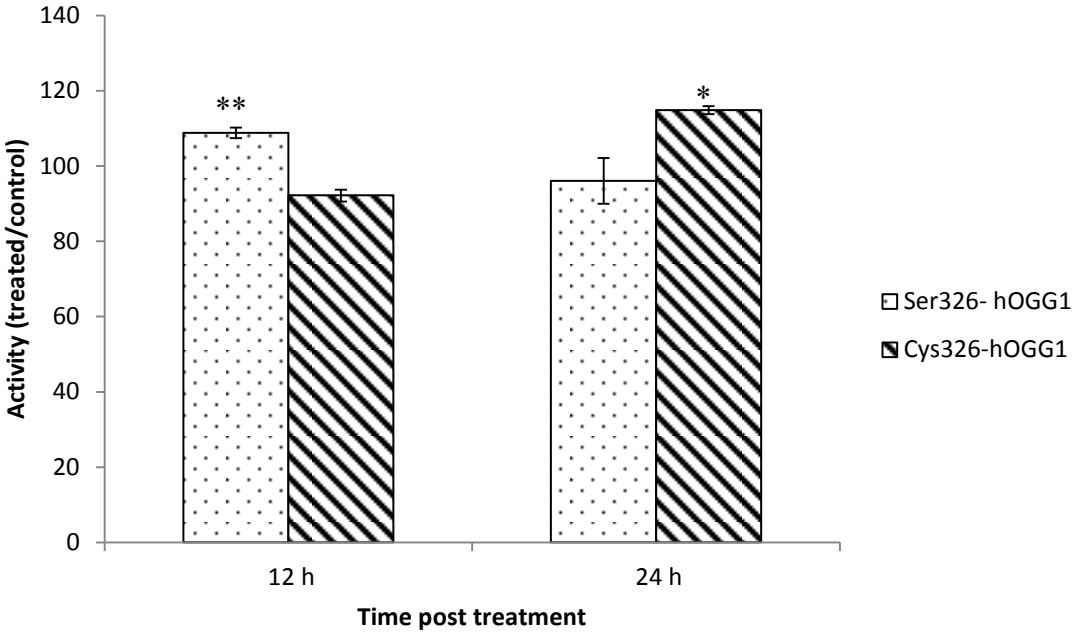

Ser326- and Cys326-hOGG1 activity in independent MEF cell clones following BSO treatment. Data are expressed as the number of positive beacon events as a percentage of untreated control, ±SEM from 4 independent experiments. *,**: Significantly different from control (*$P < 0.05$ **$P < 0.01$) as determined by 2-tailed Student's *t*-test.

Research papers

Kershaw R.M. and Hodges N.J. *Repair of oxidative DNA damage is delayed in the Ser326Cys polymorphic variant of the base excision repair protein OGG1* Submitted to mutagenesis

Mirbahai L., **Kershaw R.M.**, Green R.M., Hayden R.E., Meldrum R.A. and Hodges N.J. (2010) *Use of a molecular beacon to track the activity of base excision repair protein OGG1 in live cells* DNA Repair 9:144-152